Epigenetic Regulation of tRNA Biology in Cancer

Margalida Rosselló Tortella

Epigenetic Regulation of tRNA Biology in Cancer

Memòria presentada per **Margalida Rosselló Tortella** per optar al grau de
Doctor per la Universitat de Barcelona

UNIVERSITAT DE BARCELONA, FACULTAT DE MEDICINA
PROGRAMA DE DOCTORAT EN BIOMEDICINA 2021

Aquest treball ha estat realitzat al Grup d'Epigenètica del Càncer, primer integrat dins el Programa d'Epigenètica i Biologia del Càncer (PEBC) de l'Institut d'investigació Biomèdica de Bellvitge (IDIBELL) i posteriorment a l'Institut de Recerca contra la Leucèmia Josep Carreras (IJC)

Dr. Manel Esteller Badosa
Director i tutor

Margalida Rosselló Tortella
Doctorand

Als meus pares i padrins, que m'ho han donat tot.

A en Pep, que és el millor company d'equip.

CONTENTS

CONTENTS OF THE THESIS

Table of Contents

Contents

List of figures

Contents

List of tables

Contents

Abbreviations

5mC	5-methylcytosine (in DNA)
ACTB	β-actin
AZA	5-azacytidine
BSP	Bisulfite sequencing PCR
CANX	Calnexin
CCLE	Cancer Cell Line Encyclopedia
CDH1	E-cadherin
ChIP	Chromatin immunoprecipitation
CpG	Cytosine-phosphoryl-guanosine dinucleotide
DNMT	DNA methyltransferase
EMT	Epithelial-to-mesenchymal transition
FDR	False discovery rate
GAPDH	Glyceraldehyde-3-phosphate dehydrogenase
GTF3C1	TFIIIC subunit 1
HM450	HumanMethylation450 DNA methylation microarray
LC/MS	Liquid chromatography coupled to mass spectrometry
LMNB1	Lamin B1
mt-tRNA	Mitochondrial tRNA
ncRNA	Non-coding RNA
NMD	Nonsense-mediated mRNA decay
o2yW	Peroxywybutosine
OHyW	Hydroxywybutosine
PARP	Poly(ADP-ribose) polymerase
POLR3A	RNA polymerase III subunit A
PRF	Programmed ribosome frameshifting
qRT-PCR	Quantitative real-time PCR
RNAPII	RNA polymerase II
RNAPIII	RNA polymerase III
ROBO1	Roundabout guidance receptor 1
sgRNA	Guide RNA (for CRISPR/Cas9 system)
TCGA	The Cancer Genome Atlas
tDNA	tRNA gene
TFIIIB	General transcription factor 3B
TFIIIC	General transcription factor 3C
tiRNA	tRNA halves
tRF	tRNA-derived fragments
tRNA	Transfer RNA
TSS	Transcription start site
TYW1-5	tRNA yW-synthesizing protein 1-5
UPF1	Upstream frameshift 1
UTR	Untranslated region
VCL	Vinculin
VIM	Vimentin
yW	Wybutosine

INTRODUCTION

INTRODUCTION

The main topics of this thesis are cancer, epigenetics, and tRNA biology. This chapter will introduce some necessary background on each of them.

Cancer

Cancer refers to an enormous group of diseases that share a common feature: uncontrolled cell proliferation (Wild, 2019). The lack of growth control that leads to the transformation of a normal cell into a malignant cell is achieved through a mutation-driven process (Martincorena and Campbell, 2015). The cancer clonal evolution model postulates that cancer originates from one single abnormal cell that accumulates a series of alterations or mutations (Nowell, 1976). Like the Darwinian concept of evolution but at a smaller scale, this mutated cell would suffer successive mutations, positive selection, and selective expansion over the rest of the cell population as it would have a growth advantage.

In 2000, Hanahan and Weinberg proposed their six famous hallmarks of cancer to describe the rules governing cancer development, defining them as the capabilities that cells progressively acquire to escape from the strict regulation of cell proliferation (Hanahan and Weinberg, 2000). These hallmarks are: the sustainment of proliferative signaling, evasion of growth suppressors, resistance to cell death, enablement of replicative immortality, induction of angiogenesis, and activation of invasion and metastasis. As a result of extensive research and increased knowledge of tumor biology, in 2011 Hanahan and Weinberg revisited their original publication and added two additional new hallmarks: energetic metabolism reprogramming and immune escape (Hanahan and Weinberg, 2011); see **Figure 1**.

The gain of these features is supported by two enabling characteristics: tumor inflammation and genomic instability and mutation (Hanahan and Weinberg, 2011); see **Figure 1**. Defective genome maintenance leads to genomic aberrancies, like mutations or chromosomal rearrangements, which contribute to the mutant genotype and trigger the acquisition of the hallmarks by overactivating oncogenes or inactivating tumor suppressors.

In their renewed proposal, Hanahan and Weinberg also emphasized that tumors are more than just an individual growing mass; they are complex tissues where interactions between cells of different types occur. These cells constitute the tumor microenvironment, which includes fibroblasts, endothelial cells, and immune inflammatory cells (Hanahan and Weinberg, 2011). The tumor microenvironment cannot be overseen when studying tumor biology as these cells

Introduction

actively participate in tumorigenesis. This is well reflected by the tumor inflammation enabling characteristic, by which the tumor-infiltrated immune cells provide molecules such as growth or pro-angiogenic factors that foster the progression of the disease (Grivennikov et al., 2010).
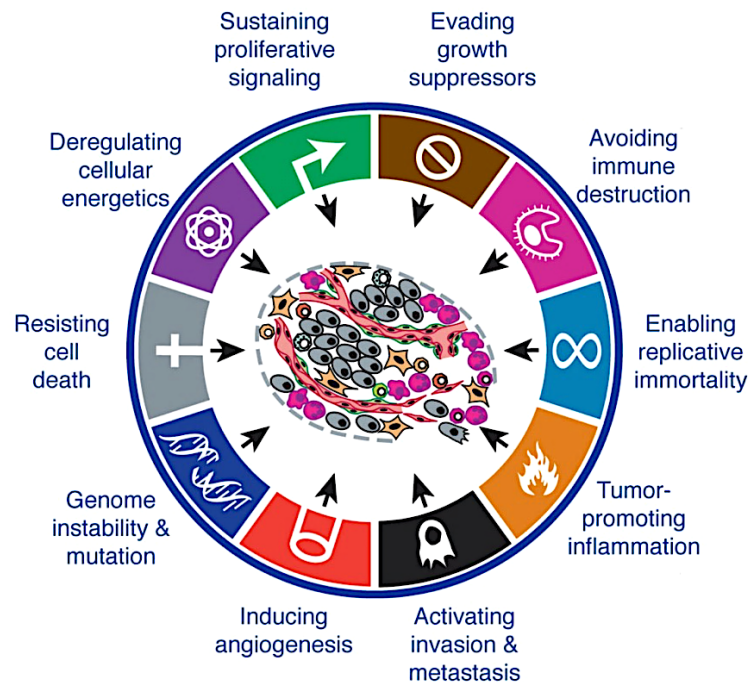
Figure 1. The hallmarks of cancer and their enabling characteristics. Summary of the eight hallmarks of cancer that normal cells acquire during their malignant transformation and the two characteristics that enable these capabilities. Adapted from Hanahan & Weinberg, 2011.

The hallmarks of cancer are essential for tumor development, thus interfering on any of them has adverse effects on the tumor. Therefore, numerous therapeutic strategies that aim to antagonize them have been developed and are currently under preclinical studies or in clinical trials, and some have already been approved for patient administration. Unfortunately, many of them result in transitory responses followed by relapses (Hanahan and Weinberg, 2011). This may be because the tumor relies on redundant signaling pathways to sustain proliferation, or because cancer cells can reduce their dependency on that particular hallmark and acquire drug resistance (Vasan et al., 2019).

Cancer is a global problem; it is currently one of the leading causes of death in a large list of countries, and improvements in life expectancy predict that its incidence will continue to rise in the coming years (Wild, 2019). Luckily, the knowledge on tumor biology is rapidly growing. According to The Art of War, it is necessary to know your enemy to defeat them. Therefore, further research on unexplored areas of study will significantly improve our understanding of this disease and direct the development of novel therapeutic approaches to stop the uncontrollable growth of cancer –also at the population level.

12

Epigenetics

In 1942, the British embryologist Conrad Waddington used the Greek word "epigenesis" to coin the term epigenetics to define the branch of biology that studies the causal interactions between genes and their products that determine how the phenotype adapts to the environment (Waddington, 1942). In 1957, Waddington also introduced the concept of epigenetic landscape to describe a cellular decision-making process during development to explain cell differentiation and tissue formation. In 1958, David Nanney used the notion of epigenetics to distinguish different types of cellular control systems. He suggested that cells had genetic components that could be expressed or not, and epigenetic components would act as auxiliary mechanisms that control the expression of specific genes (Nanney, 1958).

Research advances in the decades of 1970, 1980 and 1990 expanded the application of epigenetics to other fields, highlighting the relevance of genetic and non-genetic factors in the control of gene expression beyond developmental processes. During those years, epigenetics served as an explanation for many biological phenomena that were incomprehensible and did not fit into other genetic categories (Deans and Maggert, 2015). At that moment, epigenetic mechanisms had not been thoroughly described. The findings that DNA methylation –one of the first proposed epigenetic mechanisms– had effects on gene expression that persisted after cell division prompted Robin Holliday to offer a new definition of epigenetics, describing it as the study of the changes in gene expression that are mitotically and meiotically heritable and that do not obey to changes in DNA sequence (Holliday, 1994).

The interest in epigenetics has significantly increased since it was conceived. However, the lack of a universal definition of this field has generated ambiguities and has delayed the identification of epigenetic mechanisms despite its growing popularity (Deans and Maggert, 2015). Various scientists proposed new definitions for epigenetics, like Adrian Bird, who defined epigenetics as the structural adaptation of chromosomal regions to reflect dynamic cellular environments and different activity states (Bird, 2007).

At the molecular level, the epigenetic regulation of gene expression involves covalent modifications such as DNA methylation or histone modification, non-coding RNA (ncRNA) expression, nucleosome positioning, and histone replacement (Zhang and Pradhan, 2014); see **Figure 2**. Collectively, these mechanisms modulate chromatin accessibility to the molecular machineries that participate in gene expression regulation.

This thesis is centered exclusively in DNA methylation, which we will discuss in depth in the next section. Other epigenetic mechanisms will be commented in less detail.

Introduction
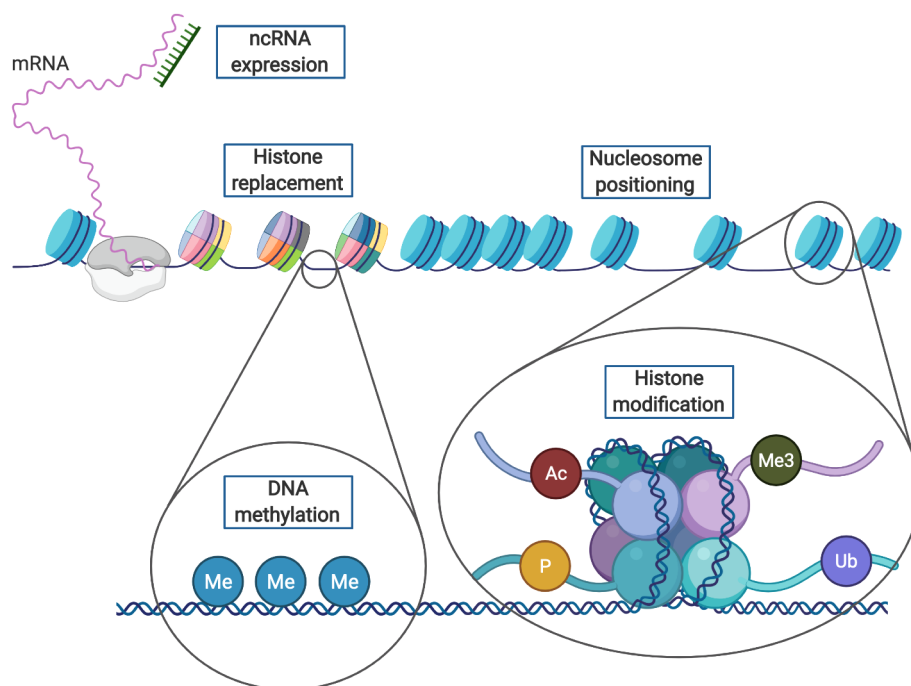
Figure 2. *Epigenetic mechanisms that regulate gene expression.* The principal epigenetic mechanisms that regulate gene expression are DNA methylation, histone modification, non-coding RNA expression, nucleosome positioning, and histone replacement.

DNA methylation

In 1975, Holliday and Pugh, on the one hand, and Riggs on the other, proposed DNA methylation to be an epigenetic mechanism as a result of their studies on chromosome X inactivation (Holliday and Pugh, 1975; Riggs, 1975). Since then, a lot of efforts have been put into the study of DNA methylation patterns and their transmission, making it one of the most studied epigenetic mechanisms.

DNA methylation mainly refers to the incorporation of a methyl group to the 5th carbon of the cytosine (5mC) of a cytosine-phosphoryl-guanosine dinucleotide (CpG). Various DNA methyltransferases (DNMT) can transfer this methyl group from an S-adenosyl methionine (SAM) molecule to the cytosine in DNA (**Figure 3**). On the one hand, DNMT1 is responsible of DNA methylation maintenance after cell division (Li et al., 1992). It is guided by the ubiquitin-like containing PHD and RING finger domains 1 (UHRF1) protein to hemimethylated DNA regions after DNA replication, where it copies the methylation pattern into the newly synthesized strand (Bostick et al., 2007). UHRF1 is subjected to a cell cycle-dependent regulation to ensure the correct timing of maintenance DNA methylation (Kernan et al., 2020). On the other hand, DNMT3A and DNMT3B are *de novo* methyltransferases (Okano et al., 1999). DNMT3A/B methyltransferase activity is enhanced by the catalytically inactive partner DNMT3L (Suetake et al., 2004).

14

DNA methylation is not permanent; it can be removed from the DNA by active or passive demethylation (**Figure 3**). Passive demethylation occurs when DNMT1 function is impaired and disrupts the transmission of the methylation pattern to newly synthesized DNA strands after replication. If this malfunction persists in a hemimethylated daughter cell, DNA replication will originate a hemimethylated double-stranded DNA and a completely unmethylated one. As a result, DNA methylation is diluted following cell division (Li et al., 1992). Active DNA demethylation is mediated by the ten-eleven translocation (TET) family of proteins. The three TETs use α-ketoglutarate and Fe^{2+} to catalyze the successive transformation of the 5'-methyl group, transforming the nucleoside into 5-hydroxymethylcytosine (5hmC), then to 5'-formylcytosine (5fC), and finally to 5'-carboxycytosine (5caC) (Ito et al., 2011). Then, the enzyme thymine DNA glycosylase (TDG) decarboxylates the 5caC to restore the unmethylated cytosine (He et al., 2011). 5hmC can be found as a stable epigenetic mark with tissue-specific distribution that participates in gene regulation and chromatin structure, being especially important in the brain and in stem cells (Cui et al., 2020).

The differential methylation status of a CpG dinucleotide can affect the binding of the transcriptional machinery to DNA (**Figure 3**). On the one hand, some transcription factors and other DNA-binding proteins are sensitive to changes in DNA methylation within their target sequences (Bartke et al., 2010; Zhu et al., 2016). For instance, CCCTC-binding factor (CTCF) binding to DNA is impeded by the presence of 5mC in its binding motif (Hashimoto et al., 2017). On the other hand, the members of the methyl-CpG-binding domains (MBD) family of proteins (MBD1-4 and MeCP2), Kaiso, and other proteins specifically bind to methylated CpG sites (Hendrich and Bird, 1998; Prokhortchouk et al., 2001). Some MBD proteins, like MBD3 and MeCP2, can also bind to 5hmC and regulate gene expression (Mellén et al., 2012; Yildirim et al., 2011).

CpG dinucleotides are not equally distributed across the genome. Instead, they tend to cluster forming CpG islands, which are typically defined as regions of more than 200 base pair (bp) with a GC content higher than a 50% (Gardiner-Garden and Frommer, 1987). It is interesting to note that approximately the 70% of human genes contain a CpG island in their 5' regulatory regions, near their transcription start site (TSS) (Saxonov et al., 2006). Methylation of promoter CpG islands robustly represses transcription either by recruiting transcriptional repressors, like MBD proteins (Schübeler, 2015), or by disrupting the binding to DNA of activating transcription factors (Cusack et al., 2020; Tate and Bird, 1993); see **Figure 4A**.

Introduction
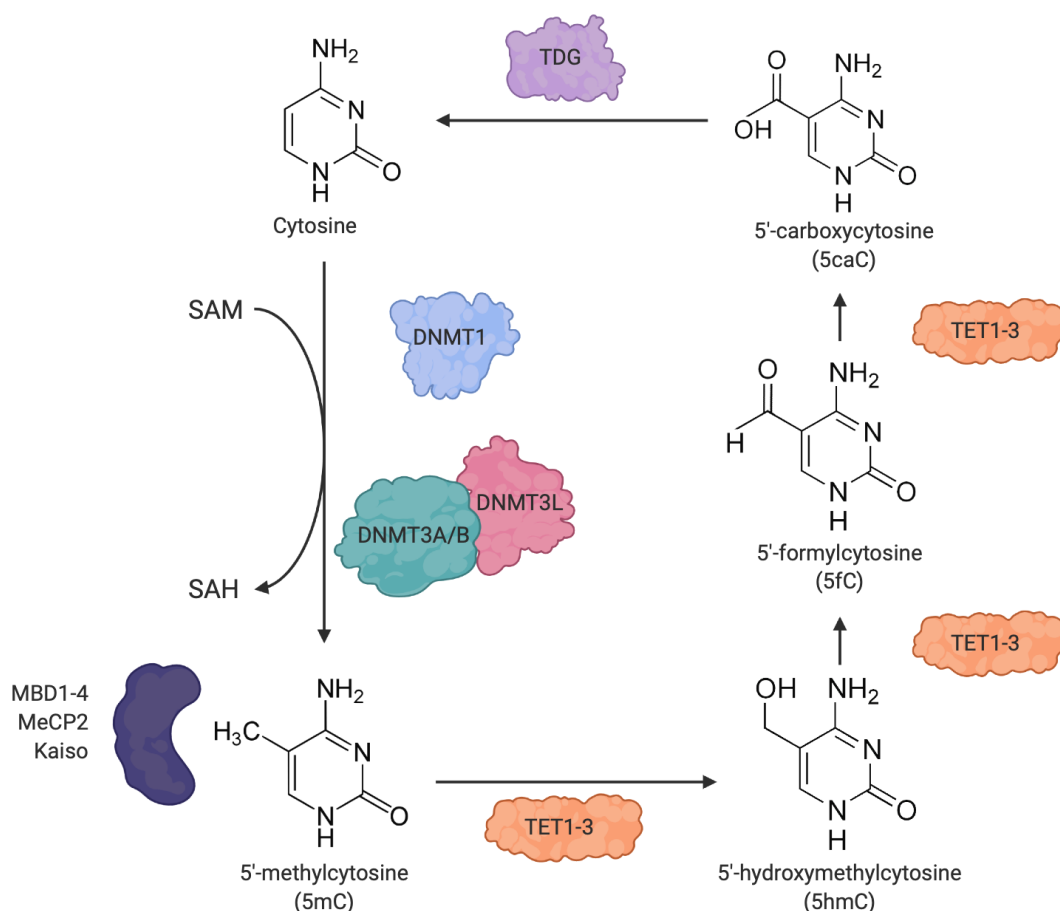
Figure 3. *Writers, readers, and erasers of DNA methylation.* 5mC is introduced *de novo* by DNMT3A/B in collaboration with DNMT3L. DNMT1 transmits the methylation pattern to newly synthesized DNA strands after replication. All DNMTs use SAM as a methyl donor. TET proteins oxidize 5mC to 5hmC, 5fC and 5caC. 5caC is excised by TDG to recover the unmethylated cytosine. 5mC serves as binding site for proteins such as MBD1-4, MeCP2, or Kaiso.

Methylation of enhancer regions is also relevant for long-distance gene expression regulation (**Figure 4B**). In fact, methylation in distal regulatory elements account for the majority of tissue-specific differentially methylated regions (Rinaldi et al., 2016). Within the gene body, DNA methylation prevents spurious RNA polymerase II (RNAPII) entry and cryptic transcription initiation (Neri et al., 2017), and affects CTCF and MeCP2 binding to modulate RNAPII elongation and facilitate alternative splicing patterns (Maunakea et al., 2013; Shukla et al., 2011); see **Figures 4C-D**.

In addition to its well-known effects on transcriptional regulation, DNA methylation is also involved in the maintenance of genomic integrity and chromosomal stability. Methylation of repetitive elements, like Alu elements, prevents their mobility and insertion in other regions of the genome (Liu et al., 1994). DNA methylation is also important for the maintenance of centromeres and controls the recombination rate in these regions (Jaco et al., 2008) as well as for the three-dimensional genomic organization of the chromatin (Buitrago et al., 2021).
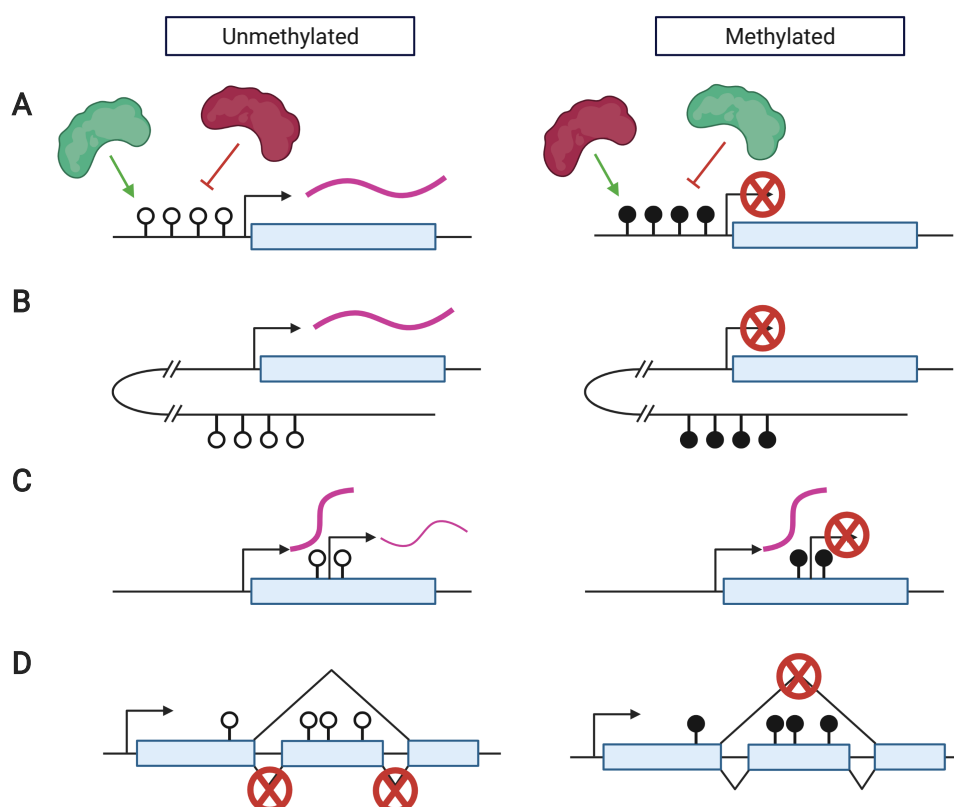
Figure 4. *Effects of DNA methylation on gene expression.* (**A**) Methylation of CpG islands in promoter regions inhibits gene expression by recruiting transcriptional repressors or by impeding transcription factor binding. (**B**) Methylation at distal regulatory regions also affects gene expression. Methylation in gene bodies (**C**) prevents spurious transcription initiation and (**D**) affects splicing patters. Black dots represent methylated CpG sites, white unmethylated cytosines are represented with white dots.

DNA methylation also exists beyond CpG dinucleotides. This is known as non-CpG methylation (Jang et al., 2017). Scientists have described methylation in CpA, CpT and CpC dinucleotides, being CpA sites the most commonly found (Ziller et al., 2011). This type of non-CpG methylation is enriched in oocytes (Guo et al., 2014), neurons and glial cells (Lister et al., 2013). Methylation in CAG and CAC occurs in embryonic stem cells and neurons, respectively (Laurent et al., 2010; Lister et al., 2013). Although non-CpG methylation frequency is very low and its function has not been elucidated yet, its presence correlates with transcriptional activity (Guo et al., 2014).

In eukaryotic cells, methylation can also be present in the 6th nitrogen of adenine to form 6mA (Heyn and Esteller, 2015; Xiao et al., 2018) It is introduced by the N^6 adenine-specific DNA methyltransferase 1 (N6AMT1) and can be removed by the AlkB homolog 1 (ALKBH1) (Xiao et al., 2018). This epigenetic mark is enriched in exon-coding regions and is associated with gene transcription activation (Xiao et al., 2018). Recently, YTH domain-containing protein 1 (YTHDC1) has been identified to be a 6mA reader that participates in chromatin organization (Woodcock et al., 2020).

Introduction

Other epigenetic mechanisms

Before the study of DNA methylation began, scientists had already acknowledged that histones played important roles in the properties of DNA and in gene expression (Allfrey et al., 1964). Histones are the small nuclear proteins that form the proteic core around which the DNA coils to form the nucleosome. Each nucleosome contains two copies of each core histone (H2A, H2B, H3 and H4) and approximately 150 bp of DNA (Lawrence et al., 2016).

Histones undergo numerous post-translational modifications. Some of them have been known for decades, such as methylation, acetylation, phosphorylation, sumoylation, ubiquitination, or ADP-ribosylation (Lawrence et al., 2016). However, more histone modifications have been discovered in the recent years, like citrullination, crotonylation, succynylation, malonylation, lactylation, or isobutyrylation (Cuthbert et al., 2004; Tan et al., 2011; Xie et al., 2012; Zhang et al., 2019; Zhu et al., 2021). All of them can take place in different positions, generating a large number of combinations that give rise to the vast complexity of the so-called "histone code" (Jenuwein and Allis, 2001).

Histone modifications are dynamic, they can be actively deposited and removed by different enzymes. Globally, these modifications influence chromatin compaction and accessibility to the transcriptional machinery, either promoting it or hampering it. Likewise, different modifications of the same residue can have opposing effects (Lawrence et al., 2016). For instance, histone acetylation reduces chromatic compaction and promotes transcription (Shogren-Knaak et al., 2006). Unlike DNA methylation, that mainly affects gene expression negatively, histone methylation effects can vary depending on the position. One clear example is trimethylation lysine residues: H3K4me3 and H3K79me3 facilitate transcription, while H3K9me3 and H4K20me3 repress it (Lawrence et al., 2016). Besides that, histone modifications also act as platforms for proteins to bind to chromatin and recruit additional ones to mediate further effects.

Nucleosomes hinder the accessibility of the replicative, transcriptional and DNA repair machineries to the DNA. Therefore, these processes usually require the repositioning of nucleosomes (Pazin et al., 1994). To overcome this situation, a group of enzymes use ATP to disrupt the interactions between DNA and histones and translocate the DNA outside of the nucleosome or eject the full nucleosome (Markert and Luger, 2020). These enzymes are called chromatin remodelers and are classified into four families: ISWI, SWI/SNF, CHD, and INO80 (Clapier et al., 2017). Chromatin remodelers are essential for the specific positioning of the nucleosomes in the genome. One example is the recruitment of SWI/SNF complex to generate a nucleosome-free region around the TSS of active promoters (Bryant et al., 2008).

Chromatin remodelers also mediate the eviction of histones from the nucleosome's octamer core to be exchanged by other histone variants (Markert and Luger, 2020). During DNA replication, canonical histones are introduced to the chromatin to form nucleosomes. However, non-canonical histone variants can replace them to perform specific functions (Buschbeck and Hake, 2017). All the variants are unique both in their sequence, timing, and function. This generates variability in nucleosome composition, structure, and stability. The deposition of certain histone variants can affect chromatin organization and gene expression (Foltz et al., 2009; Mito et al., 2005). Histone replacement can also expand the possibilities of different post-translational modifications, increasing the complexity of the histone code. In fact, this variability in histone variants is of such importance that it has been proposed to shape a nucleosome code (Bernstein and Hake, 2006).

Gene expression is not only regulated by covalent modifications and nucleosome dynamics but also by ncRNAs, which are transcribed from genomic DNA but are not translated into proteins. They can be divided into two categories: ncRNA with structural functions like transfer RNAs (tRNAs) or ribosomal RNAs (rRNAs), or ncRNA with regulatory functions such as microRNAs (miRNAs), small interfering RNAs (siRNAs) or long non-coding RNAs (lncRNAs) (Wei et al., 2017). Regulatory ncRNA comprises a very heterogeneous group of molecules with specific functions and properties that significantly contribute to gene expression regulation at various levels: from maintaining an open or closed chromatin conformation (Chu et al., 2011) to post-transcriptional gene silencing (Loewer et al., 2010; Mercer et al., 2010).

The substantial advances in the research of these mechanisms using high-throughput technologies uncovered an intricate crosstalk among different epigenetic layers. Histone variants and nucleosome positioning can influence DNA methylation patterns (Chodavarapu et al., 2010; Zilberman et al., 2008), while 5mC can recruit chromatin remodeling complexes (Harikrishnan et al., 2005). Methylation of DNA can guide and can be guided by histone modifications. For instance, MeCP2 can recruit the histone methyltransferase Suv39h1/2 to trimethylate H3K9 position (Fuks et al., 2003). H3K9 trimethylation in heterochromatic regions can recruit DNMT3A/B (Lehnertz et al., 2003). Conversely, H3K4 trimethylation at gene promoters repels *de novo* DNA methylation at CpG islands (Otani et al., 2009). DNA methylation can play regulatory roles in ncRNA expression (Diaz-Lagares et al., 2016), while ncRNA can also direct DNMT to chromatin (Wang et al., 2015).

Despite the growing knowledge on the different epigenetic layers and their participation in gene expression regulation, the real degree of interaction between epigenetic mechanisms is not completely understood yet.

Introduction

DNA methylation defects in cancer and their clinical exploit

The epigenetics field has witnessed a colossal expansion since its introduction in the early 1940s. Over the last decades, many scientists have claimed that the strict regulation of the epigenetic landscape of a cell and its effects on gene expression are crucial for many biological processes such as development or aging. The importance of these mechanisms in cell physiology is emphasized by the observation of epigenetic defects in pathologies like neurodegenerative disorders or cancer (Berdasco and Esteller, 2019).

The epigenetic landscape of a tumor cell is characterized by low levels of global DNA methylation compared to a normal cell from the healthy tissue of origin (Feinberg and Vogelstein, 1983a). This hypomethylation entails a source of chromosomal instability, since the lack of methylation in transposable elements facilitates their translocation and insertion in other genomic regions, potentially disrupting other genes and introducing mutations (Bestor, 2005; Karpf and Matsui, 2005). Another effect of DNA hypomethylation in cancer cells is the activation of oncogenes that are normally silent in healthy cells due to promoter CpG island hypermethylation (Feinberg and Vogelstein, 1983b; Wu et al., 2005).

Global genomic hypomethylation in cancer cells is accompanied by focal hypermethylation of CpG islands located at promoters of tumor suppressor genes. This event was reported for the first time as a mechanism to inactivate the expression of retinoblastoma (Rb) suppressor gene (Greger et al., 1989). Since then, numerous examples of promoter hypermethylation-associated silencing of coding and non-coding genes have been described in cancer cells (Ortiz-Barahona et al., 2020). The epigenetic inactivation of these genes supports the acquisition of the malignant features listed in the hallmarks of cancer (Ortiz-Barahona et al., 2020). It is estimated that cancer-related hypermethylation affects between 5 and 10% of the gene promoters containing CpG islands, being more frequent than genetic alterations (Ortiz-Barahona et al., 2020). Tumor cells also undergo focal methylation shifts in distal regulatory elements that provoke further effects in gene expression (Aran et al., 2013; Heyn et al., 2016). Alterations in methylation levels at enhancers and silencers disrupt chromatin three-dimensional architecture by affecting protein binding to chromatin and favoring genomic rearrangements to promote oncogenic gene expression (Valton and Dekker, 2016). Methylation in internal CpG sites can affect the use of alternative TSS and alternative splicing to yield different transcripts (Sun et al., 2020; Vizoso et al., 2015).

The cancer-associated perturbed DNA methylation signatures may originate from defects in methylation and demethylation machinery. In fact, DNMTs are frequently mutated in various types of cancer (Han et al., 2019). It is proposed that the focal hypermethylation is randomly

generated, and those alterations conferring advantages to the proliferating cell are further selected to drive the evolution of the fittest cancer cell clones (Russo et al., 2021). Therefore, it is not surprising that genes that are often mutated in a given type of cancer may also undergo promoter hypermethylation-guided silencing in that same tumor, like Rb in retinoblastoma (Gelli et al., 2019). Because of this, epigenetic gene inactivation could satisfy the widely known Knudson's two-hit hypothesis required for tumor suppressor loss (Esteller, 2008).

Epigenetic changes associated to cancer cells can be translated into clinics as potential biomarkers for cancer diagnosis, prognosis, and therapy selection. Because laborious techniques cannot be easily incorporated into the clinical practice and thus can only be used for research, the detection of CpG at specific loci constitutes the most successful epigenetic biomarker so far (Berdasco and Esteller, 2019). Epigenetic biomarkers are highly attractive in the clinical perspective because they are more stable than other RNA-based tests and they do not require special handling (Berdasco and Esteller, 2019). In addition to the primary tumor, DNA methylation is also stable in samples that are commonly used in the medical practice: cancer-specific DNA methylation patterns can be identified in easy-to-obtain, non-invasive samples like blood, urine, and saliva. Detection of cancer-derived epigenetic alterations in these samples has allowed the development of tests for early cancer diagnosis and for detection of minimal residual disease (Lianidou, 2021).

Each tumor type displays a DNA hypermethylome that characterizes it (Costello et al., 2000). This epigenetic specificity can be exploited from a clinical standpoint and be used for tumor classification and stratification. Particularly, the tumor DNA methylation profile has been of great use in the diagnosis of cancers of unknown origin and brain metastases, since the identification of the primary tumor site notably improves patients' outcome (Liu et al., 2021a; Moran et al., 2016).

The epigenetic silencing of some genes provides new opportunities for synthetic lethality strategies for cancer treatment. Numerous studies associate the promoter methylation status of some genes with differential drug response. This can be of high interest for personalized medicine because aberrant DNA methylation can serve as a biomarker for treatment response (Ortiz-Barahona et al., 2020). The most successful example is the hypermethylation of the O^6-methylguanine-DNA methyltransferase (MGMT), which renders tumors sensitive to the alkylating agents that are commonly used in chemotherapy such as temozolomide or dacarbazine (Esteller et al., 2000). Another noteworthy example that has been recently explored in clinical trials is the methylation status of the breast and ovarian cancer susceptibility gene 1 (BRCA1) in the response to poly(ADP-ribose) polymerase (PARP) inhibitors in patients with breast and ovarian cancer (Eikesdal et al., 2021; Swisher et al., 2021).

Introduction

Translational epigenetics is also reflected in epigenetic-based therapies, or epidrugs, consisting of small-molecule inhibitors that target the epigenetic machinery. The DNMT inhibitors 5-azacytidine and decitabine reached in the market in 2004 and 2006, respectively, and are currently used to treat hematological malignancies, like myelodysplastic syndrome (Berdasco and Esteller, 2019).

Despite the countless examples of possible epigenetic biomarkers and the approval of a few epidrugs in the clinical practice, many challenges remain. The use 5-azacytidine and decitabine present various limitations, hence new DNMT inhibitors are being developed. Other molecules are in preclinical or clinical studies, either as stand-alone agents or in combination with other non-epigenetic treatment options (Berdasco and Esteller, 2019). Moreover, the lack of locus specificity of the demethylating agents is the weak point of these drugs because they can re-activate silenced genes that can be detrimental for the patient (Cheishvili et al., 2015). Scientists have attempted different mechanisms to guide the epigenetic machinery to specific loci, like the use of RNA molecules to direct DNTM3A/B (Holz-Schietinger and Reich, 2012) or the development of an epigenome editing system based on the CRISPR/Cas9 system that uses a nuclease-dead Cas9 fused to an epigenomic enzyme that is directed to a specific locus by a guide RNA (Sgro and Blancafort, 2020).

Tumor-associated epigenetic alterations are not completely understood yet. However, DNA methylation profiles can provide reliable information about cancer status and the most probable clinical outcome, and help in the selection of the most suitable therapy for each patient. But the road from preclinical observations to a final clinical application is long and winding. Currently, the US Food and Drug Administration (FDA) and the European Medicine Agency (EMA) have already approved the use of a few DNA methylation-based biomarkers for cancer in vitro diagnosis, such as blood-based tests that evaluate Septin 9 (SEPT9) in the diagnosis of colorectal cancer and hepatocellular carcinoma (Kotoh et al., 2020; Song et al., 2017).

The number of proposed potential epigenetic biomarkers with apparent clinical relevance has rapidly increased in the last decades. While many of them are still under preclinical studies, some are already in clinical trials to measure their suitability for cancer diagnosis and classification (Berdasco and Esteller, 2019). Future research will probably overcome the current limitations of clinical epigenetics so that translational oncology and personalized medicine can benefit from epigenetic biomarkers for early, non-invasive cancer diagnosis as well as for treatment predictors to improve the patient's survival and reduce therapeutic costs.

tRNA biology

Hoagland and colleagues (1958) first described tRNAs as "a soluble RNA intermediate in protein synthesis". These molecules act as adaptors between the information encoded in the messenger RNA (mRNA) and the polypeptide that is being synthesized, bringing to the ribosome the amino acid specified by the mRNA codons and allowing translation. For many years, scientists had considered tRNAs as simple, housekeeping molecules without any additional regulatory function, but increasing evidence on the intricacy of tRNA biology have proven that this initial misconception was far from true. In reality, tRNA biology is much more complex than it was initially believed and tRNA defects take active part in pathological processes like neurodegeneration or cancer (Berg and Brandl, 2021; Lant et al., 2019).

tRNA sequence and structure

The first tRNA sequence was determined in 1965, and corresponded to the 77 nucleotides of the yeast tRNA[Ala] (Holley et al., 1965). The overall length of a tRNA varies from 76 to 90 bases (Sharp et al., 1985). This sequence presents internal base pairing generating stem-loop patterns that result in a characteristic and very conserved secondary structure resembling a cloverleaf (Holley et al., 1965); see **Figure 5A**. Starting from the 5' end, these stem-loop structures are named acceptor stem, D arm, anticodon stem, variable loop, and T arm, respectively. The tRNA culminates at its 3' end with a CCA trinucleotide where the amino acids are covalently attached (Deutscher, 1973). The base preceding the CCA trinucleotide is called discriminator base, and participates in the aminoacylation specificity (Crothers et al., 1972).

The cloverleaf secondary structure is folded into an L-shaped three-dimensional structure because of intramolecular interactions between the D and T arms (Shi and Moore, 2000); see **Figure 5B**. This L-shaped structure presents two branches: the acceptor domain and the anticodon domain (Kim et al., 1974). The region where D and T arms meet is termed the elbow (Zhang and Ferré-D'amaré, 2016). This structure is also well conserved across organisms, although there are some exceptions like the existence of some mitochondrial tRNA (mt-tRNA) lacking one or both D and T arms (de Bruijn et al., 1980).

The tRNA sequence has a standard numbering system, beginning with position 1 at the 5' end that pairs with base 72 at the 3' end (Sprinzl et al., 1996). The discriminator base is found at position 73, followed by the terminal 3' CCA in position 74, 75 and 76. The anticodon positions are the 34, 35 and 36. The variable loop commences at positions 44 and 45, and finishes with the bases 46, 47 and 48.

Introduction
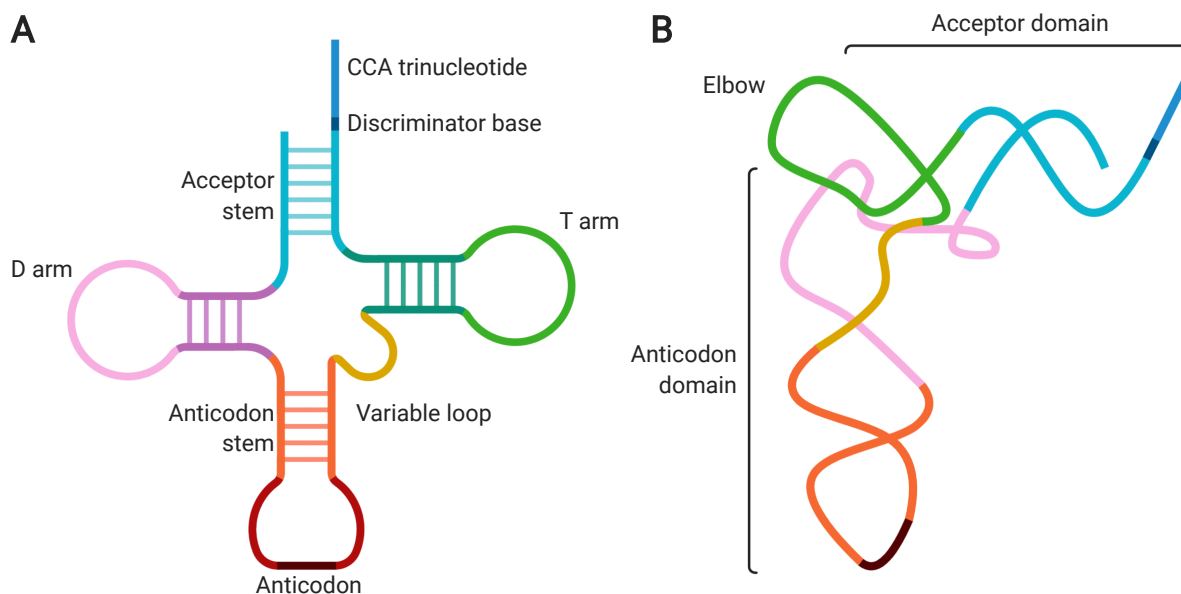
Figure 5. *Secondary and tertiary tRNA structure diagrams.* (**A**) Cloverleaf-shaped secondary structure of the tRNA molecule. (**B**) Tertiary L-shaped structure of a tRNA.

Because of the degeneracy of the genetic code, most amino acids are encoded by more than one codon. In these cases, various tRNA with different anticodon sequences can decode the same amino acid. These tRNA with different anticodons that decode the same amino acid are called isoacceptors. In higher eukaryotes, tRNA sequences present sequence variations beyond the anticodon, generating various isodecoder species for each isoacceptor (Berg and Brandl, 2021). Considering all the cytoplasmic human tRNA for the 20 proteinogenic amino acids and for selenocysteine, a total sum of 254 high confidence isodecoders are associated with 48 different isoacceptor tRNA molecules according to the GRCh37/hg19 version of the human genome (Chan and Lowe, 2016). The numbers of tRNA isoacceptors and isodecoders per amino acid are provided in **Table 1**.

Amino acid	Ala	Arg	Asn	Asp	Cys	Gln	Glu	Gly	His	Ile	Leu
Isoacceptors	3	5	1	1	1	2	2	3	1	3	5
Isodecoders	27	20	12	3	23	11	6	12	2	13	19
Amino acid	Lys	Met	Met$_i$	Phe	Pro	Sec	Ser	Thr	Trp	Tyr	Val
Isoacceptors	2	1	1	1	3	1	4	3	1	1	3
Isodecoders	19	7	2	6	7	1	18	17	5	9	15

Table 1. *Number of cytoplasmic tRNA isoacceptor and isodecoders in human cells.* For each amino acid, the number of cytoplasmatc isoacceptor tRNA species and the total sum of isodecoders for all the isoacceptors are provided. Data obtained from GtRNAdb (Chan & Lowe, 2016) for the GRCh37/hg19 version of the human genome. mt-tRNA are not included in this table.

Biogenesis and processing of tRNA

tRNAs are synthesized as a precursor species (pre-tRNA) that must undergo various processing steps to generate the functional and mature molecule (**Figure 6**). Some steps in tRNA processing are shared among all tRNAs, including transcription, 5' header and 3' trailer removal, CCA addition, and nuclear export. Splicing, nucleoside modification, and amino-acylation are specific to certain tRNA (Berg and Brandl, 2021). Because these processing steps and the proteins involved in them vary among species, the following pages will mainly focus on the particularities of cytosolic tRNA biogenesis and processing in higher eukaryotes.
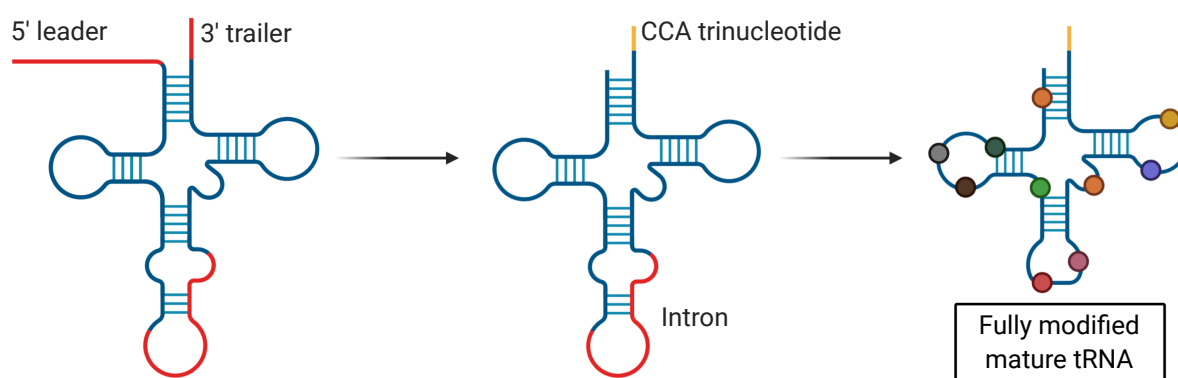
Figure 6. *General overview of pre-tRNA processing.* pre-tRNA processing consists of the removal of the 5' leader and 3' trailer sequences after transcription, the addition of the terminal CCA, intron splicing, and the chemical modification of specific nucleosides.

tRNA transcription and its regulation

In eukaryotes, the RNA polymerase III (RNAPIII) transcribes the nuclear tRNA genes (tDNA) to generate cytosolic tRNA pool (**Figure 7**). First, the hexameric general transcription factor 3C (TFIIIC) binds to the internal promoter of the tDNA, a type II promoter for RNAPIII composed of two sequences known as the A and B boxes (Galli et al., 1981; Schramm and Hernandez, 2002). Once bound, TFIIIC recruits the general transcription factor 3B (TFIIIB) at the 5' edge of the tDNA (Bieker et al., 1985). Then, TFIIIB recruits the RNAPIII and participates in tDNA promoter melting to permit transcription initiation (Kassavetis et al., 2001). Transcription termination occurs at a poly-T tract located in the non-template strand (Arimbasseri and Maraia, 2015). The retention of TFIIIB and TFIIIC to the tDNA facilitates transcription re-initiation by recycling the RNAPIII machinery (Dieci and Sentenac, 1996).

Introduction
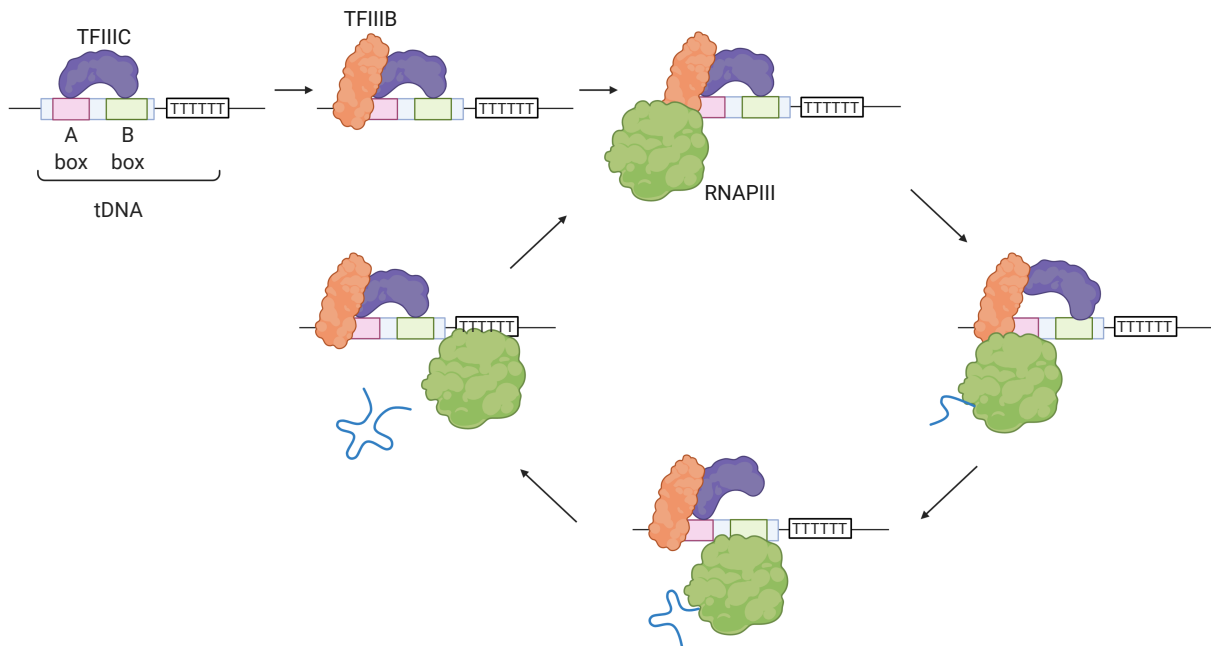
Figure 7. *tRNA transcription overview.* tRNA transcription starts with the binding of TFIIIC to the internal tDNA promoter followed by the recruitment of TFIIIB and RNAPIII. Termination occurs at a stretch of thymine residues. Then, RNAPIII is recycled to allow transcriptional re-initiation. Adapted from Berg and Brandl, 2021.

RNAPIII-mediated transcription is regulated in response to changing environmental conditions to adapt to the cellular needs. This is mainly achieved by mechanisms that control its general transcription factors (Graczyk et al., 2018). In this regard, the expression and phosphorylation status of TFIIIB and TFIIIC are regulated in response to growth and stressful conditions to affect RNAPIII activity (Chymkowitch and Enserink, 2018).

Trans-acting factors targeting TFIIIB interaction with TFIIIC or DNA can also repress RNAPIII-mediated transcription (Graczyk et al., 2018); see **Figure 8**. One example is the dimer composed by DR1 and DR1-associated protein 1 (DRAP1), which hampers TFIIIB assembly (Kantidakis et al., 2010). MAF1 is the best characterized RNAPIII transcriptional repressor. It binds to RNAPIII, hinders its interaction with TFIIIB, and rearranges its conformation to prevent transcription initiation (Desai et al., 2005; Orioli et al., 2016). Many signaling pathways modulate MAF1 activity by controlling its phosphorylation status to mediate further effects on RNAPIII transcription. Under favorable growth conditions, casein kinase 2 (CK2), cAMP-dependent protein kinase A (PKA), and the mammalian target of rapamycin complex 1 (mTORC1) phosphorylate MAF1 to inhibit its repressive activity and allow transcription. Under stressful or unfavorable conditions, protein phosphatases 4 and 2A (PP4 and PP2A) dephosphorylate MAF1 to activate it and repress transcription (Graczyk et al., 2018).

26
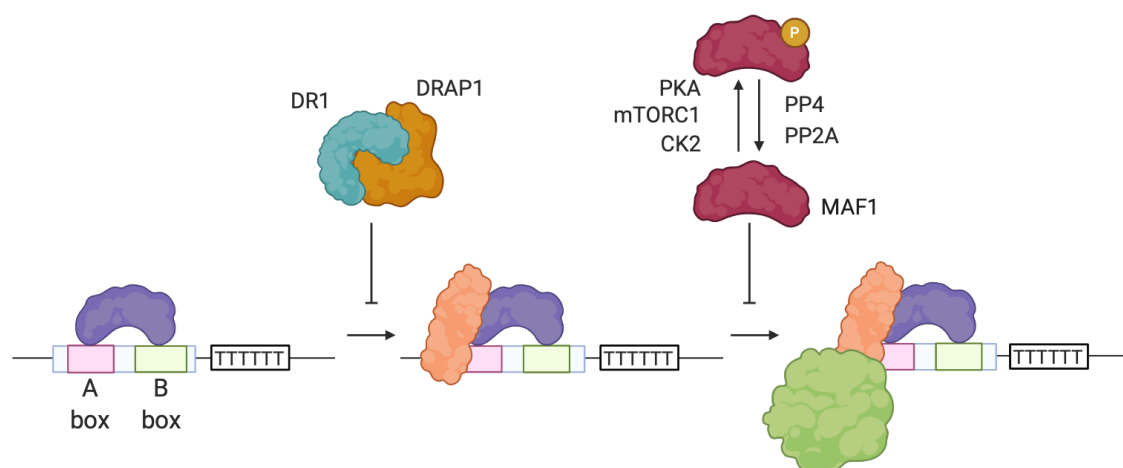
Figure 8. *Regulation of RNAPIII-mediated transcription by trans-acting factors.* TFIIIB assembly is inhibited by the dimer composed of DR1 and DRAP1. Dephosphorylation of MAF1 prevents RNAPIII transcription initiation.

The human nuclear genome contains more than 400 high confidence tDNA genes (Chan and Lowe, 2016). The emergence of novel high-throughput sequencing techniques capable of discerning small RNAs with similar sequences have shown that not all tRNAs are equally abundant among cell types and not all tDNA are uniformly transcribed (Gogakos et al., 2017; Sagi et al., 2016; Torres, 2019). Plus, tRNA repertoire is not static; it varies in response to various stimuli and has profound effects over protein synthesis, thereby affecting cellular physiology (Rak et al., 2018).

Such specificity in RNAPIII transcription cannot be explained by its apparently simple regulation mediated by the above-mentioned means, thus additional control mechanisms are required. tDNA positioning in terms of three-dimensional organization of the chromatin can influence transcription rates (Van Bortle et al., 2017). Other reports indicate that tDNA transcription can be epigenetically regulated by histone marks and nucleosome positioning (Good et al., 2013; Park et al., 2017). Studies regarding DNA methylation at tDNA loci are scarce, but it has been described that it can hamper TFIIIC binding to DNA (Bartke et al., 2010) and inhibit tRNA transcription in vitro (Besser et al., 1990). Moreover, interferences of the RNAPIII with RNAPII can also modulate tRNA expression. This was first proposed when chromatin immunoprecipitation (ChIP)-seq data revealed that RNAPII and RNAPIII colocalized in the genome (Oler et al., 2010), and it was further supported with the evidence that elongating RNAPII negatively affected the RNAPIII-mediated transcription of neighboring genes (Gerber et al., 2020). Another study revealed that RNAPII transcription factors can bind to some tDNA and modulate RNAPIII recruitment and impact their transcription (Yang et al., 2020). In conclusion, more studies are needed to completely elucidate the mechanisms governing the specificity of tDNA transcription.

Introduction

tRNA-ends processing

Pre-tRNAs contain 5'-leader and 3'-trailer sequences of variable length that must be removed (Berg and Brandl, 2021); see **Figue 9**. After pre-tRNA transcription, a La protein binds to the poly-uridine tract of the 3'-trailer sequence, protecting it from exonucleases and promoting the 5' processing in the first place (Yoo and Wolin, 1997). The 5'-leader removal is mediated by the ribonuclease P (RNase P) complex. Human nuclear RNase P is composed by one ncRNA named RPPH1 and ten proteins (Jarrous, 2017). Then, the ElaC ribonuclease Z 2 (ELAC2) cleaves the pre-tRNA after the discriminator base to remove the 3'-trailer (Schiffer et al., 2002).

Although this 5'-before-3' cleavage is the major pre-tRNA ends-processing pathway, this order can be reversed in absence of La protein (Berg and Brandl, 2021). In this scenario, the 3'-end of the pre-tRNA is unprotected, and other nucleases can process it. For instance, the RNA exonuclease 1 homolog (REXO1) can eliminate the 3'-trailer sequence prior to the 5'-end processing by RNase P (Copela et al., 2008).

Independently of the cleavage path followed, tRNA-end processing concludes with the addition of the CCA trinucleotide to the 3'-end of the molecule by the tRNA nucleotidyl transferase 1 (TRNT1) (Sprinzl and Cramer, 1979). Additionally, some tRNAs present particularities in their ends processing. One remarkable example is the 3'-5' addition of a guanosine nucleoside at the 5'-end of tRNA^{His} catalyzed by the tRNA-histidine guanylyltransferase 1 like (THG1L) (Cooley et al., 1982).
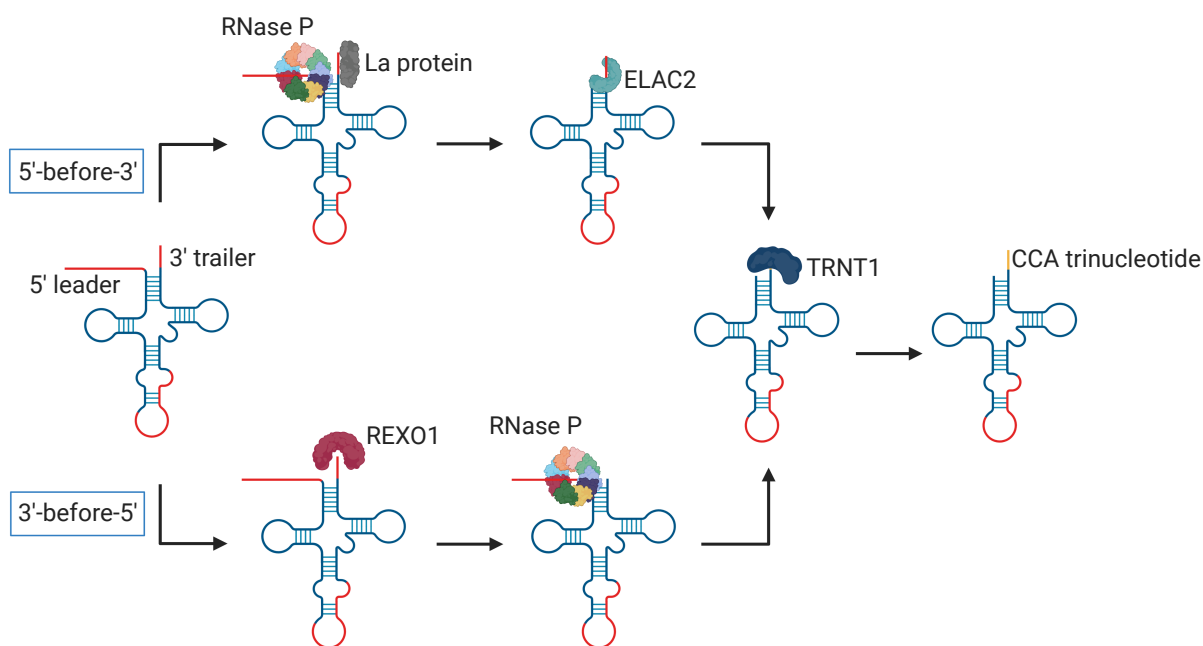
Figure 9. *tRNA-ends processing summary.* In mammals, the most prevalent pre-tRNA ends-processing mechanism is the 5'-before-3' process, where the RNase P eliminates the 5' end of the molecule before the 3' trailer is removed by ELAC2. Alternatively, the 3' end can be processed before the 5' end. tRNA-ends processing culminates with the CCA addition to the 3' end of the molecule.

tRNA introns and splicing

28 human tDNAs contain introns that must be spliced to generate the functional molecule (Chan and Lowe, 2016). These introns are enzymatically removed in the nucleus, prior to their export, by a spliceosomal-independent mechanism (Berg and Brandl, 2021; Schmidt and Matera, 2020); see **Figure 10**.

First, the intron is recognized by the tRNA-splicing endonuclease complex (TSEN) composed of four subunits (Paushkin et al., 2004). The identification of the intron is based on structural features of the pre-tRNA, as introns can differ in length and sequence but not in their location after position 37. Concretely, the TSEN complex recognizes the dimensions of the pre-tRNA and cuts what would exceed the mature tRNA size. The correct positioning of the TSEN complex requires two key nucleotides known as cardinal positions. The TSEN complex-mediated pre-tRNA cleavage results in a 2'-3'-cyclic phosphate at the 5' exon and a 5'-OH at the 3'-exon (Schmidt and Matera, 2020). The resulting exons are directly ligated by the RNA 2',3'-cyclic phosphate and 5'-OH ligase RTCB (Popow et al., 2011). This reaction is facilitated by a complex composed of the DEAD-box helicase 1 (DDX1), Ashwin (ASW), Archease (ARCH or ZBTB8OS), CGI-99, and FAM98B (Popow et al., 2014). Direct ligation of tRNA exons can be inhibited by the cleavage factor polyribonucleotide kinase subunit 1 (CLP1)-mediated phosphorylation of the 5'-OH in the 3' exon, or by the resolution of the 2',3'-cyclic phosphate in the 5' exon by the Angel homolog 2 (ANGEL2) (Hayne et al., 2020; Pinto et al., 2020).
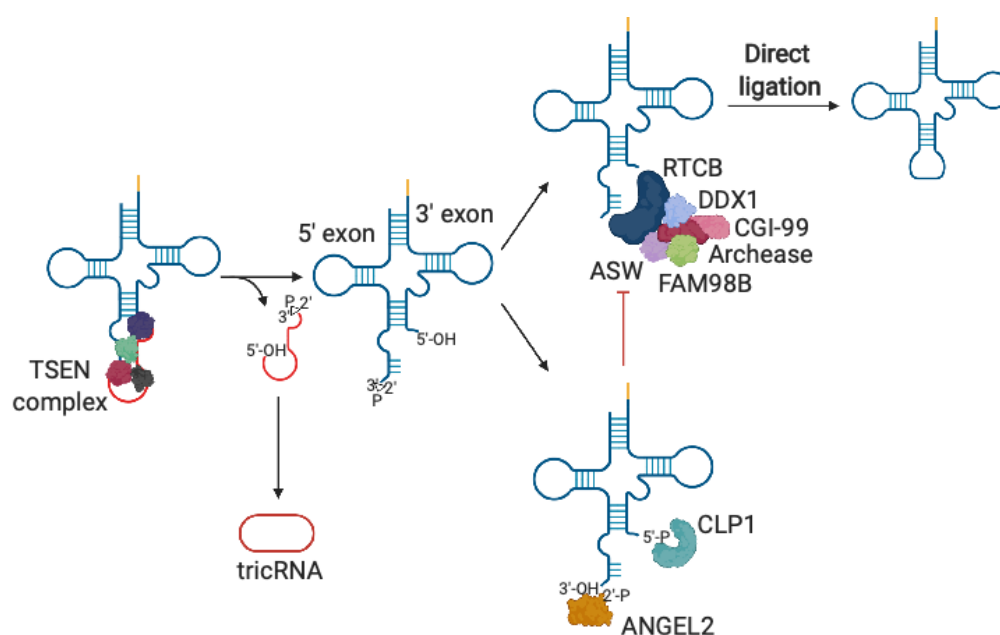
Figure 10. *pre-tRNA splicing overview.* In vertebrates, the TSEN complex recognizes the size of the immature pre-tRNA molecule and cleaves it to remove the intron. The resulting exons are directly ligated by RTCB and its assisting proteins. Direct ligation can be blocked by CLP1 or ANGEL2. The removed intron is circularized by RTCB to produce a tricRNA.

Introduction

Once excised, human tRNA introns are not discarded as waste products. Instead, they are circularized by RTCB to generate a molecule known as tRNA intronic circular RNA or tricRNA (Schmidt et al., 2019). While introns in mRNA entail a clear selective advantage that allows alternative splicing to increase proteomic diversity, the reasons underlying the presence of introns in tRNA and the functions of tricRNA remain obscure.

tRNA trafficking between nucleus and cytosol

tRNA transcription and processing occurs in the nucleus, but protein synthesis takes place in the cytosol. Therefore, tRNAs must be exported from the nucleus to participate in translation and other biological functions in the cytosol (Berg and Brandl, 2021; Chatterjee et al., 2018). In vertebrates, the primary tRNA nuclear export is mediated by various mechanisms. The best characterized nuclear exporter is the β-importin family member exportin-t (XPOT), which binds to tRNA in the nucleus in a Ran-GTP-dependent manner. Upon translocation through the nuclear pore, GTP is hydrolyzed and the tRNA is released to the cytoplasm (Kutay et al., 1998). Alternative mechanisms that can accomplish this task include the exportins 1 and 5 (XPO1 and XPO5) or the heterodimer composed by NXF1-NXT1 (Wu et al., 2015).

tRNA traffic between the nucleus and the cytosol is not a one-way process; tRNAs can be re-imported into the nucleus. This retrograde import and can be either a constitutive or a regulated process. Under certain stress conditions like nutrient deprivation or oxidative stress situation, tRNAs will be reimported to the nucleus as part of the integrated stress response (Schwenzer et al., 2019; Whitney et al., 2007). This retrograde tRNA nuclear import is mediated by the β-importin transportin 3 (TNPO3) in a Ran-GTPase-dependent manner (Murthi et al., 2010). The re-imported tRNA can be re-exported to the cytosol under favorable conditions by means that are shared with the primary export pathways (Chatterjee et al., 2018; Whitney et al., 2007).

tRNA aminoacylation

Aminoacyl-tRNA synthetases (aaRS) couple amino acids to their cognate tRNA, allowing them to serve as adaptors in translation (Berg and Brandl, 2021). tRNA aminoacylation is a two-step reaction. First, the amino acid is activated with an ATP molecule to generate an aminoacyl adenylate intermediary. Then, this activated amino acid is transferred to the 3' end of the tRNA, yielding free AMP (Gomez and Ibba, 2020). 20 different aaRS exist, one for each proteinogenic amino acid. Thus, all the isoacceptors for one amino acid compete for the same enzyme to be loaded with the correspondent amino acid (Gomez and Ibba, 2020).

tRNA recognition by the aaRS is fundamental for their correct amino acylation. All tRNA molecules display the same structural features, therefore aaRS must rely on identity elements that are specific for each tRNA (Gomez and Ibba, 2020). These identity elements include single nucleotides, nucleotide pairs, and structural motifs. The anticodon sequence or its chemical modifications can be key identity elements for many tRNA types (Commans et al., 1998; Senger et al., 1997). Other molecular particularities can act as identity elements, like the base pairing between positions 3 and 70 of the tRNA (Mcclain and Foss, 1988) or the size of the variable loop (Himeno et al., 1997). Antideterminant elements also exist to prevent the interaction between the aaRS with a noncognate tRNA (Pütz et al., 1994).

The accurate discrimination of amino acids by aaRS is also crucial for protein synthesis, since incorrect tRNA loading would provoke an amino acid misincorporation and mutations in the growing polypeptide chain. To guarantee the correct amino acid incorporation to the tRNA and ensure the highest level of fidelity in protein synthesis, some aaRS display amino acid editing mechanisms (Eldred and Schimmel, 1972). Besides the intrinsic ability of some aaRS to modify amino acids, other trans-acting proteins that target mischarged amino acids exist (Ahel et al., 2003). This is very relevant for selenocysteine charging to tRNA^{Sec}, as a SecRS does not exist. Instead, selenocysteine is formed from a serine that is loaded to tRNA^{Sec} by a series of reactions catalyzed by the o-phosphoseryl-tRNA:selenocysteinyl-tRNA synthase (Palioura et al., 2009).

tRNA surveillance and turnover

Two major tRNA surveillance pathways participate in the removal of defective precursor and mature tRNA molecules in eukaryotic cells (Berg and Brandl, 2021; Megel et al., 2015).

The nuclear surveillance pathway (**Figure 11A**) monitors aberrantly folded or un-spliced pre-tRNA in the nucleus (Megel et al., 2015; Vaňáčová et al., 2005). It involves the TRF4/AIR2/MTR4 polyadenylation (TRAMP) complex and the nuclear exosome. This complex participates in the polyadenylation at the 3' of the tRNA, which is then degraded from the 3'-end by the nuclear exosome (Kadaba et al., 2006; Megel et al., 2015).

The cytosolic surveillance pathway (**Figure 11B**), also known as rapid tRNA decay (RTD), recognizes mature tRNAs that are destabilized or that lack some nucleotide modifications, and degrades them from the 5' end (Alexandrov et al., 2006; Guy et al., 2014). In this case, the defective tRNA is marked with the addition of a second CCA triplet by TRNT1 at its 3'-end (Wilusz et al., 2011). Then, it can be eliminated in the cytosol by the exoribonuclease 1 (XRN1) or can be re-imported into the nucleus to be degraded by XRN2 (Chernyakov et al., 2008).

Introduction
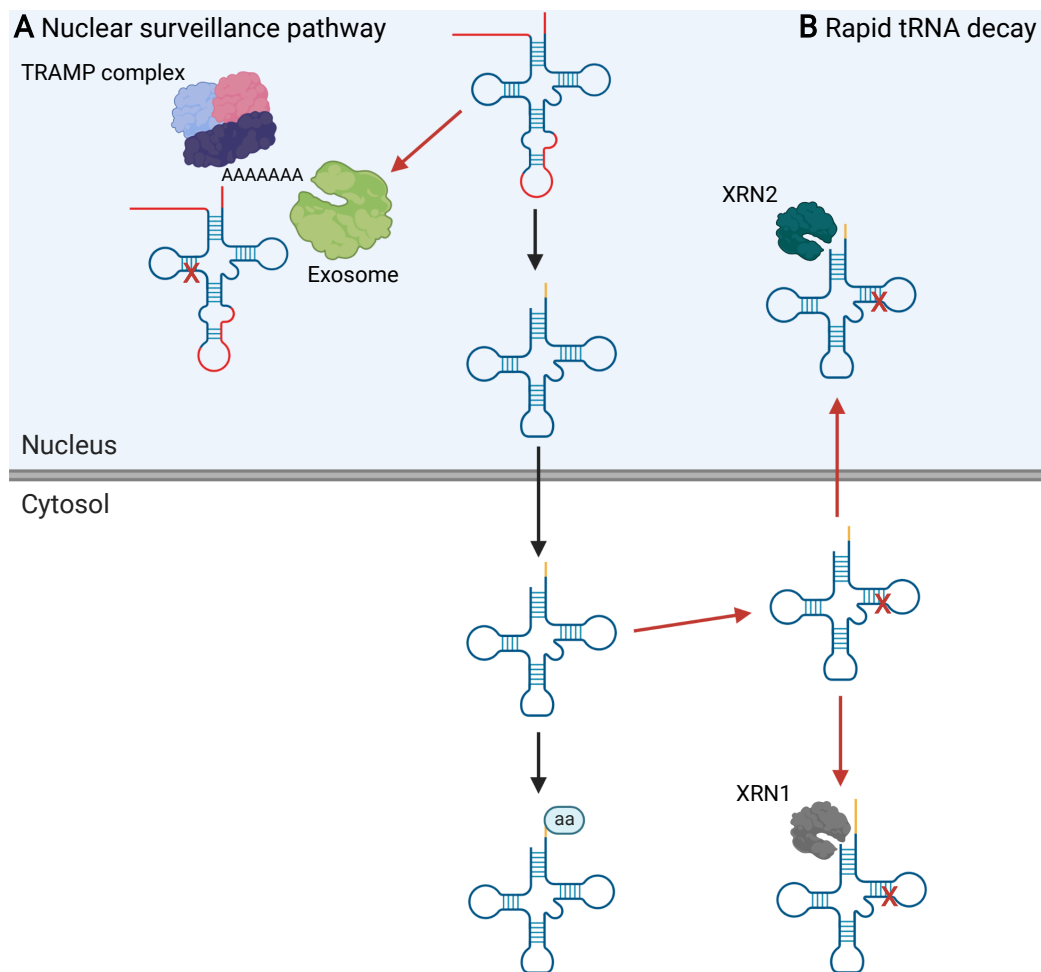
Figure 11. *Overview of the tRNA degradation mechanisms.* (**A**) The nuclear surveillance pathway primarily acts over poorly processed pre-tRNA transcripts via the TRAMP complex and the nuclear exosome. (**B**) The rapid tRNA decay targets for degradation destabilized tRNAs in the cytosol by the addition of a second CCA triplet and the activity of the cytosolic XRN1 or the nuclear XRN2.

tRNA nucleoside modifications

tRNA nucleosides undergo several modifications as a part of the molecules' post-transcriptional processing (Berg and Brandl, 2021). Some of these modifications are conserved among Bacteria, Archaea and Eukarya, while others are restricted to a few species. Despite this conservation, the enzymes that synthesize them are not evolutionary conserved –a fact that has probably delayed tRNA modification research. It is a big challenge to characterize tRNA modifications, their specific role in cell physiology, and the enzymes that participate in their deposition. However, recent developments in mass spectrometry techniques have pushed their study by facilitating the identification of novel chemical modifications. Currently, more than fifty different modifications have been described in human tRNAs (**Figure 12**), and around twelve of them can be found per tRNA molecule (Boccaletto et al., 2018; Suzuki, 2021).
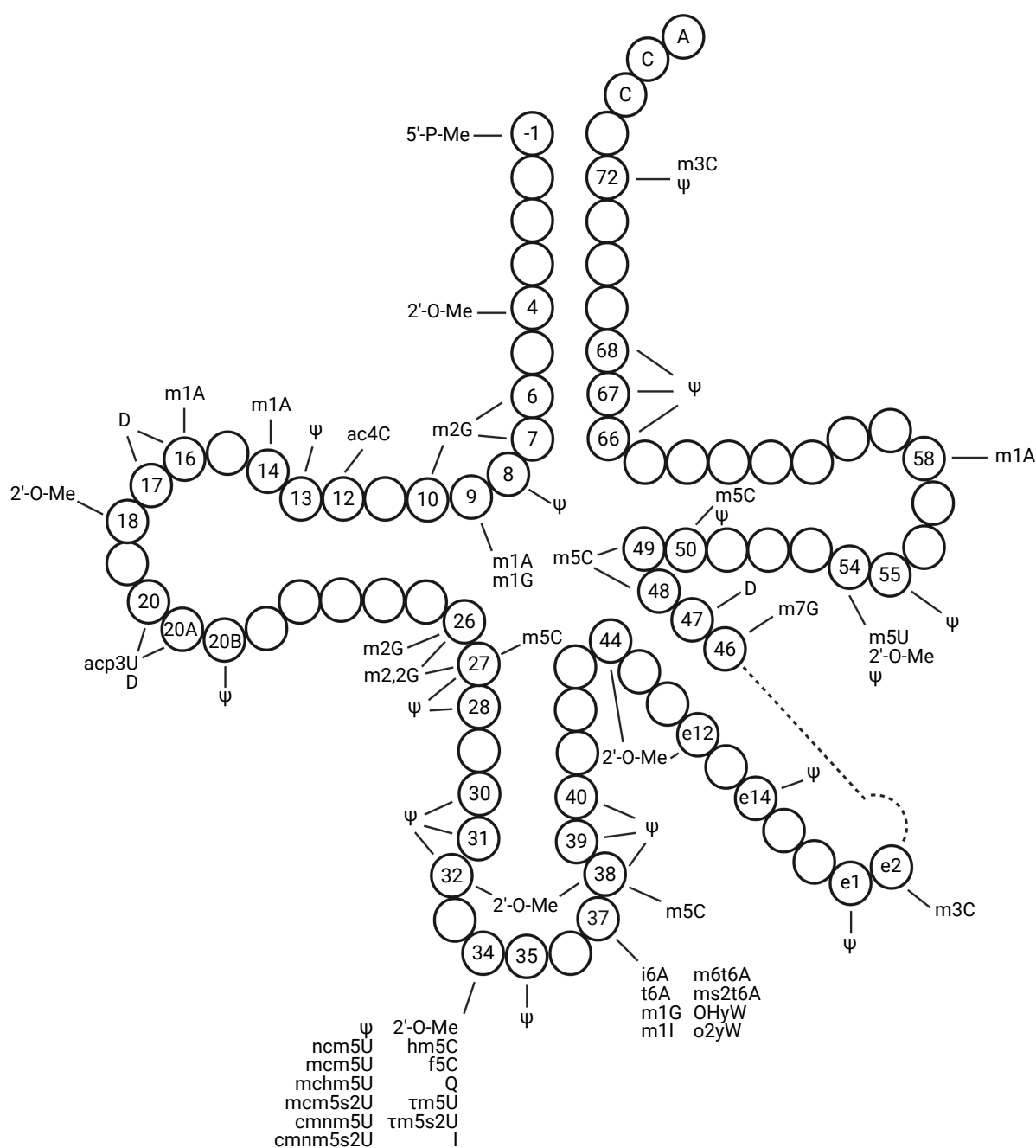
Figure 12. Integrated view of the human tRNA nucleoside modification landscape. Positions that are subjected to modification are numbered in the cloverleaf structure and the occurring modifications are indicated. Adapted from Suzuki, 2021.

tRNA cleavage and tRNA-derived small fragments

Advances in next-generation sequencing technologies allowed the discovery of novel types of small ncRNAs such as tRNA-derived small RNA fragments (tRF) (Lee et al., 2009; Su et al., 2020). tRFs constitute a novel a group of regulatory ncRNA sized between 14 and 40 nucleotides that originate from tRNA via their endonucleolytic cleavage.

Introduction

tRFs can be classified in six major groups based on the cleavage position that originates them (**Figure 13**). One of these groups consists of tRNA halves (tiRNA) derived from the cleavage of the anticodon of the mature tRNA by angiogenin (ANG). The resulting molecules are known as 5' tiRNA and 3' tiRNA (Saxena et al., 1992; Thompson et al., 2008). tRF-1 molecules arise during the pre-tRNA maturation process as a result of the removal of the 3' trailer sequence by ELAC2 (Su et al., 2020). tRF-5 and tRF-3 result from the cleavage of the D and T arms, respectively. The specific cutting site can slightly vary, originating various subtypes of different length. The ribonuclease DICER was reported to participate in their generation (Cole et al., 2009), but further analyses have demonstrated that the majority of these tRFs are produced independently of the miRNA-processing machinery (Kumar et al., 2014). Internal tRFs (i-tRFs) and tRF-2 originate from the central part of the tRNA (Su et al., 2020), yet their biogenesis is still unknown. In addition to ANG and DICER, other nucleases can act on tRNA molecules to produce fragments. Some examples are the RNase L and Schlafen 13 (SLFN13). The former generates tRNA halves to arrest protein synthesis in response to interferon signaling (Donovan et al., 2017), and the latter cleaves tRNAs between the acceptor and T stems to restrict HIV replication (Yang et al., 2018).
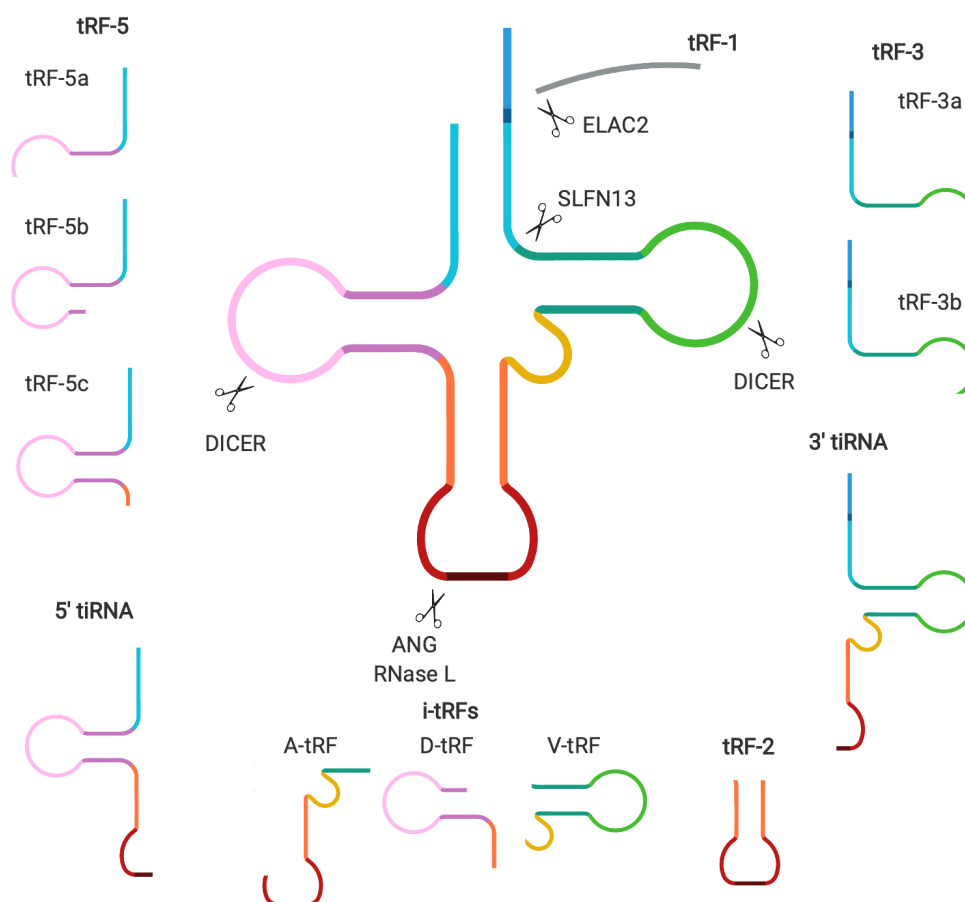
Figure 13. *Classification of tRFs according to their origin.* Types of tRF molecules and the known tRNA endonucleases cleaving sites are shown. Adapted from Su *et al.,* 2020.

tRNA functions in normal cell physiology: more than just carrying amino acids

tRNAs play a pivotal role in protein synthesis by linking the information encoded in the mRNA and the amino acids that are incorporated in the growing polypeptide chain. However, they are more than simple adaptor molecules: tRNAs and their derived fragments actively engage in protein synthesis regulation and in other molecular processes that are unrelated to translation (Rak et al., 2018).

Cytosolic tRNA repertoire modulates protein synthesis

Codon usage bias refers to the preferential use of certain synonymous codons, which can act as an additional layer of protein synthesis regulation (Liu et al., 2021b). Protein synthesis can be seen as an analogy of the supply and demand economic model. Transcripts containing the preferred codons –the demand– are more rapidly translated and highly expressed (Frumkin et al., 2018; Gardin et al., 2014), while those mRNAs with rare codons tend to be destabilized and degraded as a result of their slow translation rate (Wu et al., 2019). Codon recognition by tRNA is the rate-limiting step in protein synthesis, thus the decoding rate of a given codon is affected by the concentration of its cognate tRNA –the supply. The unequal abundance of tRNA isoacceptors markedly influences the effectivity of how synonymous codons are translated, as rare codons may take longer to be recognized by their corresponding tRNA if it is present at low concentrations (Dana and Tuller, 2014), thereby affecting the elongation rate and shaping the proteome of the cell (Rak et al., 2018). For this, codon usage bias usually correlates with the supply of the tRNA isoacceptor that decodes them (dos Reis et al., 2004).

In higher eukaryotes, tRNA isoacceptors' expression varies among human and mice tissues (Dittmar et al., 2006; Pinkard et al., 2020) in such a way that tissue-specific tRNA expression patterns mirror the codon bias of tissue-specific proteins (Dittmar et al., 2006; Hernandez-Alias et al., 2020). Also, the tRNA pools of proliferating cells are different from those of quiescent and differentiated cells, allowing the expression of different sets of proteins (Aharon-Hefetz et al., 2020; Gingold et al., 2014). Therefore, the expression of individual tRNAs must be tightly coordinated to match the specific needs of the cell at each moment.

tRNA modifications influence translation efficiency and accuracy

tRNA nucleoside modifications can be divided into two categories based on their functions: those that influence the tRNA structure and those that regulate decoding and protein synthesis

Introduction

(Jackman and Alfonzo, 2013). The first group of modifications mainly affect the hydrogen-bonding capacity of a given nucleoside, modifying its base pairing and the secondary and tertiary structure of the tRNA. For instance, pseudouridine (Ψ) and dihydrouridine (D) confer rigidity and flexibility to tRNA molecules, respectively (Motorin and Helm, 2010). The presence of 1-methyladenine (m1A) in position 9 of mt-tRNA^{Lys} disrupts a base pairing that stabilizes a non-canonical structure, thereby favoring the canonical cloverleaf secondary structure (Voigts-Hoffmann et al., 2007). The second group of modifications target the functional sites of the tRNA, including the anticodon stem or those positions that are identity elements for aminoacylation. To cite some examples, 1-methylguanine (m1G) in position 37 of yeast tRNA^{Asp} prevents its misacylation (Pütz et al., 1994) and 5-methylcytosine (m5C) in position 38 in mouse tRNA^{Asp} stimulates amino acid loading (Shanmugam et al., 2015).

Modifications at positions 34 and 37 of the tRNA are particularly important for modulating translational efficiency and accuracy (Jackman and Alfonzo, 2013). Modifications at position 34 ensure a correct codon-anticodon pairing and contribute to the stability of the interaction between the mRNA and tRNA during decoding (Agris, 2008). This nucleotide can be subjected to numerous modifications (**Figure 12**). For instance, U_{34} hypermodification affect ribosome decoding speed and protein synthesis (Nedialkova and Leidel, 2015). Modifications at position 34 can also expand or restrict the decoding capacity of the tRNA. The most prominent example of this phenomenon is adenosine deamination to inosine (I), which effectively permits a single tRNA to decode up to three different codons for the same amino acid (Crick, 1966). Modifications at position 37 contribute to the maintenance of an open loop conformation by blocking base pairing with position 33 and influencing reading frame maintenance. For example, wybutosine (yW) derivatives in tRNA^{Phe} prevent -1 ribosome frameshifting by stabilizing codon-anticodon interactions and ensure proper maintenance of the reading frame in slippery sequences (Carlson et al., 1999; Konevega et al., 2004).

The above-mentioned examples represent just the top of the iceberg of the repertoire and functions of tRNA modifications. Clearly, more research is needed to entirely understand how tRNA modifications participate in normal cell functions.

tRFs mediate diverse cellular functions

tRFs participate in cellular functions that are mainly related, but not exclusively, to protein synthesis. Some tRFs have a miRNA-like role on the regulation of translation because they can associate with P-element induced wimpy testis (PIWI) and Argonaute (AGO) proteins in RNA-induced silencing complexes (RISC) together with a target mRNA (Kuscu et al., 2018;

Zhang et al., 2016). In fact, 270 human tRFs have been predicted to participate in more than 150 million interactions with putative target transcripts (Li et al., 2021). Other tRFs interact with RNA-binding proteins and prevent their binding to other RNAs (Boskovic et al., 2020; Goodarzi et al., 2015). tRFs also participate in the silencing of transposable elements (Schorn et al., 2017) or as donors for protein post-translational modifications (Avcilar-Kucukgoze et al., 2020).

Although the current understanding of tRF function is limited to a few molecules, future advances in research methodological approaches will hopefully expand our knowledge on this new species of ncRNA as epigenetic regulators of gene expression.

tRNAs modulate translation in response to stress

Available tRNAs are a limiting factor for protein synthesis, thus diverse post-transcriptional regulatory mechanisms are combined to fine tune tRNA availability and aminoacylation. Various stress conditions that affect cellular viability can alter tRNA pools through the dynamic control of their transcription and subsequent processing steps, including modification and cleavage (**Figure 14**). At the end, this will modulate mRNA translation, reshape the proteome of the cell, and determine the response to a given cellular condition (Rak et al., 2018).

Increased translational fidelity correlates with a decreased protein yield, hence the need of a balance between protein synthesis speed and accuracy. Translational miscoding refers to the mechanism by which codons at mRNA are non-canonically decoded by tRNAs, leading to the insertion of an amino acid that is not encoded in the transcript (Wohlgemuth et al., 2010). This event was initially regarded as aberrant, but it has been recently acknowledged to serve as an adaptive mechanism. There are diverse examples of this tRNA-dependent adaptive mistranslation. For example, in response to reactive oxygen species, the extracellular signal-related kinases 1 and 2 (ERK1/2) phosphorylate MetRS to promote the misacylation of approximately 1% of all tRNAs in HeLa cells with methionine, increasing the incorporation of this amino acid into the newly synthesized proteins to enhance survival (Lee et al., 2014; Netzer et al., 2009).

Upon oxidative stress, ANG dissociates from its inhibitor and translocates from the nucleus to the cytosol to cleave tRNAs and inhibit translation (Yamasaki et al., 2009). ANG can also cleave the CCA sequence at the 3' end of the tRNA to deactivate tRNAs and rapidly repress protein synthesis (Czech et al., 2013). Oxidative stress can also trigger tRNA fragmentation in an ANG-independent manner to deplete the cellular tRNA pool of specific molecules and modulate protein synthesis of specific transcripts (Huh et al., 2021).

Introduction
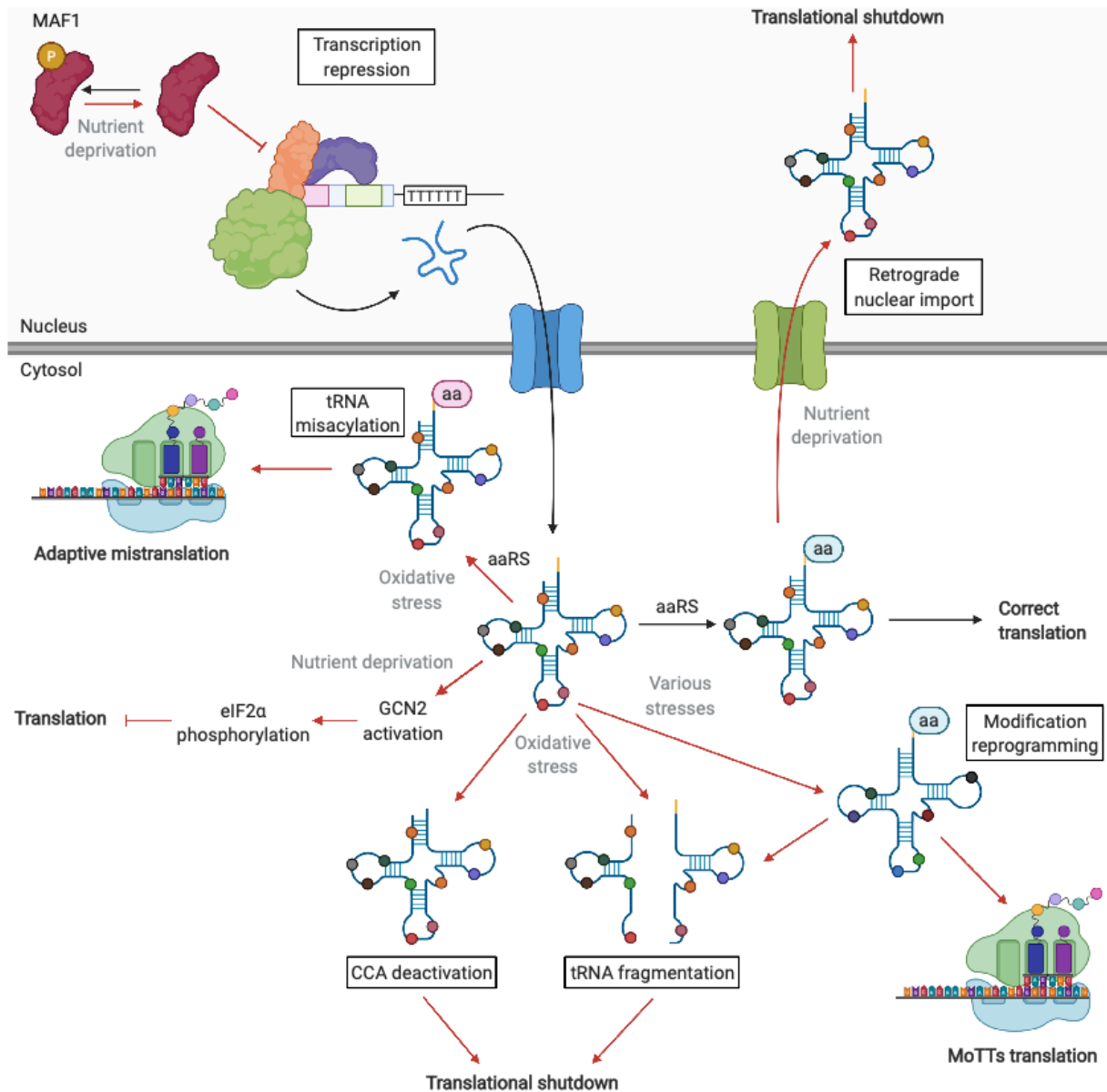
Figure 14. *Stress-induced dynamics of tRNA-related processes.* Normal tRNA metabolism and function is represented with black arrows; red arrows indicate stress-related tRNA processes. Upon nutrient starvation, MAF1 dephosphorylation reduces tDNA transcription by RNAPIII and promotes the nuclear retrograde import. The accumulation of uncharged tRNAs leads to translation repression through the phosphorylation of eIF2α. Oxidative stress promotes tRNA deactivation by CCA removal and tRNA fragmentation to reduce protein synthesis in a global or in a transcript-dependent manner. tRNA misacylation derived from oxidative stress drives adaptive mistranslation. tRNA modifications can be reprogrammed upon different cellular stresses to influence codon usage patterns and MoTTs translation or to induce tRNA destabilization and cleavage.

Under nutrient deprivation, the eIF2α kinase 4 (GCN2) phosphorylates the eIF2α at Ser51 to reduce global translation as a response to the accumulation of uncharged tRNAs (Zaborske et al., 2009). The nuclear import of certain tRNAs upon nutrient deprivation also contributes to this translational shut-down (Whitney et al., 2007). In this situation, the inhibition of mTORC1 facilitates MAF1 dephosphorylation and repression of RNAPIII to stop the synthesis of new

tRNAs (Wei et al., 2009). The repressive effects of MAF1 vary among tDNA genes, as a subset of tDNAs are unresponsive to MAF1 transcription inhibition (Turowski et al., 2016).

tRNA modification landscape is also reprogrammed under various cellular stress conditions (Chan et al., 2010; Wilusz, 2015). This can induce tRNA destabilization and cleavage, provoking further effects over protein synthesis (Rashad et al., 2020). Parallelly, translational fidelity is notably influenced by nucleoside modifications in positions 34 and 37 of the anticodon stem (Gu et al., 2014), therefore the stress-specific reprogramming of tRNA wobble base modification status will promote the selective translation of mRNAs that are critical for the response against that situation (Chan et al., 2015). These transcripts that use specific degenerate codons and whose expression can be affected by tRNA modification levels are known as modification-tunable transcripts (MoTTs), and normally encode critical stress response proteins (Endres et al., 2015; Gu et al., 2014).

Cancer-associated defects in tRNA biology

In the recent years, growing evidence exposed that tRNAs, their derived fragments, and the proteins involved in their bioprocessing are altered in tumoral cells (Santos et al., 2019). tRNA imbalance in cancer has been overlooked for many years due to the misconception of tRNAs as housekeeping molecules, but the latest advances in tRNA biology have irrefutably linked these molecules to tumor biology and postulate that they can no longer be considered passive bystanders in malignant transformation anymore (Santos et al., 2019). The details of the molecular mechanisms that orchestrate these aberrancies are still poorly known, thus a deeper understanding of cancer-associated tRNA imbalance will probably become useful from a clinical standpoint (Zeng et al., 2020).

tRNA expression variations in tumor cells

Multiple molecular pathways participate in the global regulation of RNAPIII, and their dysregulation fosters cancer development and progression. Several oncogenes and tumor suppressor genes participate in RNAPIII control by modulating the expression of its related transcription factors, their post-translational modifications, or their release from transcriptional repressors. As a result, RNAPIII will be overactivated in cancer cells and lead to a global boost in tRNA expression (Haurie et al., 2010). This increased tRNA expression associated to malignant transformation was first believed to be a natural outcome of the proliferative status of the cell, likely to respond to the greater demand of tRNA needed to sustain elevated protein

Introduction

synthesis rates (Santos et al., 2019). But, although the cancer-associated tRNA overexpression is extensive to all tumor types, not all tRNA species are equally altered (Santos et al., 2019; Zhang et al., 2018). In fact, tRNA expression variations occur at amino acid, isoacceptor and isodecoder levels in a tissue-dependent manner (Zhang et al., 2018). The molecular mechanisms that orchestrate such a precise control of tRNA abundance in cancer cells are poorly understood, but copy number alterations and epigenetic regulation have been proposed to take part in it (Hernandez-Alias et al., 2020; Park et al., 2017).

Particular changes in tRNA isoacceptor expression will allow the translation of mRNAs with certain codons and reshape the cell proteome (Benisty et al., 2020; Goodarzi et al., 2016). Alterations in the stoichiometry between tRNAs and their cognate aaRS resulting from variations in the tRNA pool composition will contribute to the differential mRNA translation as well as to elevate protein synthesis error or translational miscoding (Santos et al., 2018). In the end, these changes will foster cancer progression and metastasis (Hernandez-Alias et al., 2020) or facilitate stress adaptation (Kwon et al., 2018).

tRNA expression alterations are not simply passenger events in tumorigenesis; they actively drive it. In fact, initiator tRNA^{Met} (tRNA$_i^{Met}$) has been claimed as an oncogene. Overexpression of tRNA$_i^{Met}$ in normal breast cells induces changes in the entire tRNA repertoire, increases proliferation and inhibits apoptosis (Pavon-Eternod et al., 2013; Wang et al., 2018a). In melanoma cells, it enhances migration and invasion (Birch et al., 2016). Conversely, the reduction of tRNA$_i^{Met}$ slows glioblastoma growth (Yang et al., 2020). Interestingly, tRNA$_i^{Met}$ can be targeted by the tumor suppressor miR-34a (Wang et al., 2018a), which uncovers another molecular mechanism for specific tRNA abundance regulation.

Alterations of tRNA modifications and tRFs in cancer cells

tRNA modifications are dynamic and can be reprogrammed in response to different cellular status or stresses, including tumor growth. Nucleoside modifications in tRNA experiment shifts in fast-proliferating tumor cells compared to their matched normal tissues (Dong et al., 2016) –probably as a result of altered tRNA modifier expression (Begik et al., 2020)– in order to participate in the cellular processes that govern various stages of malignant transformation (Endres et al., 2019; Rapino et al., 2017).

Cancer-associated tRNA modification defects were acknowledged various decades ago, when scientists observed tRNA hypomodification in some tumors. For instance, the tumor-specific loss of yW derivatives in tRNA^{Phe} was first observed in the 1970s and proposed to confer

growth advantages to those cells (Grunberger et al., 1975; Kuchino et al., 1982; Mushinski and Marini, 1979). Similarly, queuosine deficiency in some tumors was associated with more advanced forms of the disease and poor differentiation status (Baranowski et al., 1994; Huang et al., 1992).

Since then, different studies have shown that the enzymes responsible of tRNA modifications can play oncogenic or tumor suppressive roles depending on the modification they deposit and the tumor type (Endres et al., 2019). One example of oncogenic tRNA modifier enzyme is the catalytic subunit of Elongator complex (ELP3). Wobble U_{34} modification introduced by ELP3 contributes to breast cancer metastasis by enhancing the translation of the lymphoid enhancer binding factor 1 (LEF1) (Delaunay et al., 2016). BRAF^{V600E}-expressing melanoma cells depend on ELP3 and the cytosolic thiouridylase subunits 1 and 2 (CTU1/2) to translate pro-survival mRNAs like the hypoxia inducible factor 1α (HIF1α) (Rapino et al., 2018). On the other way around, the human tRNA methyltransferase 9-like protein (TRMT9B/C8orf79) is an example of tumor suppressor tRNA modifying enzyme. This protein can slow the cell cycle and limit the invasive capacity of lung cancer cells (Wang et al., 2018b) and inhibit cell growth in ovarian cells (Chen et al., 2017).

Cancer-associated dysregulation of tRNA biology also includes defects in their small derivatives like tRFs and tiRNAs (Balatti et al., 2017; Yu et al., 2020). Multiple studies highlight that the expression of several tRFs is altered in human cancers in a tissue-specific manner, yet the specific mechanism of how they affect carcinogenesis remains obscure for most of them. Like tRNA modifications and their cognate enzymes, tRFs can play oncogenic and tumor suppressive roles. In breast cancer, for example, the expression of a tRF-2 derived from some tRNA species bind to YBX1, preventing its binding to the 3' untranslated region (UTR) in oncogenic mRNAs and suppressing cell growth (Goodarzi et al., 2015), while a tRF-3 derived from tRNA^{Glu} acts as tumor suppressor by displacing nucleolin from p53 mRNA, thereby increasing its expression and modulating cell proliferation (Falconi et al., 2019).

The mechanisms driving tRF alterations in cancer cells have been elucidated only for a reduced number of molecules. In some cancers, the activation of ANG contributes to the increased generation of tiRNAs and promotion of cell proliferation (Honda et al., 2015). Alterations in tRF levels can result from the aberrant expression of the tRNAs from which they are originated (Torres et al., 2019) or from alterations in their nucleoside modifications that lead to their fragmentation (Rashad et al., 2020).

Introduction

Clinical perspective of cancer-associated tRNA imbalance

The clinical relevance of cancer-associated alterations in tRNA biology is beginning to be unveiled. Some analyses report that tRNA expression can be a prognostic marker for cancer patients' overall survival (Kuang et al., 2019; Zhang et al., 2018). Interestingly, tRFs are gradually being suggested as biomarkers for cancer diagnosis, prognosis and drug sensitivity (Cui et al., 2019; Jin et al., 2021; Zhang et al., 2020b) because they can be detected in fluids that can be easily obtained from patients and serve as a diagnostic tool (Huang et al., 2020; Wu et al., 2021).

The levels of tRNA modification and their cognate enzymes have been linked to differential drug response. This indicates that the modulation of nucleoside modifications may be a promising approach to enhancer cancer chemotherapy effectivity (Begley et al., 2013; Okamoto et al., 2014; Rapino et al., 2018).

tRFs could also constitute therapeutic targets against this devastating disease, as the use of mimetic tRFs that compete with the endogenous and aberrantly expressed molecule can counteract the oncogenic features that arise from their dysregulation (Goodarzi et al., 2015).

Doubtlessly, the defects in tRNA biology play unforeseen roles in complex diseases like cancer, yet our knowledge on tumor-associated tRNA defects is scarce and many outstanding questions are still unanswered. Much remains to be discovered about tRNA alterations in cancer and how they correlate with disease features and outcome, as well as how this can be translated into the clinical practice. Over the following years, the research in cancer-specific tRNA imbalance will likely continue to grow and provide new insights into the mechanisms that are responsible for their alterations and, most importantly, how they can be therapeutically exploited in personalized medicine. Thus, this thesis aims to contribute to this blossoming field.

HYPOTHESIS AND OBJECTIVES

HYPOTHESIS AND OBJECTIVES

Hypothesis

Compelling evidence prove that tRNA are more than housekeeping molecules; in reality, their molecular functions are broader than initially thought. This is reinforced by the recent discovery that these molecules and their derived fragments are altered in pathological processes like cancer, where they have been reported to impact on patient prognosis. Interestingly, cancer cells present altered profiles of tRNA expression and modification (Endres et al., 2019; Santos et al., 2019). tRNA alterations are prevalent in many cancer types, therefore it is interesting to explore how these defects participate in tumor biology, learn how they correlate with the outcome of the disease, and evaluate their suitability to be targeted by novel therapeutic approaches.

Our knowledge of the causes and the complexity of such imbalance are still limited as the study cancer-associated tRNA defects constitute a very new discipline. Thus, much remains to be learned about the causes and consequences of cancer-associated tRNA imbalance before these alterations can be transported into the medical practice. Provided that DNA methylation lesions constitute a frequent mechanism by which cancer cells acquire their malignant features, we hypothesized that tumor-associated epigenetic alterations could guide this tRNA dysregulation. Therefore, this thesis aims to identify and characterize DNA methylation patterns that give rise to the cancer-related tRNA biology defects that promote malignant transformation and tumor progression.

To achieve our goal, we have followed different strategies that have inspired two independent studies:

- The first strategy aimed to study the causes of tRNA modification reprogramming in cancer cells. To do so, we sought to find aberrant DNA methylation patterns that could silence tRNA modifier proteins to enhance tumorigenesis. With this approach, we could identify tRNA modifying enzymes with tumor suppressive features, characterize how their loss contributes to cancer biology, and determine their clinical impact.

- The second strategy intended to evaluate if DNA methylation alterations can drive differential tRNA expression. To this end, we studied the presence and the cancer-associated variations of DNA methylation within tDNAs and their impact on their transcription, thus proposing the contribution of this epigenetic mechanism to tRNA expression regulation. Moreover, we also explored the suitability of these changes in DNA methylation events as biomarkers to predict the progression of the disease.

45

Objectives of the thesis

Study I: Role of DNA methylation defects in tumor-associated tRNA modification reprogramming

  I.   To determine if there is any tRNA modifying enzyme that is epigenetically lost in cancer by mining the available DNA methylation data from The Cancer Genome Atlas (TCGA) and an extensive panel comprising approximately 1,000 cancer cell lines.

  II.   To select a candidate gene of interest in which confirm this DNA promoter methylation and gene silencing in cancer.

  III. To characterize the cellular implications of the observed epigenetic lesion in cancer cell line models resulting from the depletion or the recovery of the gene of interest.

  IV.   To test whether the methylation status of the selected gene may serve as a prognosis biomarker in cancer.

Study II: Contribution of DNA methylation alterations to altered tRNA expression in cancer.

  I.   To evaluate if differential DNA methylation in tDNA genes varies in primary cancer samples compared to the normal tissue by analyzing the available data from TCGA and cancer cell lines.

  II.   To establish a correlation between tDNA gene methylation and the expression of the associated tRNA.

  III. To validate in cancer cell lines the observed epigenetic silencing on one or more tRNA of interest that may be subjected to this regulation according to the previous in silico analyses.

  IV.   To assess if tDNA methylation has any clinical implications in tumor progression and its utility as a predictive biomarker for cancer patients' prognosis by examining the clinical information from TCGA and generating the appropriate cellular models.

MATERIALS AND METHODS

MATERIALS AND METHODS

Cell line culture and treatments

For the first study, the four colon cancer cell lines (SW48, HT-29, HCT-116 and SW480) as well as HEK-293 cells were cultured in Dulbecco's Modified Eagle's Medium (DMEM). For the second study, the T-acute lymphoblastic leukemia (T-ALL) cell line DND41 was cultured in Roswell Park Memorial Institute (RPMI) 1640 medium at 37°C and 5% CO_2. The cell lines derived from endometrial adenocarcinoma (HEC1) and colon adenocarcinoma (SW48) were cultured in DMEM at 37°C and 5% CO_2. All media were supplemented with 10% fetal bovine serum (FBS) and 1% penicillin/streptomycin.

For DNA demethylating treatment, SW48 and HT-29 cells were treated with 1 µM 5-azacytidine (Sigma, A2385) for 96 hours, with medium renewal after 48 hours. DND41 cells were cultured with 0.5 µM 5-azacytidine for 96 hours because of their increased sensitivity to this compound. For mRNA decay analyses, cells were incubated with α-amanitin (MedChemExpress, HY-19610) at 20 µg/mL and collected after 0, 4, 8, and 24 hours.

The source of all the cell lines is provided in **Table 2**. All cell lines were authenticated by short tandem repeat profiling (LGS Standards SLU) and tested for the absence of mycoplasma.

Cell lines	Study	Source	Reference
HCT-116	I	ATCC	CCL-247
HT-29	I	ATCC	HTB-38
SW48	I, II	ATCC	CCL-231
SW480	I	ATCC	CCL-228
HEK-293	I	ATCC	CRL-1573
HEC1	II	JCRB	JCRB0042
DND41	II	DSMZ	ACC-525

Table 2. Source and commercial reference of all the cell lines used in this thesis.

DNA methylation analyses

DNA methylation microarrays: in silico DNA methylation evaluation

In silico DNA methylation analyses were carried out using the Infinium HumanMethylation450 (HM450) methylation microarray, which interrogates approximately 450 thousand CpG dinucleotides. This platform uses different fluorophores' intensities to discern whether the interrogated DNA is methylated or unmethylated, which is then normalized to a 0-to-1 value named β-value.

Materials and Methods

DNA methylation profiles from human primary tumors and healthy tissues were obtained from TCGA. Parallelly, the methylation profiles from a panel of approximately 1,000 human cancer cell lines was also obtained (Iorio et al., 2016). All these HM450 methylation microarray-derived data were data-mined to identify differentially methylated CpG islands at the promoter regions of the genes of interest. Cross-reactive CpG were automatically discarded in our analyses (Chen et al., 2013). Gene promoter CpG islands were considered hypermethylated in cancer cell lines when the average β-value of the interrogated CpG dinucleotides encompassing the 5'UTR and TSS200 regions was higher than 0.66. This threshold β-value was reduced to 0.33 in human primary tumors and healthy control samples because of possible contamination of the sample with surrounding tissues.

For internal tDNA methylation evaluation, the tDNAs' genomic location (Chan and Lowe, 2016) was used to retrieve CpG probes from the HM450 DNA methylation microarrays. The β-value thresholds to consider a tDNA hypermethylated were the same as in gene promoters.

Genomic DNA extraction

For genomic DNA extraction, cell pellets were incubated overnight with 500 µL of DNA lysis buffer (10 mM Tris pH 8.0, 100 mM NaCl, 5 mM EDTA, 1% SDS and 10 mg/mL proteinase K) at 37°C. Cell lysates were centrifuged during 15 minutes at maximum speed after the addition of 250 µL of 5 M NaCl. Then, the upper phase was transferred to a new tube and DNA was precipitated with the addition of 560 µL of isopropanol followed by centrifugation at maximum speed for 10 minutes. The DNA was washed twice with 1 mL ethanol 70% by centrifugation at maximum speed for 5 minutes. The DNA pellet was air-dried and resuspended in 50 µL of water. DNA concentration was measured using a NanoDrop.

Bisulfite DNA conversion and bisulfite-sequencing PCR (BSP)

The methylation status of gene promoter CpG islands or tDNAs that were considered of interest were interrogated by bisulfite sequencing PCR (BSP), for which bisulfite conversion of the DNA is required. This process specifically converts unmethylated cytosines to uridines that can be further evaluated by genomic sequencing.

Bisulfite conversion was performed on 2 µg of previously extracted genomic DNA using the EZ DNA Methylation-Gold kit (Zymo Research, D5006) with the following change on the manufacturer's standard protocol: DNA was incubated with the CT conversion reagent

following Bibikova's protocol (Bibikova et al., 2009). This modification of the standard protocol includes various denaturing steps that enhance the conversion of cytosines located in CG-rich genomic regions. Therefore, the incubation profile was 16 cycles at 95ºC for 30s and 50ºC 1h with a final holding step at 4ºC. DNA desulphonation and purification was conducted as stated in the standard protocol. Bisulfite-converted DNA was stored at -20ºC until further use.

BSP primers used to amplify the region of interest were designed using MethylPrimer Express (Applied Biosystems) and are listed in Table 3. These primers did not contain any CpG in their sequence to amplify the desired regions regardless of their methylation status. PCR of the bisulfite-converted genomic DNA was conducted using the Immolase DNA polymerase (Bioline, BIO-20147). BSP amplicon products were purified using the NucleoSpin Gen and PCR Clean-Up (Macherey-Nagel, 740609.250). Then, 5 µL of purification product were ligated overnight at 16ºC into the pGEMT-easy vector (Promega, AS1360) using 3 µL of 2X ligation buffer, 1 µL of pGEM-T vector and 1 µL of DNA ligase. Ligation products were transformed into competent DH5α *E. coli* by thermal shock (45 seconds at 42ºC and 2 minutes on ice) and grown in 1mL of antibiotic-free lysogeny broth (LB) medium at 37ºC for 1 hour in agitation. After that, bacteria were grown overnight at 37ºC in LB Petri dishes with ampicillin in presence of isopropyl-β-D-1-thiogalactopyranoside (IPTG) and 5-bromo-4-chloro-3-indolyl-β-D-galactopyranoside (X-gal) to differentiate the bacterial clones that incorporated the pGEMT-easy with (white colonies) or without insert (blue colonies). Single colonies were grown at 37ºC overnight in 1 mL of ampicillin positive LB medium in orbital agitation. Plasmid DNA was extracted and purified using the NucleoSpin 96 Plasmid kit (Macherey-Nagel, 740625.24) following the manufacturer's specifications. The plasmid products obtained were subjected to sequencing PCR using BigDye Terminator V3.1 sequencing kit (Applied Biosystems, 4337458), purified using the BigDye X-Terminator™ purification kit (Applied Biosystems, 4376484) and sequenced in a Hitachi 3730 DNA sequencer (Applied Biosystems) to interrogate the presence of cytosine or uracil in the BSP amplicon product to assess methylation status. The sequencing results of a minimum of 8 clones were analyzed using BioEdit software, and methylated cytosines were mapped using BSMap software.

Oligonucleotide name	Sequence (5' to 3')
BSP_TYW2_Fd	ATGTTTTTTTAGGTTGAAAAAAAAG
BSP_TYW2_Rv	AAACCAAAACTCAATCACAACT
BSP_tRNAArgTCT41_Fd	AGGATTTTTAAGGAAAAGGGTTTT
BSP_tRNAArgTCT41_Rv	ATTTTCCAACTATCCCTATCC
BSP_tRNAIleAAT81_Fd	GGTTTAGAGTTAAAATAGTTTGGATT
BSP_tRNAIleAAT81_Rv	ACCTATTCTTTTCATTTTTCACAATAA

Table 3. List of the BSP primers sequences.

Materials and Methods

RNA expression analyses

In silico RNA expression evaluation

In silico mRNA expression was analyzed in cell lines and in TCGA samples from primary tumors or normal tissue. Transcripts levels from cancer cell lines were obtained from the Broad Institute Cancer Cell Line Encyclopedia (CCLE) (Ghandi et al., 2019) and from the Catalogue of Somatic Mutations in Cancer (COSMIC) (Tate et al., 2019). mRNA expression data from TCGA cohorts was downloaded using the TCGAbiolinks Bioconductor package in the R environment (Colaprico et al., 2016).

In silico tRNA expression was analyzed in TCGA samples by using the datasets generated by Zhang and coworkers that are publicly available online (Zhang et al., 2018).

Total RNA extraction, retrotranscription and quantitative real-time PCR (qRT-PCR)

Total RNA was extracted from cell pellets using the SimplyRNA kit (Promega, AS1340) in the Maxwell RSC device (Promega, AS4500) following the manufacturer's indications. In brief, cell pellets were vigorously homogenized in a 1-thioglycerol-containing solution, lysed, and loaded onto Maxwell cartridges. Maxwell RSC device performs an automated RNA purification using magnetic particles. The total RNA product was eluted in 50 µL of RNase-free water and its concentration was measured using a NanoDrop.

2 µg of the extracted RNA were retrotranscribed using the RevertAid First Strand cDNA Synthesis kit (Thermofisher Scientific, K1622) as per manufacturer's instructions, using random hexamers to prime the retrotranscriptase. Quantitative real-time PCR (qRT-PCR) reactions were used to assess mRNA expression in cell lines. qRT-PCR primers for mRNA were designed using the online Primer3 software with a melting temperature of 60ºC and the requirement that forward and reverse primers were in different exons or in exon-exon junctions. The amplification efficiency for each pair of primers was calculated with a standard curve prior to the experiment, and only those pairs of primers displaying an efficiency between 85% and 115% were used. All qRT-PCR primers are listed in **Table 4**. Each qRT-PCR reaction was carried out using 5 ng of cDNA in 5 µL of water, 4.85 µL of SYBR Green PCR Master Mix (Life Technologies, 4312704) and 0.15 µL of forward and reverse primers mix at 10 µM. The fold change among samples was calculated using the ddCT formula (Livak and Schmittgen, 2001), using GAPDH or 28S rRNA expression as an endogenous control. All qRT-PCR experiments were performed using at least three biological replicates with technical triplicates.

52

RNA-sequencing (RNA-seq)

5 μg of total RNA from three biological replicates from each sample were used for RNA-sequencing (RNA-seq) analyses. The RNA-seq experiment was conducted at the National Center for Genomic Analysis (CNAG) and analyzed by the bioinformatics unit of the Josep Carreras Leukaemia Research Institute (IJC). In short words, the RNA-seq libraries were prepared from total RNA with TruSeq®Stranded mRNA LT Sample Prep Kit (Illumina). Each library was sequenced using TruSeq SBS Kit v4-HS, in paired-end mode with a read length of 2x76+8+8bp. We obtained between 60 and 80 million paired-end reads in a fraction of a sequencing lane on HiSeq2500 (Illumina) following the manufacturer's protocol. Raw reads were quality assessed and preprocessed using FASTQC (v0.11.7) and Trimmomatic (v0.36) software. Differential expression analysis was performed using DESeq2 Bioconductor package (Love et al., 2014), in R programming environment (v3.4.3). Gene annotations were extracted from GENECODE (v28). Genes were considered differentially expressed when log2 fold change was < -1.0 or > 1.0 and adjusted p value < 0.05.

Small RNA extraction, retrotranscription and tRNA qRT-PCR

tRNA expression in cancer cell lines was determined by qRT-PCR using commercially available, isodecoder-specific primers purchased from ArrayStar. These experiments were conducted in samples enriched in small RNA. The small RNA fraction was extracted from cell lines by direct phenol acidic extraction, which promotes DNA denaturalization, followed by a LiCl precipitation of large RNA molecules.

Fresh cell pellets were resuspended in 300 μL ice-cold resuspension buffer (0.3 M sodium acetate pH 4.5, 10 mM EDTA), to which 300 μL of cold acidic phenol:chloroform:isoamyl alcohol (125:24:1) pH 4.5 (Thermofisher Scientific, AM9722) were added. After vortexing for 90 seconds in three intervals of 30 seconds with 30 seconds pauses between steps, samples were centrifuged at maximum speed for 15 minutes at. The aqueous phase was transferred to a new centrifuge tube containing 300 μL of acidic phenol:chloroform. The samples were again vortexed for 1 minute and centrifuged at maximum speed for 15 minutes at 4ºC. The aqueous phase was transferred to a 15 mL tube containing 300 μL of acidic phenol:chloroform and 3.6 mL of ethanol. After two hours of incubation on ice, samples were centrifuged at maximum speed for 15 minutes at 4ºC and supernatant was discarded. The RNA pellets were washed twice in ethanol 80% and left to air-dry for 10 minutes. Then, they were resuspended in 90 μL of 10 mM sodium acetate pH 4.5 and 0.8 M LiCl. After centrifugation at maximum speed for 15 minutes at 4ºC, supernatant containing the small RNA fraction was recovered. Next, it was

Materials and Methods

precipitated with 10 µL of RNase-free 3 M sodium acetate pH 5.5 (Thermofisher Scientific, AM9740) and 300 µL of absolute ethanol for 40 minutes at -80ºC. Afterwards, samples were centrifuged at maximum speed for 30 minutes at 4ºC to precipitate the RNA. The RNA pellet was washed three times with ethanol 80% and vacuum-dried to eliminate all traces of ethanol. Finally, the RNA pellets were resuspended with 20 µL of RNase-free water and concentration was measured using a NanoDrop.

1 µg al the small RNA fraction was retrotranscribed using random primers with the RevertAid First Strand cDNA Synthesis kit following manufacturer's instructions. qRT-PCR were carried out using 2.5 ng of cDNA in 5 µL, 4.85 µL of SYBR Green PCR Master Mix and 0.15 µL of the commercial primer mix at 10 µM. The fold change among samples was calculated following the ddCT formula using the expression U6 snRNA as an endogenous control. The references of the commercial primers as well as for U6 determination can be found in **Table 4**.

Oligonucleotide name	Sequence (5' to 3') / Reference
qRT-PCR primer sequences	
qPCR_TYW2_Fd	CCTGCCCAAAAATTGTGTCT
qPCR_TYW2_Rv	AGAGTTCCGGTCCCAGATTT
qPCR_ROBO1_Fd	GGAGTCAGGGGCACAAGAAA
qPCR_ROBO1_Rv	GGCCTCGTTCATCTTCCTCC
qPCR_VIM_Fd	CTTAAAGGAACCAATGAGTCCCT
qPCR_VIM_Rv	AGTGAATCCAGATTAGTTTCCCTC
qPCR_CDH1_Fd	GGGGTCTGTCATGGAAGGTG
qPCR_CDH1_Rv	GAAACTCTCTCGGTCCAGCC
qPCR_GAPDH_Fd	GAAGGTGAAGGTCGGAGTC
qPCR_GAPDH_Rv	TGGACTCCACGACGTACTCA
qPCR_UPF1_Fd	CCATCCCCTTCAACCTGGTC
qPCR_UPF1_Rv	GTTGGGGAGGTTAGTCTGGC
qPCR_TUSC3_Fd	AATACTGGCGAACTCCTGGC
qPCR_TUSC3_Rv	TCCGTTCTGTCAGCAATCCA
qPCR_PVR_Fd	CTACACCTGCCTGTTCGTCA
qPCR_PVR_Rv	GGTCTGAGTGCCAGGTGATT
qPCR_NQO1_Fd	AAAGGACCCTTCCGGAGTAA
qPCR_NQO1_Rv	CCATCCTTCCAGGATTTGAA
qPCR_UPP1_Fd	CAGAGCAGGCAGTGGATACC
qPCR_UPP1_Rv	CTGCTTGTCCTTCTCCGTGT
qPCR_DUSP10_Fd	GCGAGTCCATAGCTGAAGAGG
qPCR_DUSP10_Rv	GATGACAGGAGGGTGGCTG
qPCR_28S_Fd	CAGGGGAATCCGACTGTTTA
qPCR_28S_Rv	ATGACGAGGCATTTGGCTAC
qPCR_U6_Fd	CTCGCTTCGGCAGCACA
qPCR_U6_Rv	AACGCTTCACGAATTTGCGT
Commercial references for tRNA qRT-PCR primers	
Arg-TCT-3 (Human)	AS-NR-001H-1-026 (ArrayStar)
Ile-AAT-5 (Human)	AS-NR-001H-1-080 (ArrayStar)

Table 4. *Sequences of qRT-PCR primers and reference for tRNA qRT-PCR primers.*

Protein expression analysis

Protein extraction and quantification

Total protein from cell pellets was extracted using Laemli buffer (62.5 mM Tris-HCl pH 6.8, 25% glycerol, 2% SDS, 0.01% bromophenol blue, 3% β-mercaptoethanol). Cell pellets were resuspended in Laemli buffer and mixed vigorously by vortexing for 30 seconds. Then, samples were boiled (95ºC for 5 minutes) and sonicated 30 seconds. These steps were repeated until the sample was completely dissolved. Then, Laemli protein extracts were measured on the NanoDrop to determine protein concentration, which was obtained by dividing absorbance at 260 nm by 6.

Western blot

Protein expression levels were determined by western blot. Briefly, protein extracts were subjected to electrophoretic separation in polyacrylamide gels (SDS-PAGE). The percentage of acrylamide used was dependent on the molecular weight of the protein to be immunoblotted. Then, proteins were transferred to a 0.2 µm pore nitrocellulose membrane. After that, membranes were blocked in 5% fat-free milk in phosphate buffered saline (PBS) with 1% Tween for at least 1 hour. Membranes were incubated with primary antibody overnight at 4ºC in an orbital shaker. Next day, membranes were washed in PBS with 1% Tween and incubated with a HRP-conjugated secondary antibody for 1 hour at room temperature in an orbital shaker. After washing, membranes were developed using different Luminata HRP substrates (Millipore). Images were captured using an iBright (Applied Biosystems). β-actin (ACTB), Calnexin (CANX), Lamin B1 (LMNB1), and Vinculin (VCL) were used as endogenous loading controls. All western blots were performed in triplicate. The commercial sources of all antibodies used for western blotting are listed in **Table 5**.

Antibodies	Source	Reference
anti-TYW2	Novus Bio	NBP1-76583
anti-ROBO1	Abcam	ab7279
anti-Calnexin	Cell Signaling	2679
anti-HA HRP-conjugated	Sigma	H6533
anti-PARP	Cell Signaling	9542
anti-p21	Cell Signaling	2497
anti-β-Actin HRP-conjugated	Sigma	A3854
anti-LaminB1	Abcam	ab16048
anti-Vinculin HRP-conjugated	Cell Signaling	18799
anti-rabbit HRP-conjugated secondary antibody	Sigma	A0545

Table 5. *List of the antibodies used in this thesis together with their commercial reference.*

Gene overexpression in cell lines

The genes to be overexpressed in cell lines were first cloned into the required vector. To do so, specific cloning primers were designed to be complementary to the 5' and 3'-ends of the coding region of the gene of interest. In addition, both forward and reverse primers contained overhangs. The forward primer contained a restriction site and the Kozak sequence for proper ribosome translation initiation. The reverse primer included the sequence of a protein tag and a different restriction site. The sequences of these primers are found in **Table 6**.

Primer name	Sequence (5' to 3')
TYW2_F	AAAAAAGAATTCGCCGCCACCATGAGAGAGAATGTGGTTGTTAGCAACATGGAGAGAGAAAGTGGGAAGCCCGTGGCTGT
TYW2-Flag_R	AAAAAAGCGGCCGCCTACTTATCGTCGTCATCCTTGTAATCGCCGGAGCCGCCAACTGAAGGACAGGGGCAGCATTCCAGATCCAGGACTATGTGATCCACATGGGG
PRF_RLuc_F	AAAAAAAAGCTTGCCGCCACCATGTACCCCTACGACGTGCCCGACTACGCCGGATCAGGAGCTTCCAAGGTGTACGACCCCGAGCAACGCAAAC
PRF_RLuc_R	TTTTTTGCGGCCGCGAATTCTCCTGATCCCTGCTCGTTCTTCAGCACGCGCTCCACGAAG
PRF_FLuc_F	AAAAAAGCGGCCGCGAATTCGGTACCGGATCAGGAGCCGATGCTAAGAACATTAAGAAGGGCCCTGCTCCCTTCTACC
PRF_FLuc_R	TTTTTTCTCGAGTTACACGGCGATCTTGCCGCCTTTCTTAGCCTTGATCAGGATCTC
PRF_HIV_F	AATTCAATTTTTTAGGGAAGATCTGGCCTTCCCACAAGGGAAGGCCAGGGAATTTTCTTCAGGGTAC
PRF_HIV_R	CCTGAAGAAAATTCCCTGGCCTTCCCTTGTGGGAAGGCCAGATCTTCCCTAAAAAATTG
PRF_ROBO1wt_F	AAAAAAAGAATTCCGCCCTTTTTTTAATGAATTTCAAGGAGCAGATAGTGAAATCAAGTTTGCCAAAACCCTGGAAGA
PRF_ROBO1_R	TTTTTTTGGTACCTCCATCATTCTTGGATACAGTTACACCTTGGGGTGGGGCACTGGGTGCTTCTTCCAGGGTTTTGG
PRF_ROBO1mut_F	AAAAAAAGAATTCCGCCCACTGCTAAATGAATTTCAAGGAGCAGATAGTGAAATCAAGTTTGCCAAAACCCTGGAAGA
ROBO1_F	AAAAAAAAGCTTCTCGAGGCCGCCACCATGATTGCGGAGCCCGCTCACTTTTACCTGTTTGGATTAATATGTCTCTGTTCAG
ROBO1-HA_R	TTTTTTGCGGCCGCTCAGGCGTAGTCGGGCACGTCGTAGGGGTATCCTGATCCGCTTTCAGTTTCCTCTAATTCTTCATTATTATCTTCTCCTCTTTCATATCCTCCAAGTACCTGCATTTCTGCAATATTTCTTCGACCT

Table 6. Sequences of the oligonucleotides used for cloning procedures.

cDNA from cell lines expressing the gene of interest was used as DNA template to be amplified with the Phusion High-Fidelity DNA Polymerase (Thermofisher Scientific, F-530XL). Concretely, TYW2 was cloned from HCT-116 cDNA with a Flag-tag and ROBO1 was obtained from SW480 cDNA with a HA-tag. PCR product was resolved in an agarose gel to verify the size of the amplicon, which was then purified using the NucleoSpin Gen and PCR Clean-Up. The purified PCR overexpression cassette and the vector backbone were digested with the appropriate FastDigest restriction enzymes (Thermofisher Scientific), generating overhangs that were complementary between the vector and the insert. Ligation with T4 DNA ligase (NEB Biolabs, M202L) was carried out overnight at 16 ºC using 50 ng of digested vector and insert

amount equal to three times the number of vector molecules. Ligation products were transformed into competent DH5α *E. coli* by thermal shock and grown overnight at 37ºC in LB plates with ampicillin as described in previous sections. Single colonies were grown in 10 mL LB with ampicillin in agitation overnight. The resulting plasmid was extracted from bacterial clones by miniprep using EZNA Plasmid mini kit (Omega, D6942-01) following the manufacturer's indications. The vector was sequenced to ensure the correct insertion of the overexpression cassette and the absence of mutations introduced by the DNA polymerase.

Stable gene overexpression was achieved using a lentiviral system. The vector used in this case was the pLVX-IRES-ZsGreen1 (Clontech, 632187). Lentivirus containing either the construct or the empty vector were produced by co-transfecting HEK-293 cells with 10 µg of the empty or the recombinant pLVX-IRES-ZsGreen1 plasmid, 7.5 µg psPAX2 (Addgene, 12260) and 2.5 µg pMD2.G (Addgene, 12259) using JetPrime® Transfection Reagent (Polyplus transfections, 114-75) following the manufacturer's instructions. 72 hours after transfection, virus-containing culture media was collected, filtered, and delivered to $7 \cdot 10^5$ of the desired cell lines in 6-well plates. Infection was enhanced by centrifuging the plates at 1,000 g for 90 minutes at 32ºC. After 5 passages, green cells were purified by cell sorting.

pcDNA4 T/O vector (Thermofisher Scientific, V102020) was used for transient gene overexpression in cell lines. Either the empty vector or the vector containing the gene of interest were transfected to $5 \cdot 10^5$ cells after overnight adherence using JetPrime® Transfection Reagent in 6-well plates. Cells were collected by cell scrapping after 72 hours, and RNA and protein extraction were conducted as previously described.

Gene silencing in cell lines

Gene knockout using the CRISPR/Cas9 system

The CRISPR/Cas9 system was used to generate stable knockout (KO) cell lines for the gene of interest as described previously (Ran et al., 2013). This system relies on DNA cleavage by the endonuclease Cas9 in a specific sequence that is complementary to a guide RNA (sgRNA). Unless a repair template is used, this cleavage will be repaired by the cell via non-homologous end-joining (NHEJ), resulting in InDel mutations that alter the coding reading frame and abolish the synthesis of a functional protein from this sequence. The use of two different sgRNA targeting separated loci will lead to the generation of larger deletions of the sequences encompassed between the two sgRNA.

Materials and Methods

sgRNA were designed using the online CHOPCHOP tool (Labun et al., 2016). Two sgRNA sequences were selected by minimum off-target activity and location within the first exon of the target coding gene or in the vicinity the tRNA of interest. To prepare the sgRNA oligonucleotide insert, forward and reverse DNA oligonucleotides for each sgRNA were annealed by rapid temperature ramp down, from 95ºC to 25ºC descending 5ºC per minute, generating a double-stranded DNA molecule with overhangs that are complementary to the BpiI-digested pSpCas9(BB)-2A-GFP vector (Addgene, 48138). 50 ng of the digested pSpCas9(BB)-2A-GFP plasmid and 1 μL of 1/200 diluted annealed DNA oligonucleotides were ligated using T4 DNA ligase overnight at 16ºC. Ligation product was transformed into competent DH5α *E. coli* by thermal shock, plated on ampicillin positive LB plates and left for overnight growth at 37ºC. Bacterial colonies were subjected to miniprep plasmid isolation using EZNA Plasmid mini kit to check for the correct insertion of the sgRNA by sequencing the vector as described earlier.

To generate the cell line KO model, two different sgRNA-containing pSpCas9(BB)-2A-GFP vectors were transfected simultaneously to the desired cells (unmethylated HCT-116 and SW480 cells for TYW2 KO, and HEC1 for tRNA-Arg-TCT-4-1 KO) using JetPrime® Transfection Reagent. 48 hours after transfection, green positive cells were isolated by cell sorting into 96-well plates to establish clonal cell lines and left for expansion. KO clones were first screened by amplification of the genomic region that was targeted by the sgRNA. A deletion of more than 100 base pairs will take place in case of double cleavage by the two different sgRNA, which is easily detected when genomic PCR amplicons are resolved in a 2% agarose gel by electrophoresis. Genomic DNA from KO cell lines presenting one or more truncated gene copies was subjected to Sanger sequencing to fully validate the deletion introduced with the CRISPR/Cas9 system. The sequences of the sgRNA and of the primers used to amplify the targeted genomic region are shown in **Table 7**.

Oligonucleotide name	Sequence (5' to 3')
TYW2_sgRNA1_Fd	CACCGGTAGCGCCACCGAGCCATC
TYW2_sgRNA1_Rv	AAACGATGGCTCGGTGGCGCTACC
TYW2_sgRNA2_Fd	CACCGAGGCTGATTTGCCCCGATCA
TYW2_sgRNA2_Rv	AAACTGATCGGGGCAAATCAGCCTC
TYW2-KO_seq_Fd	TGTGGTTGTTAGCAACATGGA
TYW2-KO_seq_Rv	CTCTACCCAGCCATGGTCAC
ArgTCT41_sgRNA1_Fd	CACCGTCTCTGCCGGGACTCGAACC
ArgTCT41_sgRNA1_Rv	AAACGGTTCGAGTCCCGGCAGAGAC
ArgTCT41_sgRNA2_Fd	CACCGATCCTGCTCTCTGAGCGGTG
ArgTCT41_sgRNA2_Rv	AAACCACCGCTCAGAGAGCAGGATC
ArgTCT41_KO_seq_Fd	TTCCTTTCTCTCCCCTATAGCC
ArgTCT41_KO_seq_Rv	ATCGGACCCAGAGTATTGAGAA

Table 7. *Sequences of the sgRNA and of the primers used for knockout validation.*

Transient gene silencing by siRNA transfection

siRNA transfection was used for transient gene downregulation in cell lines. Briefly, $2\cdot10^5$ cells were transfected with 50 nM siRNA that are commercially available against the gene of interest (Thermofisher Scientific: siUPF1 ID 12990, siROBO1 ID AM16708) or with a negative control (Thermofisher Scientific, AM4611) using JetPrime® Transfection Reagent following the manufacturer's specifications for siRNA transfection. After 48 hours, cells were collected by cell scraping and total RNA extraction and retrotranscription were conducted as previously described.

tRNA nucleoside liquid chromatography - mass spectrometry (LC/MS)

Liquid chromatography coupled to mass spectrometry (LC/MS) was used to assess tRNA modification status. These determinations and analyses were performed by Dr. Yuriko Sakaguchi, Dr. Kenjyo Miyauchi and Dr. Tsutomu Suzuki, from the University of Tokyo, Japan, as previously described (Sakaguchi et al., 2015).

$5\cdot10^7$ cells per condition were collected by cell scrapping. Total RNA was immediately extracted from these pellets using TRIzol reagent (Thermofisher Scientific, 15596026) according to the manufacturer's specifications. Briefly, cell pellets were resuspended in 750 µL of cold TRIzol and incubated 5 minutes at room temperature. Next, 150 µL of chloroform were added to the tubes and incubated 3 minutes at room temperature. Samples were vigorously mixed by vortexing 30 seconds and centrifuged for 15 minutes at maximum speed at 4ºC. Then, the aqueous phase containing the RNA was transferred to a new RNase-free tube. RNA was precipitated with the addition of 375 µL of isopropanol and centrifugation at maximum speed for 10 minutes at 4ºC. The RNA pellet was washed with 1 mL of ethanol 75% and centrifuged at maximum speed for 5 minutes at 4ºC.

These RNA pellets in ethanol were sent to our collaborators in the University of Tokyo. They completed the total RNA extraction protocol and subjected it to a urea-PAGE separation to isolate the tRNA fraction. Next, the purified tRNA were digested using nuclease T_1 (Wako Pure Chemical Industries, 145-08221), phosphodiesterase I (Worthington Biochemical Corporation, LS003926) and bacterial alkaline phosphatase (Takara Bio, 2120A). The resulting nucleosides were separated and analyzed using a QExactive and U3000 liquid chromatography system (Thermofisher Scientific).

Materials and Methods

-1 Programmed Ribosome Frameshifting evaluation

-1 programmed ribosome frameshifting events were evaluated using a dual luciferase reporter as described previously (Grentzmann et al., 1998). For the dual luciferase experiment, a reporter construct was generated by cloning renilla and firefly luciferases into pcDNA4 T/O vector, separated by the slippery sequence of interest (HIV, ROBO1 wild-type, and ROBO1 mutated). Should the ribosome retrocede because of a ribosome frameshift event, the new reading frame with generate a premature stop codon and firefly activity will be abolished. Briefly, Renilla and Firefly luciferases sequences were amplified with the Phusion High-Fidelity DNA Polymerase using primers that contained overhangs with different restriction sites. The vector psiCHECK-2 (Promega, C8021) was used as template for both luciferases. The slippery sequence of interest was generated by the annealing a forward and a reverse oligonucleotide, generating a double-stranded DNA molecule with overhangs that are complementary to the renilla 3'-end and to the firefly 5'-end. The cloning procedures are the ones described earlier in this section, and all the oligonucleotide sequences required are found in **Table 6**.

This reporter was transfected into 10.000 cells plated in 96-well white plates after overnight adherence using JetPrime® Transfection Reagent according to manufacturer's instructions. Firefly and renilla luminescence were determined 72 hours after transfection using the Dual Glo™ Luciferase Assay System (Promega, E2920) with the following change on the manufacturers' protocol: 45 µL of each reagent were used instead of the same volume of media. 45 µL of luciferase substrate reagent were delivered to each well and firefly luminescence was captured after a 10 minutes' incubation. Then, 45 µL of Stop&Go reagent were added to quench firefly activity and measure renilla activity. The ratio of firefly over renilla luminescence was compared between pairs of samples to estimate ribosome frameshifting frequency. A minimum of four biological replicates with technical triplicates were analyzed.

Cell migration determination

Cell migration capacity was assessed by the Transwell assay. $2 \cdot 10^5$ cells were seeded in serum-free medium in the upper chamber of an 8 µm pore Transwell insert (Corning, 3422) and left for migration to the serum-containing lower chamber for 48 hours. Then, Transwell membranes were fixed with 10% trichloroacetic acid (TCA) for 1 hour, washed with water and stained with 0.057% sulforhodamine B (SRB) in 1% acetic acid for 30 minutes. After washing the excess of SRB dye with 1% acetic acid, complete membrane pictures were taken, and ImageJ software was to calculate the percentage of membrane area occupied by cells to assess cell migration. Migration experiments were performed in triplicate.

Cell growth and viability studies

Flow cytometry analyses

Cell cycle was analyzed in bromodeoxyuridine (BrdU) labeled cells with an APC labelled anti-BrdU antibody and 7-amino-actinomycin D (7AAD) staining using an APC BrdU Flow Kit (BD Biosciences, 552598). Cells were incubated with 10 µM BrdU during 1h at 37ºC. This incubation period was reduced to 30 minutes in HCT-116 cell line and its derived cell model because of its rapid doubling time. Then, cells were collected, washed, fixed, permeabilized and treated with DNase following manufacturer's indications. After that, samples were incubated with APC-labeled anti-BrdU antibody during 30 minutes at room temperature, and total DNA was stained using 2 µL of 7AAD solution. A minimum of 10,000 cells was analyzed per sample with a FACS Canto, using FACS Diva software to quantify cell populations.

Cell death was analyzed by staining the cells with an APC labelled anti-Annexin V antibody using the APC Annexin V kit (BioLegend, 640919). Briefly, cells were incubated with 5µL of the antibody in 100 µL of 1X Annexin V binding buffer at room temperature in the dark for 15 minutes. Then, additional 400 µL of 1X Annexin V binding buffer were added to the samples. A minimum of 10,000 cells was analyzed per sample with a FACS Canto using an excitation wavelength of 633 nm. FlowJo software was used to quantify the percentage of dead cells.

SRB assay

Cell proliferation was measured by the SRB assay. 500 cells were seeded in flat-bottomed 96-well plates and left for overnight adherence. In the appropriate time points, cell medium was removed from the plate and cells were fixed with 10% TCA for 1 hour at 4ºC. Then, they were washed with twice water and stained with 0.057% SRB in 1% acetic acid for 30 minutes at room temperature. After that, cells were washed twice with 1% acetic acid and finally resuspended in 100 µL of 10 mM Tris pH 10.0. Cell mass was assessed by measuring the absorbance at 540 nm, and proliferation fold change at each time point was inferred by comparing the absorbance value to an initial value.

Drug sensitivity was measured by calculating their half maxima inhibitory concentration (IC50). 5000 cells were seeded in flat-bottomed 96-well and treated with different doses of the appropriate compounds after overnight adherence. 72 hours upon treatment, SRB assays were conducted as described above, and cell survival was estimated by comparing each drug dose to the absorbance value of the lowest dose. All drugs used were purchased from

Materials and Methods

MedChemExpress: afatinib (HY-10261), dactolisib (HY-50673), dasatinib (HY-10181), erlotinib (HY-50896), gefitinib (HY-50895), saracatinib (HY-10234), and selumetinib (HY-50706).

Chromatin immunoprecipitation (ChIP) - qPCR

Chromatin immunoprecipitation (ChIP) was conducted using the SimpleChip® Enzymatic Chromatin IP Kit (Cell Signaling, 9003). A suspension of $2 \cdot 10^7$ cells in 40 mL of culture media were cross-linked with 1.08 mL of 37% formaldehyde at room temperature for 10 minutes. The crosslink was quenched with the addition of 4 mL of 10X glycine solution for 5 minutes. Then, cells were centrifuged at 500g for 5 minutes at 4ºC and cell pellets were washed twice with 20 mL of ice-cold PBS with protease inhibitor cocktail (PIC). After the second wash, the cell pellet was resuspended in 4 mL of 1X Buffer A with 0.5 µM dithiothreitol (DTT) and PIC and incubated on ice 10 minutes. After centrifugation at 2000g for 5 minutes at 4ºC, nuclei pellets were washed once with 4 mL of 1X Buffer B with 0.5 µM of DTT. Then, nuclei pellets were resuspended with 400 µL of 1X Buffer B with 0.5 µM and 2 µL of micrococcal nuclease and incubated for 20 minutes at 37ºC with soft agitation for chromatin digestion. The digestion was stopped with 40 µL of 0.5 M of EDTA, and nuclei were pelleted by centrifugation at maximum speed at 4ºC. The nuclei were resuspended in 400 µL of 1X ChIP Buffer with PIC and sonicated to break the nuclear membranes. Nuclei lysates were clarified by centrifugation at 10,000g at 4ºC and the supernatant was recovered. 50 µL of this supernatant were used for chromatin digestion evaluation by assessing the chromatin fragments size in an 1% agarose gel, and for the determination of the chromatin concentration by NanoDrop. A volume equivalent to 5 µg of digested chromatin was scaled to a final volume of 300 µL of 1X ChIP Buffer with PIC. 6 µL of it were removed and stored until further use as a 2% input control sample. The remaining sample was incubated overnight at 4ºC with rotation with 5 µL of the primary antibody anti-GTF3C1 (Novus Bio, NB100-60657) or anti-POLR3A (Cell Signaling, 12825).

Next day, samples were incubated with 20 µL of protein G magnetic beads at 4ºC with rotation for two hours to capture the chromatin fragments bound to the antibodies. Protein G beads were pelleted with a magnetic separation rack and washed three times in 1 mL of 1X low salt buffer and once in 1 mL of 1X high salt buffer at 4ºC during 5 minutes with rotation. After that, chromatin was eluted in 150 µL of 1X ChIP Elution Buffer at 65ºC for 30 minutes with vortexing at 1200 rpm followed by magnetic separation of the magnetic beads. Finally, the IP and 2% input samples, in which 150 µL of 1X ChIP Elution buffer were added in advance, were incubated for a minimum of 2 hours at 65ºC with 6 µL of 5M NaCl and 2 µL proteinase K to reverse the crosslinking. The DNA was purified using the spin columns provided with the kit.

The quantification of the immunoprecipitated DNA was performed by qPCR. Specific primers against the desired genomic regions were designed with Primer3 software with a melting temperature of 60ºC and the requirement of an amplicon sized between 100 and 150 bp. The qPCR reactions were conducted using 0.5 µL of chromatin sample, 4.5 µL of nuclease-free water, 4.85 µL of SYBR Green PCR Master Mix and 0.15 µL of the appropriate primer mix at 10 µM. The fold change among samples was calculated as a percentage of the total chromatin following the formula $100 \cdot 2^{(CT \text{ adjusted input} - CT \text{ sample})}$. ChIP-qPCR primers are listed in **Table 8**.

Oligonucleotide name	Sequence (5' to 3')
ChIP_ArgTCT41_Fd	ATTAGAAGTCCAGCGCGCTC
ChIP_ArgTCT41_Rv	GATGGCTCGGTGATGCAGAA
ChIP_IleAAT81_Fd	GTGTGGCCGGTTAGCTCA
ChIP_IleAAT81_Rv	GGTAAGTGAAGGGCCCCAC

Table 8. *List of oligonucleotides used for ChIP-qPCR experiments.*

Statistical analyses and data availability

Statistical analyses were carried out with R, GraphPad Prism 5, or IBM SPSS software. Values of $p < 0.05$ were considered statistically significant. False discovery rate (FDR) method was used for multiple comparison p-values correction.

The association between DNA methylation status and the correspondent transcript expression was assessed by Spearman's correlation. Student's t-test was performed to compare small-sized samples and large samples following a normal distribution, as evaluated by Shapiro-Wilk test. Large samples that did not follow a Gaussian distribution were compared using a Mann Whitney U-test. Chi-squared tests were used to compare proportions and contingency tables.

Survival and other relevant clinical information of patients included in TCGA cohort of interest was obtained using the TCGAbiolinks Bioconductor R package (Colaprico et al., 2016). Logrank tests and Cox regression models, were used to estimate overall survival association to DNA methylation events or transcript expression levels.

Functional over-representation analyses of a given list of genes were performed using gene ontology biological processes gene sets included in the GSEA signature database. Top ten over-represented gene clusters resulting from a hypergeometric test FDR < 0.05 were further considered.

HCT-116 wild-type and TYW2 CRISPR/Cas9-mediated knockout RNA-seq data have been deposited in the Sequence Read Archive (SRA) repository under project code PRJNA596997.

RESULTS
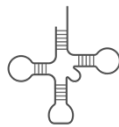
STUDY I

Role of DNA methylation defects in tumor-associated tRNA modification reprogramming

RESULTS: STUDY I

Evaluation of promoter methylation status of human tRNA modifier genes

Chemical modifications in tRNA are critical for the molecule's function at multiple levels (Suzuki, 2021). In neoplasia, aberrant patterns of tRNA modifications alter protein synthesis and contribute to the malignant cell features (Endres et al., 2019). Unfortunately, the literature concerning cancer-associated tRNA nucleoside defects is scarce and restricted to a small group of modifications or enzymes. In this study, we sought to evaluate if promoter CpG island hypermethylation-mediated silencing of tRNA modifier enzymes could participate in cancer-associated tRNA modification reprogramming and how this could contribute to tumorigenesis.

In the first place, we elaborated a curated list of human tRNA modifiers based on the gene ontology term "tRNA modification" (GO:0006400) in combination with the existing literature regarding human tRNA modifications and their cognate enzymes or their homologs in other species (**Table 9**).

Mark	Proteins	References
Adenosine		
m1A	TRMT6, TRMT61A	(Ozanick et al., 2005)
	TRMT61B	(Chujo and Suzuki, 2012)
	TRMT10C	(Vilardo et al., 2012)
	TRMT10B	(Howell et al., 2019)
	ALKBH1	(Liu et al., 2016)
	ALKBH3	(Chen et al., 2019)
	FTO	(Wei et al., 2018)
i6A	TRIT1	(Lamichhane et al., 2013)
ms2i6A	CDK5RAP1	(Reiter et al., 2012)
t6A	C14orf142, LAGE3, OSGEP, TP53RK, TPRKB	(Wan et al., 2017)
	YRDC, OSGEPL1	(Lin et al., 2018)
ms2t6A	CDKAL1	(Arragain et al., 2010)
m6t6A	TRMO	(Kimura et al., 2014)
A-to-I	ADAT1-3	(Gerber and Keller, 1999; Gerber et al., 1998)
Guanosine		
m1G	TRMT5	(Brulé et al., 2004)
	TRMT10A, TRMT10B	(Howell et al., 2019)
	TRMT10C, HSD17B10	(Vilardo et al., 2012)
m2G	TRMT11, TRMT112	(Bourgeois et al., 2017)
m2,2G	TRMT1	(Dewe et al., 2017)
m7G	METTL1, WDR4	(Alexandrov et al., 2002)
OHyW, o2yW	TRMT5, TYW1-5	(Noma et al., 2006, 2010)

Cytidine			
m3C	METLL2, METTL6	(Xu et al., 2017)	
	METTL2, DALRD3	(Lentini et al., 2020)	
	ALKBH3	(Chen et al., 2019)	
m5C	NSUN2	(Shinoda et al., 2019; Tuorto et al., 2012)	
	NSUN3	(Nakano et al., 2016)	
	NSUN6	(Haag et al., 2015)	
	TRDMT1	(Tuorto et al., 2012)	
	ALKBH1 (via hm5C)	(Kawarada et al., 2017)	
	TET2 (via hm5C)	(Shen et al., 2020)	
hm5C	ALKBH1	(Kawarada et al., 2017)	
	TET2	(Shen et al., 2020)	
f5C	ALKBH1	(Kawarada et al., 2017)	
ac4C	NAT10, THUMPD1	(Sharma et al., 2015)	
Uridine			
m5U	TRMT2A	(Carter et al., 2019)	
	TRMT2B	(Powell and Minczuk, 2020)	
ncm5U, mcm5U	ELP1-6, DPH3, KTI12, SERGEF	(Huang et al., 2005)	
mcm5U	TRMT9B, TRMT112	(Mazauric et al., 2010)	
	ALKBH8, TRMT112	(Songe-Møller et al., 2010)	
ncm5s2U, mcm5s2U	CTU1, CTU2, MOCS3, ISD11, NFS1, MPST, URM1	(Nakai et al., 2004; Noma et al., 2009)	
τm5U, cmnm5U	MTO1, GTPBP3	(Umeda et al., 2005)	
τm5s2U, cmnm5s2U	TRMU, NFS1, ISD11	(Nakai et al., 2004; Umeda et al., 2005)	
acp3U	DTWD1, DTWD2	(Takakura et al., 2019)	
D	DUSL1-4	(Xing et al., 2002)	
Ψ	PUS1	(Sibert et al., 2008)	
	PUS3	(Lecointe et al., 1998)	
	PUS7	(Behm-Ansmant et al., 2003)	
	PSU10, TRUB1, TRUB2	(Mukhopadhyay et al., 2021)	
	RPUSD2	(Behm-Ansmant et al., 2004)	
	RPUSD4	(Zaganelli et al., 2017)	
Ribose methylation			
2'-O-Me (Nm)	TARBP1	(Cavaillé et al., 1999)	
	FTSJ1, WDR6, THADA	(Guy et al., 2012)	
	TRMT13	(Wilkinson et al., 2007)	
	TRMT44	(Kotelawala et al., 2008)	
5'-P-Me	BCDIN3D	(Martinez et al., 2017)	
Others			
Q	QTRT1, QTRT2	(Chen et al., 2010)	

Table 9. *List of human tRNA modifications and the proteins involved in their deposition and removal.* This list and the references included in it were last updated in June 2021.

70

The genes included in **Table 9** were interrogated for the presence of differential methylation in their promoter regions in TCGA primary tumors and normal samples using the available data derived from the HM450 methylation microarray. Those genes that contain less than 3 CpG probes in the genomic region encompassing their TSS200 and 5'UTR or that are in sex chromosomes were excluded from the analysis. For the remaining genes (81 out of the 92 initially listed), we calculated the percentage of hypermethylated samples.

Most genes were unmethylated in both tumor and normal TCGA samples (**Figures 15, 16**). The genes that presented different methylation levels between tumor and normal tissues were the AlkB homolog 3 (ALKBH3), the dihydrouridine synthase 4-like (DUS4L), the leucine carboxyl methyltransferase 2 (LCMT2/TYW4), the pseudouridine synthase 3 (PUS3), and the tRNA methyltransferase 12 (TRMT12/TYW2).

We also conducted this analysis in a panel of almost 1,000 cell lines to corroborate the findings in TCGA cohorts (**Figure 17**). Likewise, very few genes displayed altered methylation in this set of samples compared to the normal tissue (**Figure 16**). The genes with the most variable methylation levels were TRMT9B/C8orf79 and ALKBH3, whose cancer-associated promoter hypermethylation had already been described in colon and breast cancer, respectively (Begley et al., 2013; Stefansson et al., 2017). In this analysis, DUS4L and PUS3 did not present hypermethylation in any tissue, but TYW2 and TYW4 recapitulated the results obtained in the analysis performed on TCGA sample sets.

TYW2 is silenced in colon cancer due to promoter hypermethylation

tRNA-wybutosine synthesizing proteins 2 and 4 (TYW2 and TYW4) are two of the six enzymes involved in the synthesis of the hydroxylated (OHyW) and peroxydated (o2yW) yW derivatives in position 37 of the human tRNA^{Phe} (Noma et al., 2006, 2010); see **Figure 18A**. In the late 1970s, various publications highlighted the presence of a hypomodified form of tRNA^{Phe} in tumors that lacked these residues and suggested that this phenomenon could provide growth advantages to those cells (Grunberger et al., 1975; Kuchino et al., 1982; Mushinski and Marini, 1979). Nevertheless, the cause underlying such phenomenon was never unveiled.

Since promoter CpG island hypermethylation has been extensively described as a mechanism underlying tumor suppressor silencing, we wondered the above-described epigenetic alterations impaired yW synthesis pathway and accounted for such tRNA^{Phe} hypomodification.
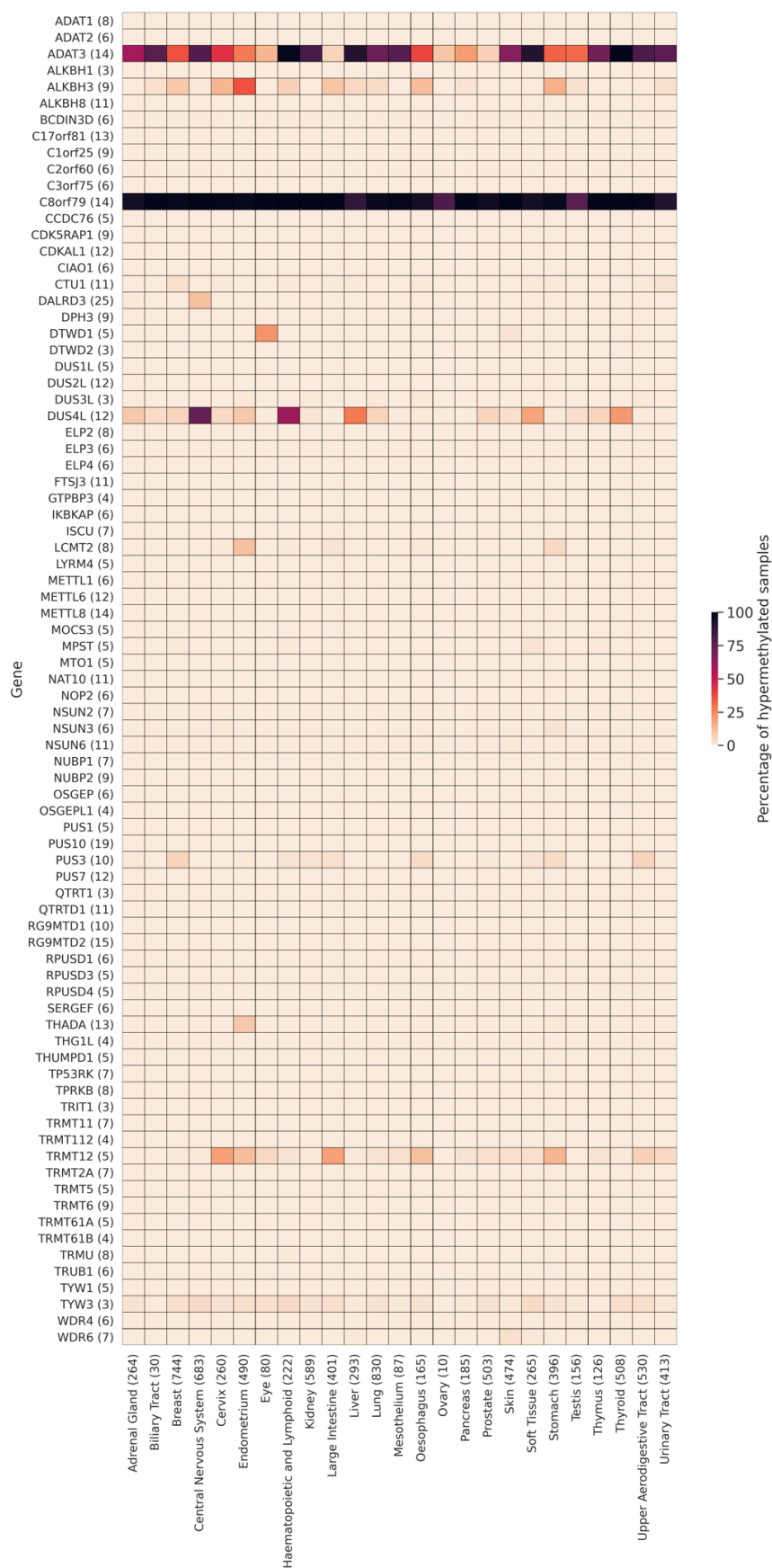
Figure 15. *Screening of tRNA modifier promoter methylation in TCGA tumor samples.* Heatmap showing the percentage of hypermethylated TCGA primary tumor samples for a total of 81 tRNA modifying enzyme genes. Numbers in brackets represent the number of probes analyzed (vertical axis) and the number of evaluated samples per tissue (horizontal axis).
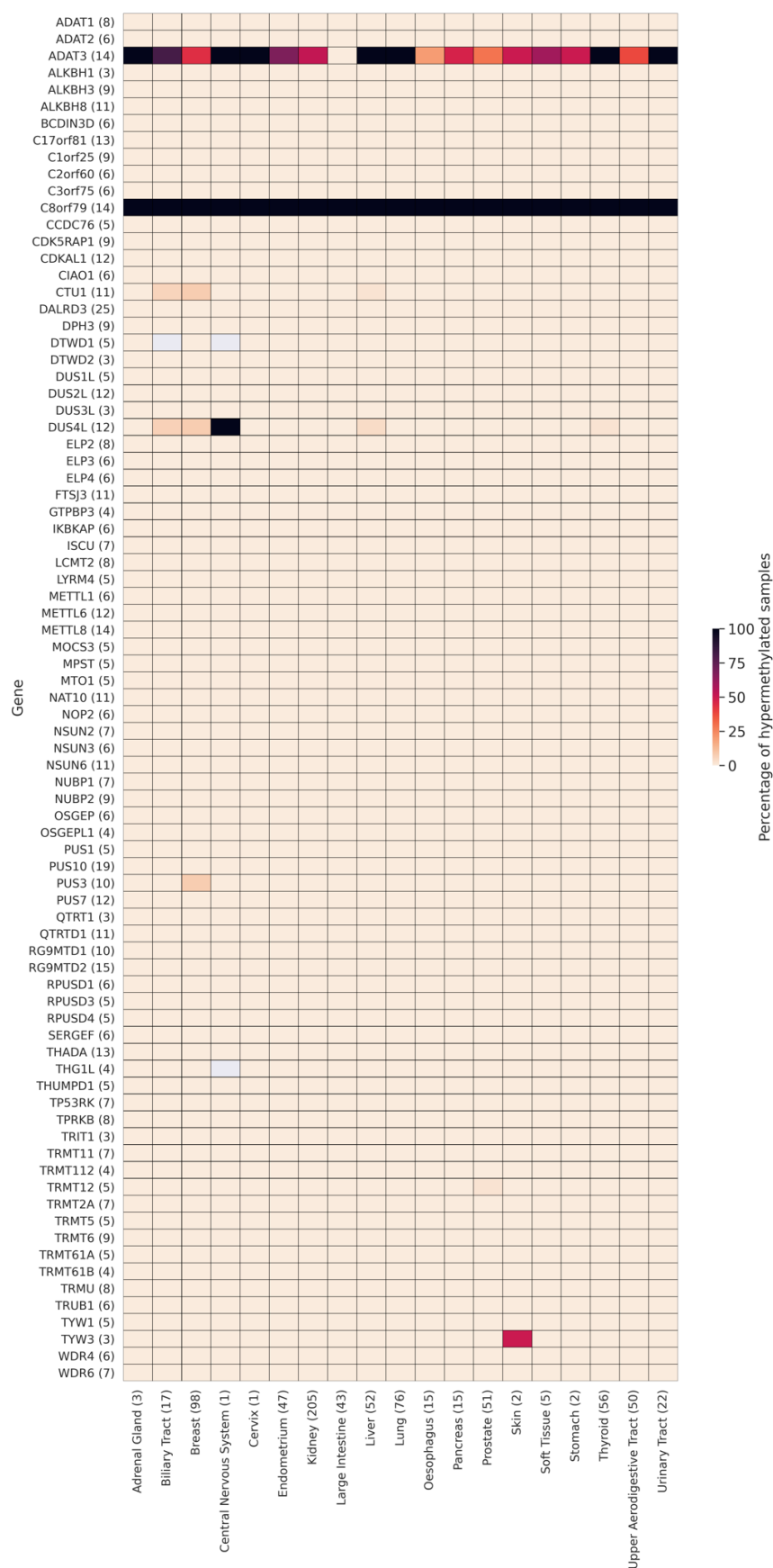
Figure 16. *Screening of tRNA modifier promoter methylation in TCGA normal samples.* Heatmap showing the percentage of hypermethylated TCGA normal tissue samples for a total of 81 tRNA modifying enzyme genes. Numbers in brackets represent the number of probes analyzed (vertical axis) and the number of evaluated samples per tissue (horizontal axis). Gray indicates missing data.
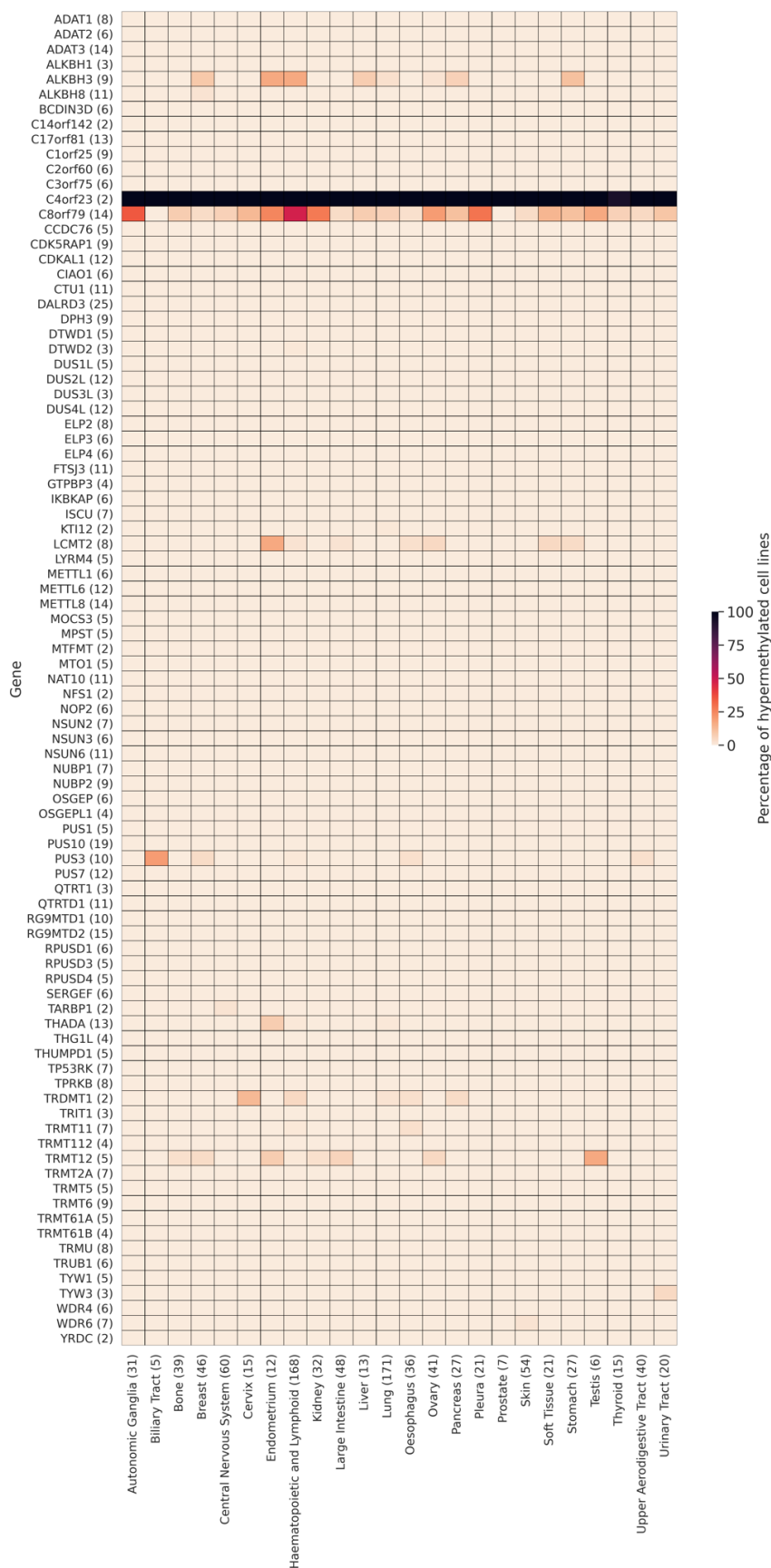
Figure 17. *Screening of tRNA modifier promoter methylation in cell lines.* Heatmap showing the percentage of hypermethylated cell lines by tissue of origin for a total of 81 genes encoding for tRNA modifying enzymes. Numbers in brackets represent the number of probes analyzed (vertical axis) and the number of evaluated cell lines per tissue (horizontal axis).

We decided to focus on TYW2 because it presented a higher number of hypermethylated cases than TYW4. In the available TCGA data, TYW2 promoter was hypermethylated in 19.0% of colorectal tumors, 17.4% of cervical tumors, 12.9% of gastric tumors, and 12.1% of uterine tumors (**Figure 15**). The examination of TCGA RNA-seq data revealed that those tissues where TYW2 expression displayed most variability matched those with the higher percentage of hypermethylated cases (**Figure 18B**). In fact, TYW2 hypermethylation negatively correlates with its expression in colorectal and cervical TCGA primary tumors (**Figure 18C**). This negative association between TYW2 promoter methylation and TYW2 transcript levels also occurred in colon cancer cell lines (**Figure 18D**).

The higher frequency of TYW2 gene promoter methylation in colorectal cancer primary tumor and cell lines and the accompanying reduction of its expression levels in silico motivated us to study of this gene in this type of tumor.
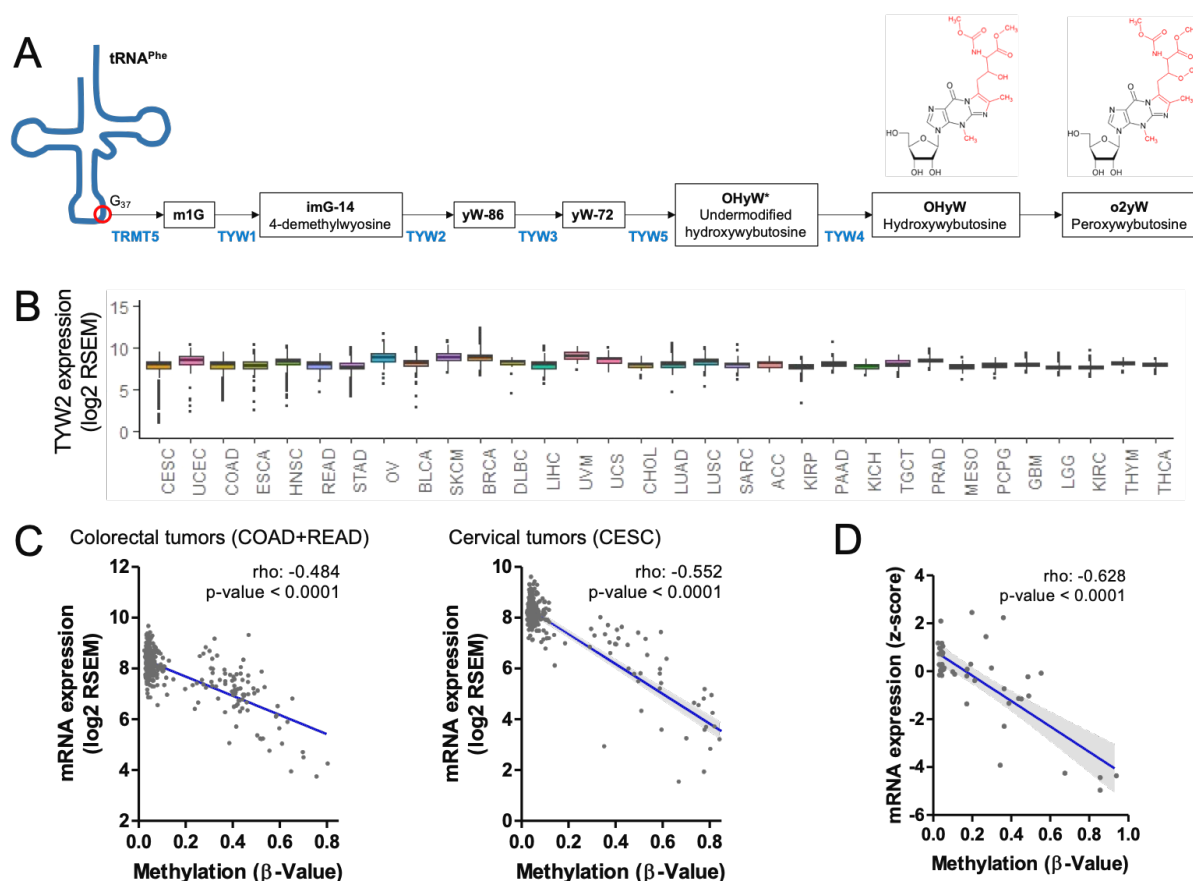
Figure 18. TYW2 promoter hypermethylation negatively correlates with its expression. (**A**) Representation of the yW derivatives synthesis pathway at position 37 of human tRNA[Phe]. The enzymes involved in each step are shown in blue. The chemical structures of OHyW and o2yW are provided. (**B**) Screening of the expression of TYW2 in TCGA datasets of solid primary tumors of TCGA. TCGA projects are ordered from higher to lower TYW2 expression standard deviation. (**C**) TYW2 methylation is significantly associated with its reduced expression in colorectal (*left*) and cervical (*right*) tumors from TCGA. Spearman's correlation, $p < 0.0001$. (**D**) TYW2 methylation is significantly associated with the loss of TYW2 transcript in colon cancer cell lines. Spearman's correlation, $p < 0.0001$.

Results: Study I

To analyze in depth the relationship between TYW2 promoter CpG island hypermethylation and the resulting transcriptional inactivation of the gene, we selected two colorectal cancer cell lines that presented TYW2 promoter hypermethylation (SW48 and HT-29) and two that were unmethylated (HCT-116 and SW480) according to the HM450-derived data (**Figure 19A**). We performed bisulfite sequencing PCR (BSP) in these four cell lines, as well as in a normal colon mucosa sample, in a genomic region that encompasses TSS and part of the 5'UTR of TYW2 gene (**Figure 19B**) to validate the HM450 methylation microarray data that was used to identify this epigenetic lesion in Sanger cell line cohort (**Figure 17**).

The two TYW2 hypermethylated cell lines showed a minimal expression of TYW2 transcript and protein compared to the unmethylated cell lines (**Figure 19C**), strengthening the correlations between TYW2 promoter methylation and transcript levels in colorectal and cervical TCGA primary tumors and in colon cancer cell lines (**Figures 18C-D**). Moreover, the DNMT inhibitor 5-azacytidine restored the expression of both TYW2 mRNA and protein in the hypermethylated SW48 and HT-29 cell lines (**Figure 19D**). This confirms the link between TYW2 promoter hypermethylation in colon cancer and the resulting transcriptional silencing.
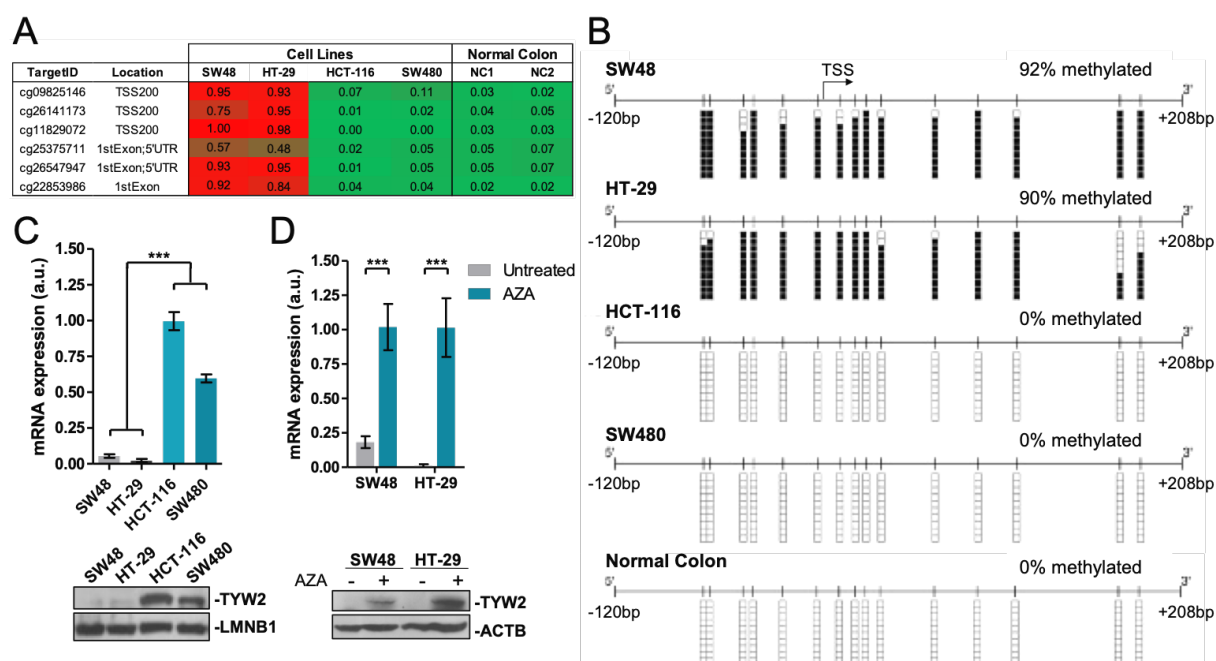
Figure 19. *TYW2 hypermethylation is associated with its transcriptional silencing.* (**A**) DNA methylation profile of the TYW2 promoter CpG island analyzed by the HM450 DNA methylation microarray of the four selected colon cancer cell lines and two normal colon mucosa samples. Single CpG absolute methylation β-values are shown (0 to 1). Red, methylated; green, unmethylated. (**B**) BSP of TYW2 promoter in four colon cancer cell lines and in normal colon mucosa. CpG dinucleotides are represented as short vertical lines. The methylation status of each CpG dinucleotide sequence is denoted with a black (methylated) or white (unmethylated) square. Single clones are shown for each sample. The TSS is marked with a black arrow. (**C**) qRT-PCR (*top*) and western blot analyses (*below*) reveal that the hypermethylated cell lines show minimal expression compared with the unmethylated cell lines. (**D**) The use of the demethylating agent 5-azacytidine (AZA) restores TYW2 expression at mRNA (*top*) and protein level (*below*) in hypermethylated SW48 and HT-29 cells. All qRT-PCR data shown represent the mean ± SD of biological triplicates analyzed using an unpaired two-tailed Student's t-test. *** $p < 0.001$.

TYW2 silencing causes the loss of yW derivatives in tRNA^{Phe}

After detecting the promoter hypermethylation-mediated TYW2 transcriptional silencing, we investigated the presence of the hypermodified OHyW and o2yW residues in tRNA^{Phe} in our colon cancer cell line panel by LC/MS (Sakaguchi et al., 2015). These determinations revealed that the fully modified nucleosides were present in the two TYW2 unmethylated and expressing cell lines (HCT-116 and SW480), while they were absent in the TYW2 hypermethylated and silenced cell lines (SW48 and HT-29) (**Figure 20**). In turn, these cell lines exhibited the intermediary 4-demethylwyosine (imG-14) (**Figure 20**), which is the direct substrate of TYW2 (**Figure 18A**). This indicates that the inactivation of TYW2 in hypermethylated cell lines blocks the synthesis of yW derivatives. Other intermediates of this pathway, like yW-86 and yW-72, were not detected in any of the cell lines, either because of their rapid conversion to other molecules in the case of HCT-116 and SW480, or because of an early arrest of the pathway in the case of SW48 and HT-29 (**Figure 20**).
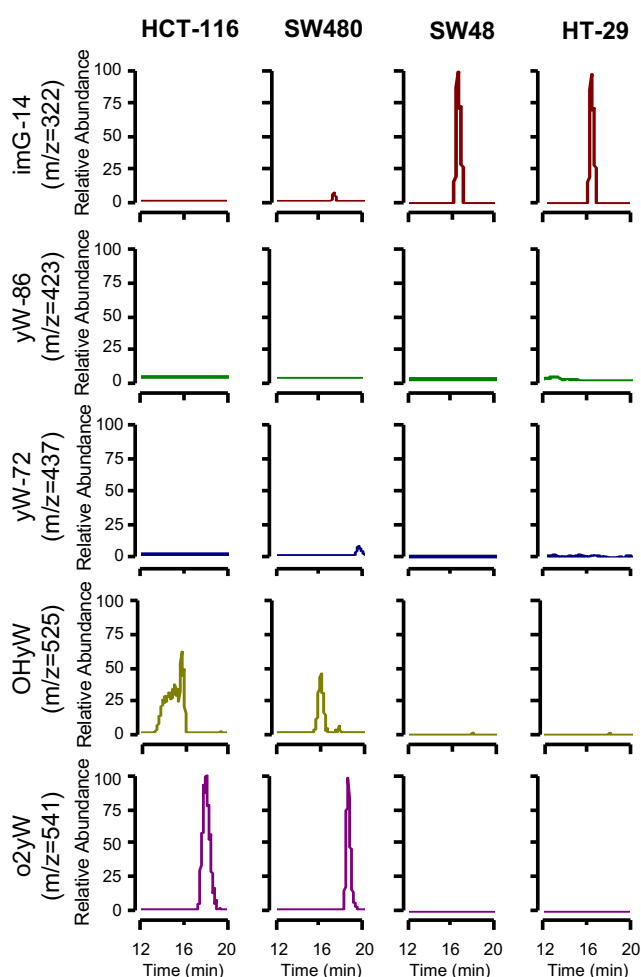
Figure 20. *TYW2-silenced colon cell lines lack OHyW and o2yW.* tRNA nucleoside analysis by LC/MS shows that OHyW and o2yW are present in the TYW2 unmethylated and expressing HCT-116 and SW480 cell lines but absent in the TYW hypermethylated and silenced SW48 and HT-29 cell lines, which accumulate imG-14.

Results: Study I

To continue investigating the association between TYW2 expression and tRNA^{Phe} modification status, we generated TYW2 KO models in HCT-116 and SW480 cell lines to imitate the effects of its epigenetic silencing. To do so, we introduced a deletion in TYW2 gene using the CRISPR/Cas9 system and confirmed it by genomic PCR and Sanger sequencing, which showed the elimination of a 234 bp fragment within the gene body (**Figure 21A**). The deletion introduced completely depleted TYW2 expression at a protein level in the two knockout models (**Figure 21B**). We also generated the reverse model by stably restoring TYW2 expression in the hypermethylated HT-29 cell line, which was verified at transcript at protein level by qRT-PCR and western blot, respectively (**Figure 21C**). OHyW and o2yW disappeared in HCT-116 and SW480 cell lines upon TYW2 silencing. Instead, they accumulated imG-14 and recapitulated the phenotype observed in the TYW2 epigenetically silenced cells (**Figure 21D**). TYW2 recovery in HT-29 cells allowed the conversion of imG-14 into OHyW and o2yW, which were not detected in the empty vector (EV)-transfected cells (**Figure 21D**). Therefore, TYW2 expression is required for the correct modification status of tRNA^{Phe} in colon cancer cell lines.
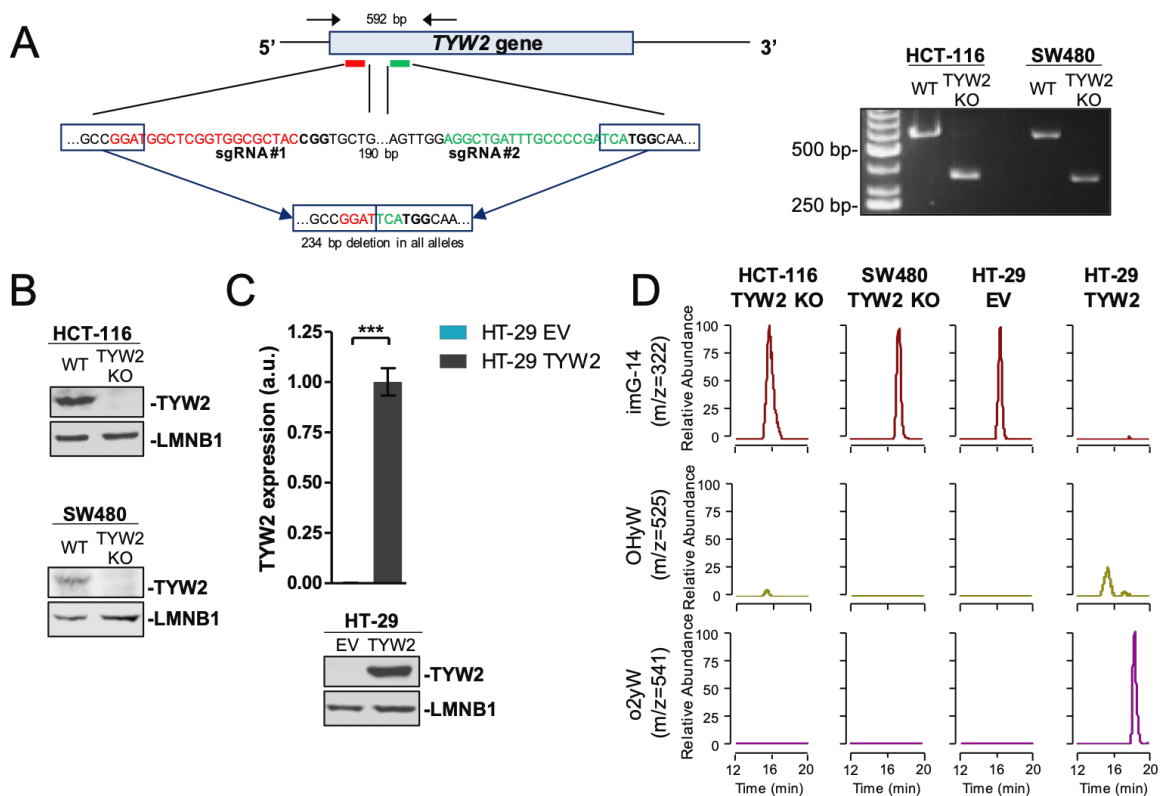
Figure 21. *Modulation of TYW2 levels affects tRNA^{Phe} modification status.* (**A**) (*Left*) Overview of the CRISPR/Cas9 sgRNA designed to target TYW2. Two sgRNA (in red and green) were transfected simultaneously and introduced a deletion of 234 bp. (*Right*) Genomic PCR performed using primers flanking the CRISPR/Cas9 targeted region (black arrows in the scheme) shows a major deletion in TYW2 gene. (**B**) Western blot proves TYW2 depletion upon the CRISPR/Cas9-mediated gene knockout in HCT-116 and SW480 cell lines. (**C**) qRT-PCR (*top*) and western blot (*below*) confirm TYW2 recovery in HT-29 cell line. qRT-PCR data shown are the mean ± SD of three biological replicates analyzed using an unpaired two-tailed Student's t-test. *** $p < 0.001$. (**D**) LC/MS shows that TYW2-silenced HCT-116 and SW480 cells lose the fully modified OHyW and o2yW and accumulate imG-14. The opposite scenario is observed upon the recovery of TYW2 in HT-29 cells.

Profiling of -1 ribosomal frameshifting in TYW2-deficient cells

Hypermodified purines at position 37 of various tRNA, like as yW and their derivatives, help maintaining the ribosome reading frame during protein synthesis to ensure translation fidelity. Concretely, yW prevents -1 ribosome frameshift events in slippery sequences as a result of proper stabilization of the codon-anticodon interaction (Carlson et al., 1999, 2001; Konevega et al., 2004). This -1 programmed ribosome frameshift (-1 PRF) occurs in sequences that are prone to ribosome slippage due to the presence of a slippery site followed by a complex secondary structure after a short spacer sequence (Dinman, 2012). This intricate secondary structure stimulates -1 PRF by pausing the elongating ribosomes and facilitating the repositioning the ribosomes and tRNAs on the slippery heptamer, thus altering the reading frame (Dinman, 2012); see **Figure 22**.
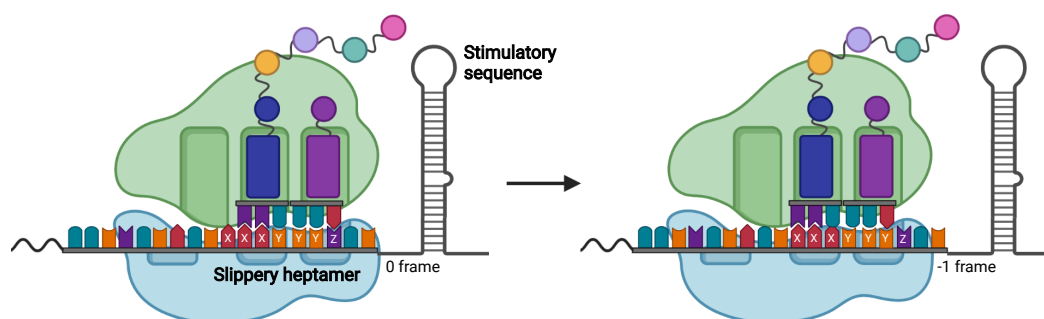
Figure 22. -1 programmed ribosome frameshifting overview. A typical -1 PRF signal is composed of a slippery site, a short spacer, and a stimulatory sequence. The slippery site consists of a heptamer with the motif X XXY YYZ, where the spaces indicate the incoming reading frame. Importantly, XXX-XXY and YYY-YYZ pairs are decoded by the same tRNA. The stimulatory sequence displays a complex secondary structure, typically a pseudoknot or a stem-loop. In short words, this stimulatory sequence pauses the ribosome on the slippery site, generating a situation that can be resolved with the re-accommodation of tRNAs in the -1 frame codons in the mRNA.

We generated a dual luciferase reporter to investigate if the tRNA[Phe] hypomodification caused by TYW2 silencing could facilitate -1 ribosome frameshifting. This construct was based on the work by Grentzmann and coworkers (1998), and resulted from the cloning of Renilla and Firefly luciferases separated by the slippery sequence from HIV (Penno et al., 2017). If ribosomes slip during the translation of this reporter and alter the reading frame, a premature stop codon emerges and prevents Firefly luciferase synthesis (**Figure 23A**). TYW2 knockout HCT-116 and SW480 cells exhibited a reduced Firefly luciferase activity compared to their wild-type counterparts (**Figure 23B**). In the opposite scenario, TYW2 recovery in HT-29 cell line increased Firefly luciferase activity compared to the EV-transfected cells (**Figure 23B**). These results demonstrate that TYW2 silencing and the loss of OHyW and o2yW in tRNA[Phe] impair ribosome reading frame maintenance and induce a phenotype that is prone to -1 PRF events in colon cancer cells.
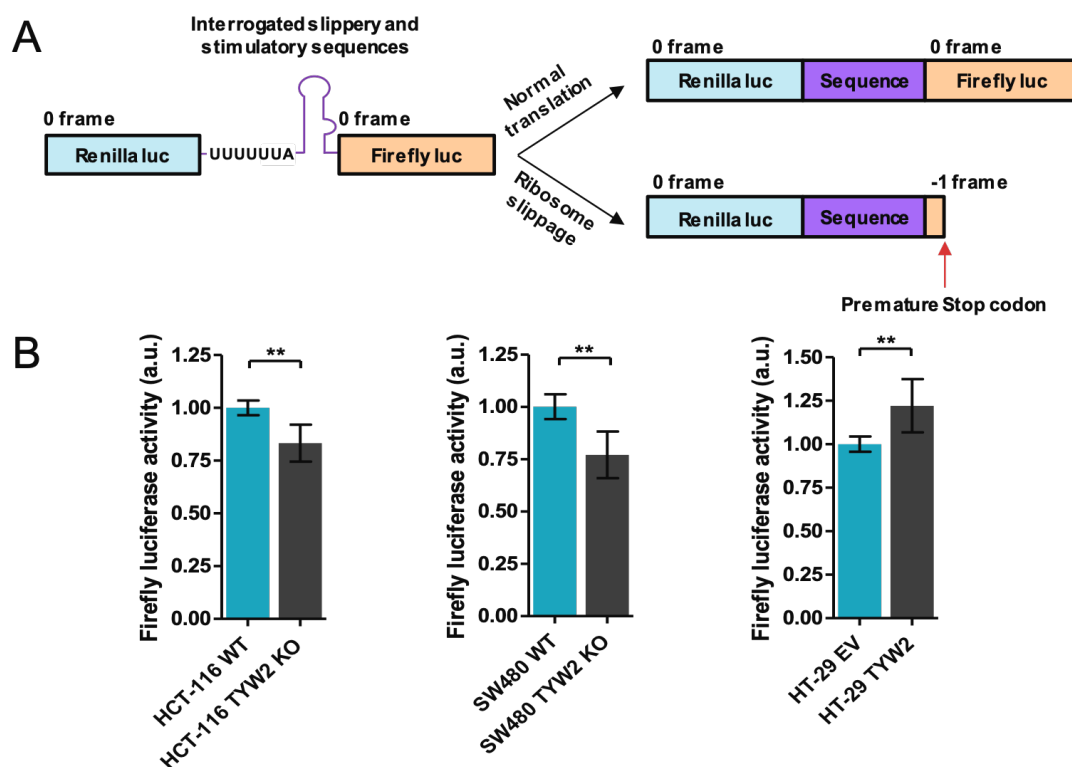
Figure 23. *TYW2 expression influences -1 ribosomal frameshifting.* (**A**) Schematic representation of the dual luciferase reporter used to monitor -1 PRF events in the colon cancer cell lines. Briefly, Renilla and Firefly luciferases are separated by the slippery and stimulatory sequences from HIV. In case of ribosome slippage, the new reading frame will abolish Firefly luciferase expression and activity due to the emergence of a premature stop codon. (**B**) HCT-116 and SW480 TYW2 knockout cell lines displayed significant reduction of Firefly luciferase activity compared to the wild-type upon the transient transfection of the dual luciferase construct. Conversely, the recovery of TYW2 in HT-29 increased Firefly luciferase activity. Data correspond to the mean ± SD of at least four biological replicates with technical triplicates. Firefly luciferase activity, normalized against Renilla activity, was compared using an unpaired two-tailed Student's t-test. ** $p < 0.01$.

Ribosome frameshifting in eukaryotic mRNAs is postulated to act as an additional layer of post-transcriptional regulation that modulates mRNA abundance (Advani and Dinman, 2016) because the introduction of a premature stop codon as a result of the ribosome slippage can induce the degradation of the affected transcript via nonsense-mediated decay (NMD). Thus, we wondered if TYW2 epigenetic silencing could promote aberrant mRNA degradation due to the defects in reading frame maintenance originated by tRNA^{Phe} hypomodification.

To explore this hypothesis, we performed RNA-seq in the TYW2-expressing HCT-116 cell line and in its TYW2-silenced derivative. This experiment revealed that the depletion of TYW2 altered the expression of 2,370 transcripts, inducing the downregulation of an 86% of them (**Figure 24A**, **Supplementary Table S1**). Parallelly, we obtained the expression of 671 of the 2,046 transcripts downregulated in HCT-116 TYW2 knockout cells from the CCLE and observed that a 61% of them (409 of 671) were also commonly under-expressed in those colon cancer cell lines harboring TYW2 promoter hypermethylation (**Figure 24B**).
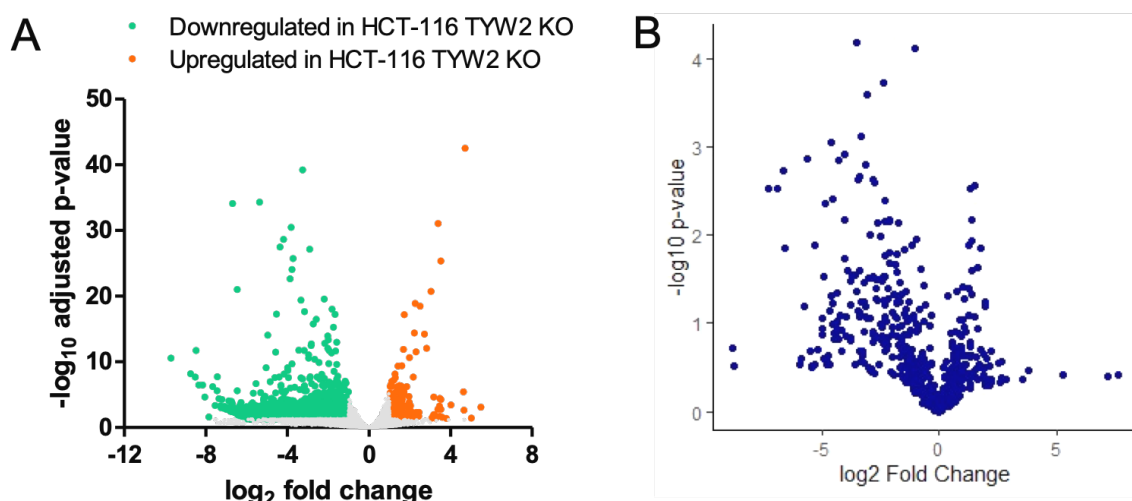
Figure 24. *TYW2 silencing alters the transcriptome of colon cancer cell lines.* (**A**) Volcano plot summarizing the results of the RNA-seq experiment conducted in HCT-116 cells and their derived CRISPR/Cas9-mediated TYW2 knockout. (**B**) Volcano plot showing the expression of 671 transcripts that are downregulated in HCT-116 upon TYW2 silencing according to the RNA-seq experiment. Data represents the log2 fold change of expression between TYW2 hypermethylated (n=4) and unmethylated colon cancer cell lines (n=43). Data normality of the methylated subset of samples was assessed using a Shapiro-Wilk test, and statistical differences among the average transcript expression were calculated using a two-tailed Student's t-test.

448 of the 671 downregulated protein-coding transcripts (**Figure 24A**) were included in a database of computationally predicted programmed -1 PRF signals (PRFdb; Belew et al., 2008). According to the PRFdb algorithm, 109 of these genes were predicted to contain at least one slippery site with UUUU/C, which is decoded by tRNA[Phe] (**Table 10**). Therefore, the expression of these transcripts may be susceptible to be directly regulated by tRNA[Phe] modification status.

These mRNAs with a predicted phenylalanine-based slippery sequence were enriched among the downregulated genes in TYW2-silenced HCT-116 cells, but their frequency in upregulated or unchanged ones as well as with all the transcripts included in the PRFdb was unaltered (**Figure 25A**). As a negative control, the transcripts containing a slippery sequence with AAAA/G, which is the codon for the frameshift-related tRNA[Lys], were not differentially enriched in any of these groups of transcripts (**Figure 25A**). Protein-coding transcripts lacking phenylalanine codons were not enriched in the set of genes downregulated in HCT-116 TYW2 knockout cell lines, indicating that their levels are unrelated to TYW2 expression in these cell line models (**Figure 25B**).

For this reason, these 109 transcripts with a putative slippery sequence decoded by tRNA[Phe] constitute bona fide candidates to be directly modulated by TYW2 epigenetic silencing in colon cancer cells.

Gene Symbol	Sites	Gene Symbol	Sites	Gene Symbol	Sites
KCNH8	GGGUUUC	LYVE1	CCCUUUU	AREG	AAAUUUC
	GGGUUUU	ACP5	CCCUUUC	BACH2	CCCUUUC
	AAAUUUC	GPR15	CCCUUUC		CCCUUUU
IFI44L	UUUUUUA	OR51I1	CCCUUUC	SYNE1	GGGUUUC
	UUUUUUC		CCCUUUU		AAAUUUC
FLRT3	GGGUUUC	ENTPD3	AAAUUUC		GGGUUUU
MSR1	AAAUUUC	SLC3A1	AAAUUUC		UUUUUUU
GPR171	UUUUUUU	GPR34	CCCUUUC		AAAUUUU
	AAAUUUC	NCF4	CCCUUUC	TMC4	UUUUUUC
GPR22	UUUUUUA	OR2AG2	CCCUUUC	SLC43A1	GGGUUUU
	AAAUUUU	GPR183	CCCUUUU	ABCA12	CCCUUUU
	UUUUUUC	TS2R31	AAAUUUU		AAAUUUC
NEGR1	AAAUUUU	C9orf50	CCCUUUC	CYP3A5	UUUUUUA
TAS2R30	AAAUUUU	LDHAL6B	CCCUUUC		AAAUUUU
GPR18	CCCUUUU	STK32A	CCCUUUC	RASIP1	CCCUUUC
	UUUUUUC	DNAH2	CCCUUUU	GPR143	GGGUUUU
EHF	CCCUUUC		UUUUUUU		AAAUUUU
OR10A4	CCCUUUU	CYP19A1	AAAUUUU	TRIM15	CCCUUUC
PKHD1	UUUUUUU	ECT2L	UUUUUUA	ANKHD1–EIF4EBP3	AAAUUUU
OR2D3	UUUUUUU		AAAUUUU	COL4A3	GGGUUUC
	UUUUUUC	F10	GGGUUUC		GGGUUUU
A2M	CCCUUUC	ANGPTL1	CCCUUUC	SERPINF2	GGGUUUC
ALK	GGGUUUC	NEXN	AAAUUUU	MUM1L1	AAAUUUU
	GGGUUUU	ZNF660	AAAUUUC	PLXNC1	AAAUUUU
	CCCUUUC	CLCNKB	CCCUUUC	SLC16A4	UUUUUUU
B3GALT2	UUUUUUA	SAMD3	CCCUUUC		UUUUUUC
ADAM20	UUUUUUA	TAS2R4	UUUUUUU	PLA2R1	AAAUUUU
ASPN	UUUUUUU		AAAUUUU		AAAUUUC
ROBO1	CCCUUUU	SLC2A3	GGGUUUU	TTYH1	CCCUUUC
	UUUUUUU	ANXA10	AAAUUUU		AAAUUUC
HSD17B2	CCCUUUU	TSHZ2	GGGUUUC	AMY2B	CCCUUUC
SFRP5	CCCUUUC	VGF	CCCUUUC		GGGUUUC
CA1	AAAUUUU	RAD51AP2	CCCUUUU	TMPRSS13	GGGUUUC
MECOM	AAAUUUC		AAAUUUU	KIAA0825	AAAUUUU
COL10A1	GGGUUUU		UUUUUUU	SLCO6A1	UUUUUUU
TAS2R46	AAAUUUU	KCNMB2	AAAUUUU	PDZD2	AAAUUUU
OR52D1	CCCUUUC	ABI3BP	CCCUUUU	FGF9	UUUUUUA
ENPP2	CCCUUUC		GGGUUUC	DDX17	AAAUUUU
ECM2	UUUUUUU	CASP10	CCCUUUC	PTPRB	UUUUUUC
CSMD4	UUUUUUA	OR51B2	CCCUUUU	TMEM200A	UUUUUUU
	UUUUUUU		GGGUUUU		GGGUUUU
	AAAUUUU	KLRK1	UUUUUUC	MATR3	UUUUUUU
	AAAUUUC	HFM1	UUUUUUU	TJP2	UUUUUUC
C17orf78	UUUUUUA		AAAUUUU	GREB1	CCCUUUC
CD33	AAAUUUC	MYH11	GGGUUUC	KIAA1257	AAAUUUC
LNX1	UUUUUUA	KIRREL2	CCCUUUC	MSH4	AAAUUUU
	UUUUUUC	ELOVL2	AAAUUUU		AAAUUUC
PKDREJ	GGGUUUC	SAMD12	AAAUUUC	ITGB8	UUUUUUU
	UUUUUUG	TCB1D19	CCCUUUU		CCCUUUU
	UUUUUUC		UUUUUUC	OMD	UUUUUUA
	UUUUUUA	ZNF84	UUUUUUU		GGGUUUU
	UUUUUUU		AAAUUUC	FUT9	AAAUUUU

Table 10. Downregulated transcripts in TYW2-silenced HCT-116 cells that contain at least one predicted slippery sequence composed of UUUU/C. The gene symbol and all the computationally predicted UUUU/C motifs per gene are provided for the 109 identified genes.
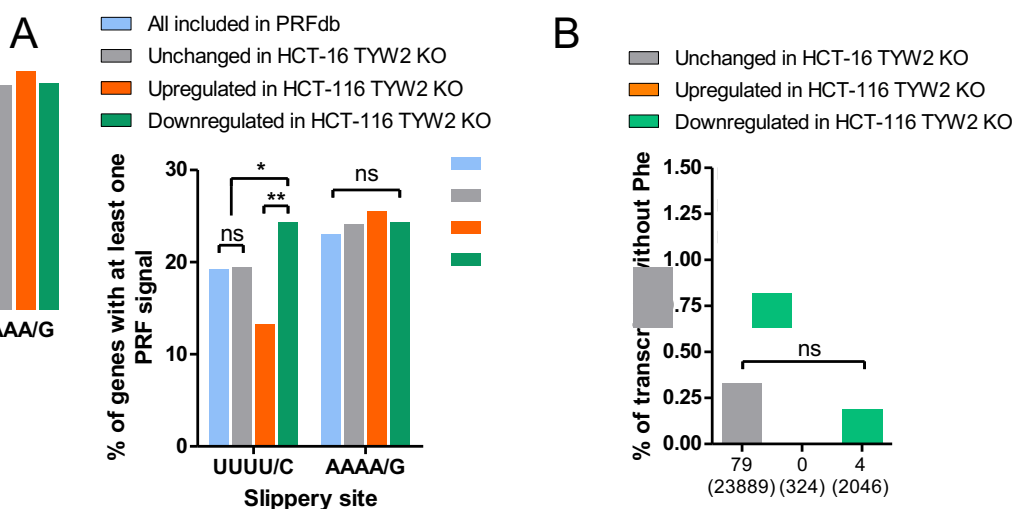
Figure 25. Transcripts downregulated in TYW2-depleted HCT-116 cells are enriched in computationally predicted -1 PRF motifs. (**A**) mRNA with at least one predicted UUUU/C -1 PRF site are enriched among the transcripts downregulated in HCT-116 TYW2 knockout cells. No enrichment is observed in the downregulated genes for transcripts containing predicted AAAA/G slippery sequences. Data represent the percentage of mRNA containing the slippery sequence of interest over the total number of protein-coding transcripts in each category. Statistical differences were assessed using Chi-squared test. ns, not significant; * $p < 0.05$; ** $p < 0.01$. (**B**) The proportion of mRNAs that lack phenylalanine codons is unaltered among the unchanged and deregulated genes in HCT-116 TYW2 knockout compared to the wild-type. The number of phenylalanine-lacking transcripts is provided below their correspondent bar in the plot. The number in brackets corresponds to the total number of genes in that category. Transcripts' sequences correspond to the Gencode v34 Genome version. Statistical differences among proportions were calculated using a Chi-squared test. ns, no significant.

Characterization of ROBO1 as a downstream target of TYW2 silencing

We hypothesized that the increased -1 PRF frequency in TYW2-silenced cells could regulate the expression of tumor suppressor genes via NMD to increase the severity of the disease. Among the 109 identified TYW2 targets that contained a predicted -1 PRF motif with UUUU/C (**Table 10**), we selected the roundabout guidance receptor 1 (ROBO1) for further validation and study because it is lost in some tumors (Rezniczek et al., 2019; Tricoli et al., 2018) and it is proposed to act as a negative regulator of cell migration in colon cancer cells (Feng et al., 2016; Huang et al., 2015; Zhang et al., 2020a).

First, we validated the downregulation of ROBO1 in CRISPR/Cas9-mediated TYW2 knockout HCT-116 and SW480 cell lines compared the wild-type at transcript and protein levels (**Figure 26A**). TYW2 recovery in the hypermethylated HT-29 cell line induced the reverse profile of ROBO1 expression, which showed an increased expression in TYW2-expressing cells compared to the EV-transfected ones (**Figure 26A**). Using α-amanitin, a specific RNAPII inhibitor, we determined that the reduced ROBO1 expression in TYW2 silenced HCT-116 and SW480 cell lines could be caused by a decrease in mRNA stability (**Figure 26B**). Conversely, TYW2 overexpression in HT-29 cells stabilized ROBO1 transcript (**Figure 26B**).
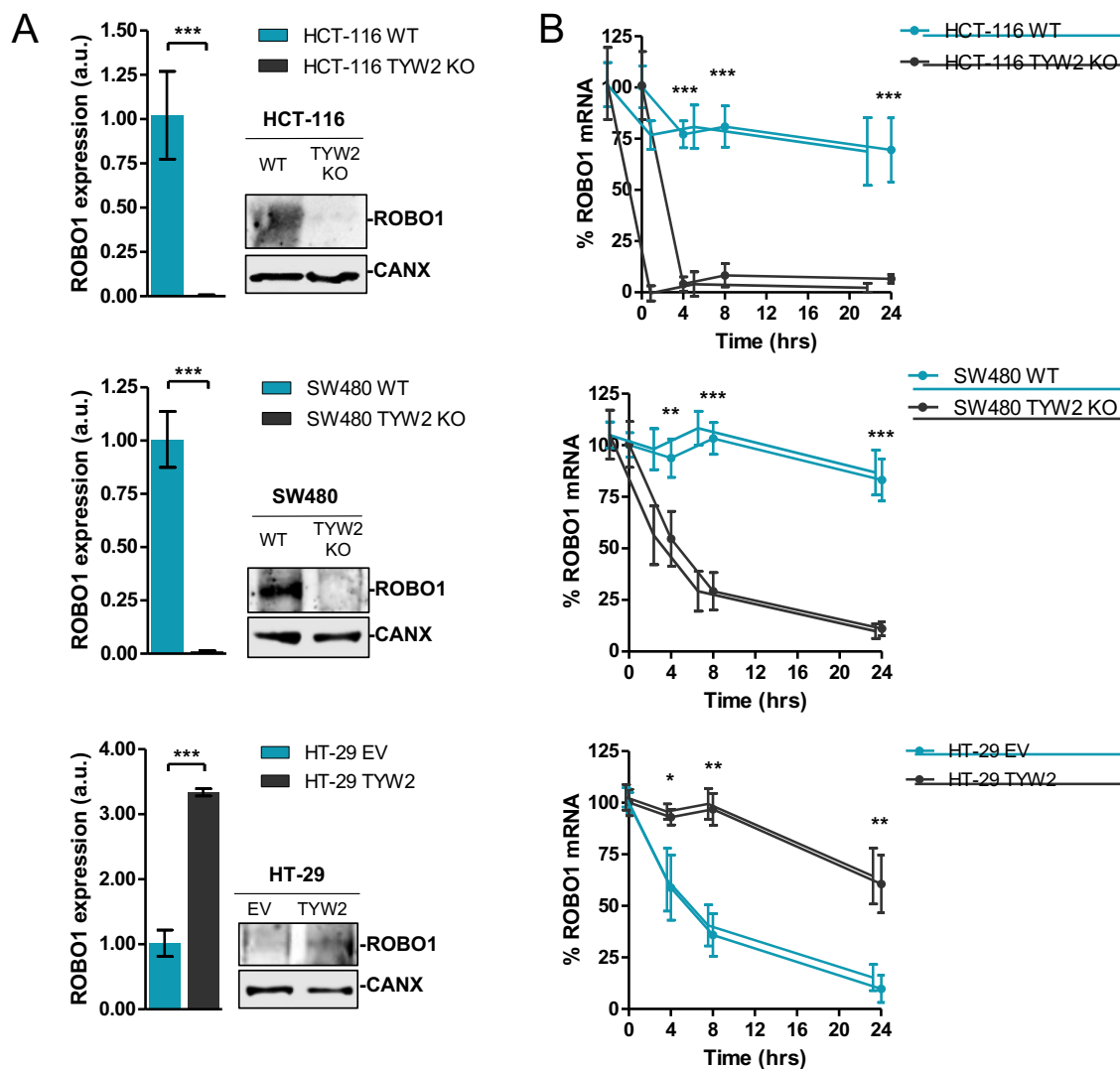
Figure 26. *ROBO1 expression is reduced in TYW2-silenced cells because of a decreased mRNA stability.* (**A**) qRT-PCR (*left*) and western blot (*right*) show that TYW2 silencing in HCT-116 and SW480 leads to ROBO1 expression reduction, while ROBO1 expression is increased in HT-29 cells upon TYW2 restoration. qRT-PCR data correspond to the mean ± SD of biological triplicates analyzed using a two-tailed Student's t-test. *** $p < 0.001$. (**B**) α-amanitin chase assays measured by qRT-PCR reveals a reduction in ROBO1 half-life in TYW2-deleted HCT-116 and SW480 compared to the wild-type and a stabilization of the transcript upon recovery of TYW2 in HT-29 cell lines. Data represents the mean ± SD of at least three biological replicates analyzed using a two-tailed Student's t-test at each time point. * $p < 0.05$; ** $p < 0.01$; *** $p < 0.001$.

Importantly, TYW2 expression did not affect the stability of other transcripts whose expression was reduced (tumor suppressor candidate 3, TUSC3) or unaltered (NAD(P)H Quinone Dehydrogenase 1, NQO1; and poliovirus receptor, PVR) that lacked any predicted -1 PRF slippery site containing UUUU/C according to the PRFdb algorithm (**Figures 27A-B**). Altogether, our results indicate that TYW2 expression levels and tRNA^Phe modification status participate in ROBO1 mRNA abundance regulation by modulating its stability.

Figure 27. *The stability of transcripts lacking predicted -1 PRF sites unaffected by TYW2 expression.*
(**A**) qRT-PCR shows that TUSC3 expression is reduced when TYW2 is silenced (*top*), while NQO1 and PVR transcript levels are unaffected by TYW2 expression (*below*). qRT-PCR data represent the mean ± SD of biological triplicates analyzed using a two-tailed Student's t-test. ns, not significant; * $p < 0.05$; *** $p < 0.001$. (**B**) α-amanitin chase assay measured by qRT-PCR of TUSC3 (*top*), NQO1 (*middle*) and PVR (*below*) does not exhibit any differences in mRNA stability between TYW2-silenced cells compared to their TYW2-expressing counterparts. Data shown correspond to the mean ± SD of at least four biological replicates analyzed by an unpaired two-tailed Student's t-test at each time point. ns, not significant.

85

Results: Study I

Next, we evaluated if the reduced stability of ROBO1 mRNA was associated with NMD. -1 PRF in ROBO1's slippery sequence would originate a premature stop codon around fifty nucleotides upstream the next exon-exon junction, which would make this transcript a good candidate to be monitored by NMD. To test our hypothesis, we targeted NMD using a siRNA targeting the RNA helicase responsible for its initiation: the up-frameshift 1 protein (UPF1) (Kurosaki et al., 2019). The reduction of UPF1 expression and the suppression of NMD increased ROBO1 levels in TYW2-deficient cells but not in the TYW2-expressing cells, corresponding to those presenting altered ROBO1 stability (**Figure 28A**). As a positive control for the assay in TYW2 silenced cells, we monitored the expression of two transcripts that are reportedly affected by UPF1 levels and undergo NMD according to Mendell et al. (2004): the uridine phosphorylase 1 (UPP1) and the dual specificity phosphatase 10 (DUSP10).
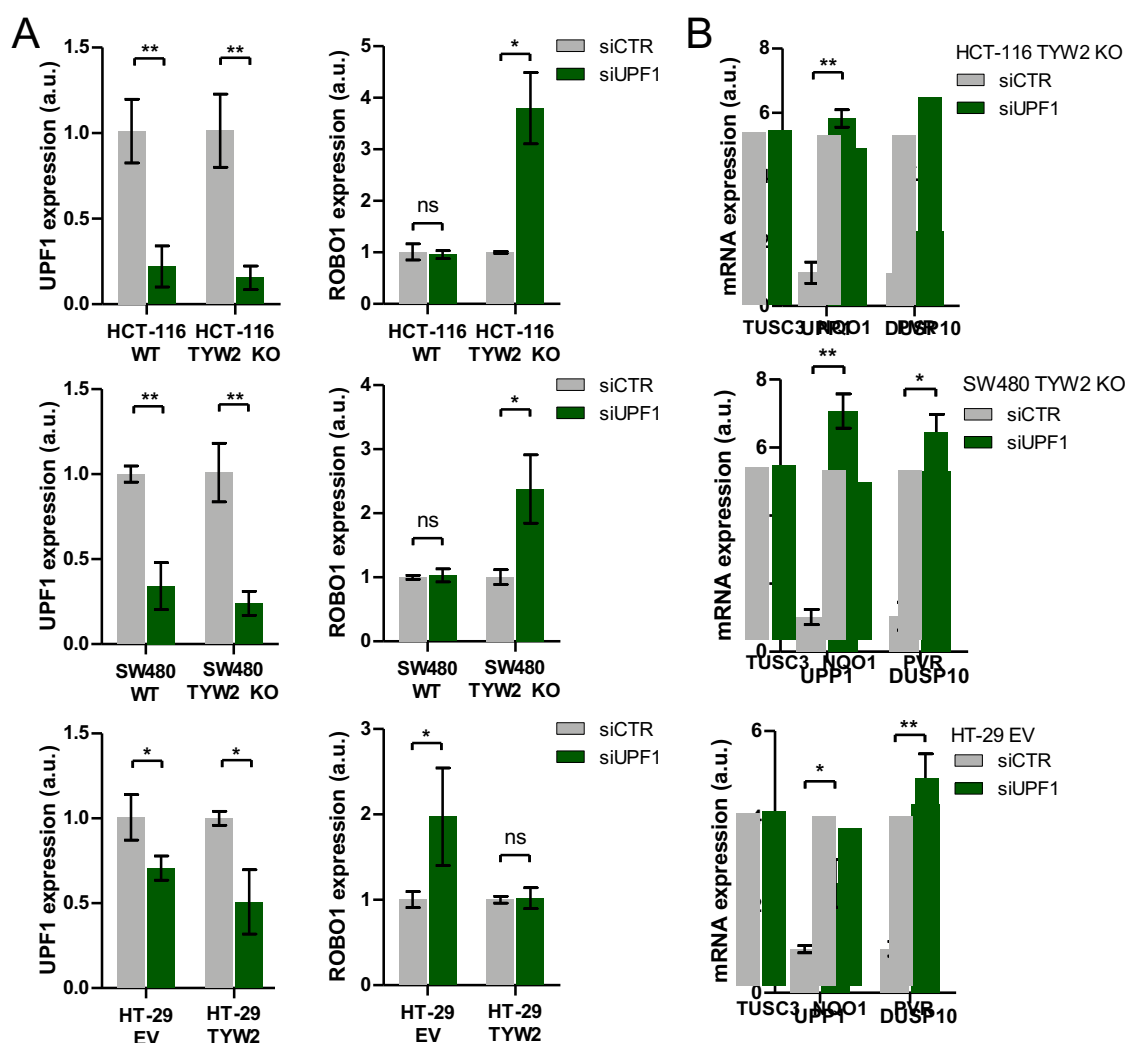
Figure 28. ROBO1 mRNA is accumulated upon NMD inhibition in TYW2-silenced cells. (**A**) Reduction of UPF1 expression using a specific siRNA (siUPF1, *left*) provokes an accumulation of ROBO1 transcript (*right*) in TYW2-silent cells compared to the cells transfected with a scrambled siRNA (siCTR), as assessed by qRT-PCR. This accumulation is not observed in their TYW2-expressing counterpart cells upon siUPF1 transfection. (**B**) UPP1 and DUSP10 levels increase in TYW2-deficient cell line models upon UPF1 knockdown. All qRT-PCR data represent the mean ± SD of biological triplicates analyzed by an unpaired two-tailed Student's t-test. ns, not significant; * $p < 0.05$; ** $p < 0.01$.

The expression of these transcripts was affected by UPF1 silencing in a similar magnitude as ROBO1 (**Figure 28B**). Overall, these results are compatible with the hypothesis that ROBO1 downregulation in TYW2-deficient cells results from increased -1 PRF events that lead to its degradation via NMD.

To irrefutably assess the impact of TYW2 loss in the induction of frameshifting during ROBO1 translation, we cloned ROBO1 predicted slippery and stimulatory sequences in the previously used dual luciferase reporter vector where -1 ribosome frameshifting originates a premature stop codon that yields a truncated protein lacking Firefly luciferase activity (**Figures 23A, 29A**). The CRISPR/Cas9-mediated deletion of TYW2 in HCT-116 and SW480 cells caused a reduction in Firefly luciferase activity compared to the wild-type cells (**Figure 29B**). Oppositely, TYW2 restoration in HT-29 cells increased Firefly activity (**Figure 29B**). Importantly, and to guarantee that the observed differences in reading frame maintenance between conditions were caused by the specific slippage of tRNA^{Phe}, we also produced a dual luciferase reporter where the phenylalanine codons (UUU) in ROBO1 slippery heptamer were replaced by leucine codons (ACU and GCU), which should not induce -1 ribosome frameshifting (**Figure 29A**). This mutation cancelled the effect of TYW2 expression levels and tRNA^{Phe} modification status on Firefly activity (**Figure 29B**).
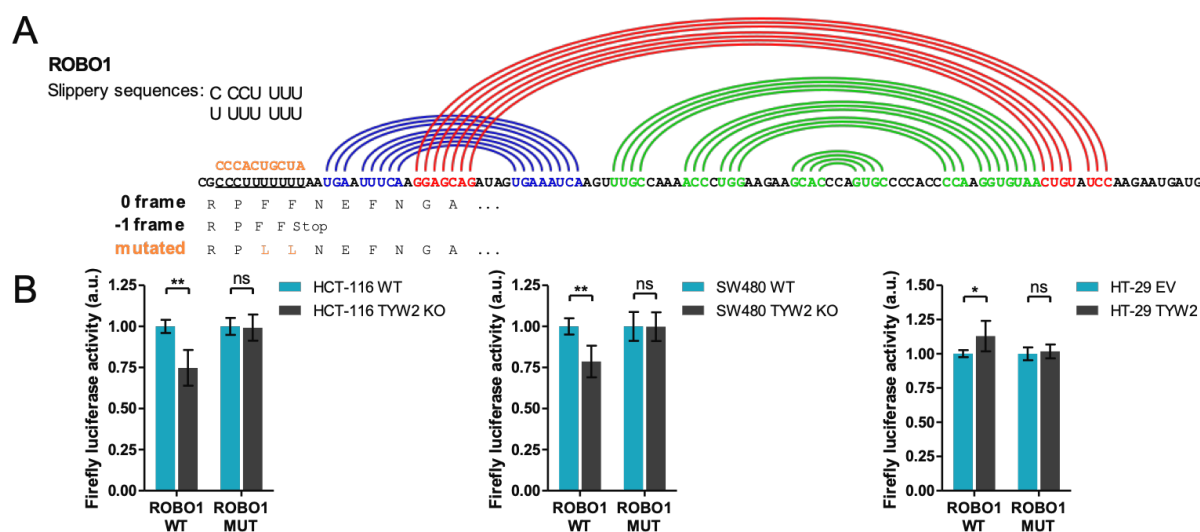
Figure 29. ROBO1 transcript contains functional -1 PRF sites. (**A**) Schematic representation of the two overlapping slippery sequences in ROBO1 predicted by the PRFdb tool. The nucleotides in colors indicate the putative folding of this sequence after the slippery heptamers decoded by tRNA^{Phe} (C CCU UUU and U UUU UUU). The amino acid sequence of the growing polypeptide chain is annotated below the RNA sequence (0 frame). In case of ribosome slippage, a premature stop codon will appear and originate a truncated protein (-1 frame). This sequence and a mutant one where phenylalanine codons are replaced by leucine (mutated; in orange) were cloned into the dual luciferase reporter designed to monitor -1 PRF. (**B**) Firefly luciferase activity is reduced in TYW2-silenced HCT-116 and SW480 cells and in EV-transfected HT-29 cells. No differences between conditions were observed when phenylalanine codons in the slippery heptamer were mutated to Leu. Data correspond to the mean ± SD of three biological replicates analyzed. Firefly luciferase activity, normalized against Renilla activity, was compared using an unpaired two-tailed Student's t-test. ns, not significant; * $p < 0.05$; ** $p < 0.01$. ROBO1 WT, wild-type Phe codons; ROBO1 MUT, mutant-introduced Leu codons.

TYW2 methylation correlates with poor clinical outcome in early-stage colorectal tumors

Having established the association between TYW2 silencing with the hypomodification of tRNA^{Phe}, the promotion -1 ribosome frameshifting events, and the induction of mRNA degradation via NMD, we evaluated if TYW2 promoter hypermethylation in primary colorectal tumors had any impact on the outcome in patients harboring this epigenetic lesion.

To do so, we studied 371 colorectal cancer cases from TCGA for which the complete clinical information was available belonging to the cohort where we had previously reported TYW2 promoter hypermethylation and transcriptional silencing. For the entire set of colorectal cancer patients (both COAD and READ projects), TYW2 promoter hypermethylation revealed a trend towards a shorter overall survival, but it was not statistically significant as assessed by the logrank test (**Figure 30A**). However, when separating patients with early- and advanced-stage tumors, those with early-stage colorectal tumors (stages I and II, n=184) presenting TYW2 epigenetic silencing displayed a significantly shorter overall survival (**Figure 30B**). Univariate Cox regression analysis reinforced the poorer prognosis in these patients with TYW2 promoter hypermethylation (Hazard Ratio [HR] = 2.98, 95% confidence interval [CI] = 1.26 to 7.08; **Figure 30B**).

The analysis of patients' overall survival based on TYW2 expression levels in the same colorectal cohort provided similar results and reinforced our previous findings. Following a similar trend, reduced TYW2 expression revealed a trend towards its association with a reduced overall survival for the entire population of TCGA colorectal cancer patients for which transcript expression and clinical information were available (n=348), although it was not significant as assessed by the logrank test (**Figure 30C**). Likewise, when patients were separated by tumor stage, early-stage colorectal patients (n=173) displaying low TYW2 transcript levels showed a significantly reduced overall survival (**Figure 30D**). A univariate Cox regression analysis supported the association of low TYW2 expression with a poorer prognosis in early-stage colorectal cancer patients (HR = 4.78, 95% CI = 2.03 to 11.27; **Figure 30D**).

In the same line as the overall survival comparisons, multivariate Cox regression analysis identified TYW2 promoter hypermethylation (HR = 2.69, 95% CI = 1.13 to 6.41; **Figure 31A**) and reduced expression (HR = 4.09, 95% CI = 1.71 to 9.79; **Figure 31B**) as independent predictors of shorter overall survival in early-stage colorectal cancer patients compared to other characteristics that have been associated with clinical outcome. Globally, these results indicate that TYW2 promoter hypermethylation and silencing is associated with poor clinical outcome in patients with early-stage colorectal cancer.
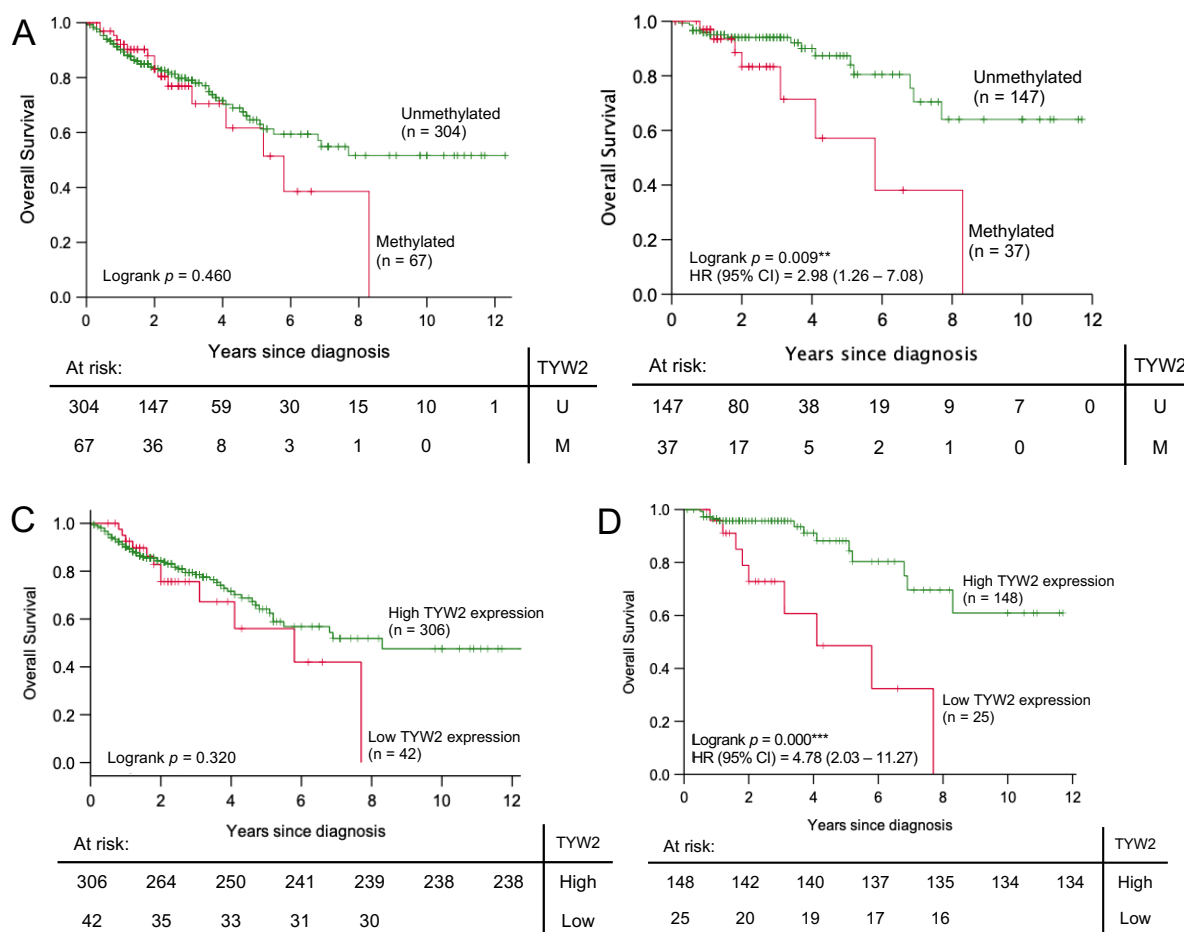
Figure 30. *TYW2 promoter hypermethylation and reduced expression are associated with shorter overall survival in patients with early-stage colorectal tumors.* (**A**, **B**) Kaplan-Meier curves according to TYW2 promoter methylation status (**A**) for the entire set of primary tumors and for (**B**) early-stage colorectal cancer patients reveal a trend towards a shorter overall survival of patients presenting hypermethylation. Green line, unmethylated cases; red line, hypermethylated cases. *p*-value corresponds to logrank test. ns, no significant; ** *p* < 0.01. (**C**, **D**) Kaplan-Meier curves according to TYW2 expression (**C**) for the entire cohort of primary tumors and (**D**) for early-stage colorectal cancer patients show a trend towards a poor prognosis in patients displaying reduced TYW2 levels. Green line, high expression (log2 TYW2 > 7.0); red line, low expression (log2 TYW2 ≤ 7.0). HR, hazard ratio; CI, confidence interval. *p*-value corresponds to logrank test. ns, no significant; ** *p* < 0.01; *** *p* < 0.001.

Epigenetic biomarkers are not only useful for predicting cancer patients' prognosis; they can also anticipate treatment response and thus allow therapy selection. Therefore, to complete the clinical profiling of TYW2 promoter hypermethylation-mediated silencing in colon cancer, we sought to analyze whether TYW2 expression could mediate the response to newly developed therapeutic agents and hence this epigenetic lesion could act as a biomarker to predict sensitivity to medical interventions. A lot of efforts have been put to design targeted therapies to interfere with the molecular pathways that underlie the acquisition of their malignant features –to counteract the hallmarks of cancer (Hanahan and Weinberg, 2011).
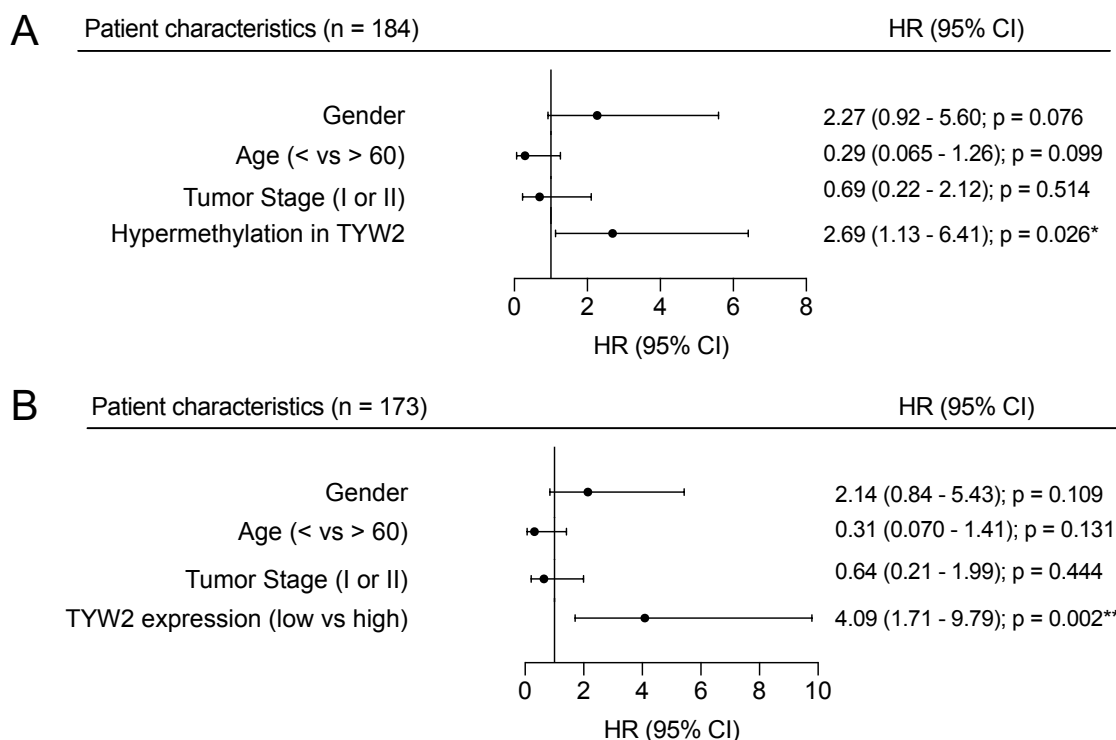
Figure 31. TYW2 hypermethylation and silencing constitute an independent prognostic factor in colon cancer. Forest plot representations of the Cox proportional hazard regression models demonstrating that (**A**) TYW2 hypermethylation and (**B**) TYW2 reduced expression (log2 TYW2 ≤ 7.0) are independent prognostic factors of poor overall survival in early-stage colorectal cancer patients. HR, hazard ratio; CI, confidence interval. ns, not significant; * $p < 0.05$; ** $p < 0.001$.

In colorectal cancer management, numerous of these targeted therapeutic strategies aim to inhibit the epidermal growth factor receptor (EGFR), the vascular endothelial growth factor receptor (VEGFR), or their related molecular pathways (Xie et al., 2020). We selected a few representative inhibitors of EGFR and its related pathways that are currently under clinical investigation (Xie et al., 2020) and tested in vitro if TYW2 expression modulation impacted cells' sensitivity to these compounds (**Figure 32**). Unfortunately, TYW2 expression did not induce differences in sensitivity against none of the compounds tested in any of our colon cancer cell line models (**Figure 32**).

Overall, although TYW2 epigenetic silencing appears to be associated with a shorter overall survival of early-staged colorectal cancer patients, its loss does not influence the response to any of the tested treatments.
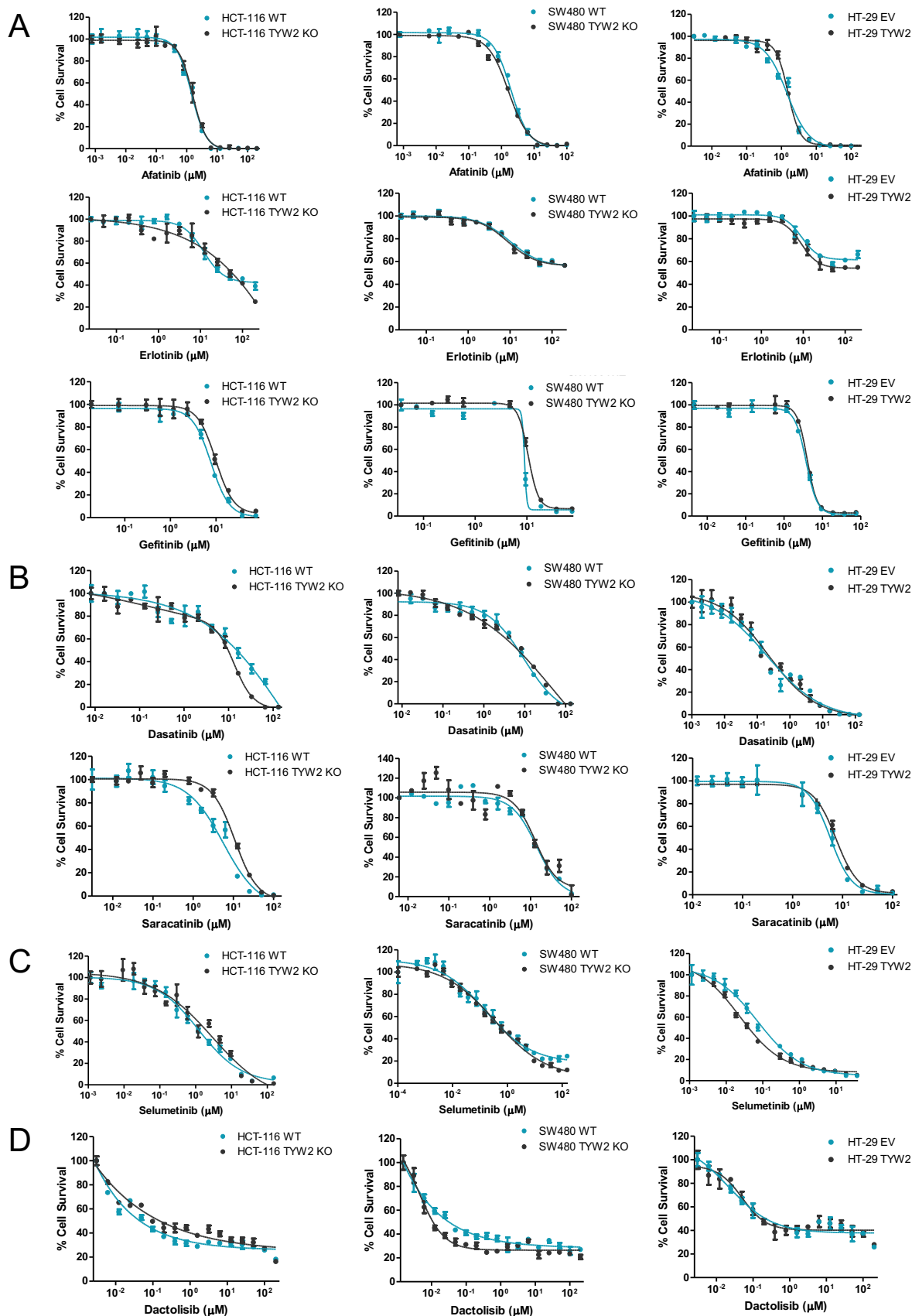
Figure 32. TYW2 expression levels do not influence the sensitivity to tyrosine kinase inhibitors that antagonize EGFR-related pathways. SRB assays show that TYW2 levels do not affect the cells' sensitivity to the tested compounds, including (**A**) three EGFR inhibitors (afatinib, erlotinib, and gefitinib), (**B**) two Src inhibitors (dasatinib and saracatinib), (**C**) one MEK inhibitor (selumetinib), and (**D**) one PI3K/mTOR inhibitor (dactolisib). IC50 graphics are representative of three independent experiments.

TYW2 silencing promotes cell migration and confers mesenchymal features

TYW2 promoter hypermethylation in colorectal cancer might permit the discrimination of those cases that, even at these initial phases, may contain transformed cells that are more prone to escape from the primary site and disseminate to other tissues, generating more advanced tumors and metastases.

The first hint of the involvement of TYW2 in these processes came from a gene set enrichment analysis using gene ontology biological process signature collections in the group of genes that were downregulated in HCT-116 upon TYW2 silencing (**Figure 24A**). The analysis showed an overrepresentation of biological process categories related to cell migration, such as "locomotion", "cell motility" and "biological adhesion" (**Figure 33**). This suggests that TYW2 deficiency in colon cancer cell lines could be related with the migration capacities of the cell.
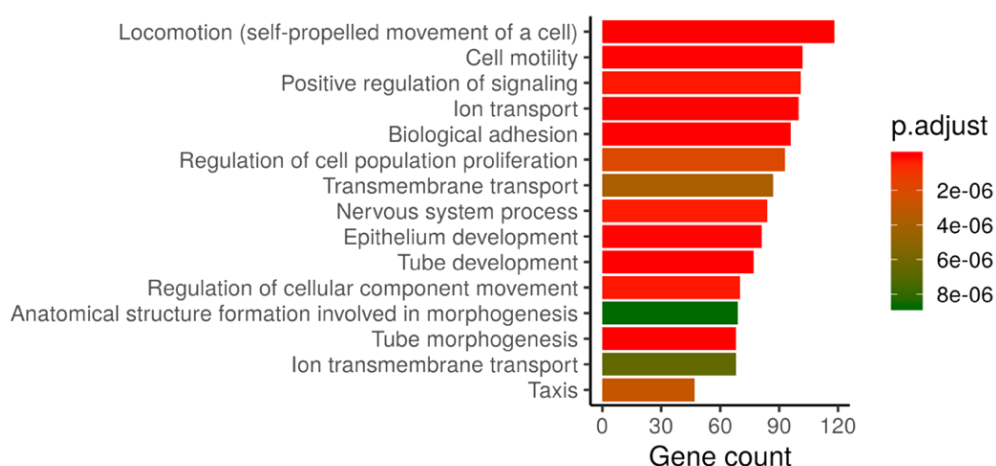
Figure 33. *Gene ontology analysis of biological process categories performed with the transcripts that are downregulated in HCT-116 TYW2 knockout cells.* The analysis reveals an enrichment of categories related to cell migration among the genes downregulated in CRISPR/Cas9-mediated TYW2 knockout in HCT-116 cells compared to the wild-type. Colors indicate the adjusted *p*-value of the functional over-representation test for each category.

To investigate this hypothesis, we tested the migration capacities in colon cancer cell line models. The CRISPR/Cas9-mediated deletion of TYW2 in the unmethylated HCT-116 and SW480 cells increased in their migration potential in comparison to their wild-type and TYW2-expressing counterparts, as determined by the Transwell migration assay (**Figure 34A**).

Seeing this, we wondered if the epithelial-to-mesenchymal transition (EMT) was involved in the increased migration capacity of TYW2-deficient cells. EMT refers to the reversible cellular program by which epithelial cells progressively lose their polarity and cell-to-cell adhesion to

gain the migratory and invasive features that are characteristic of motile mesenchymal cells (Lamouille et al., 2014). The malignant progression of many cancer types requires the activation of EMT, which provides the neoplastic cells with the capacity to disseminate to other tissues and originate a high-grade malignancy (Dongre and Weinberg, 2019).

Many molecular pathways orchestrate the regulation of EMT in cancer cells. These pathways principally converge in the downregulation of epithelial markers like E-cadherin (CDH1) and certain cytokeratines, and in the acquisition of mesenchymal markers such as Vimentin (VIM) (Lamouille et al., 2014). The TYW2-silent HCT-116 and SW480 cell lines showed a reduced expression of the epithelial marker CDH1 and an upregulation of the mesenchymal marker VIM, as assessed by qRT-PCR (**Figure 34B**). This reveals the emergence of EMT features upon TYW2 loss in colon cancer cell lines, matching the increased migration potential (**Figure 34A**) and the downregulation of ROBO1 transcript and protein due to aberrant -1 PRF events observed in these cell models (**Figure 26**).
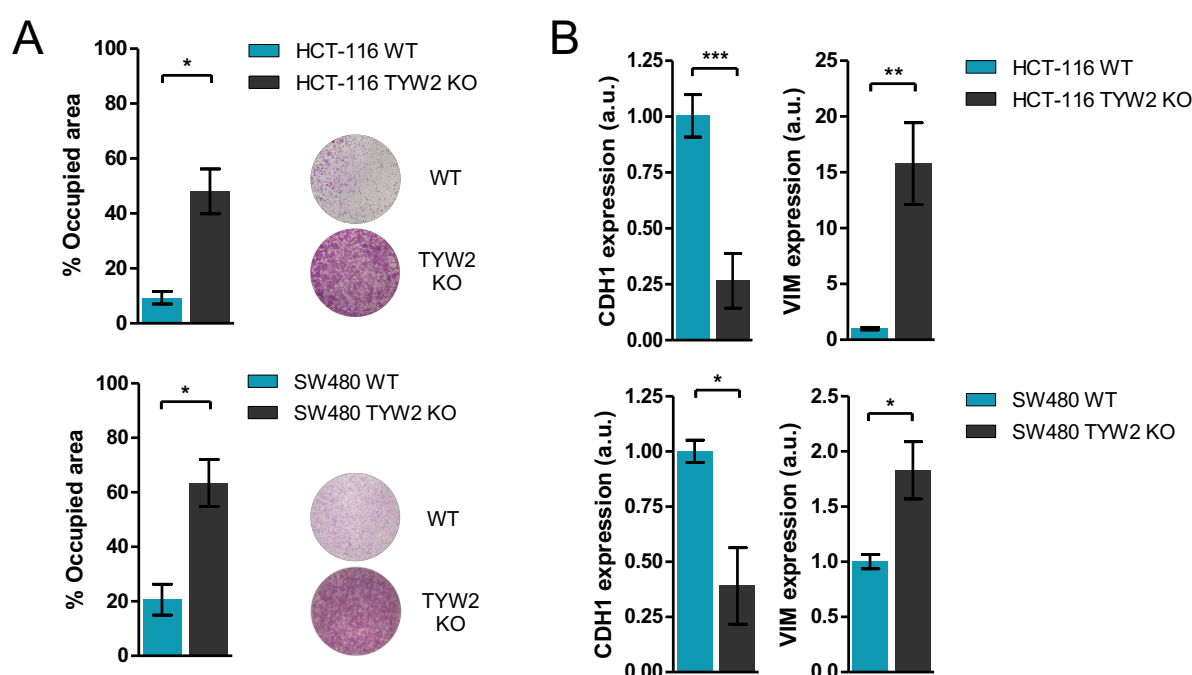
Figure 34. TYW2 silencing increases cell migration and confers mesenchymal features in a ROBO1-dependent fashion. (**A**) Transwell assay reveals an increased migration capacity of TYW2 knockout HCT-116 and SW480 cells compared to their wild-type counterparts. Data represent the mean ± SD of biological triplicates analyzed by an unpaired two-tailed Student's t-test. * $p < 0.05$. Representative images of the Transwell insert membranes are shown. (**B**) TYW2 silencing in HCT-116 and SW480 cell lines induces mesenchymal features, as assessed by qRT-PCR showing a downregulation of CDH1 expression and an increase in VIM levels. Data shown correspond to the mean ± SD of at least three biological replicates and were analyzed using an unpaired two-tailed Student's t test. * $p < 0.05$; ** $p < 0.01$; *** $p < 0.001$.

Results: Study I

To study if the mesenchymal features witnessed in TYW2 deficient colon cell lines were guided by the downregulation of ROBO1, we transiently restored its expression in the CRISPR/Cas9-mediated TYW2 knockout HCT-116 and SW480 cell lines (**Figure 35A**). ROBO1 restoration partially rescued the epithelial phenotype, as shown by an increase in CDH1 levels and a downregulation of VIM transcript (**Figure 35B**). When conducting the inverse experiment, that is depleting ROBO1 expression in wild-type HCT-116 and SW480 cell lines using a siRNA, VIM levels increased upon ROBO1 knockdown while CDH1 expression remained unaltered (**Figure 35C**). Altogether, these data point to the relationship between TYW2 expression and tRNA[Phe] modification status and the migration potential of our colon cancer cell models via ROBO1 expression modulation –although not exclusively.
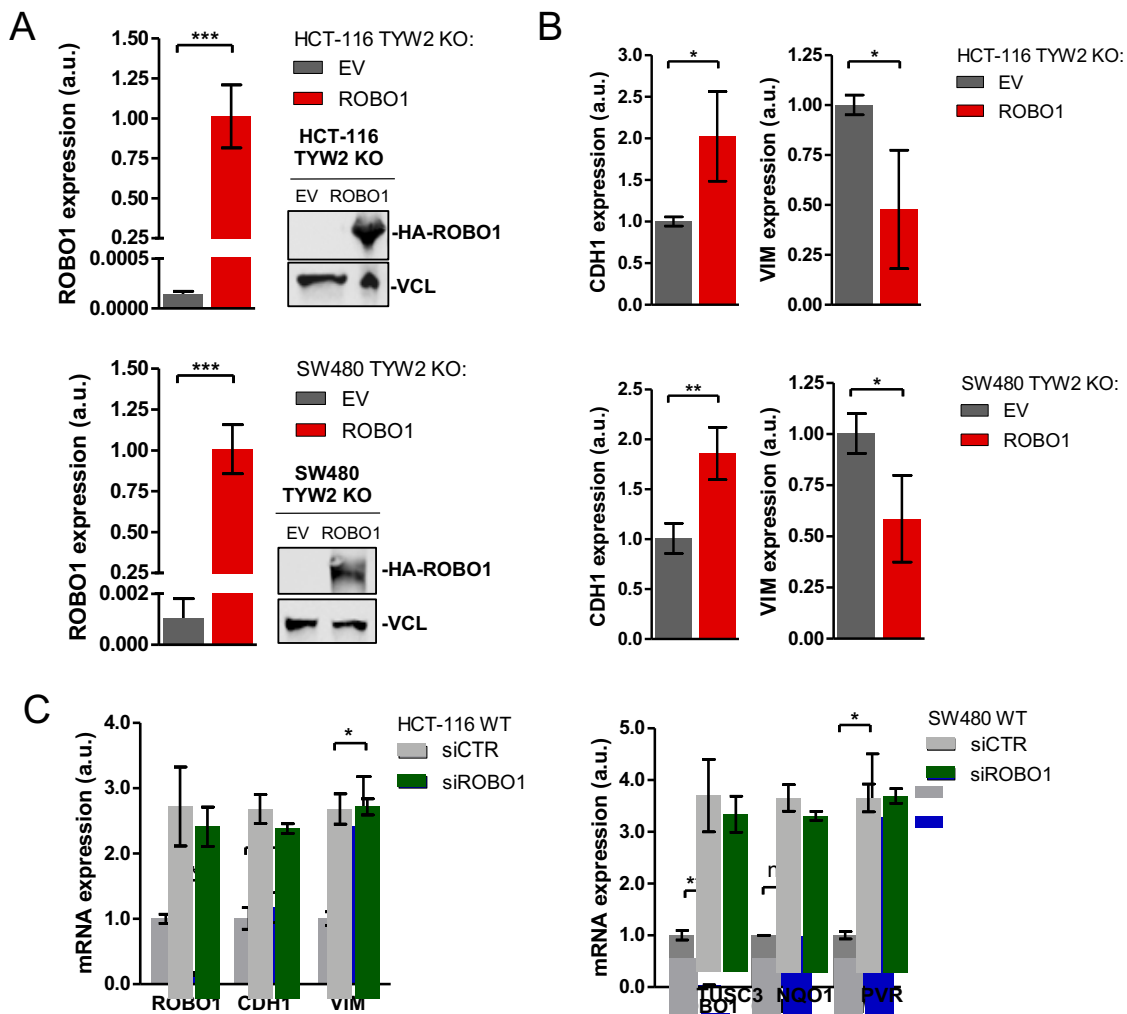
Figure 35. *ROBO1 expression restoration in TYW2 deficient cells induces the reversion of the mesenchymal characteristics.* (**A**) qRT-PCR (*left*) and western blot (*right*) confirm the efficient restoration of ROBO1 expression in HCT-116 and SW480 TYW2 knockout cell lines compared to the EV-transfected models. (**B**) qRT-PCR of CDH1 and VIM suggests a reversion of the mesenchymal features of the TYW2-depleted HCT-116 and SW480 cell lines upon ROBO1 recovery. All qRT-PCR data shown are the mean ± SD of biological triplicates and were analyzed using an unpaired two-tailed Student's t-test. * $p < 0.05$; ** $p < 0.01$; *** $p < 0.001$. (**C**) qRT-PCR experiment in wild-type HCT-116 (*left*) and SW480 (*right*) upon siROBO1 transfection increased VIM levels but not CDH1 in comparison to the siCTR-transfected cells. All qRT-PCR data shown are the mean ± SD of biological triplicates and were analyzed using an unpaired two-tailed Student's t-test. ns, not significant; * $p < 0.05$; *** $p < 0.001$.

To complete our profiling of TYW2 loss in tumor cell behavior, we analyzed the cell cycle by measuring the incorporation of BrdU and 7AAD by flow cytometry as well as the expression of p21 protein, which is a marker of cell cycle arrest (Harper et al., 1993). Cell cycle progression was unaffected by TYW2 expression in the interrogated cell line models (**Figures 36A-B**). TYW2 silencing neither affected apoptosis, as assessed by the lack of PARP cleavage evaluated by western blot (**Figure 36C**). Thus, while the results clearly suggest a role of TYW2 in cell migration, which is reinforced by the gene ontology categories overrepresented among the transcripts downregulated in TYW2-silenced HCT-116 cells (**Figure 33**), it seems that its expression does not affect cell viability (**Figure 36**).
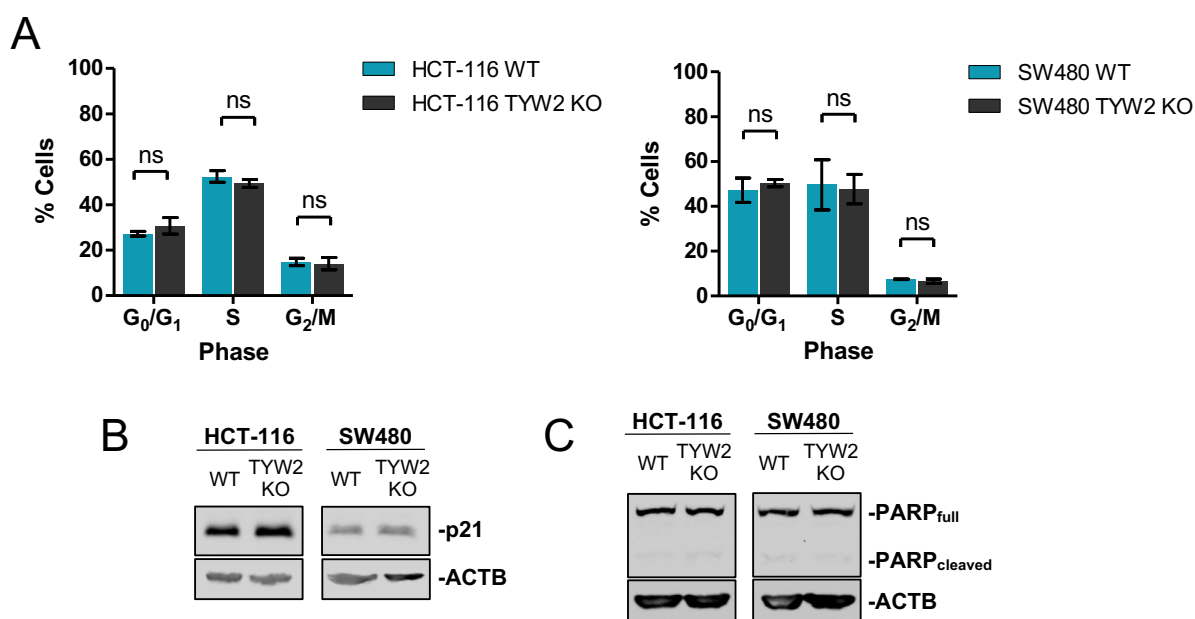
Figure 36. *TYW2 silencing does not affect cell cycle progression and cell death.* (**A**) Cell cycle analysis assessed by BrdU and 7AAD incorporation does not reveal any differences between the TYW2-expressing HCT-116 and SW480 cell lines and their derived TYW2 knockout counterparts. Data shown are the mean ± SD of biological triplicates analyzed by unpaired two-tailed Student's t-test. ns, no significant. (**B**) Western blot shows unaltered levels of p21, denoting that TYW2 expression is unrelated to cell cycle arrest. (**C**) Western blot indicates that TYW2 expression does not affect apoptosis in colon cancer cell lines, as seen by the lack of cleaved PARP.
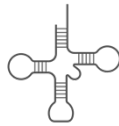
STUDY II

Contribution of DNA methylation alterations to differential tRNA expression in cancer

RESULTS: STUDY II

Tumorigenesis involves shifts in tDNA methylation patterns

The cellular tRNA pool is not static. In order to adapt to the changing cellular needs, its composition varies among tissues, in response to stress, and in disease (Rak et al., 2018). These changes in tRNA expression occur at amino acid, isoacceptor, and isodecoder levels (Pinkard et al., 2020; Zhang et al., 2018), yet the mechanisms that orchestrate such a precise regulation of tRNA abundance are poorly known.

Epigenetic mechanisms, by means of nucleosome positioning and histone modifications, control of RNAPIII activity (Good et al., 2013; Park et al., 2017), and therefore may contribute to its specificity. DNA methylation is reported to prevent TFIIIC binding to DNA (Bartke et al., 2010) and to reduce tDNA transcription in vitro (Besser et al., 1990), but the real implication of this epigenetic mechanism in the RNAPIII regulation remains unexplored. Herein, we sought evaluate if DNA methylation at tDNAs can impact their transcription rates and thus contribute to the cancer-specific alterations in tRNA expression that foster tumorigenesis.

To identify defects in the methylation of tDNA, we first retrieved the HM450 methylation microarray's probes that mapped into the genomic loci corresponding to the 416 high confidence human tDNAs (Chan and Lowe, 2016). 138 tDNAs were represented in the HM450 methylation microarray, and 95 of them were located at a greater distance than 2 kb from any other RNAPII-transcribed gene (**Figure 37**). We established this exclusion criteria and removed these genes because foreseeable interferences between elongating RNAPII and RNAPIII-mediated transcription would likely mask the effects that DNA methylation could induce on tRNA expression (Gerber et al., 2020). The elimination of cross-reactive CpGs allowed the identification of 71 tDNA that contained at least one CpG probe included in the HM450 methylation microarray. Therefore, the methylation status of these 71 genes was suitable to be efficiently interrogated with this approach (**Figure 37**).

The examination of HM450-derived data of thousands of primary tumors and normal tissues available at TCGA and of a panel encompassing approximately 1,000 cell lines revealed global differences in the tDNA methylation patterns between normal and malignant samples (**Figure 38A**). Concretely, 60 of the 71 interrogated tDNAs presented statistically significant methylation differences between normal and tumoral TCGA samples. 66 of the 71 tDNAs were differentially methylated when comparing normal TCGA samples and cancer cell lines. Most changes tended towards a methylation gain in malignant samples in both comparisons (**Figure 38B**).
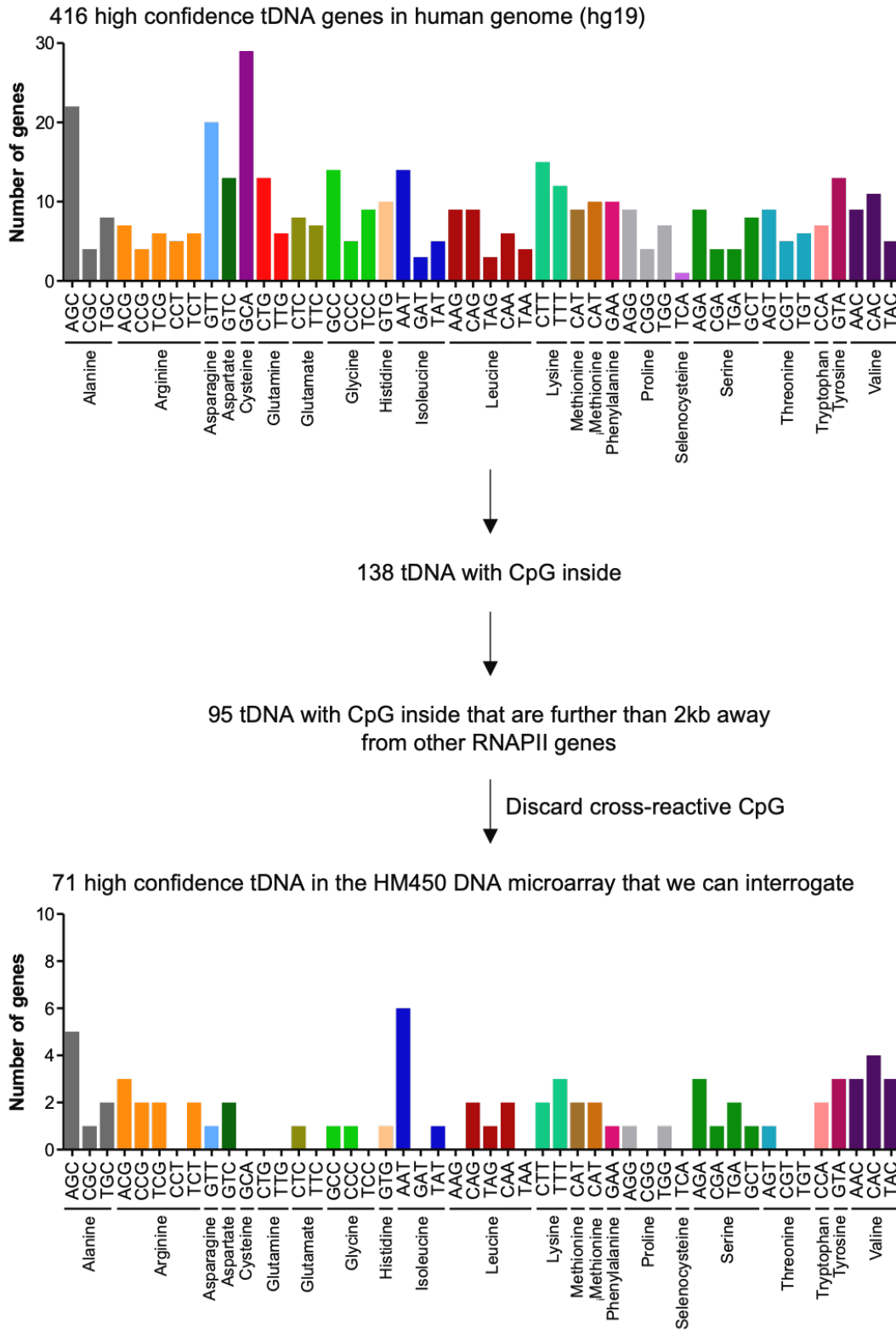
Figure 37. Interrogation of tDNA methylation using the HM450 methylation microarray. 138 tDNAs are included in the HM450 DNA methylation microarray. 95 of them are located further than 2kb from other RNAPII-transcribed. After discarding the cross-reactive CpGs, we obtain the identity of 71 tDNA genes that can be efficiently interrogated with this platform. This flowchart shows the distribution by amino acid and anticodon of all the high confidence tDNA genes (*top*) and that of the 71 genes represented in the HM450 DNA methylation microarray (*below*).

A

B

tRNA	Average normal	Average tumor	FDR Normal v Tumor		Average cells	FDR Normal v Cells	
tRNA.Ala.AGC.11.1	0.11	0.16	5.5E-34	***	0.25	2.5E-153	***
tRNA.Ala.AGC.2.1	0.06	0.07	1.5E-11	***	0.08	3.2E-03	**
tRNA.Ala.AGC.2.2	0.07	0.10	1.1E-11	***	0.11	1.2E-02	*
tRNA.Ala.AGC.3.1	0.10	0.14	2.2E-08	***	0.11	3.3E-42	***
tRNA.Ala.AGC.5.1	0.24	0.27	5.2E-12	***	0.25	5.8E-01	ns
tRNA.Ala.CGC.2.1	0.23	0.32	4.7E-16	***	0.34	1.3E-04	***
tRNA.Ala.TGC.1.1	0.06	0.10	2.7E-15	***	0.13	3.9E-44	***
tRNA.Ala.TGC.7.1	0.45	0.51	2.3E-04	***	0.46	4.1E-03	**
tRNA.Arg.ACG.2.2	0.25	0.51	1.9E-88	***	0.68	4.3E-94	***
tRNA.Arg.ACG.2.3	0.30	0.49	1.4E-72	***	0.62	1.5E-94	***
tRNA.Arg.ACG.2.4	0.20	0.29	2.3E-74	***	0.36	5.2E-83	***
tRNA.Arg.CCG.1.1	0.07	0.12	1.8E-78	***	0.20	1.5E-160	***
tRNA.Arg.CCG.1.2	0.16	0.18	1.4E-09	***	0.21	1.0E-08	***
tRNA.Arg.TCG.4.1	0.06	0.12	4.8E-61	***	0.11	4.1E-58	***
tRNA.Arg.TCG.5.1	0.08	0.11	2.2E-34	***	0.15	3.3E-114	***
tRNA.Arg.TCT.3.2	0.10	0.11	1.5E-01	ns	0.17	4.7E-125	***
tRNA.Arg.TCT.4.1	0.91	0.64	6.3E-111	***	0.37	1.2E-132	***
tRNA.Asn.GTT.8.1	0.12	0.15	7.1E-24	***	0.15	1.3E-23	***
tRNA.Asp.GTC.2.6	0.21	0.38	1.4E-95	***	0.46	2.0E-126	***
tRNA.Asp.GTC.2.9	0.30	0.42	6.5E-91	***	0.48	2.6E-119	***
tRNA.Glu.CTC.2.1	0.11	0.11	6.3E-02	ns	0.12	1.2E-06	***
tRNA.Gly.CCC.2.1	0.10	0.09	8.4E-01	ns	0.13	2.0E-63	***
tRNA.Gly.GCC.2.3	0.13	0.14	2.2E-14	***	0.16	1.4E-58	***
tRNA.His.GTG.1.5	0.15	0.22	4.2E-12	***	0.42	2.3E-139	***
tRNA.Ile.AAT.1.1	0.10	0.36	9.8E-179	***	0.66	9.7E-189	***
tRNA.Ile.AAT.2.1	0.05	0.07	4.9E-01	ns	0.08	1.5E-32	***
tRNA.Ile.AAT.3.1	0.22	0.42	6.2E-119	***	0.56	1.9E-121	***
tRNA.Ile.AAT.5.3	0.11	0.21	1.4E-62	***	0.22	6.0E-63	***
tRNA.Ile.AAT.6.1	0.32	0.55	4.7E-103	***	0.75	2.4E-167	***
tRNA.Ile.AAT.8.1	0.17	0.26	1.3E-20	***	0.30	5.9E-29	***
tRNA.Ile.TAT.3.1	0.35	0.51	8.1E-82	***	0.68	1.9E-128	***
tRNA.iMet.CAT.1.3	0.04	0.06	7.0E-02	ns	0.07	2.3E-65	***
tRNA.iMet.CAT.1.4	0.40	0.38	3.2E-09	***	0.28	1.0E-66	***
tRNA.Leu.AAG.2.1	0.20	0.26	3.4E-36	***	0.37	5.6E-158	***
tRNA.Leu.AAG.2.2	0.07	0.09	5.3E-14	***	0.09	1.7E-08	***
tRNA.Leu.CAA.2.1	0.05	0.13	1.3E-65	***	0.24	4.7E-90	***
tRNA.Leu.CAA.3.1	0.29	0.36	1.7E-13	***	0.47	5.1E-33	***
tRNA.Leu.CAG.2.1	0.42	0.54	3.6E-112	***	0.55	6.6E-87	***
tRNA.Leu.CAG.2.2	0.09	0.09	3.4E-01	ns	0.15	2.6E-105	***
tRNA.Leu.TAG.3.1	0.07	0.07	2.5E-02	*	0.06	2.2E-03	**
tRNA.Lys.CTT.2.2	0.06	0.08	5.6E-07	***	0.09	1.8E-04	***
tRNA.Lys.CTT.2.4	0.31	0.34	1.3E-02	*	0.27	6.9E-49	***
tRNA.Lys.TTT.3.2	0.09	0.09	8.4E-07	***	0.09	1.5E-01	ns
tRNA.Lys.TTT.3.4	0.04	0.04	7.3E-13	***	0.04	9.6E-19	***
tRNA.Lys.TTT.5.1	0.11	0.12	8.2E-10	***	0.17	9.6E-01	ns
tRNA.Met.CAT.3.2	0.20	0.23	8.0E-25	***	0.17	1.2E-88	***
tRNA.Met.CAT.4.2	0.08	0.25	1.3E-94	***	0.54	9.4E-120	***
tRNA.Phe.GAA.1.3	0.08	0.09	1.9E-126	***	0.09	1.1E-124	***
tRNA.Ser.AGA.2.2	0.04	0.04	4.9E-02	*	0.03	3.1E-25	***
tRNA.Ser.AGA.2.3	0.11	0.27	2.1E-83	***	0.37	1.1E-50	***
tRNA.Ser.AGA.4.1	0.29	0.37	6.1E-12	***	0.40	4.0E-01	ns
tRNA.Ser.CGA.3.1	0.08	0.13	4.0E-15	***	0.21	1.5E-04	***
tRNA.Ser.GCT.2.1	0.07	0.16	4.4E-34	***	0.27	9.8E-41	***
tRNA.Ser.TGA.1.1	0.02	0.02	6.6E-58	***	0.03	2.1E-140	***
tRNA.Ser.TGA.2.1	0.06	0.29	7.3E-168	***	0.55	5.1E-130	***
tRNA.Thr.AGT.2.1	0.06	0.06	2.4E-01	ns	0.07	1.6E-42	***
tRNA.Trp.CCA.3.2	0.06	0.15	2.3E-30	***	0.22	8.4E-36	***
tRNA.Trp.CCA.5.1	0.67	0.70	3.1E-30	***	0.86	2.4E-166	***
tRNA.Tyr.GTA.3.1	0.27	0.46	7.0E-118	***	0.58	5.0E-122	***
tRNA.Tyr.GTA.5.4	0.05	0.08	1.3E-09	***	0.18	3.9E-126	***
tRNA.Tyr.GTA.6.1	0.41	0.46	8.3E-17	***	0.57	6.7E-45	***
tRNA.Val.AAC.1.4	0.18	0.23	2.1E-120	***	0.22	7.0E-48	***
tRNA.Val.AAC.2.1	0.08	0.08	2.6E-01	ns	0.08	2.7E-01	ns
tRNA.Val.AAC.4.1	0.14	0.33	7.9E-138	***	0.63	5.3E-196	***
tRNA.Val.CAC.1.4	0.07	0.14	2.6E-01	ns	0.25	2.3E-04	***
tRNA.Val.CAC.2.1	0.18	0.28	2.5E-02	*	0.27	3.6E-04	***
tRNA.Val.CAC.4.1	0.32	0.38	1.3E-87	***	0.39	1.6E-62	***
tRNA.Val.CAC.6.1	0.37	0.52	6.2E-69	***	0.76	3.9E-151	***
tRNA.Val.TAC.1.1	0.10	0.10	8.3E-02	ns	0.10	3.2E-04	***
tRNA.Val.TAC.2.1	0.06	0.07	3.1E-01	ns	0.11	1.9E-55	***
tRNA.Val.TAC.4.1	0.09	0.29	1.6E-94	***	0.56	5.3E-107	***

Figure 38. Overview of tDNA methylation in normal and tumoral samples. (**A**) Average methylation β-values of the 71 tDNA genes of interest according to the HM450 DNA methylation microarray data available in normal (*left*) and tumor (*middle*) TCGA samples and in a panel of cell lines (*right*). (**B**) Table containing the average β-values per tDNA in TCGA normal and tumoral samples and in cell lines, as well as the FDR-adjusted *p*-values corresponding to the two-tailed Mann-Whitney U-test used to compare the methylation average between malignant samples (either TCGA tumors or cancer cell lines) and TCGA normal samples. ns, not significant; * FDR < 0.05; ** FDR < 0.01; *** FDR < 0.001.

DNA methylation patterns are different among tissues, and each tumor type displays a particular methylome (Costello et al., 2000). Therefore, we wondered whether tDNA methylation was dependent on the tissue of origin. The separation of TCGA and cell line samples according to their origin exposed that tDNA methylation was unequal among tissues in both normal and tumoral samples (**Figure 39**). Taken together, these results indicate that tumorigenesis entails epigenetic lesions in tDNAs that are unequal among tissues.
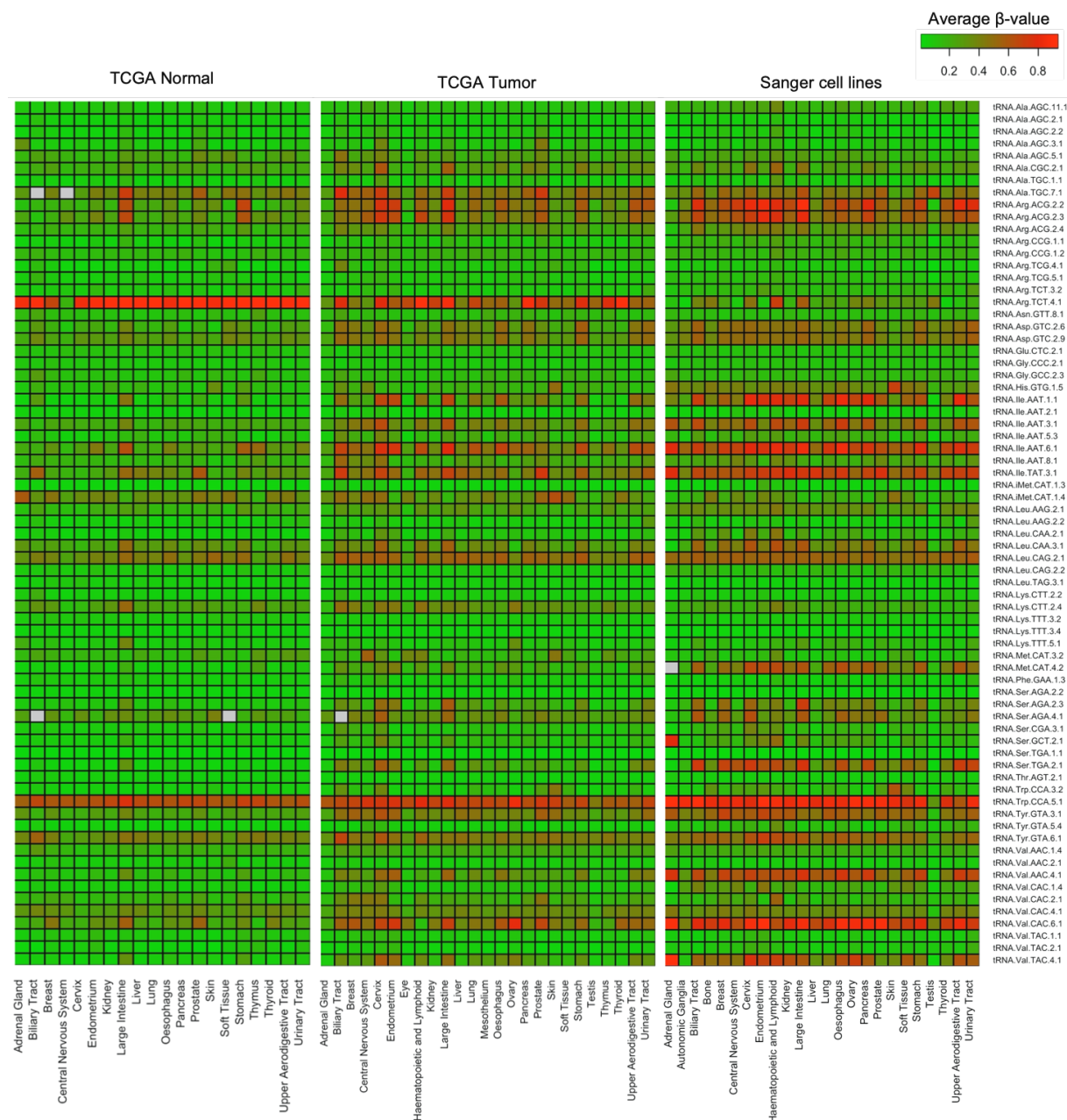
Figure 39. *Internal tDNA methylation levels in TCGA cohorts and cancer cell lines.* Heatmaps showing the HM450-derived average β-value from the for each tDNA in the different tissues from TCGA set of normal (*left*) and tumoral (*middle*) samples and in cancer cell lines (*right*). β-values span from 0 (green, unmethylated) to 1 (red, hypermethylated). Grey indicates missing values.

tDNA methylation is associated with reduced tRNA expression

Malignant cells display altered levels of some tRNAs, which can contribute to tumorigenesis (Santos et al., 2019). The observation that tDNA methylation profiles diverge between normal and tumoral samples prompted us to investigate whether these differences could guide cancer-associated variations in the expression of specific tRNAs.

To address this, we used the publicly available tRNA expression data generated by Zhang and coworkers (2018), who developed a computational pipeline to profile tRNA levels in TCGA samples using miRNA-seq datasets. By computing the Spearman's correlation between the methylation status of a given tDNA and the expression of its cognate tRNA, we discovered a negative association between tRNA methylation and expression in 60 out of the 71 pairs when considering all TCGA tumoral samples ($\rho < 0$; **Figure 40A**). However, only three of the tRNA expression and methylation pairs displayed a relevant negative Spearman's correlation coefficient ($\rho \leq -0.2$) that was statistically significant (FDR ≤ 0.05): tRNA-Arg-TCT-4-1, tRNA-Ile-AAT-8-1, and tRNA-Val-CAC-2-1.

Because tDNA methylation levels varied among tissues (**Figure 39**), we also investigated if the association between tDNA methylation and tRNA expression was dependent on the origin of the sample. To explore this question, we performed the same analysis in 25 tissues, which is a total sum of 1,775 Spearman's correlations (**Figure 40A**). 1,073 of them revealed a negative association between tDNA methylation and tRNA expression ($\rho < 0$), but only 114 of these cases presented a statistically significant robust anticorrelation ($\rho \leq -0.2$, FDR ≤ 0.05; **Figure 40B**). tRNA-Arg-TCT-4-1, tRNA-Ile-AAT-8-1, and tRNA-Val-CAC-2-1 were the tRNAs presenting the highest frequency of tissues displaying a negative correlation between tDNA methylation and tRNA expression (**Figure 40C**).

This negative association between tDNA methylation and tRNA levels in TCGA samples suggests an epigenetic control of tRNA expression. Ensuing our findings, we aimed to study in more detail the relationship between tDNA methylation and tRNA expression by providing additional support of the epigenetic silencing of two tDNA genes whose methylation is susceptible to impact tRNA expression according to our in silico results: tRNA-Arg-TCT-4-1 and tRNA-Ile-AAT-8-1 (**Figure 40C**). tRNA-Arg-TCT-4-1 is hypermethylated in most normal tissues and demethylated in tumoral samples. Conversely, tRNA-Ile-AAT-8-1 is unmethylated in normal tissues and hypermethylated in cancer (**Figures 38, 39**). We selected two cancer cell lines that were hypermethylated in these two genes according to the HM450 methylation microarray data: DND41 and SW48 (**Figure 41A**). We confirmed by BSP the methylation status of the two tDNA genes in both cell lines (**Figure 41B**). Both tDNAs are represented in the HM450 microarray by a single probe located in the internal tDNA promoter (Marck et al., 2006), hence BSP provided a comprehensive view of the methylation profile for each of them.
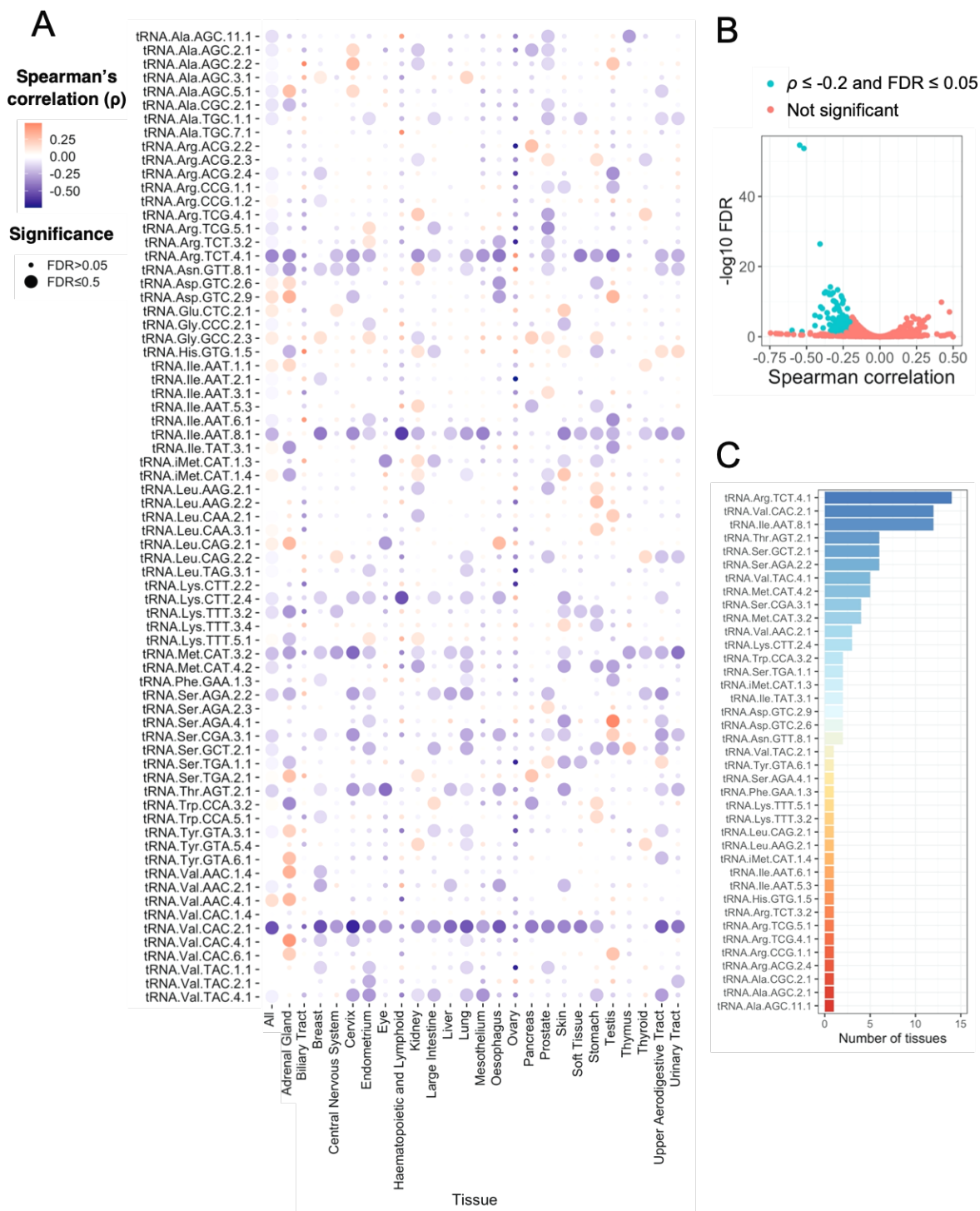
Figure 40. *tDNA methylation is negatively associated with tRNA expression in TCGA.* (**A**) Dotplot showing the Spearman's ρ of the correlation between tDNA gene methylation and the expression of their cognate tRNA in all TCGA malignant samples (*left column*, All) and subdivided by tissue of origin. Red and purple indicate a positive and negative correlation according to the Spearman's ρ, respectively. Dot size denotes the statistical significance of each correlation. Blanks correspond to missing values in *p*-value calculations. (**B**) Volcano plot representing the ρ and -log10 FDR of each computed Spearman's correlation by tissue from panel A. 114 robust, statistically significant associations (ρ ≤ -0.2, FDR ≤ 0.05) are shown in blue. (**C**) Barplot summarizing the tissue frequency of all the statistically significant negative associations between tDNA methylation and tRNA expression from panel B.

A

TargetID	MapInfo	tRNA	Cell line	
			DND-41	**SW-48**
cg12798524	1:159111423	tRNA-Arg-TCT-4-1	0.969	0.940
cg21339923	6:27636378	tRNA-Ile-AAT-8-1	0.808	0.917
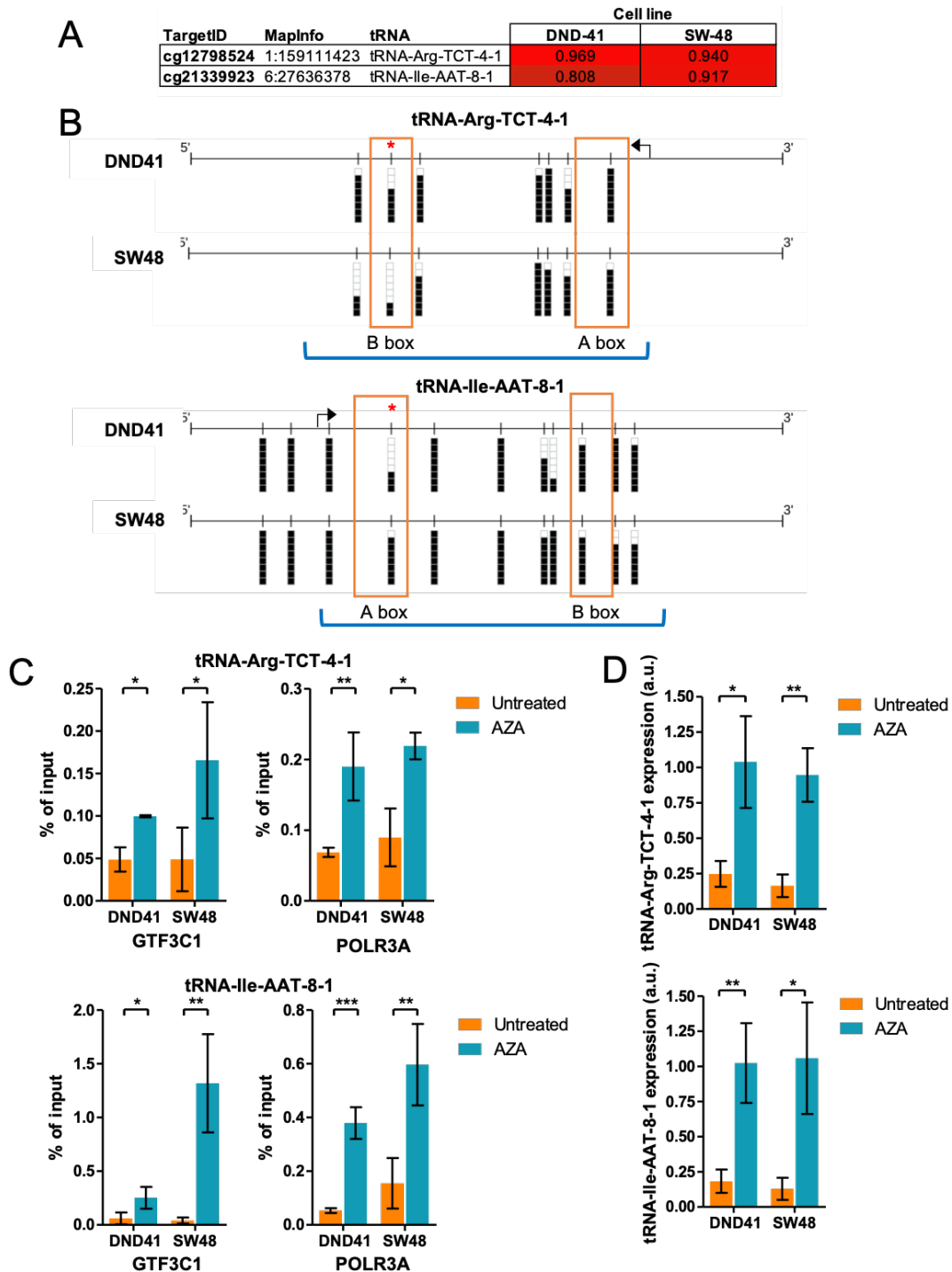
Figure 41. tDNA methylation represses tRNA expression in DND41 and SW48 cell lines. (**A**) HM450-derived DNA methylation β-values corresponding to single CpGs are shown for tRNA-Arg-TCT-4-1 and tRNA-Ile-AAT-8-1 in DND41 genes and SW48. (**B**) BSP of tRNA-Arg-TCT-4-1 (*top*) and tRNA-Ile-AAT-8-1 (*below*) genes in DND41 and SW48 cell lines. The tDNA sequence is indicated with a blue bracket, and the A and B boxes are represented with orange rectangles. The TSS is marked with a black arrow. CpG dinucleotides are represented as short vertical lines, and their methylation status is denoted with black (methylated) or white (unmethylated) squares. The CpG included in the HM450 microarray is marked with a red asterisk. (**C**) ChIP-qPCR indicate an increased binding of GTF3C1 (*left*) and POLR3A (*right*) to tRNA-Arg-TCT-4-1 (*top*) and tRNA-Ile-AAT-8-1 (*below*) genes upon treatment with 5-azacytidine (AZA) in DND41 and SW48 cell lines. Data represent the mean ± SD of biological triplicates analyzed using an unpaired two-tailed Student's t-test. * $p < 0.05$; ** $p < 0.01$; *** $p < 0.001$. (**D**) qRT-PCR shows a recovery of tRNA-Arg-TCT-4-1 (*top*) and tRNA-Ile-AAT-8-1 (*below*) expression in DND41 and SW48 cell lines after the use of 5'-azacytidine (AZA). All qRT-PCR data correspond to the mean ± SD of biological triplicates analyzed using the unpaired two-tailed Student's t-test. * $p < 0.05$; ** $p < 0.01$.

105

To evaluate if DNA methylation truly affected tRNA expression, we subjected these cell lines to a demethylating treatment with 5-azacytidine. ChIP-qPCR experiments revealed an increased binding of the TFIIIC subunit 1 (GTF3C1) and the RNAPIII subunit A (POLR3A) to the two tDNA of interest upon DNA demethylation, indicating that this epigenetic mark prevents the binding of RNAPIII transcriptional machinery to DNA (**Figure 41C**). Additionally, qRT-PCR experiments exposed that this demethylating treatment with 5-azacytidine also increased the expression levels of both tRNAs in the two interrogated hypermethylated cell lines (**Figure 41D**). Globally, our findings show that DNA methylation can actively repress RNAPIII-mediated tDNA transcription and therefore negatively impact tRNA expression, which is in accordance with the relationship between tDNA methylation and tRNA expression that arose from our in silico analysis conducted in TCGA samples (**Figure 40A**).

tDNA methylation can predict the patients' clinical outcome in TCGA cohorts

Apart from modulating gene expression to promote the malignant transformation of the cell and facilitate cancer progression, tumor-specific alterations in DNA methylation can be translated into the clinical practice as biomarkers for predicting the evolution of the disease (Ortiz-Barahona et al., 2020). Provided that the expression of some tRNA has been associated to differential overall survival of cancer patients (Kuang et al., 2019; Zhang et al., 2018), we sought to evaluate if the observed alterations in tDNA methylation that are likely to modulate tRNA expression in tumorigenesis had any impact on the outcome of cancer patients and therefore could serve as predictive biomarkers for the disease.

With this aim, we analyzed the clinical information from 31 TCGA projects to assess if these differential tDNA methylation events could anticipate patients' overall survival. For 442 of the 2,201 cases, we could not define two groups of patients to compare due to the lack of differential tDNA methylation. By performing logrank tests, we identified 86 cases in which the methylation status of a specific tDNA was significantly associated with differences in patients' survival probability (**Figure 42A**). 56 of these cases were confirmed to be predictive prognostic factors for cancer patients' outcome according to univariate Cox regression analyses (**Figure 42B**). The tRNA pool composition differs among tissues to match the cellular needs and allow the expression of different sets of proteins (Dittmar et al., 2006), therefore whether methylation predicts an increased or a reduced survival time should be evaluated individually for every tDNA and tumor (**Figure 42B**). Concretely, 50 of the altered tDNA methylation events that were associated to differential overall survival entailed a worse prognosis (**Figure 42B**).
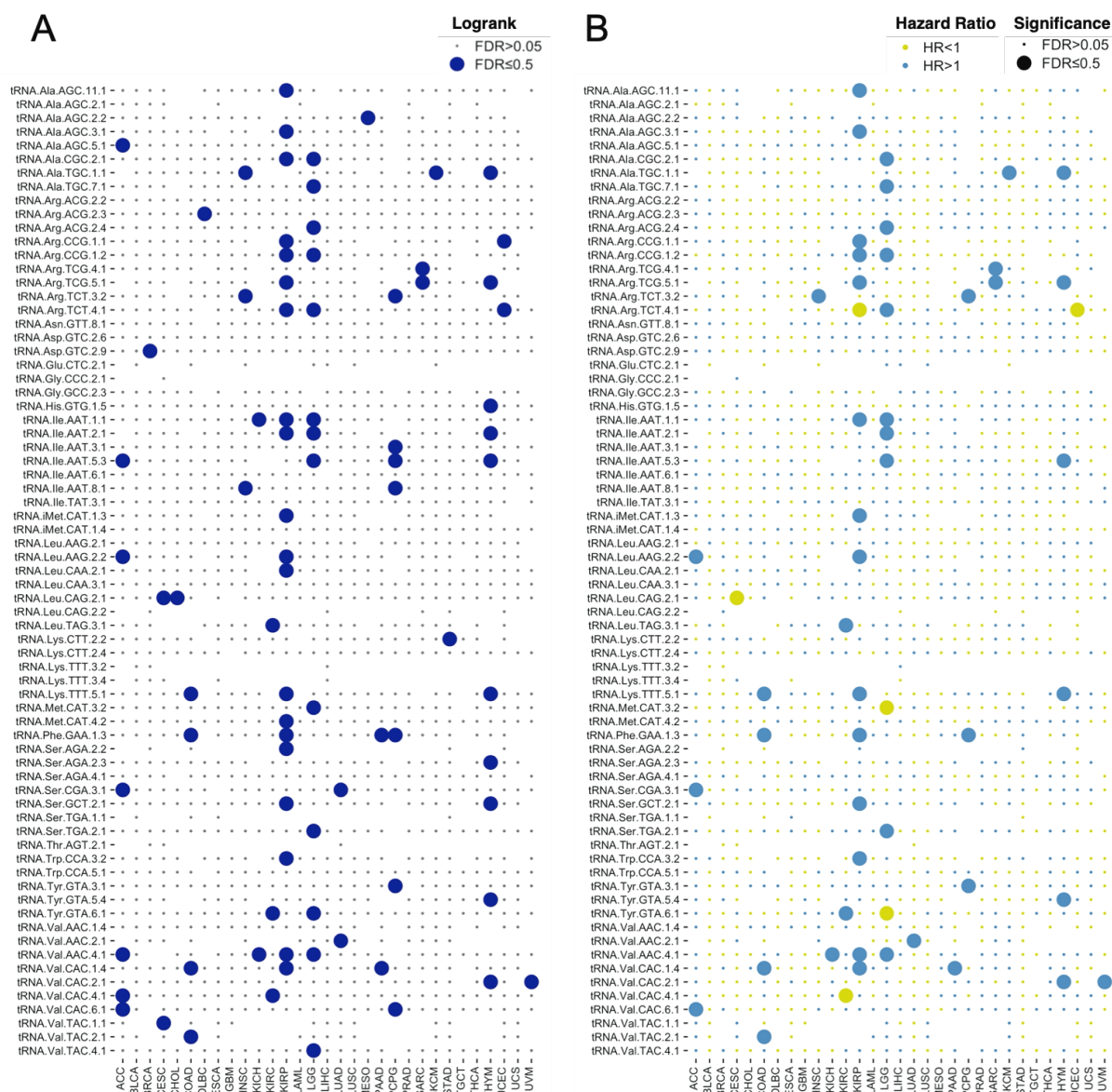
Figure 42. *tDNA methylation predicts different overall survival in cancer patients.* (**A**) Dotplot showing the FDR-corrected *p*-values of the logrank tests used to compare the overall survival of patients displaying differential methylation status of the 71 tDNAs from the HM450 microarray. Methylation cases that are significantly associated (FDR ≤ 0.05) with different prognosis are represented in dark blue. Blanks denote missing values. (**B**) Dotplot representing the predicted prognosis of the differential tDNA methylation events according to univariate Cox regression models. Large-sized points indicate statistical significance (FDR ≤ 0.05). Yellow and blue represent favorable (HR < 1) and unfavorable (HR > 1) prognosis, respectively. Blanks indicate missing values. HR, hazard ratio.

To highlight an interesting example, the methylation levels of tRNA-Arg-TCT-4-1 are significantly associated with patients' overall survival and modified risk of the disease in three TCGA projects: kidney renal papillary cell carcinoma (KIRP), uterine corpus endometrial carcinoma (UCEC) and lower grade glioma (LGG). The hypermethylation of this gene in KIRP and in UCEC –conserved from the normal tissue– was associated to a better prognosis and larger overall survival (**Figure 43**), suggesting that its cancer-specific DNA hypomethylation

can be oncogenic in these tumors. Oppositely, its tumor-associated hypermethylation in LGG patients correlated with a worse prognosis and shorter overall survival (**Figure 43**), meaning that it may display tumor suppressive roles in this tumor type.
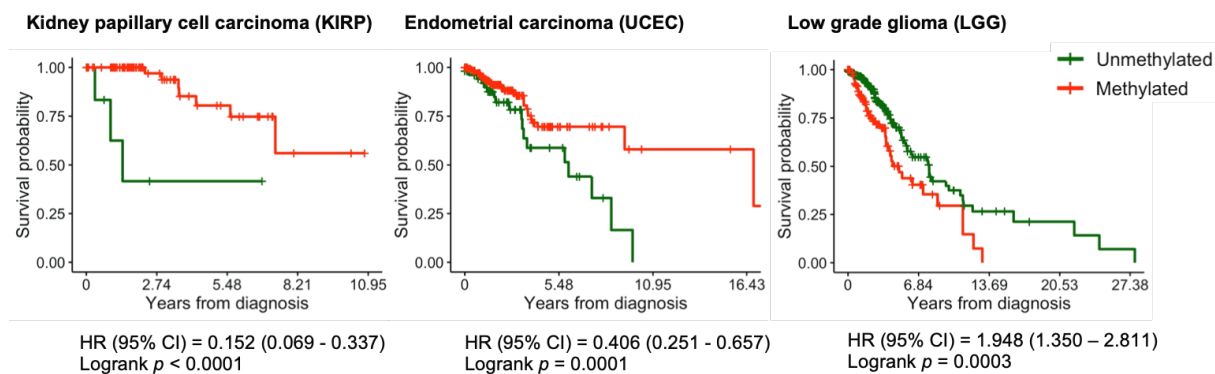
Figure 43. Effects of tRNA-Arg-TCT-4-1 methylation on cancer patients' overall survival. Kaplan-Meier curves show that tRNA-Arg-TCT-4-1 hypermethylation is associated with larger overall survival in KIRP (*left*) and UCEC (*middle*) TCGA cohorts. Hypermethylation of this gene in LGG patients (*right*) is associated with a shorter overall survival. Green, unmethylated cases; red, hypermethylated cases. HR, hazard ratio; CI, confidence interval. *p*-values correspond to logrank tests to compare survival proportions between groups. HR and CI are those from univariate Cox regression analyses.

tRNA-Arg-TCT-4-1 silencing reduces endometrial cancer cell growth

Changes in tRNA expression can drive tumorigenesis as they can confer advantages to the cancer cell (Hernandez-Alias et al., 2020; Pavon-Eternod et al., 2009). Our findings suggest that DNA methylation can repress tDNA transcription by the RNAPIII machinery, and therefore tumor-specific alterations in tDNA methylation landscape may contribute to the differences observed in tRNA expression levels. Additionally, the altered methylation of some tDNA is associated with differences in overall survival in patients with some types of tumors, which can depend on the tissue and should be interrogated separately.

Our analyses have identified tRNA-Arg-TCT-4-1 as a promising candidate to participate in tumorigenesis. This gene is hypermethylated in most normal tissues and is demethylated during malignant transformation (**Figure 39**). tRNA-Arg-TCT-4-1 hypomethylation was associated with a shorter overall survival in KIRP and UCEC TCGA cohorts (**Figure 43**), where it accounts for an 8% and 29% of cases, respectively (**Figure 44A**). The percentage of tRNA-Arg-TCT-4-1 demethylated cases was of 93% for renal cancer cell lines and 100% for endometrial cell lines (**Figure 39**). In both tumor types, the hypomethylation of this gene is accompanied by increased tRNA levels (**Figure 44B**), consistent with the higher tRNA-Arg-TCT-4-1 expression observed in tumor samples compared to normal ones (**Figure 44C**).
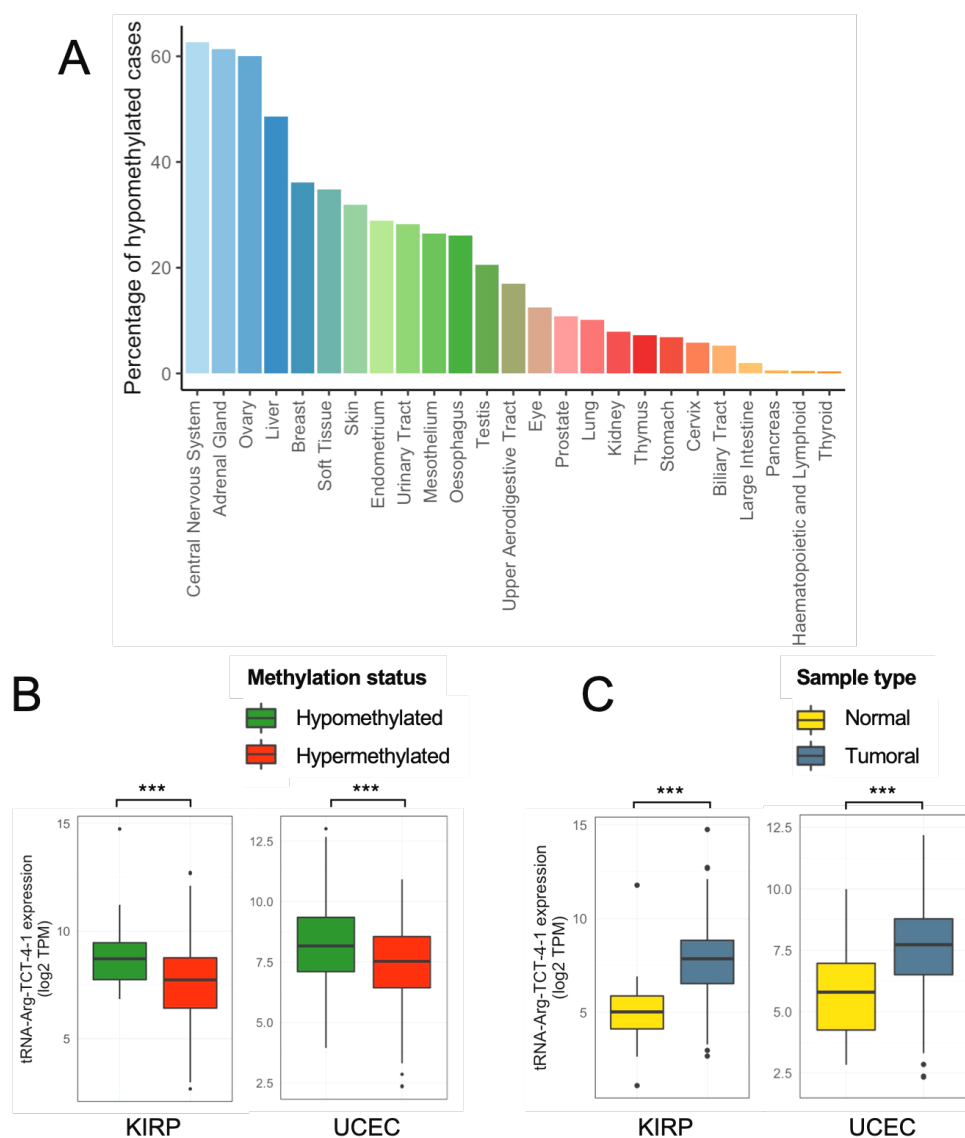
Figure 44. *tRNA-Arg-TCT-4-1 hypomethylation in KIRP and UCEC TCGA cohorts correlates with an increased tRNA expression.* (**A**) Frequency of primary tumors derived from TCGA presenting tRNA-Arg-TCT-4-1 hypomethylation. (**B**) tRNA-Arg-TCT-4-1 methylation is associated with a reduced tRNA expression in KIRP (*left*) and UCEC (*right*) TCGA primary tumors. (**C**) tRNA-Arg-TCT-4-1 expression is increased in KIRP (*left*) and UCEC (*right*) TCGA primary tumors compared to their matched normal tissue. Statistical differences in tRNA expression between groups of samples were determined using a two-sided Mann-Whitney U-test; *** $p < 0.001$.

The higher percentage of demethylated cases in the UCEC cohort of primary tumors inspired us to investigate and confirm the oncogenic role of this demethylation in endometrial cancer. First, we selected one endometrial cancer cell lines (HEC1) and confirmed the hypo-methylation of tRNA-Arg-TCT-4-1 tDNA (**Figure 45A**) that was first observed in the HM450-derived data (**Figure 39**). HEC1 presented an increased GTF3C1 and POLR3A binding to tRNA-Arg-TCT-4-1 gene (**Figure 45B**) and a higher expression of this tRNA (**Figure 45C**) than those observed in the hypermethylated DND41 and SW48 cell lines, supporting that tDNA hypermethylation can repress tRNA expression.
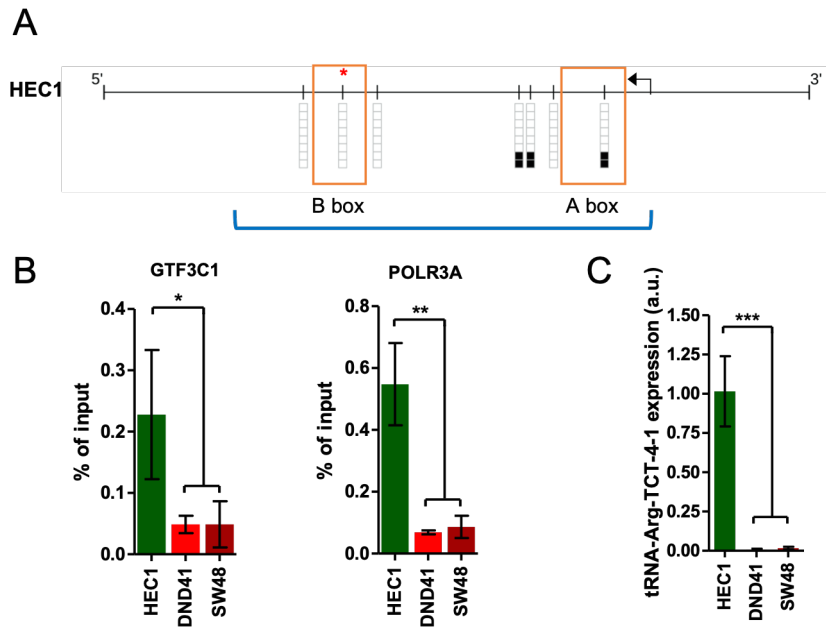
Figure 45. *tRNA-Arg-TCT-4-1 is hypomethylated and highly expressed in HEC1 endometrial cancer cell line.* (**A**) BSP confirms the hypomethylation of tRNA-Arg-TCT-4-1 in HEC1 cell line. The tDNA gene sequence is indicated with a blue bracket. The orange rectangles correspond to the A and B boxes of the tDNA gene (Marck et al., 2006). The TSS is marked with a black arrow. CpG dinucleotides are represented as short vertical lines, and their methylation status is denoted with black (methylated) or white (unmethylated) squares. The CpG represented in the HM450 methylation microarray is marked with a red asterisk. (**B**) ChIP-qPCR experiment shows an increased binding of GTF3C1 (*left*) and POLR3A (*right*) to tRNA-Arg-TCT-4-1 gene in HEC1 compared to DND41 and SW48 cell lines. Data represent the mean ± SD of biological triplicates analyzed using an unpaired two-tailed Student's t-test. * $p < 0.05$; ** $p < 0.01$; (**C**) qRT-PCR reveals an increased tRNA-Arg-TCT-4-1 expression in HEC1 compared to the hypermethylated DND41 and SW48 cell lines. Data represent the mean ± SD of biological triplicates analyzed by an unpaired two-tailed Student's t-test. *** $p < 0.001$.

To further study the role of tRNA-Arg-TCT-4-1 in endometrial cancer progression, we used the CRISPR/Cas9 system to eliminate this tDNA from HEC1 cell line and imitate its hypermethylation-associated silencing (**Figure 46A**). The deletion introduced was confirmed by genomic PCR and Sanger sequencing in two knockout clones (**Figure 46A**), which showed a minimal tRNA-Arg-TCT-4-1 expression compared to the wild-type cell line (**Figure 46B**).

tRNA-Arg-TCT-4-1 depletion resulted in a reduced cell growth of the two HEC1 knockout clones (**Figure 46C**). This phenotype was not driven by an induction of apoptosis (**Figure 46D**). Instead, it was caused by an accumulation of cells in the G_0/G_1 phase of the cell cycle in detriment of the S and G_2/M phases (**Figure 46E**). Additionally, tRNA-Arg-TCT-4-1 silencing also reduced cell migration in the two HEC1 knockout clones (**Figure 46F**). Globally, our results indicate that tRNA-Arg-TCT-4-1 increased expression promotes HEC1 cell growth and migration. This agrees with the poorer prognosis of those endometrial cancer patients that harbor tRNA-Arg-TCT-4-1 hypomethylation and confirms the oncogenicity of the resulting tRNA overexpression in this type of tumor.
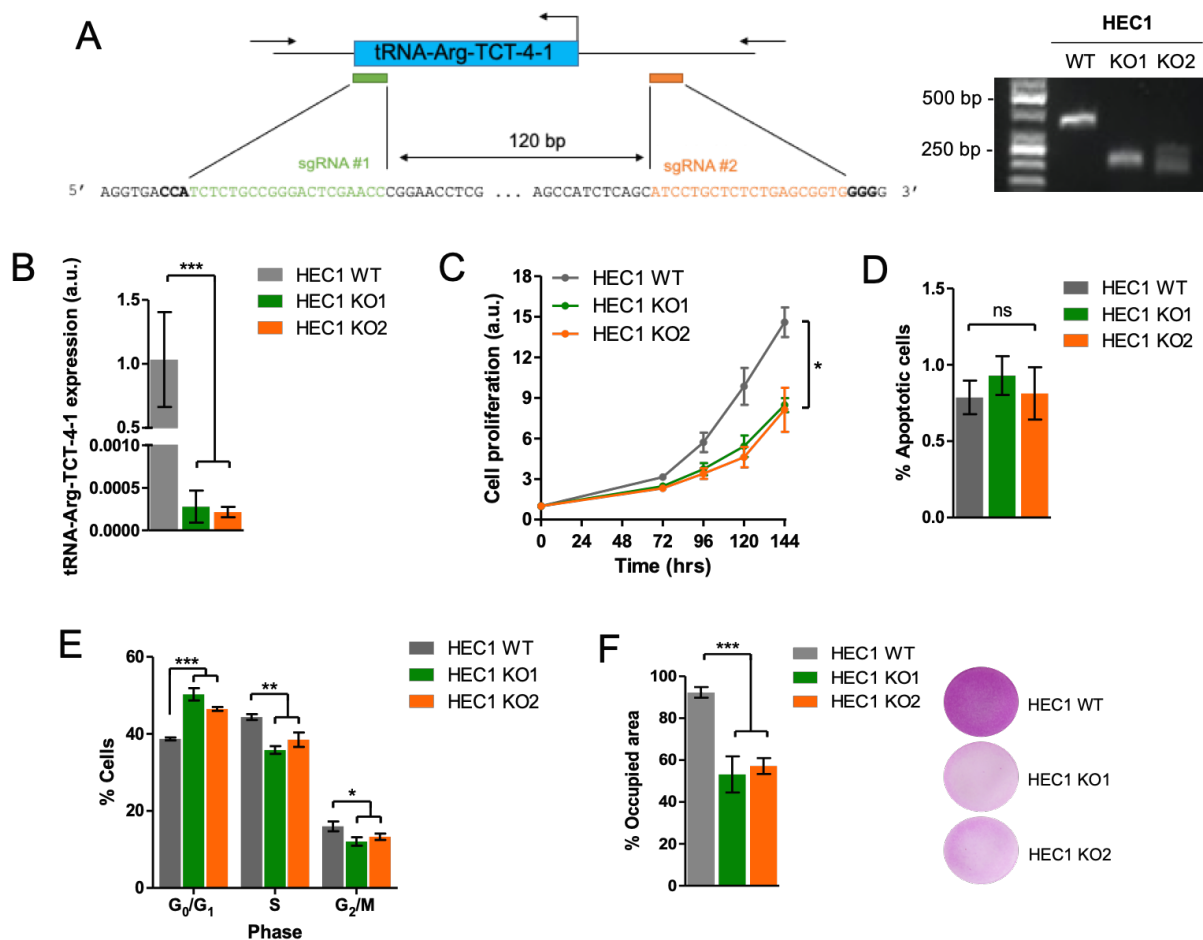
Figure 46. tRNA-Arg-TCT-4-1 silencing reduces HEC1 cell growth and migration. (**A**) (*Left*) Overview of the CRISPR/Cas9 system targeting tRNA-Arg-TCT-4-1 gene. Two different sgRNA (in green and orange) were used to eliminate this tDNA. (*Right*) Genomic PCR using a pair of primers flanking tRNA-Arg-TCT-4-1 (black arrows in the left) shows a deletion in two HEC1 knockout clones. (**B**) qRT-PCR confirms the silencing of tRNA-Arg-TCT-4-1 in HEC1 knockout cells. Data are the mean ± SD of biological triplicates analyzed using the unpaired two-tailed Student's t-test. *** $p < 0.001$. (**C**) SRB assay shows a reduced growth of two HEC1 knockout cells. Data at each time points represent the mean ± SD of four biological replicates. Statistical differences were assessed using an unpaired two-tailed Student's t-test at the 144 hours final time point. * $p < 0.05$. (**D**) Annexin V staining assessed by flow cytometry indicates the lack of differences in apoptotic cell population upon tRNA-Arg-TCT-4-1 knockout in HEC1 cells. Data shown represent the mean ± SD of independent biological triplicates analyzed by unpaired two-tailed Student's t-test. ns, not significant. (**E**) Cell cycle analysis reveals an accumulation of tRNA-Arg-TCT-4-1-depleted HEC1 cells in G_0/G_1 phase. Data shown are the mean ± SD of biological triplicates analyzed by unpaired two-tailed Student's t-test. * $p < 0.05$. (**F**) Transwell assay shows a reduced migration capacity of tRNA-Arg-TCT-4-1-silenced HEC1 cells. Data represent the mean ± SD of biological triplicates analyzed by an unpaired two-tailed Student's t-test. *** $p < 0.001$. Representative images of the Transwell insert membranes are shown.

111

DISCUSSION

DISCUSSION

tRNAs are essential molecules that allow the translation of the genetic code into amino acids. Extensive research during the last 50 years has revealed that, despite their apparently simple structure and function, tRNAs are more than simple adaptors in protein synthesis; they are pivotal in normal cell physiology (Berg and Brandl, 2021). This is supported by the fact that tRNA levels are tightly regulated to match the codon usage patterns of a given cell type or status in order to meet the cellular specific needs (Gingold et al., 2014; Sagi et al., 2016). Moreover, the nucleoside modifications of tRNA are critical for their function at multiple levels, such as translation efficiency and fidelity, wobbling, or fragmentation (Suzuki, 2021). Therefore, tRNA biology is very complex and relies on strictly regulated processes that are reportedly altered in pathological processes including cancer (Santos et al., 2019).

For many years, scientists considered tRNAs as nothing more than bare adaptors in translation and therefore they believed them to be simple observers of tumorigenesis. Yet this belief has been proven incorrect: not only tRNA biology imbalance is associated to malignant transformation, it actually actively contributes to it (Santos et al., 2019). Cancer-specific tRNA dysregulation is a very new and still unexplored field of research, thus further studies are required to fully understand the molecular mechanisms that account for these alterations as well as their connection with tumor biology.

DNA methylation alterations constitute a frequent mechanism by which cancer cells acquire their malignant features (Ortiz-Barahona et al., 2020), but their involvement in tRNA biology dysregulation had not been explored in depth yet. For this reason, the main purpose of this thesis is the description of epigenetic lesions that support tumor-associated tRNA biology alterations. With this intention, we designed and performed two independent projects to unveil the epigenetic regulation of tRNA biology in cancer.

In the first study, we identified the tumor-specific epigenetic silencing of TYW2 as a mechanism to induce tRNA^Phe hypomodification at position 37, a phenomenon that was observed for the first time more than forty years ago but whose causes and consequences have remained obscure since then. Our findings connected this epigenetic defect to a phenotype that enhances -1 ribosome frameshifting events to ultimately confer increased migratory capacities and mesenchymal features to the transformed colon cells.

In the second study, we provided relevant insights about the effects of tumor-associated tDNA methylation changes on tRNA expression and revealed that DNA hypomethylation guided the oncogenic tRNA-Arg-TCT-4-1 overexpression in endometrial cancer.

Discussion

Most importantly from the clinical perspective, the epigenetic alterations identified in both studies can anticipate the patients' outcome, thus they may serve as biomarkers for the identification of high-risk patients that might benefit from a more comprehensive surveillance or alternative therapeutic approaches.

The Art of War teaches us that "the opportunity of defeating the enemy is provided by the enemy himself": the more we understand tumor biology, the better we will fight this devastating disease. As the number of reports showing the connection of tRNA defects with tumor biology continues to grow, it is becoming evident that they are relevant for the disease. Hence, tRNAs represent promising candidates to be thoroughly examined so that researchers can learn their implications in tumorigenesis and uncover how their imbalance can eventually be exploited in cancer management.

Role of DNA methylation defects in tumor-associated tRNA modification reprogramming

Promoter hypermethylation drives TYW2 silencing and tRNA^{Phe} hypomodification

Defects in RNA nucleoside modifications, collectively named the epitranscriptome, have emerged as promising sources of biomarkers for cancer diagnosis and prognosis (Amalric et al., 2021). More specifically, tRNA modifications can be reprogrammed to adapt to the cell specific needs, such as the increased proliferation rate of cancer cells (Endres et al., 2019). As a matter of fact, the tRNA modification landscape in fast-proliferating cells is different than in their normal tissue of origin (Dong et al., 2016), likely as a mechanism to fine tune protein synthesis to enhance tumorigenesis (Endres et al., 2019).

The expression of various tRNA modifiers is altered in neoplasia (Begik et al., 2020; Zhang et al., 2018), which induces a tumor-associated tRNA modification reprogramming. The alterations in tRNA modifier enzymes can play oncogenic or tumor suppressive roles depending on the modification that they catalyze and on the tumor type (Endres et al., 2019). Most studies focus in the overexpression of tRNA modifiers, such as METTL1, ELP3, or NSUN2, which are proposed to drive oncogenesis (Dai et al., 2021; Delaunay et al., 2016; Frye et al., 2010). Although less studied, tRNA hypomodification has also been reported in malignant cells. Several decades ago, scientists proposed that the loss of certain tRNA modifications, like yW or queuosine, could confer advantages to the tumor cell to foster the progression of the disease and conjectured that these tRNA modifications and their cognate enzymes displayed tumor suppressive features (Baranowski et al., 1994; Kuchino et al., 1982).

116

We hypothesized that tumor suppressive tRNA modifier proteins could undergo promoter hypermethylation-guided silencing in cancer cells. The screening of the HM450-derived DNA methylation data comprising the promoter regions of 81 tRNA modifier enzymes from approximately 10,000 tumor samples and normal healthy tissues available at TCGA and from 1,000 cell lines allowed the identification of candidate proteins that could potentially perform these proposed tumor suppressive roles (**Figures 15-17**). Interestingly, this analysis highlighted two genes whose promoters had been previously reported to be hypermethylated in tumor cells, TRMT9B/C8orf79 and ALKBH3 (Begley et al., 2013; Stefansson et al., 2017), reinforcing the suitability of our approach for the identification of candidate genes that are epigenetically inactivated in cancer.

Two proteins belonging to the yW synthesis pathway, TRMT12/TYW2 and LCMT2/TYW4, (Noma et al., 2006) emerged as attractive candidates for further study (**Figures 15-17**). But apparently contradicting our findings, TYW2 amplification and overexpression have been described in various tumor types (Begik et al., 2020; Manning et al., 2020; Wang et al., 2019; Zhang et al., 2018), a phenomenon that has been associated to a shorter overall survival in head & neck and breast cancer TCGA cohorts (Manning et al., 2020; Wang et al., 2019). This would indicate that TYW2 is an oncogene, against its proposed tumor suppressive role that arises from our analysis.

However, we disregarded this discrepancy between our results and the scientific literature. Genomic amplification highlights loci where putative oncogenes may map, but to irrefutably prove that a specific gene drives the amplification is complicated because the amplicon can contain many genes (Albertson, 2006). TYW2 is located in the large arm of chromosome 8, less than 4 Mb away of the master oncogene MYC. MYC is amplified in 21% of all human cancer cases and considered to be a major oncogenic driver (Schaub et al., 2018). Besides, the studies that discuss the impact of this tumor-associated TYW2 amplification are limited to the in silico screening of the clinicopathological information from TCGA and do not provide details about the molecular function and relevance of this alteration (Wang et al., 2019). TYW2 and MYC amplification co-occur in various tumor types, including breast, colorectal, and head and neck cancer (**Figure 47**); therefore, it cannot be rejected that MYC amplification may be the real cause of such clinical outcomes. Moreover, the robust negative correlation between TYW2 promoter methylation and transcript levels in TCGA tumor samples and in cell lines (**Figure 18**), on the one hand, and TYW2 expression recovery in hypermethylated cell lines upon a DNA demethylation on the other (**Figure 19**), demonstrate that TYW2 promoter hypermethylation is functional regardless of its copy number.

Discussion
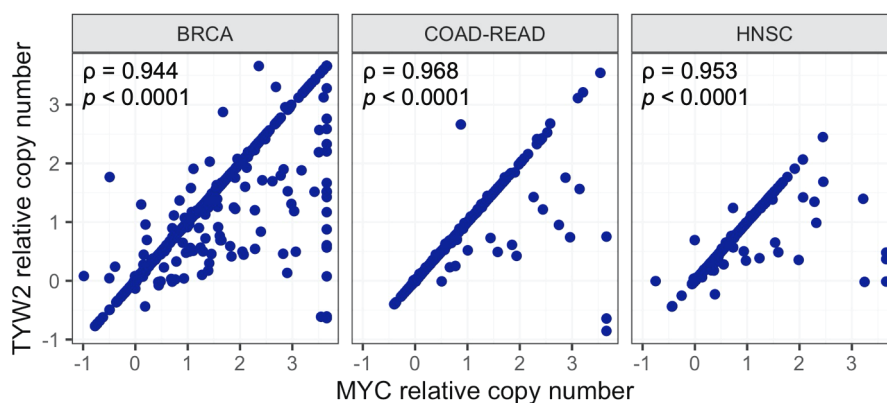
Figure 47. TYW2 and MYC amplification co-occur frequently in cancer. TYW2 and MYC copy number are strongly associated in breast (BRCA, *left*), colorectal (COAD-READ, *middle*), and head and neck (HNSC, *right*) TCGA tumor samples. Data represents the capped relative linear copy number values. Positive and negative values indicate amplification and deletion, respectively. The association between both variables was assessed using Spearman's correlation.

The expression of tRNA modifiers is pivotal for the correct modification of tRNA nucleosides. In this study, we showed that TYW2 silencing in colon cancer cell lines, either because of its epigenetic loss or its introduced deletion using the CRISPR/Cas9 system, leads to the hypomodification of tRNA[Phe], as proven by the absence of OHyW and o2yW and the emergence of the intermediary residue imG-14 –the substrate of TYW2 (**Figures 20, 21**). Back in the late 1970s, hypomodified forms of tRNA[Phe] lacking the yW derivatives were described in some tumor cells, and were then postulated to confer growth advantages to the transformed cells (Grunberger et al., 1975; Kuchino et al., 1982; Mushinski and Marini, 1979). Thus, TYW2 epigenetic loss entails a plausible mechanism to explain the cancer-associated tRNA[Phe] hypomodification discovered more than forty years ago.

tRNA[Phe] hypomodification enhances -1 ribosome frameshifting to fine tune mRNA abundance

Chemical modifications in tRNA nucleosides are critical for their stability and function at multiple levels (Suzuki, 2021). In this sense, defects in tRNA modifications affecting functional sites of the molecule can interfere with a correct protein synthesis. Hypermodification of the position 37 of tRNA[Phe], for instance, is key to ensure the maintenance of the ribosome reading frame during the translation of slippery sequences by preventing -1 ribosome frameshifting due to the proper stabilization of the codon-anticodon interaction (Konevega et al., 2004). In fact, its depletion stimulates such translational errors (Carlson et al., 1999, 2001). In agreement with the existing literature, reduced TYW2 levels and the resulting tRNA[Phe] hypomodification incremented -1 ribosome frameshifting frequency in our colon cancer cell lines (**Figure 23**).

-1 PRF events are considered a regulatory mechanism of gene expression. The emergence of a premature stop codon in non-mutated mRNAs as a result of ribosome frameshifting would be detected by the NMD machinery, which would degrade the affected transcript to prevent the production of a C-terminally truncated protein (Advani and Dinman, 2016; Kurosaki et al., 2019). NMD controls the abundance of approximately a 10% of non-mutated transcripts, therefore it must be strictly controlled to avoid undesired mRNA degradation and changes in gene expression that could result in disease (Kurosaki et al., 2019). Overall, our findings exemplify how translational defects derived from changes in tRNA modifications can lead to mRNA decay in tumor cells. The RNA-seq experiment in HCT-116 cell models revealed that TYW2 silencing provoked the alteration of 2,370 transcripts, inducing the downregulation of an 86% of them. Most of these downregulated transcripts were also commonly under-expressed in those colon cancer cell lines harboring TYW2 promoter hypermethylation (**Figure 24**).

From the 2,046 transcripts downregulated in TYW2-depleted HCT-116 cell lines (**Figure 24**), only 671 encode proteins. 448 of them are included in the PRFdb (Belew et al., 2008), and 109 are predicted to contain at least one slippery site encoding phenylalanine codons based on the algorithm of this database (**Table 10**). Interestingly, mRNAs containing predicted slippery sequences based on phenylalanine codons were enriched among the downregulated transcripts (**Figure 25**). Therefore, this type of motif may participate in the regulation of mRNA abundance in a cellular context that presents defects in ribosome frameshifting prevention.

These 109 transcripts represent potential candidates to be directly regulated by the translational defects driven by the tRNA[Phe] hypomodification arising from TYW2 silencing. However, 109 genes represent only a small fraction of the 2,046 downregulated genes upon TYW2 silencing in HCT-116 cell line. Therefore, the alterations observed for most of the transcripts, which are ncRNAs or lack predicted -1 PRF sites, must be due to indirect effects. TUSC3, for instance, is downregulated upon TYW2 silencing in our colon cancer cell line models by a mechanism unrelated to its degradation (**Figure 27**). These indirect effects could be the outcome of many molecular pathways. One example that comes to mind to support this hypothesis would be transcription factors that are directly regulated by -1 PRF and NMD, and whose expression and activity are susceptible to affect larger groups of genes. Membrane receptors and secreted ligands with autocrine functions constitute another group of proteins that can also interfere with the performance of downstream signaling pathways, hence potentially affecting the expression of numerous genes. The list of 109 genes that might be guided to NMD because of tRNA[Phe] hypomodification and increased frameshifting frequency includes various transcription factors, secreted ligands, and membrane receptors that can account for these indirect changes in transcript levels (**Table 10**).

Discussion

Ribosome frameshifting guides ROBO1 to NMD and increases migration capacity

NMD controls the abundance of approximately a 10% of non-mutated transcripts, therefore it must be strictly controlled to avoid undesired mRNA degradation that could result in disease (Kurosaki et al., 2019). As a matter of fact, NMD activity is often altered in tumorigenesis, where it can play a dual role: it can protect against the disease or aggravate it, depending on the genomic context of the tumor (Nogueira et al., 2021). On the one hand, it can act as a tumor suppressor by repressing non-mutated transcripts involved in the control cell proliferation and migration (Wang et al., 2011) or by preventing the production of dominant-negative mutant proteins that would, if expressed, foster the tumorigenic process (Fan et al., 2001). On the other hand, cancer cells can take advantage of NMD to downregulate tumor suppressor genes carrying non-sense mutations and increase the severity of the disease (Lindeboom et al., 2016). In fact, the inhibition of NMD has been used to identify candidate susceptibility genes in cancer (Ivanov et al., 2007; Johnson et al., 2012). In this sense, we hypothesized that the incremented frequency of ribosome frameshifting due to tRNA^{Phe} hypomodification could direct non-mutated tumor suppressors to NMD in TYW2 silenced cells.

We propose that this is the case of ROBO1. TYW2-silenced colon cancer cell lines present reduced levels of ROBO1 transcript and protein because of a decreased mRNA stability (**Figure 26**). ROBO1 transcript recovery upon NMD inhibition using a siRNA against UPF1 in TYW2-deficient cells but not in TYW2-expressing cells (**Figure 28**) indicates that it is only degraded via NMD in absence of TYW2 –in those cells lacking the fully modified tRNA^{Phe} that should prevent ribosome frameshifting.

The magnitude of ROBO1 mRNA restoration after NMD blocking seems to have little correlation with the velocity of its degradation. However, we must bear in mind that NMD activity is not completely abolished in our experiment, as siUPF1 did not fully eliminate UPF1 expression (**Figure 28**). Consequently, and as a means to monitor the degree of NMD inhibition, we evaluated the expression of two positive controls that undergo NMD (UPP1 and DUSP10; Mendell et al., 2004), and observed that siUPF1 transfection induced their accumulation in a magnitude similar to that observed for ROBO1 restoration (**Figure 28**).

Globally, these results fit with the assumption that the increased ribosome frameshifting in TYW2-depleted cells (**Figure 29**) triggers ROBO1 transcript degradation via NMD. Moreover, the replacement of the phenylalanine codons in ROBO1 slippery heptamer by leucine eliminated the observed differences in reading frame maintenance according to TYW2 expression levels. This confirmed that defects in tRNA^{Phe} modification status guided ribosome frameshifting on this slippery sequence (**Figure 29**).

120

The SLIT/ROBO axis was first described in the field of axon guidance and neuronal migration and proved to be important for neuronal development (Brose et al., 1999), but in the last decade, diverse investigations have established the relationship between this signaling pathway and malignant transformation. The expression of SLIT and ROBO proteins are altered in a variety of tumors, where they can play both oncogenic and tumor suppressive roles and have either positive or negative effects on tumor progression. Additional research is needed to clarify this dual role in neoplasia (Jiang et al., 2019).

Recent studies indicate that the SLIT/ROBO axis participates in cancer cell migration and metastasis, but its specific role seems to be dependent on the cellular context (Jiang et al., 2019). ROBO1 signaling has been connected to cancer progression, functioning either as an oncogene or a tumor suppressor gene depending on its association with different interactors (Chiang et al., 2019). Regarding its proposed tumor suppressive roles, ROBO1 is lost in some tumors (Rezniczek et al., 2019; Tricoli et al., 2018) and it is reported to act as a negative regulator of cell growth (Chen et al., 2021) and migration (Feng et al., 2016; Huang et al., 2015; Zhang et al., 2020a). This is compatible with the increased migration and mesenchymal features of TYW2-deficient cells presenting ROBO1 downregulation (**Figures 33, 34**).

The restoration of ROBO1 in the TYW2 knockout cell models partially reverted the mesenchymal features (**Figure 35**). In the opposite scenario, ROBO1 knockdown in TYW2-expressing cells partially induced these mesenchymal features (**Figure 35**). Together, these results help clarifying the role of ROBO1 in colon cancer by providing evidence of its participation in EMT, supporting previous reports claiming that ROBO1 reduces cell migration (Feng et al., 2016; Xia et al., 2019). At the same time, our results also reveal that ROBO1 downregulation must cooperate with additional mechanisms to increase TYW2-deficient cells' migration capacity provided that the modulation of its expression only affects EMT moderately (**Figure 35**). This comes as no surprise given the number of genes related to cell migration that are deregulated upon TYW2 silencing in HCT-116 cell lines (**Figure 33, Table S1**).

Overall, the reduction in ROBO1 levels because of TYW2 silencing provides an illustrative example of how defects in tRNA nucleoside modifications impair protein synthesis in a way that might participate in tumorigenesis (**Figure 48**). In our study, we have robustly connected TYW2 silencing with increased -1 ribosome frameshift frequency, but it cannot be ruled out that tRNA[Phe] hypomodification could mediate additional effects on protein synthesis. On the one hand, tRNA modification reprogramming can modulate tRNA fragmentation (Orellana et al., 2021; Pereira et al., 2021; Rashad et al., 2020), thereby altering the composition of the cytosolic tRNA pool. It is conceivable that tRNA[Phe] hypomodification, apart from influencing the decoding capacity of the molecule, may alter stability of the molecule and promote its

Discussion

degradation. The resulting distorted tRNA pool with a reduced abundance of tRNA[Phe] could diminish the translation efficiency of transcripts enriched with phenylalanine codons. On the other hand, tRNA modifications can represent identity elements required for their recognition and aminoacylation by the appropriate aaRS (Gomez and Ibba, 2020). In this sense, tRNA[Phe] hypermodification at position 37 is relevant for its discrimination by PheRS in *E. coli* (Giegé and Eriani, 2014). Although this has not been studied in higher eukaryotes, it is possible that the loss of these residues that are specific of tRNA[Phe] may provoke its misacylation and facilitate translational miscoding, providing proteins with incorrect amino acids. Error-prone translational machinery entails a source of mutations; therefore, such alleged fidelity errors might foster tumorigenesis (Ou et al., 2019). However, whether any of these two hypothetic scenarios contributes to the disease is unknown.
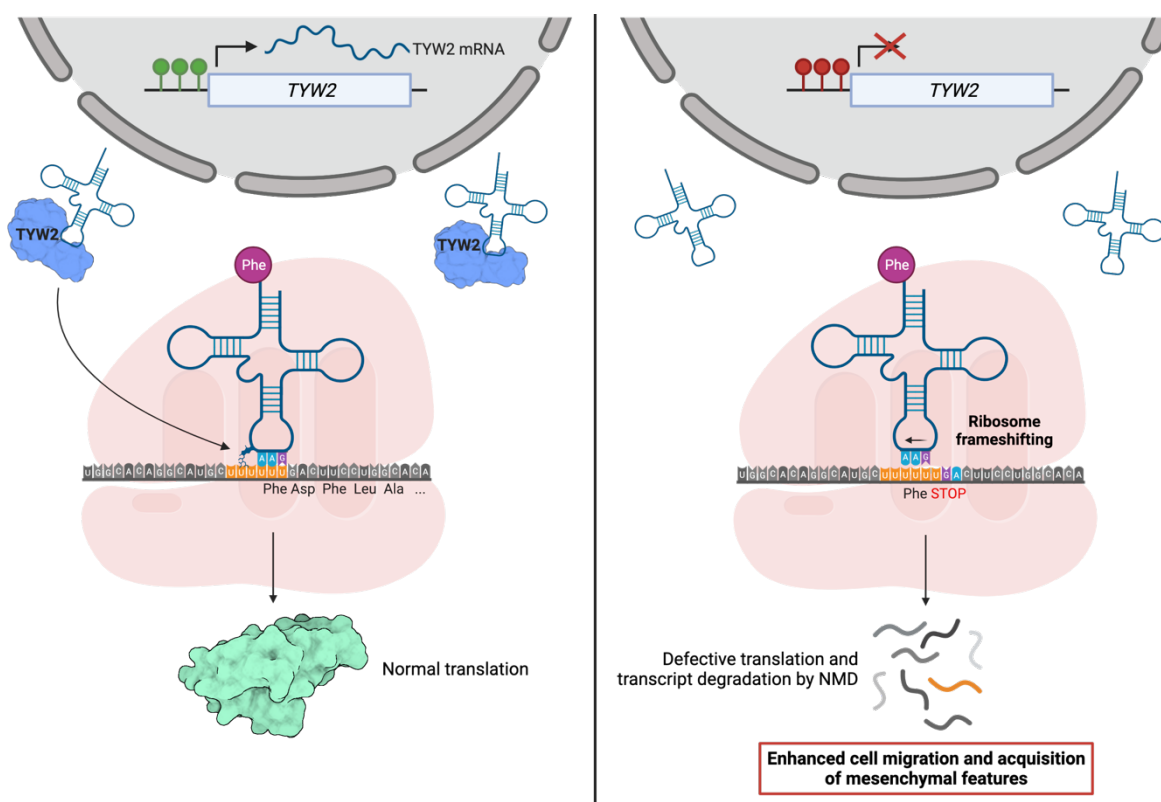
Figure 48. *Effects of TYW2 epigenetic silencing on tumor cell biology.* TYW2 hypermethylation-guided silencing results in tRNA[Phe] hypomodification. Defects in tRNA[Phe] modification at position 37 enhance -1 ribosome frameshifting at slippery sites, which directs the affected mRNA to degradation via NMD. At the end, these translational defects can foster the tumorigenic process by allowing the emergence of mesenchymal features and an increase in cell migration.

TYW2 epigenetic inactivation predicts poor clinical outcome of TCGA colorectal cancer cohort

From the clinical standpoint, colorectal cancer is one of the most prevalent neoplasia. Last year, in the United States, it accounted for an 8.6% of newly diagnosed cancer cases and for a 9% of cancer-associated deaths (Siegel et al., 2020). Most primary colorectal tumors are

122

surgically extirpated, but up to a 45% of patients with apparently localized forms of the disease succumb to relapse because residual malignant cells have colonized distant tissues before the clinical intervention (Tauriello et al., 2017). The identification of high-risk, early-stage colorectal cancer patients that are susceptible of presenting this characteristic may be relevant in the design of the most adequate therapeutic strategy, such as the administration of adjuvant chemotherapy after the surgical procedure. Hence the importance of unraveling biomarkers to predict cancer dissemination at early stages.

Epigenetic lesions promoting cell migration would favor the progression of early-staged tumors whose cells must escape from the primary site to spread the disease. Cancer-associated TYW2 silencing would fit in this category. This epigenetic lesion can be detected in early events of tumorigenesis, such as pre-cancerous lesions like high-grade colon adenomas (Fan et al., 2020), and it can contribute to disseminate the disease by enhancing cell migration and the acquisition of mesenchymal features (**Figures 33, 34**).

TYW2 hypermethylation and reduced expression are associated with poor clinical outcome only in early-staged colorectal cancer patients (**Figures 30, 31**), those with localized tumors that have not invaded surrounding tissues yet. Those primary tumors that have already disseminated to other tissues and generated metastases would not need a positive selection based on migratory advantages. This may be the reason why the performance of patients with advanced forms of the disease is unaffected by TYW2 levels. In conclusion, TYW2 promoter hypermethylation could be a biomarker for early dissemination of those colorectal tumors that at first glance seem restricted to the primary site but have already invaded other tissues.

In addition to surgical interventions, chemotherapy is the most frequently used therapeutic approach for colorectal cancer patients. Nonetheless, conventional chemotherapy and radiotherapy present certain limitations, like systemic toxicity or unpredictable resistance. In contraposition, targeted therapies directly act on tumoral cells inhibiting the molecular mechanisms that sustain the hallmarks of cancer (Hanahan and Weinberg, 2011; Xie et al., 2020). In 2004, the FDA approved the first targeted therapies to treat colon cancer: the monoclonal antibodies cetuximab and bevacizumab that inhibited EGFR and VEGFR signaling, respectively. Since then, a large number of compounds that antagonize these molecular pathways have been developed and brought into clinical studies (Xie et al., 2020). Additionally, numerous small kinase inhibitors that target EGFR, VEGFR, or their related pathways are under clinical trials to treat colon cancer, either as stand-alone agents or in combination with standard chemotherapy (Martinelli et al., 2020; Xie et al., 2020).

Discussion

Unfortunately, not all targeted therapies are equally effective in all patients, hence the importance of developing therapeutic interventions that are individualized to each patient (Collins and Varmus, 2015). With this personalized approach, the unique features of the patients' tumors are used to select the most suitable treatment option. In our study, we evaluated whether TYW2 expression is associated to differential drug response to determine its feasibility as a biomarker for targeted treatment selection in personalized medicine. To do so, we studied how TYW2 levels influence the cells' sensitivity to seven small molecules that are currently being tested in clinical trials. However, our analyses did not reveal any differences in drug sensitivity depending on TYW2 expression for any of the tested agents (**Figure 32**), indicating that TYW2 promoter hypermethylation cannot predict their therapeutic efficacy and thus rejecting its proposal as a biomarker for EGFR-targeted therapy selection in colon cancer.

At this point, it is tempting to speculate about alternative ways to exploit TYW2 promoter hypermethylation-associated silencing to turn it against the tumoral cell. Because of the reading frame alterations derived from tRNA^{Phe} hypomodification in TYW2-silenced cells, the truncated proteins that originate this defective translation likely contain non-encoded amino acids. After their clearance, their resulting fragments can be transported to the cell surface and be presented as neoantigens. The recognition of these mutant antigens –absent in normal, healthy cells– by tumor-infiltrated lymphocytes is susceptible to generate an immunologic response against that cancer cell, therefore rendering the tumor sensitive to immunotherapy (De Mattos-Arruda et al., 2020). If true, patients harboring TYW2 hypermethylation could benefit from receiving immune checkpoint inhibitors that boost the immune response against the tumor (Xie et al., 2020). Whether TYW2 promoter hypermethylation can be a double-edged sword in cancer remains unknown but may be explored in the future.

Contribution of DNA methylation alterations to differential tRNA expression in cancer

Tumorigenesis entails variations in tDNA methylation to modulate tRNA expression

Variations in tRNA expression occur in tumorigenesis. From a general perspective, malignant cells present a global increment in tRNA levels. This was first acknowledged as a natural outcome of the increased protein synthesis that accompanied the uncontrolled division of cancer cells. This belief was supported by the number of oncogenes and tumor suppressors that participate in RNAPIII transcriptional control (Graczyk et al., 2018). The tumor-associated deregulation of these molecular pathways cooperate to overactivate the RNAPIII to boost tRNA

expression and sustain the increased translation rates (Haurie et al., 2010; Santos et al., 2019). However, not all tRNAs are equally distorted in cancer. Their alterations occur at amino acid, isoacceptor, and isodecoder levels, and they differ among tumor types (Pinkard et al., 2020; Zhang et al., 2018). This means that the mechanisms that motivate this dysregulation must act specifically on each tRNA to allow such specificity.

The abundance of a molecule is controlled by their synthesis and degradation rates. Regarding tRNA degradation, the two major surveillance pathways potentially modulate the levels of all tRNA (**Figure 11**), and therefore cannot explain specific differences in tRNA expression. Alterations in tRNA processing steps that are molecule-specific, such as splicing, amino-acylation, or modification, may influence the levels of concrete tRNAs. tRNA modification defects, for instance, can lead to tRNA fragmentation (Orellana et al., 2021; Pereira et al., 2021; Rashad et al., 2020), and may contribute to modulate the abundance of specific tRNAs. As discussed earlier, alterations in tRNA modifications are usually driven by defects in their cognate enzymes, therefore their expression variations could result in specific changes in tRNA expression (Orellana et al., 2021).

On the contrary, if the disequilibrium in tRNA levels originates from a defective synthesis, defects in the common steps of tRNA biogenesis, such as the global regulation of RNAPIII machinery or pre-tRNA ends-processing, cannot explain such precision in tRNA pool disequilibrium. Therefore, the genomic context of each individual tDNA may account for the specificity of their transcription by the RNAPIII. In fact, the position of each tDNA in the three-dimensional chromatin organization (Van Bortle et al., 2017), the epigenetic landscape (Good et al., 2013; Park et al., 2017), the transcription of neighboring genes by the RNAPII (Gerber et al., 2020), and the binding of RNAPII-related transcription factors (Yang et al., 2020) are known to influence RNAPIII activity and affect tRNA expression.

Surprisingly, the role of DNA methylation in this regulation is poorly known, and its real degree of implication in tRNA expression control remains unexplored. So far, only one work proposed DNA methylation as a regulatory mechanism for tRNA expression, but it did not evaluate it in detail (Hernandez-Alias et al., 2020). Seeing the lack of information about the engagement of DNA methylation in the modulation of RNAPIII activity, we sought to study whether it could impact RNAPIII-mediated transcription, on the one hand, and if cancer-associated variations in DNA methylation could guide tRNA expression alterations on the other.

The gene annotation of the HM450 methylation microarray does not include tDNAs, a fact that has likely delayed the study of their methylation. Therefore, to address our goal, we first needed to identify all the CpG sites from the HM450 microarray that were located within the

Discussion

loci corresponding to the 416 high confidence tDNAs (GRCh37/hg19 version). Unfortunately, tDNAs are poorly represented in the HM450 methylation microarray as only 138 of them are included in it (**Figure 37**). For this reason, other high-throughput methods (e.g., reduced representation bisulfite sequencing or whole-genome bisulfite sequencing) would provide more comprehensive information about the methylation status of all tDNAs. However, the HM450 methylation microarray presented an extraordinary advantage compared to all these alternative techniques: the outstanding quantity of data available. Although the number of genes that we could analyze with the HM450 microarray data is limited, we could study them in almost 1,000 cell lines and in 10,000 TCGA samples, for which the clinical information was also available.

43 of these 138 tDNAs were located inside or closer than 2 kb from RNAPII-transcribed genes (**Figure 37**). We excluded these genes from our analysis because interferences between elongating RNAPII and RNAPIII machineries at the same loci (Gerber et al., 2020) could mask the presumed effects of tDNA methylation on tRNA expression, if any. Changes in the expression of RNAPII-transcribed genes could potentially modulate the transcription of neighboring tDNAs regardless of their methylation, but it has not been explored in our study.

The elimination of cross-reactive CpGs permitted the final identification of 71 tDNAs whose methylation could be efficiently interrogated with HM450-derived data (**Figure 37**). 60 of these tDNAs presented global methylation differences between tumor and normal TCGA samples (**Figure 38**). Moreover, these alterations in tDNA methylation were uneven among tissues (**Figure 39**), and may therefore contribute to the methylome that is specific of each tumor type (Costello et al., 2000). Undoubtedly, 71 represents only a small fraction of the total number of human tDNA but taken together, our findings revealed that tumorigenesis involves shifts in tDNA methylation patterns that are characteristic among different tissues. The possibility that other tDNAs can also present DNA methylation variations is not to be rejected despite our inability to evaluate it with the HM450 methylation microarray data, so we cannot determine the real extent of tDNA methylation variations in malignant transformation.

To our knowledge, this is the first time that increased DNA methylation levels are directly connected to tRNA silencing. The first hint of the hypermethylation-mediated tRNA transcriptional inactivation came from evaluating the correlation between tDNA methylation and tRNA expression in TCGA tumoral samples (**Figure 40**) using the data generated by Zhang and collaborators (2018). Our analysis highlighted three tDNAs whose hyper-methylation strongly correlated with a reduced expression of their cognate tRNA: tRNA-Arg-TCT-4-1, tRNA-Ile-AAT-8-1, and tRNA-Val-CAC-2-1.

DNA methylation is known to prevent TFIIIC binding to DNA (Bartke et al., 2010) and to reduce tDNA transcription in vitro (Besser et al., 1990). In line with the previous literature, and supporting our previous in silico findings, DNA demethylation upon the administration of 5'-azacytidine increased the binding of the RNAPIII transcriptional machinery to tRNA-Arg-TCT-4-1 and tRNA-Ile-AAT-8-1 genes and restored their expression in two cell lines that were hypermethylated for these two tDNAs (**Figure 41**). Although we have only provided evidence for tDNA hypermethylation-guided silencing for two tRNA species (**Figure 41**), the fact that DNA methylation can modulate tDNA transcription and tRNA expression might be extrapolated to other tDNAs including those whose methylation we are unable to evaluate with the HM450 methylation microarray.

All in all, we showed that the expression of some tRNAs can be epigenetically modulated in cancer (**Figure 49**). tDNA methylation defects appear to actively participate in the regulation of tRNA expression in malignant cells, and the unequal shifts in tDNA methylation that occur among tumor types (**Figure 39**) may guide tissue-specific changes in tRNA expression (**Figure 40**). Therefore, we believe that tDNA methylation alterations can contribute to the tissue- and tumor- specific changes in tRNA expression.
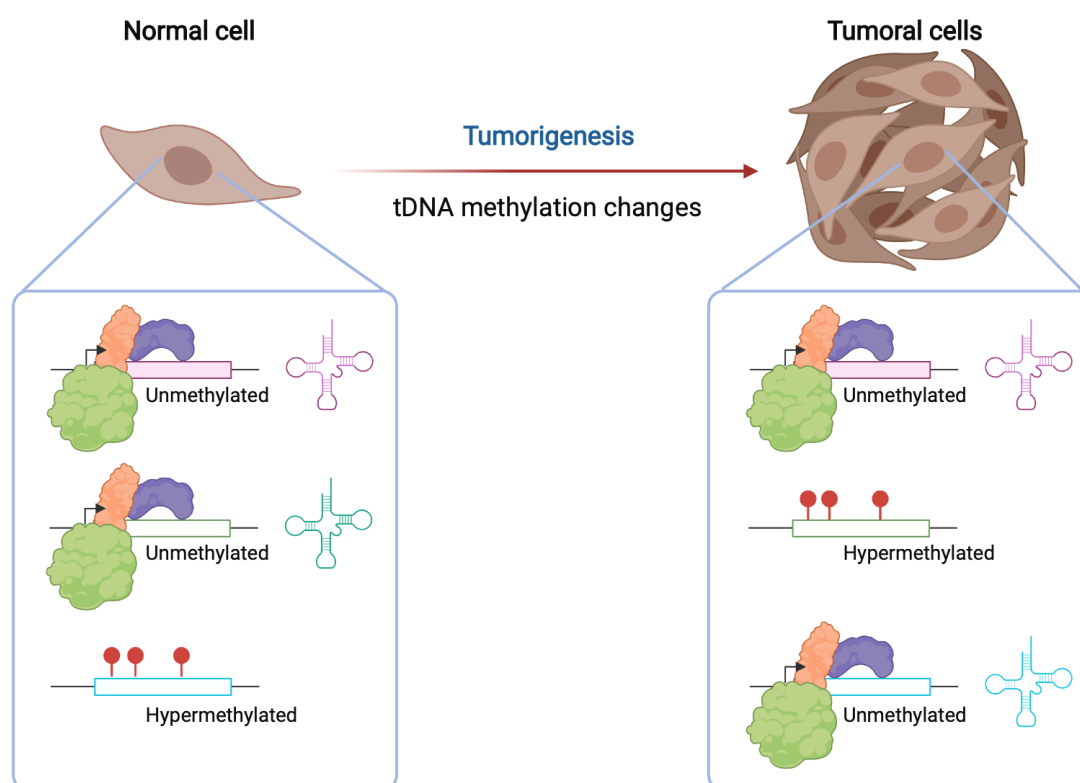
Figure 49. *tDNA methylation contributes to cancer-associated differential tRNA expression.* Human tumorigenesis entails changes in tDNA methylation, which may participate in the regulation of tRNA expression and contribute to the malignant cell's altered tRNA pool.

Discussion

Most of the tDNA methylation shifts observed between normal and tumoral samples tended towards hypermethylation in malignant samples (**Figures 38, 39**), suggesting that those tRNAs are silenced upon tumorigenesis. This would go against the cancer-associated global increase in tRNA expression, but would rather explain how certain tRNA molecules are silenced in cancer regardless of RNAPIII overactivation (Zhang et al., 2018).

The tumor-associated distortion of the tRNA pool composition at the amino acid and isoacceptor levels clearly facilitate the translation of transcripts that take advantage of the codon usage bias to encode growth-related proteins (Benisty et al., 2020; Gingold et al., 2014). However, alterations at the isodecoder level are more intriguing. Because all the isodecoders from a given isoacceptor family are functionally equivalent in terms of protein synthesis, the tRNA pool disequilibrium at the this level is believed to drive alterations in the abundance of tRFs (Torres et al., 2019).

We believe that the cancer-associated differential tRNA expression originated from defects in tDNA methylation entails a source for variations in tRF levels. The levels of numerous tRFs are altered upon tumorigenesis to foster the disease (Balatti et al., 2017; Yu et al., 2020), but the cause of their dysregulation is unknown in most cases. In view of our results, tDNA hypermethylation-associated tRNA silencing possibly contributes to it. One interesting case to note is the downregulation of a tumor suppressor 5'-tiRNA derived from tRNA-Val-CAC-2-1 in breast cancer (Mo et al., 2019), which originates from a tRNA that, according to our in silico results, undergoes hypermethylation-mediated silencing in cancer (**Figure 40**).

Our study principally provides insights on the contribution of DNA methylation to cancer-associated changes in tRNA expression. However, DNA methylation not only represses the transcription of proximal genes; it can also affect further regions of the chromatin (Buitrago et al., 2021). In this sense, the binding of TFIIIC to tDNA can promote three-dimensional chromatin rearrangements that can affect the expression of distant genes (Van Bortle and Corces, 2012; Kirkland et al., 2013). In fact, human tDNAs can act as insulators that, via TFIIIC binding, allow long-distance chromatin contacts, thus blocking RNAPII-transcribed genes' enhancers to reduce their expression (Raab et al., 2012). Therefore, tumor-related tDNA methylation shifts may have broader consequences on gene expression beyond the control of their own transcription, although this hypothesis is out of the scope of the present study.

DNA hypomethylation drives the oncogenic overexpression of tRNA-Arg-TCT-4-1

Cancer-associated DNA methylation lesions can be incorporated into the clinical practice as biomarkers for the disease (Berdasco and Esteller, 2019). Herein, we have shown that tDNA methylation defects can anticipate patients' overall survival probability in certain types of tumors (**Figure 42**), supporting the assumption that alterations in tRNA and tRF levels actively participate in tumorigenesis as it has already been described in the scientific literature (Jin et al., 2021; Pavon-Eternod et al., 2009; Zhang et al., 2018). Not all differential methylation events predicted the same trend patients' prognosis (**Figure 42**), reinforcing the idea that the specificity of the alterations in tRNA expression among different tumor types.

tRNA-Arg-TCT-4-1 constitutes the most illustrative example to support our claims. This tRNA is one of the six isodecoders that exist for tRNA^{ArgTCT} in humans. According to the previous literature, this isodecoder is only expressed in high levels in the central nervous system (Ishimura et al., 2014; Torres et al., 2019), the only normal tissue where it is hypomethylated (**Figure 39**). Zhang and coworkers' analysis of TCGA datasets (2018) revealed that this tRNA is overexpressed in tumor samples from 12 TCGA projects compared to their matched normal tissues. The cancer-associated hypomethylation and overexpression of this tRNA appears to have clinical impact. Our results revealed that tumor-specific tRNA-Arg-TCT-4-1 hypomethylation was clinically relevant in KIRP and UCEC cohorts from TCGA (**Figures 42, 43**), where it stands for an 8% and 29% of cases, respectively (**Figure 44**). Overall, the cancer-associated hypomethylation of this tDNA and the resulting overexpression of this tRNA perfectly coincides with the reports showing that the increased expression of tRNA^{ArgTCT} (the isoacceptor family to which tRNA-Arg-TCT-4-1 belongs) is associated to a shorter overall survival in the kidney clear cell carcinoma (Zhang et al., 2018) and sarcoma (Orellana et al., 2021) TCGA cohorts.

Interestingly, the expression of tRNA-Arg-TCT-4-1 is associated to a proliferative status of the cell according to the work of Gingold and coworkers (2014). Recently, Aharon-Hefetz et al. (2020) and Benisty et al. (2020) have provided further evidence that this tRNA is highly expressed in actively proliferating cells. Moreover, it has been recently discovered that the overexpression of tRNA-Arg-TCT-4-1 promotes malignant transformation, as its ectopic expression in the acute myeloid leukemia cell line MOLM-13 enhances cancer progression (Orellana et al., 2021). Altogether, these works highlight this tRNA as an attractive candidate for further study. Notably, the depletion of tRNA-Arg-TCT-4-1 in HEC1 cell line –recapitulating its hypermethylation-guided silencing observed in normal endometrial tissue– reduced cell growth and migration (**Figure 46**). In their work, Orellana and collaborators showed that tRNA-Arg-TCT-4-1 overexpression remodels the cell proteome by promoting the translation of

Discussion

transcripts enriched in AGA codons that participate in cell cycle regulation (Orellana et al., 2021), which fits with the slower cell cycle that tRNA-Arg-TCT-4-1 knockout HEC1 cells display (**Figure 46**). Taken together, our in vitro findings support the oncogenic role of the cancer-associated and hypomethylation-guided tRNA-Arg-TCT-4-1 overexpression in UCEC TCGA cohort that is inferred from the shorter overall survival of those patients that harbor this epigenetic alteration (**Figure 43**).

The prognosis for advanced forms of endometrial cancer is poor, and therapeutic options beyond surgery and first-line chemotherapy are limited (Lee et al., 2017). Hence the necessity to describe biomarkers that predict its aggressiveness to spot high-risk patients that would need a more comprehensive vigilance or that would benefit from receiving adjuvant therapy after the surgical resection of the tumor (Lee et al., 2017).

Unlike in other gynecologic cancers, the roles of tRNAs and their derived fragments in endometrial cancer remain unexplored. Future studies that evaluate in more detail tRNA-Arg-TCT-4-1 hypomethylation may determine if this event can satisfy the requirements to be used as a predictive biomarker in the clinical practice for the management of endometrial cancer. In parallel, the lack of targeted therapies approved for endometrial cancer management (Lee et al., 2017) may encourage the exploration of tRNA-Arg-TCT-4-1 silencing with antisense oligonucleotides as a novel therapeutic approach to tackle this disease.

CONCLUSIONS

CONCLUSIONS

Taken together, our findings prove that cancer cells benefit from DNA methylation alterations to modulate tRNA biology and foster tumorigenesis. First and foremost, we have shown that cancer cells benefit from DNA methylation defects to reprogram tRNA nucleoside modification, on the one hand, and modulate tRNA expression on the other. Globally, the results presented in this thesis contribute to our understanding of the mechanisms underlying the tRNA biology imbalance reported in tumor cells and may lay the foundation of future works concerning cancer-associated tRNA dysregulation from the epigenetic point of view.

The specific conclusions of each study reported in this thesis are the following:

Study I: Role of DNA methylation defects in tumor-associated tRNA modification reprogramming

I.   Promoter hypermethylation inactivates TYW2 expression in certain tumor types, such as colorectal and cervical carcinomas.

II. The epigenetic silencing of TYW2 leads to the hypomodification of tRNA^{Phe} in colon cancer cell lines. In this sense, TYW2 promoter CpG island hypermethylation-mediated silencing sheds light to the causes of the tRNA^{Phe} hypomodification reported more than forty years ago.

III. tRNA^{Phe} hypomodification induces a phenotype that is prone to induce -1 PRF events.

IV. Increased frequency of -1 PRF events due to tRNA^{Phe} hypomodification promotes the downregulation of mRNAs containing slippery sites via NMD in TYW2-deficient colon cell lines. ROBO1 constitutes a representative example of this proposed regulatory mechanism.

V.   TYW2 promoter hypermethylation and reduced transcript levels are associated with a poor clinical outcome in early-stage colorectal cancer patients.

VI. Reduced TYW2 expression increases the migration capacity of colon cancer cell lines and confers them mesenchymal features.

This work was published in:

Rosselló-Tortella, M., Llinàs-Arias, P., Sakaguchi, Y., Miyauchi, K., Davalos, V., Setien, F., Calleja-Cervantes, M.E., Piñeyro, D., et al. (2020). Epigenetic loss of the transfer RNA-modifying enzyme TYW2 induces ribosome frameshifts in colon cancer. Proc. Natl. Acad. Sci. USA *117*, 20785–20793.

Conclusions

Study II: Contribution of DNA methylation alterations to differential tRNA expression in cancer.

I. Human tumorigenesis entails differences in tDNA methylation patterns, mostly inducing a gain of methylation in malignant samples.

II. tDNA hypermethylation reduces tRNA expression by preventing the binding of the RNAPIII transcriptional machinery to DNA, which supports the negative association that exists between tDNA methylation and tRNA expression in TCGA.

III. Differential tDNA methylation levels can predict the survival probability and prognosis of patients with certain types of tumors in TCGA cohorts.

IV. tRNA-Arg-TCT-4-1 gene is hypermethylated in normal endometrial tissue and hypomethylated in cancer, where it plays oncogenic roles and is associated to a shorter overall survival and poor prognosis.

V. tRNA-Arg-TCT-4-1 expression supports tumor progression, as its silencing in HEC1 endometrial cancer cell line reduces cell growth and migration.

This work was submitted to Molecular Cancer on July 21st, 2021, as:

Roselló-Tortella, M., Bueno-Costa, A., Martínez-Verbo, L., Villanueva, L., and Esteller, M. DNA methylation-associated dysregulation of transfer RNA expression in human cancer.

REFERENCES

REFERENCES

Advani, V.M., and Dinman, J.D. (2016). Reprogramming the genetic code: The emerging role of ribosomal frameshifting in regulating cellular gene expression. BioEssays *38*, 21–26.

Agris, P.F. (2008). Bringing order to translation: The contributions of transfer RNA anticodon-domain modifications. EMBO Rep. *9*, 629–635.

Aharon-Hefetz, N., Frumkin, I., Mayshar, Y., Dahan, O., Pilpel, Y., and Rak, R. (2020). Manipulation of the human tRNA pool reveals distinct tRNA sets that act in cellular proliferation or cell cycle arrest. Elife *9*, e58461.

Ahel, I., Korencic, D., Ibba, M., and Söll, D. (2003). Trans-editing of mischarged tRNAs. Proc. Natl. Acad. Sci. USA *100*, 15422–15427.

Albertson, D.G. (2006). Gene amplification in cancer. Trends Genet. *22*, 447–455.

Alexandrov, A., Martzen, M.R., and Phizicky, E.M. (2002). Two proteins that form a complex are required for 7-methylguanosine modification of yeast tRNA. RNA *8*, 1253–1266.

Alexandrov, A., Chernyakov, I., Gu, W., Hiley, S.L., Hughes, T.R., Grayhack, E.J., and Phizicky, E.M. (2006). Rapid tRNA decay can result from lack of nonessential modifications. Mol. Cell *21*, 87–96.

Allfrey, V.G., Faulkner, R., and Mirsky, A.E. (1964). Acetylation and methylation of histones and their possible role in the regulation of RNA synthesis. Proc. Natl. Acad. Sci. USA *51*, 786–794.

Amalric, A., Bastide, A., Attina, A., Choquet, A., Vialaret, J., Lehmann, S., David, A., and Hirtz, C. (2021). Quantifying RNA modifications by mass spectrometry: a novel source of biomarkers in oncology. Crit. Rev. Clin. Lab. Sci. Epub ahead of print; doi: 10.1080/10408363.2021.1958743.

Aran, D., Sabato, S., and Hellman, A. (2013). DNA methylation of distal regulatory sites characterizes dysregulation of cancer genes. Genome Biol. *14*, R21.

Arimbasseri, A.G., and Maraia, R.J. (2015). Mechanism of Transcription Termination by RNA Polymerase III Utilizes a Non-template Strand Sequence-Specific Signal Element. Mol. Cell *58*, 1124–1132.

Arragain, S., Handelman, S.K., Forouhar, F., Wei, F.Y., Tomizawa, K., Hunt, J.F., Douki, T., Fontecave, M., Mulliez, E., and Atta, M. (2010). Identification of eukaryotic and prokaryotic methylthiotransferase for biosynthesis of 2-methylthio-N6-threonylcarbamoyladenosine in tRNA. J. Biol. Chem. *285*, 28425–28433.

Avcilar-Kucukgoze, I., Gamper, H., Polte, C., Hou, Y.-M., Dong, D.W., Ignatova, Z., Kraetzner, R., Shtutman, M., and Kashina, A. (2020). tRNA Arg-Derived Fragments Can Serve as Arginine Donors for Protein Arginylation. Cell Chem. Biol. *27*, 839–849.

Balatti, V., Nigita, G., Veneziano, D., Drusco, A., Stein, G.S., Messier, T.L., Farina, N.H., Lian, J.B., Tomasello, L., Liu, C. gong, et al. (2017). tsRNA signatures in cancer. Proc. Natl. Acad. Sci. USA *114*, 8071–8076.

Baranowski, W., Dirheimer, G., Jakowicki, J.A., and Keith, G. (1994). Deficiency of Queuine, a Highly Modified Purine Base, in Transfer RNAs from Primary and Metastatic Ovarian Malignant Tumors in Women. Cancer Res. *54*, 4468–4471.

Bartke, T., Vermeulen, M., Xhemalce, B., Robson, S.C., Mann, M., and Kouzarides, T. (2010). Nucleosome-interacting proteins regulated by DNA and histone methylation. Cell *143*, 470–484.

Begik, O., Lucas, M.C., Liu, H., Ramirez, J.M., Mattick, J.S., and Novoa, E.M. (2020). Integrative analyses of the RNA modification machinery reveal tissue- And cancer-specific signatures. Genome Biol. *21*, 97.

References

Begley, U., Sosa, M.S., Avivar-valderas, A., Patil, A., Endres, L., Estrada, Y., Chan, C.T.Y., Su, D., Dedon, P.C., Aguirre-ghiso, J.A., et al. (2013). A human tRNA methyltransferase 9-like protein prevents tumour growth by regulating LIN9 and HIF1- a. EMBO Mol. Med. *5*, 366–383.

Behm-Ansmant, I., Urban, A., Ma, X., Yu, Y.T., Motorin, Y., and Branlant, C. (2003). The Saccharomyces cerevisiae U2 snRNA:pseudouridine-synthase Pus7p is a novel multisite-multisubstrate RNA:ψ-synthase also acting on tRNAs. RNA *9*, 1371–1382.

Behm-Ansmant, I., Grosjean, H., Massenet, S., Motorin, Y., and Branlant, C. (2004). Pseudouridylation at position 32 of mitochondrial and cytoplasmic tRNAs requires two distinct enzymes in Saccharomyces cerevisiae. J. Biol. Chem. *279*, 52998–53006.

Belew, A.T., Hepler, N.L., Jacobs, J.L., and Dinman, J.D. (2008). PRFdb: a database of computationally predicted eukaryotic programmed -1 ribosomal frameshift signals. BMC Genomics *9*, 339.

Benisty, H., Weber, M., Hernandez-Alias, X., Schaefer, M.H., and Serrano, L. (2020). Mutation bias within oncogene families is related to proliferation-specific codon usage. Proc. Natl. Acad. Sci. USA *117*, 30848–30856.

Berdasco, M., and Esteller, M. (2019). Clinical epigenetics: seizing opportunities for translation. Nat. Rev. Genet. *20*, 109–127.

Berg, M.D., and Brandl, C.J. (2021). Transfer RNAs: diversity in form and function. RNA Biol. *18*, 316–339.

Bernstein, E., and Hake, S.B. (2006). The nucleosome: A little variation goes a long way. In Biochemistry and Cell Biology, (National Research Council of Canada), pp. 505–517.

Besser, D., Götz, F., Schulze-Forster, K., Wagner, H., Kröger, H., and Simon, D. (1990). DNA methylation inhibits transcription by RNA polymerase III of a tRNA gene, but not of a 5S rRNA gene. FEBS Lett. *269*, 358–362.

Bestor, T.H. (2005). Transposons reanimated in mice. Cell *122*, 322–325.

Bibikova, M., Le, J., Barnes, B., Saedinia-Melnyk, S., Zhou, L., Shen, R., and Gunderson, K.L. (2009). Genome-wide DNA methylation profiling using Infinium® assay. Epigenomics *1*, 177–200.

Bieker, J.J., Martin, P.L., and Roeder, R.G. (1985). Formation of a rate-limiting intermediate in 5S RNA gene transcription. Cell *40*, 119–127.

Birch, J., Clarke, C.J., Campbell, A.D., Campbell, K., Mitchell, L., Liko, D., Kalna, G., Strathdee, D., Sansom, O.J., Neilson, M., et al. (2016). The initiator methionine tRNA drives cell migration and invasion leading to increased metastatic potential in melanoma. Biol. Open *5*, 1371–1379.

Bird, A. (2007). Perceptions of epigenetics. Nature *447*, 396–398.

Boccaletto, P., MacHnicka, M.A., Purta, E., Pitkowski, P., Baginski, B., Wirecki, T.K., De Crécy-Lagard, V., Ross, R., Limbach, P.A., Kotter, A., et al. (2018). MODOMICS: A database of RNA modification pathways. 2017 update. Nucleic Acids Res. *46*, D303–D307.

Van Bortle, K., and Corces, V.G. (2012). tDNA insulators and the emerging role of TFIIIC in genome organization. Transcription *3*, 277–284.

Van Bortle, K., Phanstiel, D.H., and Snyder, M.P. (2017). Topological organization and dynamic regulation of human tRNA genes during macrophage differentiation. Genome Biol. *18*, 180.

Boskovic, A., Bing, X.Y., Kaymak, E., and Rando, O.J. (2020). Control of noncoding RNA production and histone levels by a 5' tRNA fragment. Genes Dev. *34*, 118–131.

Bostick, M., Jong, K.K., Estève, P.O., Clark, A., Pradhan, S., and Jacobsen, S.E. (2007). UHRF1 plays a role in maintaining DNA methylation in mammalian cells. Science *317*, 1760–1764.

Bourgeois, G., Marcoux, J., Saliou, J.M., Cianférani, S., and Graille, M. (2017). Activation mode of the eukaryotic m2G10 tRNA methyltransferase Trm11 by its partner protein Trm112. Nucleic Acids Res. *45*, 1971–1982.

Brose, K., Bland, K.S., Kuan, H.W., Arnott, D., Henzel, W., Goodman, C.S., Tessier-Lavigne, M., and Kidd, T. (1999). Slit proteins bind robo receptors and have an evolutionarily conserved role in repulsive axon guidance. Cell *96*, 795–806.

de Bruijn, M.H.L., Schreier, P.H., Eperon, I.C., Barrell, B.G., Chen, E.Y., Armstrong, P.W., Wong, J.F.H., and Roe, B.A. (1980). A mammalian mitochondrial serine transfer RNA lacking the "dihydrouridine" loop and stem. Nucleic Acids Res. *8*, 5213–5222.

Brulé, H., Elliott, M., Redlak, M., Zehner, Z.E., and Holmes, W.M. (2004). Isolation and characterization of the human tRNA-(N1G37) methyltransferase (TRM5) and comparison to the Escherichia coli TrmD protein. Biochemistry *43*, 9243–9255.

Bryant, G.O., Prabhu, V., Floer, M., Wang, X., Spagna, D., Schreiber, D., and Ptashne, M. (2008). Activator control of nucleosome occupancy in activation and repression of transcription. PLoS Biol. *6*, e317.

Buitrago, D., Labrador, M., Arcon, J.P., Lema, R., Flores, O., Esteve-Codina, A., Blanc, J., Villegas, N., Bellido, D., Gut, M., et al. (2021). Impact of DNA methylation on 3D genome structure. Nat. Commun. *12*, 3243.

Buschbeck, M., and Hake, S.B. (2017). Variants of core histones and their roles in cell fate decisions, development and cancer. Nat. Rev. Mol. Cell Biol. *18*, 299–314.

Carlson, B.A., Kwon, S.Y., Chamorro, M., Oroszlan, S., Hatfield, D.L., and Lee, B.J. (1999). Transfer RNA modification status influences retroviral ribosomal frameshifting. Virology *255*, 2–8.

Carlson, B.A., Mushinski, J.F., Henderson, D.W., Kwon, S.Y., Crain, P.F., Lee, B.J., and Hatfield, D.L. (2001). 1-Methylguanosine in place of Y base at position 37 in phenylalanine tRNA is responsible for its shiftiness in retroviral ribosomal frameshifting. Virology *279*, 130–135.

Carter, J.M., Emmett, W., Mozos, I.R., Kotter, A., Helm, M., Ule, J., and Hussain, S. (2019). FICC-Seq: a method for enzyme-specified profiling of methyl-5-uridine in cellular RNA. Nucleic Acids Res. *47*, e113.

Cavaillé, J., Chetouani, F., and Bachellerie, J.P. (1999). The yeast Saccharomyces cerevisiae YDL112w ORF encodes the putative 2'- O-ribose methyltransferase catalyzing the formation of Gm18 in tRNAs. RNA *5*, 66–81.

Chan, P.P., and Lowe, T.M. (2016). GtRNAdb 2.0: An expanded database of transfer RNA genes identified in complete and draft genomes. Nucleic Acids Res. *44*, D184–D189.

Chan, C.T.Y., Dyavaiah, M., DeMott, M.S., Taghizadeh, K., Dedon, P.C., and Begley, T.J. (2010). A quantitative systems approach reveals dynamic control of tRNA modifications during cellular stress. PLoS Genet. *6*, e1001247.

Chan, C.T.Y., Deng, W., Li, F., Demott, M.S., Babu, I.R., Begley, T.J., and Dedon, P.C. (2015). Highly Predictive Reprogramming of tRNA Modifications Is Linked to Selective Expression of Codon-Biased Genes. Chem. Res. Toxicol. *28*, 978–988.

Chatterjee, K., Nostramo, R.T., Wan, Y., and Hopper, A.K. (2018). tRNA dynamics between the nucleus, cytoplasm and mitochondrial surface: Location, location, location. Biochim. Biophys. Acta - Gene Regul. Mech. *1861*, 373–386.

Cheishvili, D., Boureau, L., and Szyf, M. (2015). DNA demethylation and invasive cancer: Implications for therapeutics. Br. J. Pharmacol. *172*, 2705–2715.

Chen, H.M., Wang, J., Zhang, Y.F., and Gao, Y.H. (2017). Ovarian cancer proliferation and apoptosis are regulated by human transfer RNA methyltransferase 9-likevia LIN9. Oncol. Lett. *14*, 4461–4466.

References

Chen, Q., Shen, P., Ge, W.L., Yang, T.Y., Wang, W.J., Meng, L.D., Huang, X.M., Zhang, Y.H., Cao, S.J., Miao, Y., et al. (2021). Roundabout homolog 1 inhibits proliferation via the YY1-ROBO1-CCNA2-CDK2 axis in human pancreatic cancer. Oncogene *40*, 2772–2784.

Chen, Y.A., Lemire, M., Choufani, S., Butcher, D.T., Grafodatskaya, D., Zanke, B.W., Gallinger, S., Hudson, T.J., and Weksberg, R. (2013). Discovery of cross-reactive probes and polymorphic CpGs in the Illumina Infinium HumanMethylation450 microarray. Epigenetics *8*, 203–209.

Chen, Y.C., Kelly, V.P., Stachura, S. V., and Garcia, G.A. (2010). Characterization of the human tRNA-guanine transglycosylase: Confirmation of the heterodimeric subunit structure. RNA *16*, 958–968.

Chen, Z., Qi, M., Shen, B., Luo, G., Wu, Y., Li, J., Lu, Z., Zheng, Z., Dai, Q., and Wang, H. (2019). Transfer RNA demethylase ALKBH3 promotes cancer progression via induction of tRNA-derived small RNAs. Nucleic Acids Res. *47*, 2533–2545.

Chernyakov, I., Whipple, J.M., Kotelawala, L., Grayhack, E.J., and Phizicky, E.M. (2008). Degradation of several hypomodified mature tRNA species in Saccharomyces cerevisiae is mediated by Met22 and the 5′-3′ exonucleases Rat1 and Xrn1. Genes Dev. *22*, 1369–1380.

Chiang, T.-S., Lin, M.-C., Tsai, M.-C., Chen, C.-H., Jang, L.-T., and Lee, F.-J.S. (2019). ADP-ribosylation factor–like 4A interacts with Robo1 to promote cell migration by regulating Cdc42 activation. Mol. Biol. Cell *30*, 69–81.

Chodavarapu, R.K., Feng, S., Bernatavichute, Y. V., Chen, P.Y., Stroud, H., Yu, Y., Hetzel, J.A., Kuo, F., Kim, J., Cokus, S.J., et al. (2010). Relationship between nucleosome positioning and DNA methylation. Nature *466*, 388–392.

Chu, C., Qu, K., Zhong, F.L., Artandi, S.E., and Chang, H.Y. (2011). Genomic Maps of Long Noncoding RNA Occupancy Reveal Principles of RNA-Chromatin Interactions. Mol. Cell *44*, 667–678.

Chujo, T., and Suzuki, T. (2012). Trmt61B is a methyltransferase responsible for 1-methyladenosine at position 58 of human mitochondrial tRNAs. RNA *18*, 2269–2276.

Chymkowitch, P., and Enserink, J.M. (2018). Regulation of tRNA synthesis by posttranslational modifications of RNA polymerase III subunits. Biochim. Biophys. Acta - Gene Regul. Mech. *1861*, 310–319.

Clapier, C.R., Iwasa, J., Cairns, B.R., and Peterson, C.L. (2017). Mechanisms of action and regulation of ATP-dependent chromatin-remodelling complexes. Nat. Rev. Mol. Cell Biol. *18*, 407–422.

Colaprico, A., Silva, T.C., Olsen, C., Garofano, L., Cava, C., Garolini, D., Sabedot, T.S., Malta, T.M., Pagnotta, S.M., Castiglioni, I., et al. (2016). TCGAbiolinks: An R/Bioconductor package for integrative analysis of TCGA data. Nucleic Acids Res. *44*, e71.

Cole, C., Sobala, A., Lu, C., Thatcher, S.R., Bowman, A., Brown, J.W.S., Green, P.J., Barton, G.J., and Hutvagner, G. (2009). Filtering of deep sequencing data reveals the existence of abundant Dicer-dependent small RNAs derived from tRNAs. RNA *15*, 2147–2160.

Collins, F.S., and Varmus, H. (2015). A New Initiative on Precision Medicine. N. Engl. J. Med. *372*, 793–795.

Commans, S., Lazard, M., Delort, F., Blanquet, S., and Plateau, P. (1998). tRNA Anticodon Recognition and Specification within Subclass IIb Aminoacyl-tRNA Synthetases. J. Mol. Biol. *278*, 801–813.

Cooley, L., Appel, B., and Soll, D. (1982). Post-transcriptional nucleotide addition is responsible for the formation of the 5' terminus of histidine tRNA. Proc. Natl. Acad. Sci. USA *79*, 6475–6479.

Copela, L.A., Fernandez, C.F., Sherrer, R.L., and Wolin, S.L. (2008). Competition between the Rex1 exonuclease and the La protein affects both Trf4p-mediated RNA quality control and pre-tRNA maturation. RNA *14*, 1214–1227.

Costello, J.F., Frühwald, M.C., Smiraglia, D.J., Rush, L.J., Robertson, G.P., Gao, X., Wright, F.A., Feramisco, J.D., Peltomäki, P., Lang, J.C., et al. (2000). Aberrant CpG-island methylation has non-random and tumour-type-specific patterns. Nat. Genet. *24*, 132–138.

Crick, F.H.C. (1966). Codon—anticodon pairing: The wobble hypothesis. J. Mol. Biol. *19*, 548–555.

Crothers, D.M., Seno, T., and Söll, G. (1972). Is there a discriminator site in transfer RNA? Proc. Natl. Acad. Sci. USA *69*, 3063–3067.

Cui, X.-L., Nie, J., Ku, J., Dougherty, U., West-szymanski, D.C., Collin, F., Ellison, C.K., Sieh, L., Ning, Y., Deng, Z., et al. (2020). A human tissue map of 5-hydroxymethylcytosines exhibits tissue specificity through gene and enhancer modulation. Nat. Commun. *11*, 6161.

Cui, Y., Huang, Y., Wu, X., Zheng, M., Xia, Y., Fu, Z., Ge, H., Wang, S., and Xie, H. (2019). Hypoxia-induced tRNA-derived fragments, novel regulatory factor for doxorubicin resistance in triple-negative breast cancer. J. Cell. Physiol. *234*, 8740–8751.

Cusack, M., King, H.W., Spingardi, P., Kessler, B.M., Klose, R.J., and Kriaucionis, S. (2020). Distinct contributions of DNA methylation and histone acetylation to the genomic occupancy of transcription factors. Genome Res. *30*, 1393–1406.

Cuthbert, G.L., Daujat, S., Snowden, A.W., Erdjument-Bromage, H., Hagiwara, T., Yamada, M., Schneider, R., Gregory, P.D., Tempst, P., Bannister, A.J., et al. (2004). Histone deimination antagonizes arginine methylation. Cell *118*, 545–553.

Czech, A., Wende, S., Mörl, M., Pan, T., and Ignatova, Z. (2013). Reversible and Rapid Transfer-RNA Deactivation as a Mechanism of Translational Repression in Stress. PLoS Genet. *9*, e1003767.

Dai, Z., Liu, H., Liao, J., Huang, C., Ren, X., Zhu, W., Zhu, S., Peng, B., Li, S., Lai, J., et al. (2021). N7-Methylguanosine tRNA modification enhances oncogenic mRNA translation and promotes intrahepatic cholangiocarcinoma progression. Mol. Cell *81*, 3339–3355.

Dana, A., and Tuller, T. (2014). The effect of tRNA levels on decoding times of mRNA codons. Nucleic Acids Res. *42*, 9171–9181.

Deans, C., and Maggert, K.A. (2015). What do you mean, "Epigenetic"? Genetics *199*, 887–896.

Delaunay, S., Rapino, F., Tharun, L., Zhou, Z., Heukamp, L., Termathe, M., Shostak, K., Klevernic, I., Florin, A., Desmecht, H., et al. (2016). Elp3 links tRNA modification to IRES-dependent translation of LEF1 to sustain metastasis in breast cancer. J. Exp. Med. *213*, 2503–2523.

Desai, N., Lee, J.H., Upadhya, R., Chu, Y., Moir, R.D., and Willis, I.M. (2005). Two steps in Maf1-dependent repression of transcription by RNA polymerase III. J. Biol. Chem. *280*, 6455–6462.

Deutscher, M.P. (1973). Synthesis and Functions of the -C-C-A Terminus of Transfer RNA. Prog. Nucleic Acid Res. Mol. Biol. *13*, 51–92.

Dewe, J.M., Fuller, B.L., Lentini, J.M., Kellner, S.M., and Fu, D. (2017). TRMT1-Catalyzed tRNA Modifications Are Required for Redox Homeostasis To Ensure Proper Cellular Proliferation and Oxidative Stress Survival. Mol. Cell. Biol. *37*, e00214-17.

Diaz-Lagares, A., Crujeiras, A.B., Lopez-Serra, P., Soler, M., Setien, F., Goyal, A., Sandoval, J., Hashimoto, Y., Martinez-Cardús, A., Gomez, A., et al. (2016). Epigenetic inactivation of the p53-induced long noncoding RNA TP53 target 1 in human cancer. Proc. Natl. Acad. Sci. USA *113*, E7535–E7544.

Dieci, G., and Sentenac, A. (1996). Facilitated recycling pathway for RNA polymerase III. Cell *84*, 245–252.

Dinman, J.D. (2012). Mechanisms and implications of programmed translational frameshifting. Wiley Interdiscip. Rev. RNA *3*, 661–673.

Dittmar, K.A., Goodenbour, J.M., and Pan, T. (2006). Tissue-specific differences in human transfer RNA expression. PLoS Genet. *2*, 2107–2115.

References

Dong, C., Niu, L., Song, W., Xiong, X., Zhang, X., Zhang, Z., Yang, Y., Yi, F., Zhan, J., Zhang, H., et al. (2016). tRNA modification profiles of the fast-proliferating cancer cells. Biochem. Biophys. Res. Commun. *476*, 340–345.

Dongre, A., and Weinberg, R.A. (2019). New insights into the mechanisms of epithelial–mesenchymal transition and implications for cancer. Nat. Rev. Mol. Cell Biol. *20*, 69–84.

Donovan, J., Rath, S., Kolet-Mandrikov, D., and Korennykh, A. (2017). Rapid RNase L–driven arrest of protein synthesis in the dsRNA response without degradation of translation machinery. RNA *23*, 1660–1671.

Eikesdal, H.P., Yndestad, S., Elzawahry, A., Llop-Guevara, A., Gilje, B., Blix, E.S., Espelid, H., Lundgren, S., Geisler, J., Vagstad, G., et al. (2021). Olaparib monotherapy as primary treatment in unselected triple negative breast cancer. Ann. Oncol. *32*, 240–249.

Eldred, E.W., and Schimmel, P.R. (1972). Rapid deacylation by isoleucyl transfer ribonucleic acid synthetase of isoleucine-specific transfer ribonucleic acid aminoacylated with valine. J. Biol. Chem. *247*, 2961–2964.

Endres, L., Dedon, P.C., and Begley, T.J. (2015). Codon-biased translation can be regulated by wobble-base tRNA modification systems during cellular stress responses. RNA Biol. *12*, 603–614.

Endres, L., Fasullo, M., and Rose, R. (2019). TRNA modification and cancer: Potential for therapeutic prevention and intervention. Future Med. Chem. *11*, 885–900.

Esteller, M. (2008). Epigenetics in cancer. N Engl J Med *358*, 1148–1159.

Esteller, M., Garcia-Foncillas, J., Andion, E., Goodman, S.N., Hidalgo, O.F., Vanaclocha, V., Baylin, S.B., and Herman, J.G. (2000). Inactivation of the DNA-Repair Gene MGMT and the Clinical Response of Gliomas to Alkylating Agents . N. Engl. J. Med. *343*, 1350–1354.

Falconi, M., Giangrossi, M., Zabaleta, M.E., Wang, J., Gambini, V., Tilio, M., Bencardino, D., Occhipinti, S., Belletti, B., Laudadio, E., et al. (2019). A novel 3'-tRNAGlu-derived fragment acts as a tumor suppressor in breast cancer by targeting nucleolin. FASEB J. *33*, 13228–13240.

Fan, J., Li, J., Guo, S., Tao, C., Zhang, H., Wang, W., Zhang, Y., Zhang, D., Ding, S., and Zeng, C. (2020). Genome-wide DNA methylation profiles of low- And high-grade adenoma reveals potential biomarkers for early detection of colorectal carcinoma. Clin. Epigenetics *12*, 56.

Fan, S., Yuan, R., Ma, Y.X., Meng, Q., Goldberg, I.D., and Rosen, E.M. (2001). Mutant BRCA1 genes antagonize phenotype of wild-type BRCA1. Oncogene 2001 2057 *20*, 8215–8235.

Feinberg, A.P., and Vogelstein, B. (1983a). Hypomethylation distinguishes genes of some human cancers from their normal counterparts. Nature *301*, 89–92.

Feinberg, A.P., and Vogelstein, B. (1983b). Hypomethylation of ras oncogenes in primary human cancers. Biochem. Biophys. Res. Commun. *111*, 47–54.

Feng, Y., Feng, L., Yu, D., Zou, J., and Huang, Z. (2016). srGAP1 mediates the migration inhibition effect of Slit2-Robo1 in colorectal cancer. J. Exp. Clin. Cancer Res. *35*, 191.

Foltz, D.R., Jansen, L.E.T., Bailey, A.O., Yates, J.R., Bassett, E.A., Wood, S., Black, B.E., and Cleveland, D.W. (2009). Centromere-Specific Assembly of CENP-A Nucleosomes Is Mediated by HJURP. Cell *137*, 472–484.

Frumkin, I., Lajoie, M.J., Gregg, C.J., Hornung, G., Church, G.M., and Pilpel, Y. (2018). Codon usage of highly expressed genes affects proteome-wide translation efficiency. Proc. Natl. Acad. Sci. USA *115*, E4940–E4949.

Frye, M., Dragoni, I., Chin, S.F., Spiteri, I., Kurowski, A., Provenzano, E., Green, A., Ellis, I.O., Grimmer, D., Teschendorff, A., et al. (2010). Genomic gain of 5p15 leads to over-expression of Misu (NSUN2) in breast cancer. Cancer Lett. *289*, 71–80.

Fuks, F., Hurd, P.J., Wolf, D., Nan, X., Bird, A.P., and Kouzarides, T. (2003). The methyl-CpG-binding protein MeCP2 links DNA methylation to histone methylation. J. Biol. Chem. *278*, 4035–4040.

Galli, G., Hofstetter, H., and Birnstiel, M.L. (1981). Two conserved sequence blocks within eukaryotic tRNA genes are major promoter elements. Nature *294*, 626–631.

Gardin, J., Yeasmin, R., Yurovsky, A., Cai, Y., Skiena, S., and Futcher, B. (2014). Measurement of average decoding rates of the 61 sense codons in vivo. Elife *3*, e03735.

Gardiner-Garden, M., and Frommer, M. (1987). CpG Islands in vertebrate genomes. J. Mol. Biol. *196*, 261–282.

Gelli, E., Pinto, A.M., Somma, S., Imperatore, V., Cannone, M.G., Hadjistilianou, T., De Francesco, S., Galimberti, D., Currò, A., Bruttini, M., et al. (2019). Evidence of predisposing epimutation in retinoblastoma. Hum. Mutat. *40*, 201–206.

Gerber, A.P., and Keller, W. (1999). An adenosine deaminase that generates inosine at the wobble position of tRNAs. Science *286*, 1146–1149.

Gerber, A., Grosjean, H., Melcher, T., and Keller, W. (1998). Tad1p, a yeast tRNA-specific adenosine deaminase, is related to the mammalian pre-mRNA editing enzymes ADAR1 and ADAR2. EMBO J. *17*, 4780–4789.

Gerber, A., Ito, K., Chu, C.S., and Roeder, R.G. (2020). Gene-Specific Control of tRNA Expression by RNA Polymerase II. Mol. Cell *78*, 765–778.

Ghandi, M., Huang, F.W., Jané-Valbuena, J., Kryukov, G. V., Lo, C.C., McDonald, E.R., Barretina, J., Gelfand, E.T., Bielski, C.M., Li, H., et al. (2019). Next-generation characterization of the Cancer Cell Line Encyclopedia. Nature *569*, 503–508.

Giegé, R., and Eriani, G. (2014). Transfer RNA Recognition and Aminoacylation by Synthetases. In ELS, (American Cancer Society), pp. 1–18.

Gingold, H., Tehler, D., Christoffersen, N.R., Nielsen, M.M., Asmar, F., Kooistra, S.M., Christophersen, N.S., Christensen, L.L., Borre, M., Sørensen, K.D., et al. (2014). A dual program for translation regulation in cellular proliferation and differentiation. Cell *158*, 1281–1292.

Gogakos, T., Brown, M., Garzia, A., Meyer, C., Hafner, M., and Tuschl, T. (2017). Characterizing Expression and Processing of Precursor and Mature Human tRNAs by Hydro-tRNAseq and PAR-CLIP. Cell Rep. *20*, 1463–1475.

Gomez, M.A.R., and Ibba, M. (2020). Aminoacyl-tRNA synthetases. RNA *26*, 910–936.

Good, P.D., Kendall, A., Ignatz-Hoover, J., Miller, E.L., Pai, D.A., Rivera, S.R., Carrick, B., and Engelke, D.R. (2013). Silencing near tRNA genes is nucleosome-mediated and distinct from boundary element function. Gene *526*, 7–15.

Goodarzi, H., Liu, X., Nguyen, H.C.B., Zhang, S., Fish, L., and Tavazoie, S.F. (2015). Endogenous tRNA-derived fragments suppress breast cancer progression via YBX1 displacement. Cell *161*, 790–802.

Goodarzi, H., Nguyen, H.C.B., Zhang, S., Dill, B.D., Molina, H., and Tavazoie, S.F. (2016). Modulated expression of specific tRNAs drives gene expression and cancer progression. Cell *165*, 1416–1427.

Graczyk, D., Cieśla, M., and Boguta, M. (2018). Regulation of tRNA synthesis by the general transcription factors of RNA polymerase III - TFIIIB and TFIIIC, and by the MAF1 protein. Biochim. Biophys. Acta - Gene Regul. Mech. *1861*, 320–329.

Greger, V., Passarge, E., Höpping, W., Messmer, E., and Horsthemke, B. (1989). Epigenetic changes may contribute to the formation and spontaneous regression of retinoblastoma. Hum. Genet. *83*, 155–158.

References

Grentzmann, G., Ingram, J.A., Kelly, P.J., Gesteland, R.F., and Atkins, J.F. (1998). A dual-luciferase reporter system for studying recoding signals. RNA *4*, 479–486.

Grivennikov, S.I., Greten, F.R., and Karin, M. (2010). Immunity, Inflammation, and Cancer. Cell *140*, 883–899.

Grunberger, D., Weinstein, I.B., and Mushinski, J.F. (1975). Deficiency of the Y base in hepatoma phenylalanine tRNA. Nature *253*, 66–67.

Gu, C., Begley, T.J., and Dedon, P.C. (2014). TRNA modifications regulate translation during cellular stress. FEBS Lett. *588*, 4287–4296.

Guo, H., Zhu, P., Yan, L., Li, R., Hu, B., Lian, Y., Yan, J., Ren, X., Lin, S., Li, J., et al. (2014). The DNA methylation landscape of human early embryos. Nature *511*, 606–610.

Guy, M.P., Podyma, B.M., Preston, M.A., Shaheen, H.H., Krivos, K.L., Limbach, P.A., Hopper, A.K., and Phizicky, E.M. (2012). Yeast Trm7 interacts with distinct proteins for critical modifications of the tRNAPhe anticodon loop. RNA *18*, 1921–1933.

Guy, M.P., Young, D.L., Payea, M.J., Zhang, X., Kon, Y., Dean, K.M., Grayhack, E.J., Mathews, D.H., Fields, S., and Phizicky, E.M. (2014). Identification of the determinants of tRNA function and susceptibility to rapid tRNA decay by high-throughput in vivo analysis. Genes Dev. *28*, 1721–1732.

Haag, S., Warda, A.S., Kretschmer, J., Günnigmann, M.A., Höbartner, C., and Bohnsack, M.T. (2015). NSUN6 is a human RNA methyltransferase that catalyzes formation of m5C72 in specific tRNAs. RNA *21*, 1532–1543.

Han, M., Jia, L., Lv, W., Wang, L., and Cui, W. (2019). Epigenetic Enzyme Mutations: Role in Tumorigenesis and Molecular Inhibitors. Front. Oncol. *9*, 194.

Hanahan, D., and Weinberg, R.A. (2000). The Hallmarks of Cancer. Cell *100*, 57–70.

Hanahan, D., and Weinberg, R.A. (2011). Hallmarks of cancer: The next generation. Cell *144*, 646–674.

Harikrishnan, K.N., Chow, M.Z., Baker, E.K., Pal, S., Bassal, S., Brasacchio, D., Wang, L., Craig, J.M., Jones, P.L., Sif, S., et al. (2005). Brahma links the SWI/SNF chromatin-remodeling complex with MeCP2-dependent transcriptional silencing. Nat. Genet. *37*, 254–264.

Harper, W.J., Adami, G.R., Wei, N., Keyomarsi, K., and Elledge, S.J. (1993). The p21 Cdk-interacting protein Cip1 is a potent inhibitor of G1 cyclin-dependent kinases. Cell *75*, 805–816.

Hashimoto, H., Wang, D., Horton, J.R., Zhang, X., Corces, V.G., and Cheng, X. (2017). Structural Basis for the Versatile and Methylation-Dependent Binding of CTCF to DNA. Mol. Cell *66*, 711–720.

Haurie, V., Durrieu-Gaillard, S., Dumay-Odelot, H., Da Silva, D., Rey, C., Prochazkova, M., Roeder, R.G., Besser, D., and Teichmann, M. (2010). Two isoforms of human RNA polymerase III with specific functions in cell growth and transformation. Proc. Natl. Acad. Sci. USA *107*, 4176–4181.

Hayne, C.K., Schmidt, C.A., Haque, M.I., Matera, A.G., and Stanley, R.E. (2020). Reconstitution of the human tRNA splicing endonuclease complex: insight into the regulation of pre-tRNA cleavage. Nucleic Acids Res. *48*, 7609–7622.

He, Y.F., Li, B.Z., Li, Z., Liu, P., Wang, Y., Tang, Q., Ding, J., Jia, Y., Chen, Z., Li, N., et al. (2011). Tet-mediated formation of 5-carboxylcytosine and its excision by TDG in mammalian DNA. Science *333*, 1303–1307.

Hendrich, B., and Bird, A. (1998). Identification and characterization of a family of mammalian methyl CpG-binding proteins. Genet. Res. *72*, 59–72.

Hernandez-Alias, X., Benisty, H., Schaefer, M.H., and Serrano, L. (2020). Translational efficiency across healthy and tumor tissues is proliferation-related. Mol. Syst. Biol. *16*, e9275.

Heyn, H., and Esteller, M. (2015). An adenine code for DNA: A second life for N6-methyladenine. Cell *161*, 710–713.

Heyn, H., Vidal, E., Ferreira, H.J., Vizoso, M., Sayols, S., Gomez, A., Moran, S., Boque-Sastre, R., Guil, S., Martinez-Cardus, A., et al. (2016). Epigenomic analysis detects aberrant super-enhancer DNA methylation in human cancer. Genome Biol. *17*, 11.

Himeno, H., Yoshida, S., Soma, A., and Nishikawa, K. (1997). Only one nucleotide insertion to the long variable arm confers an efficient serine acceptor activity upon Saccharomyces cerevisiae tRNA(Leu) in vitro. J. Mol. Biol. *268*, 704–711.

Hoagland, M.B., Stephenson, M.L., F., S.J., Hecht, L.I., and Zamecnik, P.C. (1958). A soluble ribonucleic acid intermediate in protein synthesis. J. Biol. Chem. *231*, 241–257.

Holley, R.W., Apgar, J., Everett, G.A., Madison, J.T., Marquisee, M., Merrill, S.H., Penswick, J.R., and Zamir, A. (1965). Structure of a ribonucleic acid. Science *147*, 1462–1465.

Holliday, R. (1994). Epigenetics: An overview. Dev. Genet. *15*, 453–457.

Holliday, R., and Pugh, J.E. (1975). DNA modification mechanisms and gene activity during development. Science *187*, 226–232.

Holz-Schietinger, C., and Reich, N.O. (2012). RNA modulation of the human DNA methyltransferase 3A. Nucleic Acids Res. *40*, 8550–8557.

Honda, S., Loher, P., Shigematsu, M., Palazzo, J.P., Suzuki, R., Imoto, I., Rigoutsos, I., and Kirino, Y. (2015). Sex hormone-dependent tRNA halves enhance cell proliferation in breast and prostate cancers. Proc. Natl. Acad. Sci. USA *112*, E3816–E3825.

Howell, N.W., Jora, M., Jepson, B.F., Limbach, P.A., and Jackman, J.E. (2019). Distinct substrate specificities of the human tRNA methyltransferases TRMT10A and TRMT10B. RNA *25*, 1366–1376.

Huang, B.-S., Wu, R.-T., and Chien, K.-Y. (1992). Relationship of the Queuine Content of Transfer Ribonucleic Acids to Histopathological Grading and Survival in Human Lung Cancer. Cancer Res. *52*, 4606–4700.

Huang, B., Johansson, M.J.O., and Byström, A.S. (2005). An early step in wobble uridine tRNA modification requires the Elongator complex. RNA *11*, 424–436.

Huang, Y., Ge, H., Zheng, M., Cui, Y., Fu, Z., Wu, X., Xia, Y., Chen, L., Wang, Z., Wang, S., et al. (2020). Serum tRNA-derived fragments (tRFs) as potential candidates for diagnosis of nontriple negative breast cancer. J. Cell. Physiol. *235*, 2809–2824.

Huang, Z., Wen, P., Kong, R., Cheng, H., Zhang, B., Quan, C., Bian, Z., Chen, M., Zhang, Z., Chen, X., et al. (2015). USP33 mediates Slit-Robo signaling in inhibiting colorectal cancer cell migration. Int. J. Cancer *136*, 1792–1802.

Huh, D., Passarelli, M.C., Gao, J., Dusmatova, S.N., Goin, C., Fish, L., Pinzaru, A.M., Molina, H., Ren, Z., McMillan, E.A., et al. (2021). A stress-induced tyrosine-tRNA depletion response mediates codon-based translational repression and growth suppression. EMBO J. *40*, e106696.

Iorio, F., Knijnenburg, T.A., Vis, D.J., Bignell, G.R., Menden, M.P., Schubert, M., Aben, N., Gonçalves, E., Barthorpe, S., Lightfoot, H., et al. (2016). A Landscape of Pharmacogenomic Interactions in Cancer. Cell *166*, 740–754.

Ishimura, R., Nagy, G., Dotu, I., Zhou, H., Yang, X.L., Schimmel, P., Senju, S., Nishimura, Y., Chuang, J.H., and Ackerman, S.L. (2014). Ribosome stalling induced by mutation of a CNS-specific tRNA causes neurodegeneration. Science *345*, 455–459.

Ito, S., Shen, L., Dai, Q., Wu, S.C., Collins, L.B., Swenberg, J.A., He, C., and Zhang, Y. (2011). Tet proteins can convert 5-methylcytosine to 5-formylcytosine and 5-carboxylcytosine. Science *333*, 1300–1303.

References

Ivanov, I., Lo, K.C., Hawthorn, L., Cowell, J.K., and Ionov, Y. (2007). Identifying candidate colon cancer tumor suppressor genes using inhibition of nonsense-mediated mRNA decay in colon cancer cells. Oncogene *26*, 2873–2884.

Jackman, J.E., and Alfonzo, J.D. (2013). Transfer RNA modifications: Nature's combinatorial chemistry playground. Wiley Interdiscip. Rev. RNA *4*, 35–48.

Jaco, I., Canela, A., Vera, E., and Blasco, M.A. (2008). Centromere mitotic recombination in mammalian cells. J. Cell Biol. *181*, 885–892.

Jang, H.S., Shin, W.J., Lee, J.E., and Do, J.T. (2017). CpG and Non-CpG Methylation in Epigenetic Gene Regulation and Brain Function. Genes (Basel). *8*, 148.

Jarrous, N. (2017). Roles of RNase P and Its Subunits. Trends Genet. *33*, 594–603.

Jenuwein, T., and Allis, C.D. (2001). Translating the histone code. Science *293*, 1074–1080.

Jiang, Z., Liang, G., Xiao, Y., Qin, T., Chen, X., Wu, E., Ma, Q., and Wang, Z. (2019). Targeting the SLIT/ROBO pathway in tumor progression: molecular mechanisms and therapeutic perspectives. Ther. Adv. Med. Oncol. *11*, 1758835919855238.

Jin, F., Yang, L., Wang, W., Yuan, N., Zhan, S., Yang, P., Chen, X., Ma, T., and Wang, Y. (2021). A novel class of tsRNA signatures as biomarkers for diagnosis and prognosis of pancreatic cancer. Mol. Cancer *20*, 95.

Johnson, J.K., Waddell, N., and Chenevix-Trench, G. (2012). The application of nonsense-mediated mRNA decay inhibition to the identification of breast cancer susceptibility genes. BMC Cancer *12*, 246.

Kadaba, S., Wang, X., and Anderson, J.T. (2006). Nuclear RNA surveillance in Saccharomyces cerevisiae: Trf4p-dependent polyadenylation of nascent hypomethylated tRNA and an aberrant form of 5S rRNA. RNA *12*, 508–521.

Kantidakis, T., Ramsbottom, B.A., Birch, J.L., Dowding, S.N., and White, R.J. (2010). mTOR associates with TFIIIC, is found at tRNA and 5S rRNA genes, and targets their repressor Maf1. Proc. Natl. Acad. Sci. USA *107*, 11823–11828.

Karpf, A.R., and Matsui, S.I. (2005). Genetic disruption of cytosine DNA methyltransferase enzymes induces chromosomal instability in human cancer cells. Cancer Res. *65*, 8635–8639.

Kassavetis, G.A., Letts, G.A., and Geiduschek, E.P. (2001). The RNA polymerase III transcription initiation factor TFIIIB participates in two steps of promoter opening. EMBO J. *20*, 2823–2834.

Kawarada, L., Suzuki, T., Ohira, T., Hirata, S., Miyauchi, K., and Suzuki, T. (2017). ALKBH1 is an RNA dioxygenase responsible for cytoplasmic and mitochondrial tRNA modifications. Nucleic Acids Res. *45*, 7401–7415.

Kernan, J., Martinez-Chacin, R., Wang, X., Tiedemann, R., Bonacci, T., Choudhury, R., Bolhuis, D., Damrauer, J., Yan, F., Harrison, J., et al. (2020). In silico APC/C substrate discovery reveals cell cycle degradation of chromatin regulators including UHRF1. PLOS Biol. *18*, e3000975.

Kim, S.H., Sussman, J.L., Suddath, F.L., Quigley, G.J., McPherson, A., Wang, A.H., Seeman, N.C., and RICH, A. (1974). The general structure of transfer RNA molecules. Proc. Natl. Acad. Sci. USA *71*, 4970–4974.

Kimura, S., Miyauchi, K., Ikeuchi, Y., Thiaville, P.C., De Crécy-Lagard, V., and Suzuki, T. (2014). Discovery of the β-barrel-type RNA methyltransferase responsible for N6-methylation of N6-threonylcarbamoyladenosine in tRNAs. Nucleic Acids Res. *42*, 9350–9365.

Kirkland, J.G., Raab, J.R., and Kamakaka, R.T. (2013). TFIIIC bound DNA elements in nuclear organization and insulation. Biochim. Biophys. Acta - Gene Regul. Mech. *1829*, 418–424.

Konevega, A.L., Soboleva, N.G., Makhno, V.I., Semenkov, Y.P., Wintermeyer, W., Rodnina, M. V, and Katunin, V.I. (2004). Purine bases at position 37 of tRNA stabilize codon-anticodon interaction in the ribosomal A site by stacking and Mg2+-dependent interactions. RNA *10*, 90–101.

Kotelawala, L., Grayhack, E.J., and Phizicky, E.M. (2008). Identification of yeast tRNA Um44 2′-O-methyltransferase (Trm44) and demonstration of a Trm44 role in sustaining levels of specific tRNASer species. RNA *14*, 158–169.

Kotoh, Y., Suehiro, Y., Saeki, I., Hoshida, T., Maeda, M., Iwamoto, T., Matsumoto, T., Hidaka, I., Ishikawa, T., Takami, T., et al. (2020). Novel Liquid Biopsy Test Based on a Sensitive Methylated SEPT9 Assay for Diagnosing Hepatocellular Carcinoma. Hepatol. Commun. *4*, 461–470.

Kuang, M., Zheng, D., Tao, X., Peng, Y., Pan, Y., Zheng, S., Zhang, Y.Y., Li, H., Yuan, C., Zhang, Y.Y., et al. (2019). tRNA-based prognostic score in predicting survival outcomes of lung adenocarcinomas. Int. J. Cancer *145*, 1982–1990.

Kuchino, Y., Borek, E., Grunberger, D., Mushinski, J.F., and Nishimura, S. (1982). Changes of post-transcriptional modification of wye base in tumor-specific tRNAPhe. Nucleic Acids Res. *10*, 6421–6432.

Kumar, P., Anaya, J., Mudunuri, S.B., and Dutta, A. (2014). Meta-analysis of tRNA derived RNA fragments reveals that they are evolutionarily conserved and associate with AGO proteins to recognize specific RNA targets. BMC Biol. *12*, 78.

Kurosaki, T., Popp, M.W., and Maquat, L.E. (2019). Quality and quantity control of gene expression by nonsense-mediated mRNA decay. Nat. Rev. Mol. Cell Biol. *20*, 406–420.

Kuscu, C., Kumar, P., Kiran, M., Su, Z., Malik, A., and Dutta, A. (2018). tRNA fragments (tRFs) guide Ago to regulate gene expression post-transcriptionally in a Dicer-independent manner. RNA *24*, 1093–1105.

Kutay, U., Lipowsky, G., Izaurralde, E., Bischoff, F.R., Schwarzmaier, P., Hartmann, E., and Görlich, D. (1998). Identification of a tRNA-specific nuclear export receptor. Mol. Cell *1*, 359–369.

Kwon, N.H., Lee, M.R., Kong, J., Park, S.K., Hwang, B.J., Kim, B.G., Lee, E.S., Moon, H.G., and Kim, S. (2018). Transfer-RNA-mediated enhancement of ribosomal proteins S6 kinases signaling for cell proliferation. RNA Biol. *15*, 635–648.

Labun, K., Montague, T.G., Gagnon, J.A., Thyme, S.B., and Valen, E. (2016). CHOPCHOP v2: a web tool for the next generation of CRISPR genome engineering. Nucleic Acids Res. *44*, W272–W276.

Lamichhane, T.N., Mattijssen, S., and Maraia, R.J. (2013). Human Cells Have a Limited Set of tRNA Anticodon Loop Substrates of the tRNA Isopentenyltransferase TRIT1 Tumor Suppressor. Mol. Cell. Biol. *33*, 4900–4908.

Lamouille, S., Xu, J., and Derynck, R. (2014). Molecular mechanisms of epithelial-mesenchymal transition. Nat. Rev. Mol. Cell Biol. *15*, 178–196.

Lant, J.T., Berg, M.D., Heinemann, I.U., Brandl, C.J., and O'Donoghue, P. (2019). Pathways to disease from natural variations in human cytoplasmic tRNAs. J. Biol. Chem. *294*, 5294–5308.

Laurent, L., Wong, E., Li, G., Huynh, T., Tsirigos, A., Ong, C.T., Low, H.M., Sung, K.W.K., Rigoutsos, I., Loring, J., et al. (2010). Dynamic changes in the human methylome during differentiation. Genome Res. *20*, 320–331.

Lawrence, M., Daujat, S., and Schneider, R. (2016). Lateral Thinking: How Histone Modifications Regulate Gene Expression. Trends Genet. *32*, 42–56.

Lecointe, F., Simos, G., Sauer, A., Hurt, E.C., Motorin, Y., and Grosjean, H. (1998). Characterization of yeast protein Deg1 as pseudouridine synthase (Pus3) catalyzing the formation of Ψ38 and Ψ39 in tRNA anticodon loop. J. Biol. Chem. *273*, 1316–1323.

References

Lee, J.Y., Kim, D.G., Kim, B.G., Yang, W.S., Hong, J., Kang, T., Oh, Y.S., Kim, K.R., Han, B.W., Hwang, B.J., et al. (2014). Promiscuous methionyl-tRNA synthetase mediates adaptive mistranslation to protect cells against oxidative stress. J. Cell Sci. *127*, 4234–4245.

Lee, Y.C., Lheureux, S., and Oza, A.M. (2017). Treatment strategies for endometrial cancer: Current practice and perspective. Curr. Opin. Obstet. Gynecol. *29*, 47–58.

Lee, Y.S., Shibata, Y., Malhotra, A., and Dutta, A. (2009). A novel class of small RNAs: tRNA-derived RNA fragments (tRFs). Genes Dev. *23*, 2639–2649.

Lehnertz, B., Ueda, Y., Derijck, A.A.H.A., Braunschweig, U., Perez-Burgos, L., Kubicek, S., Chen, T., Li, E., Jenuwein, T., and Peters, A.H.F.M. (2003). Suv39h-mediated histone H3 lysine 9 methylation directs DNA methylation to major satellite repeats at pericentric heterochromatin. Curr. Biol. *13*, 1192–1200.

Lentini, J.M., Alsaif, H.S., Faqeih, E., Alkuraya, F.S., and Fu, D. (2020). DALRD3 encodes a protein mutated in epileptic encephalopathy that targets arginine tRNAs for 3-methylcytosine modification. Nat. Commun. *11*, 2510.

Li, E., Bestor, T.H., and Jaenisch, R. (1992). Targeted mutation of the DNA methyltransferase gene results in embryonic lethality. Cell *69*, 915–926.

Li, N., Shan, N., Lu, L., and Wang, Z. (2021). tRFtarget: a database for transfer RNA-derived fragment targets. Nucleic Acids Res. *49*, D254–D260.

Lianidou, E. (2021). Detection and relevance of epigenetic markers on ctDNA: recent advances and future outlook. Mol. Oncol. *15*, 1683–1700.

Lin, H., Miyauchi, K., Harada, T., Okita, R., Takeshita, E., Komaki, H., Fujioka, K., Yagasaki, H., Goto, Y.I., Yanaka, K., et al. (2018). CO2-sensitive tRNA modification associated with human mitochondrial disease. Nat. Commun. *9*, 1875.

Lindeboom, R.G.H., Supek, F., and Lehner, B. (2016). The rules and impact of nonsense-mediated mRNA decay in human cancers. Nat. Genet. *48*, 1112–1118.

Lister, R., Mukamel, E.A., Nery, J.R., Urich, M., Puddifoot, C.A., Johnson, N.D., Lucero, J., Huang, Y., Dwork, A.J., Schultz, M.D., et al. (2013). Global epigenomic reconfiguration during mammalian brain development. Science *341*, 1237905.

Liu, F., Clark, W., Luo, G., Wang, X., Fu, Y., Wei, J., Wang, X., Hao, Z., Dai, Q., Zheng, G., et al. (2016). ALKBH1-Mediated tRNA Demethylation Regulates Translation. Cell *167*, 816-828.e16.

Liu, H., Chen, J., Chen, H., Xia, J., Wang, O., Xie, J., Li, M., Guo, Z., Chen, G., and Yan, H. (2021a). Identification of the origin of brain metastases based on the relative methylation orderings of CpG sites. Epigenetics *16*, 908–916.

Liu, W. man, Maraia, R.J., Rubin, C.M., and Schmid, C.W. (1994). Alu transcripts: Cytoplasmic localisation and regulation by DNA methylation. Nucleic Acids Res. *22*, 1087–1095.

Liu, Y., Yang, Q., and Zhao, F. (2021b). Synonymous but Not Silent: The Codon Usage Code for Gene Expression and Protein Folding. Annu. Rev. Biochem. *90*, 375–401.

Livak, K.J., and Schmittgen, T.D. (2001). Analysis of relative gene expression data using real-time quantitative PCR and the 2-ΔΔCT method. Methods *25*, 402–408.

Loewer, S., Cabili, M.N., Guttman, M., Loh, Y.H., Thomas, K., Park, I.H., Garber, M., Curran, M., Onder, T., Agarwal, S., et al. (2010). Large intergenic non-coding RNA-RoR modulates reprogramming of human induced pluripotent stem cells. Nat. Genet. *42*, 1113–1117.

Love, M.I., Huber, W., and Anders, S. (2014). Moderated estimation of fold change and dispersion for RNA-seq data with DESeq2. Genome Biol. *15*, 550.

Manning, M., Jiang, Y., Wang, R., Liu, L., Rode, S., Bonahoom, M., Kim, S., and Yang, Z.Q. (2020). Pan-cancer analysis of RNA methyltransferases identifies FTSJ3 as a potential regulator of breast cancer progression. RNA Biol. *17*, 474–486.

Marck, C., Kachouri-Lafond, R., Lafontaine, I., Westhof, E., Dujon, B., and Grosjean, H. (2006). The RNA polymerase III-dependent family of genes in hemiascomycetes: Comparative RNomics, decoding strategies, transcription and evolutionary implications. Nucleic Acids Res. *34*, 1816–1835.

Markert, J., and Luger, K. (2020). Nucleosomes Meet Their Remodeler Match. Trends Biochem. Sci. *46*, 41–50.

Martincorena, I., and Campbell, P.J. (2015). Somatic mutation in cancer and normal cells. Science *349*, 1483–1489.

Martinelli, E., Ciardiello, D., Martini, G., Troiani, T., Cardone, C., Vitiello, P.P., Normanno, N., Rachiglio, A.M., Maiello, E., Latiano, T., et al. (2020). Implementing anti-epidermal growth factor receptor (EGFR) therapy in metastatic colorectal cancer: challenges and future perspectives. Ann. Oncol. *31*, 30–40.

Martinez, A., Yamashita, S., Nagaike, T., Sakaguchi, Y., Suzuki, T., and Tomita, K. (2017). Human BCDIN3D monomethylates cytoplasmic histidine transfer RNA. Nucleic Acids Res. *45*, 5423–5436.

De Mattos-Arruda, L., Vazquez, M., Finotello, F., Lepore, R., Porta, E., Hundal, J., Amengual-Rigo, P., Ng, C.K.Y., Valencia, A., Carrillo, J., et al. (2020). Neoantigen prediction and computational perspectives towards clinical benefit: recommendations from the ESMO Precision Medicine Working Group. Ann. Oncol. *31*, 978–990.

Maunakea, A.K., Chepelev, I., Cui, K., and Zhao, K. (2013). Intragenic DNA methylation modulates alternative splicing by recruiting MeCP2 to promote exon recognition. Cell Res. *23*, 1256–1269.

Mazauric, M.H., Dirick, L., Purushothaman, S.K., Bjö Rk, G.R., and Lapeyre, B. (2010). Trm112p is a 15-kDa zinc finger protein essential for the activity of two tRNA and one protein methyltransferases in yeast. J. Biol. Chem. *285*, 18505–18515.

Mcclain, W.H., and Foss, K. (1988). Changing the identity of a tRNA by introducing a G-U wobble pair near the 3′ acceptor end. Science *240*, 793–796.

Megel, C., Morelle, G., Lalande, S., Duchêne, A.M., Small, I., and Maréchal-Drouard, L. (2015). Surveillance and cleavage of eukaryotic tRNAs. Int. J. Mol. Sci. *16*, 1873–1893.

Mellén, M., Ayata, P., Dewell, S., Kriaucionis, S., and Heintz, N. (2012). MeCP2 binds to 5hmC enriched within active genes and accessible chromatin in the nervous system. Cell *151*, 1417–1430.

Mendell, J.T., Sharifi, N.A., Meyers, J.L., Martinez-Murillo, F., and Dietz, H.C. (2004). Nonsense surveillance regulates expression of diverse classes of mammalian transcripts and mutes genomic noise. Nat. Genet. *36*, 1073–1078.

Mercer, T.R., Qureshi, I.A., Gokhan, S., Dinger, M.E., Li, G., Mattick, J.S., and Mehler, M.F. (2010). Long noncoding RNAs in neuronal-glial fate specification and oligodendrocyte lineage maturation. BMC Neurosci. *11*, 14.

Mito, Y., Henikoff, J.G., and Henikoff, S. (2005). Genome-scale profiling of histone H3.3 replacement patterns. Nat. Genet. *37*, 1090–1097.

Mo, D., Jiang, P., Yang, Y., Mao, X., Tan, X., Tang, X., Wei, D., Li, B., Wang, X., Tang, L., et al. (2019). A tRNA fragment, 5′-tiRNA Val , suppresses the Wnt/β-catenin signaling pathway by targeting FZD3 in breast cancer. Cancer Lett. *457*, 60–73.

Moran, S., Martínez-Cardús, A., Sayols, S., Musulén, E., Balañá, C., Estival-Gonzalez, A., Moutinho, C., Heyn, H., Diaz-Lagares, A., de Moura, M.C., et al. (2016). Epigenetic profiling to classify cancer of unknown primary: a multicentre, retrospective analysis. Lancet Oncol. *17*, 1386–1395.

Motorin, Y., and Helm, M. (2010). TRNA stabilization by modified nucleotides. Biochemistry *49*, 4934–4944.

References

Mukhopadhyay, S., Deogharia, M., and Gupta, R. (2021). Mammalian nuclear TRUB1, mitochondrial TRUB2, and cytoplasmic PUS10 produce conserved pseudouridine 55 in different sets of tRNA. RNA *27*, 66–79.

Murthi, A., Shaheen, H.H., Huang, H.Y., Preston, M.A., Lai, T.P., Phizicky, E.M., and Hopper, A.K. (2010). Regulation of tRNA bidirectional nuclear-cytoplasmic trafficking in Saccharomyces cerevisiae. Mol. Biol. Cell *21*, 639–649.

Mushinski, J.F., and Marini, M. (1979). Tumor-associated Phenyiaianyl Transfer RNA Found in a Wide Spectrum of Rat and Mouse Tumors but Absent in Normal Adult, Fetal, and Regenerating Tissues. Cancer Res. *39*, 1253–1256.

Nakai, Y., Umeda, N., Suzuki, T., Nakai, M., Hayashi, H., Watanabe, K., and Kagamiyama, H. (2004). Yeast Nfs1p Is Involved in Thio-modification of Both Mitochondrial and Cytoplasmic tRNAs. J. Biol. Chem. *279*, 12363–12368.

Nakano, S., Suzuki, T., Kawarada, L., Iwata, H., Asano, K., and Suzuki, T. (2016). NSUN3 methylase initiates 5-formylcytidine biogenesis in human mitochondrial tRNA Met. Nat. Chem. Biol. *12*, 546–551.

Nanney, D.L. (1958). Epigenetic control systems. Proc. Natl. Acad. Sci. USA *44*, 712–717.

Nedialkova, D.D., and Leidel, S.A. (2015). Optimization of Codon Translation Rates via tRNA Modifications Maintains Proteome Integrity. Cell *161*, 1606–1618.

Neri, F., Rapelli, S., Krepelova, A., Incarnato, D., Parlato, C., Basile, G., Maldotti, M., Anselmi, F., and Oliviero, S. (2017). Intragenic DNA methylation prevents spurious transcription initiation. Nature *543*, 72–77.

Netzer, N., Goodenbour, J.M., David, A., Dittmar, K.A., Jones, R.B., Schneider, J.R., Boone, D., Eves, E.M., Rosner, M.R., Gibbs, J.S., et al. (2009). Innate immune and chemically triggered oxidative stress modifies translational fidelity. Nature *462*, 522–526.

Nogueira, G., Fernandes, R., García-Moreno, J.F., and Romão, L. (2021). Nonsense-mediated RNA decay and its bipolar function in cancer. Mol. Cancer *20*, 72.

Noma, A., Kirino, Y., Ikeuchi, Y., and Suzuki, T. (2006). Biosynthesis of wybutosine, a hyper-modified nucleoside in eukaryotic phenylalanine tRNA. EMBO J. *25*, 2142–2154.

Noma, A., Sakaguchi, Y., and Suzuki, T. (2009). Mechanistic characterization of the sulfur-relay system for eukaryotic 2-thiouridine biogenesis at tRNA wobble positions. Nucleic Acids Res. *37*, 1335–1352.

Noma, A., Ishitani, R., Kato, M., Nagao, A., Nureki, O., and Suzuki, T. (2010). Expanding role of the jumonji C domain as an RNA hydroxylase. J. Biol. Chem. *285*, 34503–34507.

Nowell, P.C. (1976). The clonal evolution of tumor cell populations. Science *194*, 23–28.

Okamoto, M., Fujiwara, M., Hori, M., Okada, K., Yazama, F., Konishi, H., Xiao, Y., Qi, G., Shimamoto, F., Ota, T., et al. (2014). tRNA Modifying Enzymes, NSUN2 and METTL1, Determine Sensitivity to 5-Fluorouracil in HeLa Cells. PLoS Genet. *10*.

Okano, M., Bell, D.W., Haber, D.A., and Li, E. (1999). DNA methyltransferases Dnmt3a and Dnmt3b are essential for de novo methylation and mammalian development. Cell *99*, 247–257.

Oler, A.J., Alla, R.K., Roberts, D.N., Wong, A., Hollenhorst, P.C., Chandler, K.J., Cassiday, P.A., Nelson, C.A., Hagedorn, C.H., Graves, B.J., et al. (2010). Human RNA polymerase III transcriptomes and relationships to Pol II promoter chromatin and enhancer-binding factors. Nat. Struct. Mol. Biol. *17*, 620–628.

Orellana, E.A., Liu, Q., Yankova, E., Pirouz, M., De Braekeleer, E., Zhang, W., Lim, J., Aspris, D., Sendinc, E., Garyfallos, D.A., et al. (2021). METTL1-mediated m7G modification of Arg-TCT tRNA drives oncogenic transformation. Mol. Cell *81*, 3323–3338.

Orioli, A., Praz, V., Lhôte, P., and Hernandez, N. (2016). Human MAF1 targets and represses active RNA polymerase III genes by preventing recruitment rather than inducing long-term transcriptional arrest. Genome Res. *26*, 624–634.

Ortiz-Barahona, V., Joshi, R.S., and Esteller, M. (2020). Use of DNA Methylation Profiling in Translational Oncology. Semin. Cancer Biol. Epub ahead of print; doi:10.1016/j.semcancer.2020.12.011

Otani, J., Nankumo, T., Arita, K., Inamoto, S., Ariyoshi, M., and Shirakawa, M. (2009). Structural basis for recognition of H3K4 methylation status by the DNA methyltransferase 3A ATRX-DNMT3-DNMT3L domain. EMBO Rep. *10*, 1235–1241.

Ou, X., Cao, J., Cheng, A., Peppelenbosch, M.P., and Pan, Q. (2019). Errors in translational decoding: tRNA wobbling or misincorporation? PLOS Genet. *15*, e1008017.

Ozanick, S., Krecic, A., Andersland, J., and Anderson, J.T. (2005). The bipartite structure of the tRNA m1A58 methyltransferase from S. cerevisiae is conserved in humans. RNA *11*, 1281–1290.

Palioura, S., Sherrer, R.L., Steitz, T.A., Soil, D., and Simonovic, M. (2009). The human SepSecS-tRNASec complex reveals the mechanism of selenocysteine formation. Science *325*, 321–325.

Park, J.L., Lee, Y.S., Kunkeaw, N., Kim, S.Y., Kim, I.H., and Lee, Y.S. (2017). Epigenetic regulation of noncoding RNA transcription by mammalian RNA polymerase III. Epigenomics *9*, 171–187.

Paushkin, S. V., Patel, M., Furia, B.S., Peltz, S.W., and Trotta, C.R. (2004). Identification of a human endonuclease complex reveals a link between tRNA splicing and pre-mRNA 3′ end formation. Cell *117*, 311–321.

Pavon-Eternod, M., Gomes, S., Geslain, R., Dai, Q., Rosner, M.R., and Pan, T. (2009). tRNA over-expression in breast cancer and functional consequences. Nucleic Acids Res. *37*, 7268–7280.

Pavon-Eternod, M., Gomes, S., Rosner, M.R., and Pan, T. (2013). Overexpression of initiator methionine tRNA leads to global reprogramming of tRNA expression and increased proliferation in human epithelial cells. RNA *19*, 461–466.

Pazin, M.J., Kamakaka, R.T., and Kadonaga, J.T. (1994). ATP-dependent nucleosome reconfiguration and transcriptional activation from preassembled chromatin templates. Science *266*, 2007–2011.

Penno, C., Kumari, R., Baranov, P. V, Sinderen, D. Van, and Atkins, J.F. (2017). Specific reverse transcriptase slippage at the HIV ribosomal frameshift sequence: potential implications for modulation of GagPol synthesis. Nucleic Acids Res. *45*, 10156–10167.

Pereira, M., Soares, A.R., Ribeiro, D.R., Pinheiro, M.M., Ferreira, M., and Kellner, S. (2021). m5U54 tRNA hypomodification by lack of TRMT2A drives the generation of tRNA-derived small RNAs. Int. J. Mol. Sci. *22*, 2491.

Pinkard, O., McFarland, S., Sweet, T., and Coller, J. (2020). Quantitative tRNA-sequencing uncovers metazoan tissue-specific tRNA regulation. Nat. Commun. *11*, 4104.

Pinto, P.H., Kroupova, A., Schleiffer, A., Mechtler, K., Jinek, M., Weitzer, S., and Martinez, J. (2020). ANGEL2 is a member of the CCR4 family of deadenylases with 2′,3′-cyclic phosphatase activity. Science *369*, 524–530.

Popow, J., Englert, M., Weitzer, S., Schleiffer, A., Mierzwa, B., Mechtler, K., Trowitzsch, S., Will, C.L., Lührmann, R., Söll, D., et al. (2011). HSPC117 is the essential subunit of a human tRNA splicing ligase complex. Science *331*, 760–764.

Popow, J., Jurkin, J., Schleiffer, A., and Martinez, J. (2014). Analysis of orthologous groups reveals archease and DDX1 as tRNA splicing factors. Nature *511*, 104–107.

Powell, C.A., and Minczuk, M. (2020). TRMT2B is responsible for both tRNA and rRNA m5U-methylation in human mitochondria. RNA Biol. *17*, 451–462.

References

Prokhortchouk, A., Hendrich, B., Jørgensen, H., Ruzov, A., Wilm, M., Georgiev, G., Bird, A., and Prokhortchouk, E. (2001). The p120 catenin partner Kaiso is a DNA methylation-dependent transcriptional repressor. Genes Dev. *15*, 1613–1618.

Pütz, J., Florentz, C., Benseler, F., and Giegé, R. (1994). A single methyl group prevents the mischarging of a tRNA. Nat. Struct. Biol. *1*, 580–582.

Raab, J.R., Chiu, J., Zhu, J., Katzman, S., Kurukuti, S., Wade, P.A., Haussler, D., and Kamakaka, R.T. (2012). Human tRNA genes function as chromatin insulators. EMBO J. *31*, 330–350.

Rak, R., Dahan, O., and Pilpel, Y. (2018). Repertoires of tRNAs: The Couplers of Genomics and Proteomics. Annu. Rev. Cell Dev. Biol. *34*, 239–264.

Ran, F.A., Hsu, P.D., Wright, J., Agarwala, V., Scott, D.A., and Zhang, F. (2013). Genome engineering using the CRISPR-Cas9 system. Nat. Protoc. *8*, 2281–2308.

Rapino, F., Delaunay, S., Zhou, Z., Chariot, A., and Close, P. (2017). tRNA Modification: Is Cancer Having a Wobble? Trends in Cancer *3*, 249–252.

Rapino, F., Delaunay, S., Rambow, F., Zhou, Z., Tharun, L., De Tullio, P., Sin, O., Shostak, K., Schmitz, S., Piepers, J., et al. (2018). Codon-specific translation reprogramming promotes resistance to targeted therapy. Nature *558*, 605–609.

Rashad, S., Han, X., Sato, K., Mishima, E., Abe, T., Tominaga, T., and Niizuma, K. (2020). The stress specific impact of ALKBH1 on tRNA cleavage and tiRNA generation. RNA Biol. *17*, 1092–1103.

dos Reis, M., Savva, R., and Wernisch, L. (2004). Solving the riddle of codon usage preferences: A test for translational selection. Nucleic Acids Res. *32*, 5036–5044.

Reiter, V., Matschkal, D.M.S., Wagner, M., Globisch, D., Kneuttinger, A.C., Müller, M., and Carell, T. (2012). The CDK5 repressor CDK5RAP1 is a methylthiotransferase acting on nuclear and mitochondrial RNA. Nucleic Acids Res. *40*, 6235–6240.

Rezniczek, G.A., Grunwald, C., Hilal, Z., Scheich, J., Reifenberger, G., Tannapfel, A., and Tempfer, C.B. (2019). ROBO1 expression in metastasizing breast and ovarian cancer: SLIT2-induced Chemotaxis Requires Heparan Sulfates (Heparin). Anticancer Res. *39*, 1267–1273.

Riggs, A.D. (1975). X inactivation, differentiation, and DNA methylation. Cytogenet. Genome Res. *14*, 9–25.

Rinaldi, L., Datta, D., Serrat, J., Morey, L., Solanas, G., Avgustinova, A., Blanco, E., Pons, J.I., Matallanas, D., Von Kriegsheim, A., et al. (2016). Dnmt3a and Dnmt3b Associate with Enhancers to Regulate Human Epidermal Stem Cell Homeostasis. Cell Stem Cell *19*, 491–501.

Russo, G., Tramontano, A., Iodice, I., Chiariotti, L., and Pezone, A. (2021). Epigenome chaos: Stochastic and deterministic dna methylation events drive cancer evolution. Cancers (Basel). *13*, 1800.

Sagi, D., Rak, R., Gingold, H., Adir, I., Maayan, G., Dahan, O., Broday, L., Pilpel, Y., and Rechavi, O. (2016). Tissue- and Time-Specific Expression of Otherwise Identical tRNA Genes. PLoS Genet. *12*, e1006264.

Sakaguchi, Y., Miyauchi, K., Kang, B. Il, and Suzuki, T. (2015). Nucleoside Analysis by Hydrophilic Interaction Liquid Chromatography Coupled with Mass Spectrometry. In Methods in Enzymology, (Elsevier Inc.), pp. 19–28.

Santos, M., Pereira, P.M., Varanda, A.S., Carvalho, J., Azevedo, M., Mateus, D.D., Mendes, N., Oliveira, P., Trindade, F., Pinto, M.T., et al. (2018). Codon misreading tRNAs promote tumor growth in mice. RNA Biol. *15*, 773–786.

Santos, M., Fidalgo, A., Varanda, A.S., Oliveira, C., and Santos, M.A.S. (2019). tRNA Deregulation and Its Consequences in Cancer. Trends Mol. Med. *25*, 853–865.

Saxena, S.K., Rybak, S.M., Davey, R.T., Youle, R.J., and Ackerman, E.J. (1992). Angiogenin is a cytotoxic, tRNA-specific ribonuclease in the RNase A superfamily. J. Biol. Chem. *267*, 21982–21986.

Saxonov, S., Berg, P., and Brutlag, D.L. (2006). A genome-wide analysis of CpG dinucleotides in the human genome distinguishes two distinct classes of promoters. Proc. Natl. Acad. Sci. USA *103*, 1412–1417.

Schaub, F.X., Dhankani, V., Berger, A.C., Trivedi, M., Richardson, A.B., Shaw, R., Zhao, W., Zhang, X., Ventura, A., Liu, Y., et al. (2018). Pan-cancer Alterations of the MYC Oncogene and Its Proximal Network across the Cancer Genome Atlas. Cell Syst. *6*, 282–300.

Schiffer, S., Rösch, S., and Marchfelder, A. (2002). Assigning a function to a conserved group of proteins: The tRNA 3′-processing enzymes. EMBO J. *21*, 2769–2777.

Schmidt, C.A., and Matera, A.G. (2020). tRNA introns: Presence, processing, and purpose. Wiley Interdiscip. Rev. RNA *11*, e1583.

Schmidt, C.A., Giusto, J.D., Bao, A., Hopper, A.K., and Matera, A.G. (2019). Molecular determinants of metazoan tricRNA biogenesis. Nucleic Acids Res. *47*, 6452–6465.

Schorn, A.J., Gutbrod, M.J., LeBlanc, C., and Martienssen, R. (2017). LTR-Retrotransposon Control by tRNA-Derived Small RNAs. Cell *170*, 61–71.

Schramm, L., and Hernandez, N. (2002). Recruitment of RNA polymerase III to its target promoters. Genes Dev. *16*, 2593–2620.

Schübeler, D. (2015). Function and information content of DNA methylation. Nature *517*, 321–326.

Schwenzer, H., Jühling, F., Chu, A., Pallett, L.J., Baumert, T.F., Maini, M., and Fassati, A. (2019). Oxidative Stress Triggers Selective tRNA Retrograde Transport in Human Cells during the Integrated Stress Response. Cell Rep. *26*, 3416–3428.

Senger, B., Auxilien, S., Englisch, U., Cramer, F., and Fasiolo, F. (1997). The modified wobble base inosine in yeast tRNA(Ile) is a positive determinant for aminoacylation by isoleucyl-tRNA synthetase. Biochemistry *36*, 8269–8275.

Sgro, A., and Blancafort, P. (2020). Epigenome engineering: new technologies for precision medicine. Nucleic Acids Res. *48*, 12453–12482.

Shanmugam, R., Fierer, J., Kaiser, S., Helm, M., Jurkowski, T.P., and Jeltsch, A. (2015). Cytosine methylation of tRNA-Asp by DNMT2 has a role in translation of proteins containing poly-Asp sequences. Cell Discov. *1*, 15010.

Sharma, S., Langhendries, J.L., Watzinger, P., Kotter, P., Entian, K.D., and Lafontaine, D.L.J. (2015). Yeast Kre33 and human NAT10 are conserved 18S rRNA cytosine acetyltransferases that modify tRNAs assisted by the adaptor Tan1/THUMPD1. Nucleic Acids Res. *43*, 2242–2258.

Sharp, S.J., Schaack, J., Cooley, L., Burke, D.J., and Soll, D. (1985). Structure and transcription of eukaryotic tRNA gene. Crit. Rev. Biochem. Mol. Biol. *19*, 107–144.

Shen, H., Ontiveros, R.J., Owens, M.C., Liu, M.Y., Ghanty, U., Kohli, R.M., and Liu, K.F. (2020). TET-mediated 5-methylcytosine oxidation in tRNA promotes translation. J. Biol. Chem. *296*, 100087.

Shi, H., and Moore, P.B. (2000). The crystal structure of yeast phenylalanine tRNA at 1.93 Å resolution: A classic structure revisited. RNA *6*, 1091–1105.

Shinoda, S., Kitagawa, S., Nakagawa, S., Wei, F.Y., Tomizawa, K., Araki, K., Araki, M., Suzuki, T., and Suzuki, T. (2019). Mammalian NSUN2 introduces 5-methylcytidines into mitochondrial tRNAs. Nucleic Acids Res. *47*, 8734–8745.

Shogren-Knaak, M., Ishii, H., Sun, J.M., Pazin, M.J., Davie, J.R., and Peterson, C.L. (2006). Histone H4-K16 acetylation controls chromatin structure and protein interactions. Science *311*, 844–847.

References

Shukla, S., Kavak, E., Gregory, M., Imashimizu, M., Shutinoski, B., Kashlev, M., Oberdoerffer, P., Sandberg, R., and Oberdoerffer, S. (2011). CTCF-promoted RNA polymerase II pausing links DNA methylation to splicing. Nature *479*, 74–79.

Sibert, B.S., Fischel-Ghodsian, N., and Patton, J.R. (2008). Partial activity is seen with many substitutions of highly conserved active site residues in human Pseudouridine synthase 1. RNA *14*, 1895–1906.

Siegel, R.L., Miller, K.D., and Jemal, A. (2020). Cancer statistics, 2020. CA. Cancer J. Clin. *70*, 7–30.

Song, L., Jia, J., Peng, X., Xiao, W., and Li, Y. (2017). The performance of the SEPT9 gene methylation assay and a comparison with other CRC screening tests: A meta-analysis. Sci. Rep. *7*, 3032.

Songe-Møller, L., van den Born, E., Leihne, V., Vågbø, C.B., Kristoffersen, T., Krokan, H.E., Kirpekar, F., Falnes, P.Ø., and Klungland, A. (2010). Mammalian ALKBH8 Possesses tRNA Methyltransferase Activity Required for the Biogenesis of Multiple Wobble Uridine Modifications Implicated in Translational Decoding. Mol. Cell. Biol. *30*, 1814–1827.

Sprinzl, M., and Cramer, F. (1979). The -C-C-A End of tRNA and Its Role in Protein Biosynthesis. Prog. Nucleic Acid Res. Mol. Biol. *22*, 1–69.

Sprinzl, M., Steegborn, C., Hübel, F., and Steinberg, S. (1996). Compilation of tRNA sequences and sequences of tRNA genes. Nucleic Acids Res. *24*, 68–72.

Stefansson, O.A., Hermanowicz, S., van der Horst, J., Hilmarsdottir, H., Staszczak, Z., Jonasson, J.G., Tryggvadottir, L., Gudjonsson, T., and Sigurdsson, S. (2017). CpG promoter methylation of the ALKBH3 alkylation repair gene in breast cancer. BMC Cancer *17*, 469.

Su, Z., Wilson, B., Kumar, P., and Dutta, A. (2020). Noncanonical Roles of tRNAs: tRNA Fragments and Beyond. Annu. Rev. Genet. *54*, 47–69.

Suetake, I., Shinozaki, F., Miyagawa, J., Takeshima, H., and Tajima, S. (2004). DNMT3L stimulates the DNA methylation activity of Dnmt3a and Dnmt3b through a direct interaction. J. Biol. Chem. *279*, 27816–27823.

Sun, X., Tian, Y., Wang, J., Sun, Z., and Zhu, Y. (2020). Genome-wide analysis reveals the association between alternative splicing and DNA methylation across human solid tumors. BMC Med. Genomics *13*, 4.

Suzuki, T. (2021). The expanding world of tRNA modifications and their disease relevance. Nat. Rev. Mol. Cell Biol. *22*, 375–392.

Swisher, E.M., Kwan, T.T., Oza, A.M., Tinker, A. V., Ray-Coquard, I., Oaknin, A., Coleman, R.L., Aghajanian, C., Konecny, G.E., O'Malley, D.M., et al. (2021). Molecular and clinical determinants of response and resistance to rucaparib for recurrent ovarian cancer treatment in ARIEL2 (Parts 1 and 2). Nat. Commun. *12*, 2487.

Takakura, M., Ishiguro, K., Akichika, S., Miyauchi, K., and Suzuki, T. (2019). Biogenesis and functions of aminocarboxypropyluridine in tRNA. Nat. Commun. *10*, 5542.

Tan, M., Luo, H., Lee, S., Jin, F., Yang, J.S., Montellier, E., Buchou, T., Cheng, Z., Rousseaux, S., Rajagopal, N., et al. (2011). Identification of 67 histone marks and histone lysine crotonylation as a new type of histone modification. Cell *146*, 1016–1028.

Tate, P.H., and Bird, A.P. (1993). Effects of DNA methylation on DNA-binding proteins and gene expression. Curr. Opin. Genet. Dev. *3*, 226–231.

Tate, J.G., Bamford, S., Jubb, H.C., Sondka, Z., Beare, D.M., Bindal, N., Boutselakis, H., Cole, C.G., Creatore, C., Dawson, E., et al. (2019). COSMIC: The Catalogue Of Somatic Mutations In Cancer. Nucleic Acids Res. *47*, D941–D947.

Tauriello, D.V.F., Calon, A., Lonardo, E., and Batlle, E. (2017). Determinants of metastatic competency in colorectal cancer. Mol. Oncol. *11*, 97–119.

154

Thompson, D.M., Lu, C., Green, P.J., and Parker, R. (2008). tRNA cleavage is a conserved response to oxidative stress in eukaryotes. RNA *14*, 2095–2103.

Torres, A.G. (2019). Enjoy the Silence: Nearly Half of Human tRNA Genes Are Silent. Bioinform. Biol. Insights *13*, 1–3.

Torres, A.G., Reina, O., Attolini, C.S.O., and De Pouplana, L.R. (2019). Differential expression of human tRNA genes drives the abundance of tRNA-derived fragments. Proc. Natl. Acad. Sci. USA *116*, 8451–8456.

Tricoli, J. V., Boardman, L.A., Patidar, R., Sindiri, S., Jang, J.S., Walsh, W.D., McGregor, P.M., Camalier, C.E., Mehaffey, M.G., Furman, W.L., et al. (2018). A mutational comparison of adult and adolescent and young adult (AYA) colon cancer. Cancer *124*, 1070–1082.

Tuorto, F., Liebers, R., Musch, T., Schaefer, M., Hofmann, S., Kellner, S., Frye, M., Helm, M., Stoecklin, G., and Lyko, F. (2012). RNA cytosine methylation by Dnmt2 and NSun2 promotes tRNA stability and protein synthesis. Nat. Struct. Mol. Biol. *19*, 900–905.

Turowski, T.W., Leśniewska, E., Delan-Forino, C., Sayou, C., Boguta, M., and Tollervey, D. (2016). Global analysis of transcriptionally engaged yeast RNA polymerase III reveals extended tRNA transcripts. Genome Res. *26*, 933–944.

Umeda, N., Suzuki, T., Yukawa, M., Ohya, Y., Shindo, H., Watanabe, K., and Suzuki, T. (2005). Mitochondria-specific RNA-modifying enzymes responsible for the biosynthesis of the wobble base in mitochondrial tRNAs: Implications for the molecular pathogenesis of human mitochondrial diseases. J. Biol. Chem. *280*, 1613–1624.

Valton, A.L., and Dekker, J. (2016). TAD disruption as oncogenic driver. Curr. Opin. Genet. Dev. *36*, 34–40.

Vaňáčová, Š., Wolf, J., Martin, G., Blank, D., Dettwiler, S., Friedlein, A., Langen, H., Keith, G., and Keller, W. (2005). A New Yeast Poly(A) Polymerase Complex Involved in RNA Quality Control. PLoS Biol. *3*, e189.

Vasan, N., Baselga, J., and Hyman, D.M. (2019). A view on drug resistance in cancer. Nature *575*, 299–309.

Vilardo, E., Nachbagauer, C., Buzet, A., Taschner, A., Holzmann, J., and Rossmanith, W. (2012). A subcomplex of human mitochondrial RNase P is a bifunctional methyltransferase-extensive moonlighting in mitochondrial tRNA biogenesis. Nucleic Acids Res. *40*, 11583–11593.

Vizoso, M., Ferreira, H.J., Lopez-Serra, P., Carmona, F.J., Martínez-Cardús, A., Girotti, M.R., Villanueva, A., Guil, S., Moutinho, C., Liz, J., et al. (2015). Epigenetic activation of a cryptic TBC1D16 transcript enhances melanoma progression by targeting EGFR. Nat. Med. *21*, 741–750.

Voigts-Hoffmann, F., Hengesbach, M., Kobitski, A.Y., Van Aerschot, A., Herdewijn, P., Ulrich Nienhaus, G., and Helm, M. (2007). A methyl group controls conformational equilibrium in human mitochondrial tRNALys. J. Am. Chem. Soc. *129*, 13382–13383.

Waddington, C.H. (1942). Canalization of development and the inheritance of acquired characters. Nature *150*, 563–565.

Wan, L.C.K., Maisonneuve, P., Szilard, R.K., Lambert, J.P., Ng, T.F., Manczyk, N., Huang, H., Laister, R., Caudy, A.A., Gingras, A.C., et al. (2017). Proteomic analysis of the human KEOPS complex identifies C14ORF142 as a core subunit homologous to yeast Gon7. Nucleic Acids Res. *45*, 805–817.

Wang, B., Li, D., Kovalchuk, I., Apel, I.J., Chinnaiyan, A.M., Wóycicki, R.K., Cantor, C.R., and Kovalchuk, O. (2018a). miR-34a directly targets tRNAiMet precursors and affects cellular proliferation, cell cycle, and apoptosis. Proc. Natl. Acad. Sci. USA *115*, 7392–7397.

Wang, D., Zavadil, J., Martin, L., Parisi, F., Friedman, E., Levy, D., Harding, H., Ron, D., and Gardner, L.B. (2011). Inhibition of Nonsense-Mediated RNA Decay by the Tumor Microenvironment Promotes Tumorigenesis. Mol. Cell. Biol. *31*, 3670–3680.

References

Wang, K., Zheng, M., and Ren, Y. (2019). Overexpression of TRMT12 may independently predict poor overall survival in patients with head and neck squamous cell carcinoma. Onco. Targets. Ther. *12*, 7269–7279.

Wang, L., Zhao, Y., Bao, X., Zhu, X., Kwok, Y.K.Y., Sun, K., Chen, X., Huang, Y., Jauch, R., Esteban, M.A., et al. (2015). LncRNA Dum interacts with Dnmts to regulate Dppa2 expression during myogenic differentiation and muscle regeneration. Cell Res. *25*, 335–350.

Wang, S., Liu, X., Huang, J., Zhang, Y., Sang, C., Li, T., and Yuan, J. (2018b). Expression of KIAA1456 in lung cancer tissue and its effects on proliferation, migration and invasion of lung cancer cells. Oncol. Lett. *16*, 3791–3795.

Wei, J., Liu, F., Lu, Z., Fei, Q., Ai, Y., He, P.C., Shi, H., Cui, X., Su, R., Klungland, A., et al. (2018). Differential m6A, m6Am, and m1A Demethylation Mediated by FTO in the Cell Nucleus and Cytoplasm. Mol. Cell *71*, 973-985.e5.

Wei, J.W., Huang, K., Yang, C., and Kang, C.S. (2017). Non-coding RNAs as regulators in epigenetics (Review). Oncol. Rep. *37*, 3–9.

Wei, Y., Tsang, C.K., and Zheng, X.F.S. (2009). Mechanisms of regulation of RNA polymerase III-dependent transcription by TORC1. EMBO J. *28*, 2220–2230.

Whitney, M.L., Hurto, R.L., Shaheen, H.H., and Hopper, A.K. (2007). Rapid and reversible nuclear accumulation of cytoplasmic tRNA in response to nutrient availability. Mol. Biol. Cell *18*, 2678–2686.

Wild, C.P. (2019). The global cancer burden: necessity is the mother of prevention. Nat. Rev. Cancer *19*, 123–124.

Wilkinson, M.L., Crary, S.M., Jackman, J.E., Grayhack, E.J., and Phizicky, E.M. (2007). The 2′-O-methyltransferase responsible for modification of yeast tRNA at position 4. RNA *13*, 404–413.

Wilusz, J.E. (2015). Controlling translation via modulation of tRNA levels. Wiley Interdiscip. Rev. RNA *6*, 453–470.

Wilusz, J.E., Whipple, J.M., Phizicky, E.M., and Sharp, P.A. (2011). tRNAs marked with CCACCA are targeted for degradation. Science *334*, 817–821.

Wohlgemuth, I., Pohl, C., and Rodnina, M. V (2010). Optimization of speed and accuracy of decoding in translation. EMBO J. *29*, 3701–3709.

Woodcock, C.B., Horton, J.R., Zhou, J., Bedford, M.T., Blumenthal, R.M., Zhang, X., and Cheng, X. (2020). Biochemical and structural basis for YTH domain of human YTHDC1 binding to methylated adenine in DNA. Nucleic Acids Res. *48*, 10329–10341.

Wu, H., Chen, Y., Liang, J., Shi, B., Wu, G., Zhang, Y., Wang, D., Li, R., Yi, X., Zhang, H., et al. (2005). Hypomethylation-linked activation of PAX2 mediates tamoxifen-stimulated endometrial carcinogenesis. Nature *438*, 981–987.

Wu, J., Bao, A., Chatterjee, K., Wan, Y., and Hopper, A.K. (2015). Genome-wide screen uncovers novel pathways for tRNA processing and nuclear–cytoplasmic dynamics. Genes Dev. *29*, 2633–2644.

Wu, Q., Medina, S.G., Kushawah, G., Devore, M.L., Castellano, L.A., Hand, J.M., Wright, M., and Bazzini, A.A. (2019). Translation affects mRNA stability in a codon-dependent manner in human cells. Elife *8*, e45396.

Wu, Y., Yang, X., Jiang, G., Zhang, H., Ge, L., Chen, F., Li, J., Liu, H., and Wang, H. (2021). 5′-tRF-GlyGCC: a tRNA-derived small RNA as a novel biomarker for colorectal cancer diagnosis. Genome Med. *13*, 20.

Xia, Y., Wang, L., Xu, Z., Kong, R., Wang, F., Yin, K., Xu, J., Li, B., He, Z., Wang, L., et al. (2019). Reduced USP33 expression in gastric cancer decreases inhibitory effects of Slit2-Robo1 signalling on cell migration and EMT. Cell Prolif. *52*, e12606.

Xiao, C. Le, Zhu, S., He, M., Chen, D., Zhang, Q., Chen, Y., Yu, G., Liu, J., Xie, S.Q., Luo, F., et al. (2018). N6-Methyladenine DNA Modification in the Human Genome. Mol. Cell *71*, 306–318.

Xie, Y., Hong, N., Chen, Y.X., and Fang, J.Y. (2020). Comprehensive review of targeted therapy for colorectal cancer. Signal Transduct. Target. Ther. *5*, 22.

Xie, Z., Dai, J., Dai, L., Tan, M., Cheng, Z., Wu, Y., Boeke, J.D., and Zhao, Y. (2012). Lysine succinylation and lysine malonylation in histones. In Molecular and Cellular Proteomics, (American Society for Biochemistry and Molecular Biology), pp. 100–107.

Xing, F., Martzen, M.R., and Phizicky, E.M. (2002). A conserved family of Saccharomyces cerevisiae synthases effects dihydrouridine modification of tRNA. RNA *8*, 370–381.

Xu, L., Liu, X., Sheng, N., Oo, K.S., Liang, J., Chionh, Y.H., Xu, J., Ye, F., Gao, Y.G., Dedon, P.C., et al. (2017). Three distinct 3-methylcytidine (m3C) methyltransferases modify tRNA and mRNA in mice and humans. J. Biol. Chem. *292*, 14695–14703.

Yamasaki, S., Ivanov, P., Hu, G.F., and Anderson, P. (2009). Angiogenin cleaves tRNA and promotes stress-induced translational repression. J. Cell Biol. *185*, 35–42.

Yang, J., Smith, D.K., Ni, H., Wu, K., Huang, D., Pan, S., Sathe, A.A., Tang, Y., Liu, M.L., Xing, C., et al. (2020). SOX4-mediated repression of specific tRNAs inhibits proliferation of human glioblastoma cells. Proc. Natl. Acad. Sci. USA *117*, 5782–5790.

Yang, J.Y., Deng, X.Y., Li, Y.S., Ma, X.C., Feng, J.X., Yu, B., Chen, Y., Luo, Y.L., Wang, X., Chen, M.L., et al. (2018). Structure of Schlafen13 reveals a new class of tRNA/rRNA- targeting RNase engaged in translational control. Nat. Commun. *9*, 1165.

Yildirim, O., Li, R., Hung, J.H., Chen, P.B., Dong, X., Ee, L.S., Weng, Z., Rando, O.J., and Fazzio, T.G. (2011). Mbd3/NURD complex regulates expression of 5-hydroxymethylcytosine marked genes in embryonic stem cells. Cell *147*, 1498–1510.

Yoo, C.J., and Wolin, S.L. (1997). The yeast La protein is required for the 3' endonucleolytic cleavage that matures tRNA precursors. Cell *89*, 393–402.

Yu, M., Lu, B., Zhang, J., Ding, J., Liu, P., and Lu, Y. (2020). TRNA-derived RNA fragments in cancer: Current status and future perspectives. J. Hematol. Oncol. *13*, 121.

Zaborske, J.M., Narasimhan, J., Jiang, L., Wek, S.A., Dittmar, K.A., Freimoser, F., Pan, T., and Wek, R.C. (2009). Genome-wide analysis of tRNA charging and activation of the eIF2 kinase Gcn2p. J. Biol. Chem. *284*, 25254–25267.

Zaganelli, S., Rebelo-Guiomar, P., Maundrell, K., Rozanska, A., Pierredon, S., Powell, C.A., Jourdain, A.A., Hulo, N., Lightowlers, R.N., Chrzanowska-Lightowlers, Z.M., et al. (2017). The pseudouridine synthase RPUSD4 is an essential component of mitochondrial RNA granules. J. Biol. Chem. *292*, 4519–4532.

Zeng, T., Hua, Y., Sun, C., Zhang, Y., Yang, F., Yang, M., Yang, Y., Li, J., Huang, X., Wu, H., et al. (2020). Relationship between tRNA-derived fragments and human cancers. Int. J. Cancer *147*, 3007–3018.

Zhang, G., and Pradhan, S. (2014). Mammalian epigenetic mechanisms. IUBMB Life *66*, 240–256.

Zhang, J., and Ferré-D'amaré, A.R. (2016). The tRNA elbow in structure, recognition and evolution. Life *6*, 3.

Zhang, D., Tang, Z., Huang, H., Zhou, G., Cui, C., Weng, Y., Liu, W., Kim, S., Lee, S., Perez-Neut, M., et al. (2019). Metabolic regulation of gene expression by histone lactylation. Nature *574*, 575–580.

Zhang, L., Qin, Y., Wu, G., Wang, J., Cao, J., Wang, Y., Wu, D., Yang, K., Zhao, Z., He, L., et al. (2020a). PRRG4 promotes breast cancer metastasis through the recruitment of NEDD4 and downregulation of Robo1. Oncogene *39*, 7196–7208.

References

Zhang, X., He, X., Liu, C., Liu, J., Hu, Q., Pan, T., Duan, X., Liu, B., Zhang, Y., Chen, J., et al. (2016). IL-4 Inhibits the Biogenesis of an Epigenetically Suppressive PIWI-Interacting RNA To Upregulate CD1a Molecules on Monocytes/Dendritic Cells. J. Immunol. *196*, 1591–1603.

Zhang, Y., Qian, H., He, J., and Gao, W. (2020b). Mechanisms of tRNA-derived fragments and tRNA halves in cancer treatment resistance. Biomark. Res. *8*, 52.

Zhang, Z., Ye, Y., Gong, J., Ruan, H., Liu, C.J., Xiang, Y., Cai, C., Guo, A.Y., Ling, J., Diao, L., et al. (2018). Global analysis of tRNA and translation factor expression reveals a dynamic landscape of translational regulation in human cancers. Commun. Biol. *1*, 234.

Zhu, H., Wang, G., and Qian, J. (2016). Transcription factors as readers and effectors of DNA methylation. Nat. Rev. Genet. *17*, 551–565.

Zhu, Z., Han, Z., Halabelian, L., Yang, X., Ding, J., Zhang, N., Ngo, L., Song, J., Zeng, H., He, M., et al. (2021). Identification of lysine isobutyrylation as a new histone modification mark. Nucleic Acids Res. *49*, 177–189.

Zilberman, D., Coleman-Derr, D., Ballinger, T., and Henikoff, S. (2008). Histone H2A.Z and DNA methylation are mutually antagonistic chromatin marks. Nature *456*, 125–129.

Ziller, M.J., Müller, F., Liao, J., Zhang, Y., Gu, H., Bock, C., Boyle, P., Epstein, C.B., Bernstein, B.E., Lengauer, T., et al. (2011). Genomic distribution and Inter-Sample variation of Non-CpG methylation across human cell types. PLoS Genet. *7*, e1002389.

ANNEXES

ANNEXES

Table 11. *Differentially expressed transcripts upon TYW2 depletion in HCT-116 cells.* The gene symbol, log2 fold change (log2FC), and adjusted *p*-value (adj pval) are provided for the 2,370 genes whose expression is altered in TYW2-knockout HCT-116 cells according to the RNA-seq experiment.

Gene symbol	log2FC	adj pval	Gene symbol	log2FC	adj pval
TMPRSS15	-9.71	2.84E-11	FABP6	-2.65	7.77E-06
AF127936.9	-8.75	6.74E-09	CCDC102B	-2.65	4.94E-07
TUSC3	-8.52	2.09E-08	EPGN	-2.65	6.27E-03
ZNF502	-8.48	1.81E-12	CTC-277H1.6	-2.65	4.95E-02
AF127577.13	-8.34	3.24E-07	RP11-268P4.6	-2.64	4.06E-02
CSRNP3	-8.15	3.20E-07	RP11-717D12.1	-2.64	3.83E-02
RP11-154H23.1	-8.06	2.22E-05	RN7SL600P	-2.64	4.37E-02
RP11-650J17.1	-7.85	2.50E-02	RP11-416A17.6	-2.64	1.92E-03
MAP6	-7.67	5.68E-07	GPX2	-2.64	9.04E-03
AC012370.2	-7.54	4.26E-04	AC009303.1	-2.64	4.24E-02
SCN9A	-7.45	2.49E-06	RP11-93M12.1	-2.63	3.25E-03
ZNF493	-7.44	1.91E-08	MIR3687-2	-2.63	5.03E-03
PCDH15	-7.35	3.98E-05	RP11-177H22.2	-2.63	1.32E-02
NRIP1	-7.35	3.11E-62	CTD-2104P17.1	-2.63	2.18E-02
GS1-124K5.13	-7.28	4.87E-04	RP11-19E18.1	-2.63	4.00E-02
RP11-577O19.1	-7.26	9.39E-04	RP11-785H5.2	-2.62	2.07E-02
KCNH8	-7.20	5.56E-05	RP11-682B13.2	-2.62	2.38E-02
RP11-713M15.1	-7.13	1.14E-03	BCL2L14	-2.62	1.48E-03
CTA-331F8.1	-7.12	8.64E-04	ANKRD22	-2.61	2.28E-04
RP11-418J17.2	-7.12	8.83E-04	RP11-487I9.2	-2.61	8.33E-03
AC114763.1	-7.09	5.91E-04	C19orf35	-2.61	9.48E-03
IFI44L	-7.02	9.13E-04	IFI44	-2.61	5.90E-06
RP11-54I5.1	-7.00	1.73E-03	RP11-31F15.2	-2.61	5.56E-03
RP11-420A21.1	-6.90	8.92E-04	RP11-203H2.1	-2.61	2.26E-02
AC003989.4	-6.88	8.42E-05	CTC-448F2.5	-2.60	8.78E-03
RNA5SP278	-6.83	2.65E-03	RP11-419I17.2	-2.60	3.42E-02
RBM22P4	-6.82	2.66E-03	C9orf50	-2.60	3.07E-03
MIR181B2	-6.81	2.84E-03	RP11-261E12.2	-2.60	3.39E-02
MIR548AQ	-6.78	3.54E-03	RN7SL558P	-2.59	3.94E-02
RN7SL108P	-6.75	3.23E-03	GVINP1	-2.59	4.31E-03
AC103881.1	-6.74	1.02E-04	RP6-99M1.3	-2.59	2.09E-03
RP11-327O17.2	-6.71	2.24E-04	RP11-91P24.1	-2.59	4.10E-02
AIRN	-6.70	3.81E-03	KB-1125A3.12	-2.59	7.24E-03
TACSTD2	-6.69	7.82E-35	RP11-98J23.1	-2.58	1.82E-02
RP11-650J17.2	-6.67	4.15E-03	MESTIT1	-2.58	4.52E-02
RP11-340C20.3	-6.63	4.36E-03	SATB1	-2.58	3.18E-17
ASTN1	-6.60	1.09E-03	IL1RN	-2.58	1.56E-02
AF127577.11	-6.59	2.25E-03	TMPRSS4	-2.58	1.48E-05
RP11-27H1.1	-6.57	1.36E-03	RP1-274L14.2	-2.57	1.01E-02
FLRT3	-6.57	5.18E-03	EEF1AL1	-2.57	6.25E-04
EYA1	-6.54	2.89E-03	AC018462.2	-2.56	3.49E-02
RN7SL683P	-6.54	5.55E-03	AKR1C3	-2.56	3.18E-05
RNU11-6P	-6.50	4.31E-03	NCRNA00093	-2.56	1.75E-02
RP11-767L7.2	-6.48	6.55E-03	BCL11A	-2.56	1.10E-04

CAPN6	-6.46	9.10E-22	RF00019	-2.56	1.98E-02
RP1-168P16.3	-6.46	2.54E-06	AP000699.2	-2.56	4.71E-02
RP11-666F17.1	-6.46	6.40E-03	RP11-823P9.3	-2.55	1.98E-02
MAB21L2	-6.44	1.27E-02	CTC-448F2.6	-2.55	1.96E-08
RP11-319G9.1	-6.43	2.75E-03	IGKV1OR-2	-2.55	4.99E-02
RP11-6E2.1	-6.42	2.75E-03	AC114737.6	-2.54	4.20E-03
RP11-39E3.5	-6.41	7.91E-03	LDHAL6B	-2.54	3.14E-02
RNA5SP38	-6.40	5.92E-03	SARNP	-2.54	1.80E-02
MSR1	-6.39	2.49E-03	RP11-333E13.1	-2.53	1.62E-02
RF00019	-6.36	8.30E-03	LINC00216	-2.53	7.07E-03
RP11-430C17.1	-6.36	5.81E-03	ANGPTL3	-2.53	4.73E-02
RP11-775J23.2	-6.35	6.34E-04	RP11-290D2.3	-2.53	3.54E-02
RP11-270M14.4	-6.33	6.34E-03	AQP7P4	-2.52	1.54E-03
RP11-115H15.2	-6.33	3.86E-04	RP11-359M6.1	-2.52	3.30E-02
RP11-905F6.1	-6.33	6.40E-03	RP11-332O19.3	-2.52	2.32E-02
GPR171	-6.32	6.70E-03	RP11-236P2.2	-2.51	9.15E-05
KB-1090H4.2	-6.31	1.11E-02	CTD-2541M15.3	-2.51	1.52E-02
ZNF831	-6.29	3.74E-03	RP11-669N7.2	-2.51	4.46E-03
AC002429.5	-6.29	2.04E-02	RP3-326I13.1	-2.50	4.46E-02
CYP4A22	-6.29	1.11E-03	RP13-192B19.2	-2.50	6.75E-03
AC133965.1	-6.28	1.31E-02	RP3-467K16.4	-2.50	2.86E-02
CYCSP29	-6.27	1.05E-02	ACSM1	-2.50	4.75E-02
ISX	-6.27	1.52E-04	RP11-305L7.7	-2.50	1.32E-05
RP11-573N10.1	-6.27	3.14E-03	MNS1	-2.50	4.45E-06
RP11-318K15.2	-6.26	1.01E-02	RP11-27M24.3	-2.50	3.72E-02
RP11-197K3.1	-6.26	8.14E-03	RP5-849H19.3	-2.49	4.24E-02
CSF2RB	-6.26	6.67E-04	RP11-517I3.1	-2.49	2.44E-02
RP11-338E21.2	-6.25	1.04E-02	AC009502.4	-2.49	4.57E-02
RP11-3K15.1	-6.25	4.08E-03	GPRASP1	-2.49	5.43E-04
CTD-3118D7.1	-6.22	1.11E-02	AC058791.1	-2.49	2.94E-02
TBX5	-6.20	5.49E-03	RP11-152H18.4	-2.49	1.20E-02
RP11-90P5.1	-6.19	1.20E-02	RP11-102M11.1	-2.49	3.42E-02
C11orf76	-6.17	1.07E-02	RP11-204J18.3	-2.48	2.21E-02
RP11-343L14.1	-6.14	9.56E-03	CTD-2233K9.1	-2.48	6.04E-03
NPAS3	-6.13	9.27E-03	RP11-303G3.6	-2.48	7.25E-03
RP11-196H14.2	-6.11	1.45E-02	RP11-627K11.3	-2.47	3.78E-02
SCN3A	-6.11	1.14E-03	AP000525.10	-2.47	4.01E-05
RP11-317F4.1	-6.10	5.68E-03	RORA	-2.47	5.87E-03
AC010967.1	-6.10	2.69E-02	RP11-631M6.3	-2.47	4.82E-02
RP11-759F5.1	-6.10	1.07E-02	EDDM13	-2.47	2.03E-02
RP11-115D19.2	-6.10	1.41E-03	KRT39	-2.46	1.91E-02
RP5-1092L12.2	-6.09	1.01E-02	AC008277.1	-2.46	2.48E-02
RP11-374M1.4	-6.07	1.14E-02	RP11-75C10.9	-2.46	4.42E-02
AC106873.2	-6.07	6.34E-03	LL22NC03-N14H11.1	-2.45	1.28E-10
RP11-298C2.1	-6.06	2.91E-02	ABCG8	-2.45	4.89E-02
RP11-305D15.6	-6.05	2.87E-03	RP11-616K22.1	-2.45	4.97E-02
AC022173.2	-6.05	1.45E-02	EID3	-2.45	1.74E-03
RP11-155G15.1	-6.04	3.25E-02	CTC-421K24.1	-2.45	2.87E-02
AC011747.3	-6.03	1.71E-02	ERVW-1	-2.44	1.03E-02
RN7SL568P	-6.02	4.22E-02	RP11-1221G12.3	-2.44	7.25E-04
RP11-11N9.1	-6.02	3.19E-02	CTB-49A3.2	-2.43	1.87E-02
RP11-44N11.1	-6.01	2.52E-03	RP5-1033H22.2	-2.43	1.61E-02

RP4-593M8.1	-6.01	3.20E-02	RP11-410E4.1	-2.43	4.60E-02
RP11-438D8.4	-6.01	3.23E-02	RP11-333I13.1	-2.43	1.15E-02
SND1-IT1	-6.01	6.70E-04	PCAT1	-2.43	6.48E-04
SVOP	-6.00	1.82E-02	GNRHR	-2.43	1.01E-02
MIR3140	-6.00	3.65E-02	RP11-627K11.7	-2.42	2.28E-02
RP11-115A14.1	-5.99	7.42E-03	STK32A	-2.42	2.13E-02
RNA5SP129	-5.99	3.56E-02	AC002543.2	-2.42	1.32E-02
AC037193.1	-5.98	1.28E-02	CTB-134H23.3	-2.41	4.60E-02
AC140076.1	-5.98	1.28E-02	CTD-2547E10.4	-2.41	2.62E-03
RP11-1123I8.1	-5.98	4.91E-02	RP11-474P2.6	-2.41	4.99E-02
RP11-703M24.5	-5.98	3.52E-02	DNAH2	-2.41	4.39E-08
RNU6-626P	-5.97	1.51E-02	SMIM18	-2.41	2.84E-02
RP11-359B20.1	-5.96	1.34E-02	CYP19A1	-2.41	7.80E-04
PSG7	-5.95	3.57E-02	P4HA3	-2.40	1.68E-05
RP11-351C8.1	-5.95	3.98E-02	HMGB1P14	-2.40	2.89E-02
SLC5A1	-5.94	5.46E-47	RP11-380G5.2	-2.40	2.42E-02
RP11-21M7.2	-5.93	3.85E-02	CTD-2124B8.1	-2.40	1.82E-02
DUXAP7	-5.93	1.55E-02	RF00019	-2.40	4.10E-02
AC132807.1	-5.93	3.89E-02	RP1-69D17.3	-2.39	1.75E-02
RP11-508N12.2	-5.92	3.85E-02	RP11-855A2.1	-2.38	2.61E-02
AL592528.1	-5.92	1.71E-02	ZNF671	-2.38	1.99E-02
RP11-43D2.2	-5.92	4.01E-02	AC093620.5	-2.37	1.42E-02
RNY4P6	-5.92	3.85E-02	ADAM12	-2.36	8.35E-03
RP11-156K23.2	-5.92	2.92E-03	RP11-544A12.8	-2.36	1.60E-02
RP11-522L3.5	-5.92	1.41E-02	RF00019	-2.36	4.43E-02
FMO6P	-5.91	1.42E-02	AC097639.4	-2.36	1.19E-02
RP1-102G20.2	-5.91	3.86E-02	RENBP	-2.36	3.15E-02
HIST1H4B	-5.90	1.60E-02	RP11-974F13.5	-2.36	3.76E-04
RP11-117F22.1	-5.88	2.46E-02	RP3-354N19.3	-2.36	1.67E-02
RP5-1154E9.8	-5.88	4.23E-02	RP4-671O14.6	-2.35	4.16E-03
CTD-2563K22.1	-5.87	2.37E-02	RP11-226E21.4	-2.35	7.65E-03
IFNK	-5.87	4.23E-02	RP11-16E23.4	-2.35	1.02E-02
RP11-185E12.2	-5.87	1.56E-02	PPP1R1B	-2.35	1.57E-03
AC079807.3	-5.87	2.61E-03	RP11-512H23.2	-2.34	2.25E-02
AC096775.2	-5.86	4.24E-02	BAALC	-2.34	2.05E-02
CEACAMP2	-5.86	4.27E-02	ECT2L	-2.34	2.58E-03
AP000563.2	-5.86	3.44E-02	RP11-11N5.3	-2.34	2.40E-02
RP11-522L3.1	-5.85	4.74E-03	LAMA1	-2.34	1.30E-04
RP5-1174J21.2	-5.84	4.84E-02	NEDD9	-2.34	4.33E-03
AC010967.3	-5.83	4.68E-02	RP11-317B17.4	-2.33	5.98E-03
RN7SL329P	-5.82	1.78E-03	AQP7P1	-2.33	1.75E-04
RP11-108K3.3	-5.82	6.30E-03	RP11-149B9.2	-2.32	1.58E-02
RP11-345I18.3	-5.82	1.71E-02	CTD-2353F22.1	-2.32	6.70E-03
CTD-2197I11.1	-5.82	2.64E-02	RP1-46F2.2	-2.32	7.98E-09
RP11-192K2.2	-5.81	2.17E-02	RP5-891H21.4	-2.32	2.47E-02
CPS1-IT1	-5.81	4.67E-02	LMO3	-2.32	3.82E-02
CTD-2340D6.2	-5.81	2.62E-02	GAS5-AS1	-2.32	1.89E-02
AC011742.3	-5.81	2.14E-02	F10	-2.31	1.15E-05
RP11-6N13.4	-5.81	4.68E-02	RP11-65J3.14	-2.31	2.16E-02
RP11-390D11.1	-5.80	4.71E-02	BTN1A1	-2.30	2.60E-02
RP11-396D18.1	-5.80	4.71E-02	AC011747.4	-2.30	3.95E-04
SNORA70B	-5.80	4.71E-02	MRPS36P2	-2.29	4.57E-02

AC019171.4	-5.79	6.68E-03	APOBEC3G	-2.29	3.49E-07
RP11-33E24.3	-5.79	4.76E-02	GRM7	-2.29	3.17E-02
RP11-175B12.2	-5.79	2.94E-04	AC093690.1	-2.29	3.08E-03
UPP2	-5.77	1.57E-02	CKMT2	-2.28	1.40E-03
TRPS1	-5.76	1.88E-02	AQP7P2	-2.28	6.26E-03
EPHA7	-5.76	1.53E-02	RP11-161H23.10	-2.28	5.99E-03
RP11-420K10.1	-5.75	5.42E-03	RP11-159F24.5	-2.28	4.37E-02
RP11-242F11.2	-5.74	2.14E-02	ANGPTL1	-2.27	2.37E-02
RP11-657O9.1	-5.74	2.91E-02	FSD2	-2.27	2.75E-02
EGFEM1P	-5.74	2.03E-02	CYP2T2P	-2.27	1.87E-02
TSPYL6	-5.73	4.21E-04	RP11-792A8.3	-2.26	1.57E-02
PAK7	-5.73	3.20E-02	PDE4D	-2.26	3.34E-03
AC006077.4	-5.72	3.04E-02	TMEM130	-2.26	3.54E-02
RP11-47J17.3	-5.72	1.24E-02	AC097721.2	-2.26	1.13E-02
RP11-36N20.1	-5.72	1.71E-04	RP11-642A1.1	-2.26	2.99E-02
AC016894.1	-5.71	2.04E-02	TMEM154	-2.26	9.13E-04
RP11-697N18.1	-5.70	6.07E-03	TTLL9	-2.26	9.01E-03
LARP4P	-5.69	2.12E-02	SYCP3	-2.26	1.64E-02
CTC-459M5.2	-5.69	7.38E-03	VGLL3	-2.26	7.50E-04
P2RY14	-5.68	6.65E-04	SDR42E2	-2.25	1.74E-02
RP11-364F11.1	-5.67	5.95E-06	RP11-385D13.3	-2.25	2.51E-02
RP11-402L5.1	-5.67	1.38E-02	RP5-1021I20.5	-2.25	2.88E-02
RP11-552M6.1	-5.67	1.09E-02	RP11-91H12.4	-2.24	4.03E-02
RP11-1336O20.2	-5.65	3.18E-04	RP11-752D24.2	-2.24	4.25E-02
AC009310.1	-5.64	2.95E-02	RP11-111A21.1	-2.24	4.48E-02
RP11-36N20.2	-5.64	4.30E-03	OTOG	-2.24	6.33E-03
RP11-474P2.5	-5.64	2.34E-02	NUTM2G	-2.24	2.73E-03
RBPMSLP	-5.63	2.36E-02	AL590762.11	-2.23	2.52E-02
LRRC4	-5.62	8.75E-03	HHIP	-2.23	3.30E-02
RP11-12I24.2	-5.62	7.07E-03	FOXN4	-2.23	1.42E-05
RP11-138A9.2	-5.61	7.43E-04	RPL7AP34	-2.23	9.06E-03
RP11-255L13.1	-5.60	1.18E-03	RP11-434C1.1	-2.22	7.88E-03
MAB21L1	-5.60	2.51E-02	TMEM139	-2.22	2.54E-07
RP11-1250I15.3	-5.59	1.57E-02	MIR3648-2	-2.22	5.46E-03
RP11-474L11.5	-5.58	4.88E-04	RP11-702L15.1	-2.22	1.89E-02
RP11-522L3.4	-5.58	1.65E-02	MAML3	-2.22	5.58E-07
AC007790.3	-5.57	2.64E-02	WISP2	-2.22	1.57E-02
RP1-101D8.1	-5.57	2.65E-02	AC091801.1	-2.22	2.71E-02
RP11-674I16.1	-5.56	4.03E-03	KRT20	-2.21	6.70E-03
RP11-182M20.2	-5.56	2.67E-02	CTD-3051D23.4	-2.21	3.10E-02
AC104781.1	-5.56	2.85E-02	LIN28A	-2.21	1.84E-02
RP11-624G19.1	-5.56	2.68E-02	RP11-342D14.1	-2.21	4.87E-06
RP1-102G20.3	-5.56	1.67E-02	RP11-520B13.7	-2.21	2.47E-02
RP11-351O1.3	-5.55	2.80E-02	RP11-57H14.5	-2.21	2.32E-02
FILIP1L	-5.55	3.29E-03	RP11-4B16.1	-2.21	3.97E-02
RP11-522L3.3	-5.54	1.76E-02	WI2-1896O14.1	-2.21	4.62E-02
RERG	-5.54	2.13E-07	PKIB	-2.20	2.74E-20
RP11-333H9.6	-5.54	8.77E-03	MIR3648-1	-2.20	5.74E-03
AC013410.1	-5.53	1.95E-02	SSTR2	-2.20	2.91E-03
DIRC3	-5.51	2.16E-03	EXTL3-AS1	-2.20	1.50E-02
CTC-349C3.2	-5.50	1.51E-02	RP4-565E6.1	-2.20	1.49E-03
CNNM1	-5.49	4.15E-02	AZGP1	-2.20	5.76E-03

RP11-269G24.2	-5.49	3.20E-02	CTD-2024I7.1	-2.20	4.60E-02
RP11-506B4.2	-5.48	3.20E-02	AC013448.1	-2.20	1.75E-03
OR51J1	-5.48	2.62E-03	TRPV6	-2.20	4.88E-04
MIR624	-5.48	3.16E-02	CTA-390C10.10	-2.19	6.11E-07
RP11-393I2.2	-5.47	5.31E-04	RP11-583F2.2	-2.19	1.96E-02
RNA5SP168	-5.47	3.17E-02	CRYBA1	-2.19	3.39E-02
AF129408.15	-5.47	3.17E-02	AC006509.8	-2.19	3.78E-02
CTA-298G8.1	-5.46	1.62E-02	NEXN	-2.19	6.75E-03
OR51Q1	-5.46	5.47E-03	CEP295NL	-2.19	4.09E-02
RP11-346J10.1	-5.46	1.99E-02	RP11-231I16.1	-2.19	1.98E-02
RP11-391L3.3	-5.46	1.34E-02	ZNF660	-2.18	3.20E-02
FGF14	-5.46	8.96E-04	FXYD3	-2.18	1.67E-05
CTD-2008P7.9	-5.45	1.04E-02	EPB41L4A	-2.18	3.31E-08
ST7OT2	-5.45	1.25E-03	CASP4	-2.18	1.51E-13
RP11-538D9.2	-5.45	3.28E-02	RP11-266L9.2	-2.18	9.93E-03
RF00561	-5.43	1.75E-02	CH17-52D20.1	-2.18	3.39E-03
RP11-89N17.1	-5.43	1.74E-02	NCKAP1L	-2.18	1.02E-02
RN7SKP72	-5.43	3.40E-02	VTCN1	-2.18	5.26E-03
RP11-72B4.2	-5.42	2.01E-02	RP11-304F15.4	-2.17	4.19E-02
RP11-1029M24.4	-5.40	1.41E-02	ESR1	-2.17	4.97E-02
XXbac-B476C20.14	-5.40	1.88E-02	BST2	-2.17	1.30E-04
RP11-669C19.1	-5.39	3.62E-02	HULC	-2.17	9.47E-04
SRSF12	-5.39	1.65E-02	RP11-317B17.2	-2.17	3.47E-03
RP11-560B16.5	-5.39	3.62E-02	RP11-353N4.5	-2.17	2.75E-02
KB-1205A7.2	-5.39	1.06E-03	ANKRD20A5P	-2.17	1.35E-04
RP11-52J3.2	-5.38	1.50E-03	RP11-268I9.2	-2.16	2.98E-02
ZNF652P	-5.37	7.91E-03	RP11-382A20.7	-2.16	3.14E-02
AC023590.1	-5.37	3.63E-02	RP11-332H18.3	-2.16	2.95E-02
RND3	-5.37	5.03E-35	RP11-400F19.12	-2.15	2.30E-02
RP11-44D5.1	-5.36	1.39E-02	ZMAT1	-2.15	1.20E-04
RP11-8L18.2	-5.36	7.43E-04	EIF4E1B	-2.15	2.46E-02
RP11-223C24.2	-5.35	3.94E-02	RP11-498P14.2	-2.15	1.86E-02
AC007098.1	-5.35	3.84E-02	LHFP	-2.14	9.63E-03
RP11-295M3.2	-5.35	1.76E-02	RP11-769O8.1	-2.14	1.32E-02
RP11-212F11.1	-5.35	2.87E-02	RP11-289H16.1	-2.14	1.85E-02
RP5-916O11.3	-5.35	4.94E-03	RP11-146E13.5	-2.14	4.15E-03
RP11-8L18.3	-5.33	1.36E-02	GP6	-2.14	4.70E-03
MIR4435-2	-5.32	4.10E-02	RP11-794G24.1	-2.13	8.88E-03
OR7A19P	-5.32	4.87E-06	CTD-2349P21.5	-2.13	7.93E-03
RP3-388N13.1	-5.31	1.16E-02	RP11-227G15.11	-2.13	4.04E-02
RP11-417B4.4	-5.30	4.46E-02	RP11-343N15.1	-2.13	2.05E-02
AC093166.4	-5.28	4.39E-02	CTC-343N3.1	-2.13	1.77E-02
PSG1	-5.28	6.11E-03	RP11-495P10.10	-2.12	2.67E-02
OR1AA1P	-5.26	4.44E-02	CLCNKB	-2.12	9.13E-04
RP11-605F14.3	-5.25	1.06E-02	AC138972.2	-2.12	4.70E-02
AC092839.4	-5.25	4.72E-02	RP11-34P13.9	-2.11	4.25E-02
AC090516.2	-5.25	1.18E-02	SPDYE3	-2.11	4.89E-02
RP11-338E21.3	-5.25	1.57E-02	CECR1	-2.11	4.08E-02
RP5-1163L11.3	-5.25	4.64E-02	RP11-697N18.3	-2.11	2.40E-02
KCTD4	-5.24	3.89E-04	RP11-380B4.3	-2.10	4.41E-02
RP11-454K7.3	-5.24	1.74E-02	PSMD10P	-2.10	1.85E-02
RN7SL706P	-5.24	1.06E-02	RP11-344E13.3	-2.10	4.77E-02

AC055764.1	-5.22	4.74E-02	SAMD3	-2.10	6.65E-04
RP1-245G19.2	-5.22	3.54E-02	AC090516.1	-2.10	2.74E-02
RP11-356I18.1	-5.22	1.70E-03	RP11-563J2.2	-2.09	4.88E-02
AC092431.2	-5.22	2.87E-02	FOXJ1	-2.09	1.04E-02
RP11-254F7.1	-5.22	2.00E-02	FAM65C	-2.09	1.29E-02
BLID	-5.21	2.58E-03	RP11-342K2.1	-2.09	1.03E-03
KB-1205A7.1	-5.20	8.77E-04	RP11-692D12.1	-2.08	1.92E-02
AC104058.1	-5.19	8.40E-03	RP11-163E9.1	-2.07	2.38E-02
CTD-2566J3.2	-5.19	7.10E-03	CTD-2540L5.3	-2.07	2.76E-02
RP3-472M2.2	-5.19	3.09E-03	TNFAIP8L3	-2.07	2.09E-02
RP11-264E23.1	-5.19	7.31E-03	SPDYE8P	-2.06	3.41E-03
RN7SL801P	-5.19	1.86E-02	CTA-747E2.11	-2.06	3.34E-02
RP11-85F14.1	-5.18	2.27E-02	AC096670.3	-2.06	6.40E-03
RP11-641C17.1	-5.18	2.68E-02	RP5-1158E12.3	-2.06	1.82E-02
RP11-142O6.1	-5.18	2.04E-02	LRG1	-2.06	3.97E-03
RN7SL430P	-5.17	2.05E-02	RP11-213H15.3	-2.06	1.11E-02
GPR22	-5.17	5.09E-05	TAS2R4	-2.05	3.14E-03
RP11-617F23.2	-5.17	3.30E-02	MIRLET7A2	-2.05	3.56E-02
AC090627.1	-5.16	7.73E-05	DPRXP4	-2.05	2.58E-02
RP11-436I24.1	-5.15	2.34E-03	RP11-2H3.7	-2.05	1.81E-02
RP11-539G18.1	-5.15	3.11E-05	AC003029.4	-2.04	4.19E-02
RP11-756D7.1	-5.15	8.72E-03	LAMA4	-2.04	3.23E-04
RP11-369L4.1	-5.14	3.70E-02	RP11-496I2.5	-2.04	2.53E-03
RP11-956A19.1	-5.14	5.22E-03	RP11-139K1.2	-2.04	2.55E-02
RF00019	-5.13	1.67E-02	TENM3	-2.04	2.30E-02
PRSS48	-5.13	4.71E-03	CTA-228A9.4	-2.03	1.64E-02
RPL6P12	-5.13	9.90E-03	AP1M2	-2.03	1.12E-14
RP11-665C16.5	-5.12	2.70E-02	AC008746.12	-2.03	3.86E-02
AC018804.3	-5.12	3.64E-02	CH17-52D20.2	-2.03	5.04E-03
ZFP64P1	-5.11	1.99E-02	KB-1836B5.1	-2.03	2.79E-02
CTC-298B17.1	-5.10	1.75E-05	RP13-580F15.2	-2.03	4.41E-02
RP11-600P18.4	-5.10	3.80E-02	GALNT3	-2.02	8.90E-13
RP11-193F5.2	-5.10	1.94E-04	TRIM17	-2.02	1.59E-02
RP11-264L1.1	-5.10	8.88E-03	RN7SKP80	-2.02	2.23E-02
SLCO5A1	-5.10	2.16E-05	MB	-2.02	6.06E-05
RP5-1029F21.4	-5.09	3.19E-02	SMTNL1	-2.01	2.29E-04
CTD-2286N8.1	-5.09	2.78E-02	AP000347.3	-2.01	1.13E-02
RP11-390N6.1	-5.08	2.25E-04	RP11-927P21.12	-2.01	4.67E-02
RF00017	-5.07	4.16E-03	RP11-474D14.2	-2.01	2.40E-02
MIR619	-5.07	2.96E-02	CTD-2353F22.2	-2.01	2.27E-05
U51244.2	-5.07	2.98E-02	SLC2A3	-2.01	9.39E-06
RP11-809C18.3	-5.06	1.06E-03	CC2D2B	-2.01	1.18E-02
OR51M1	-5.06	2.84E-03	IL1RAPL1	-2.01	3.42E-04
RP1-272J12.1	-5.06	2.64E-02	AC005488.12	-2.01	3.76E-02
AC025627.4	-5.06	3.51E-02	ANKFN1	-2.00	1.02E-02
CTC-448F2.4	-5.05	8.11E-10	KLF12	-2.00	4.31E-14
RP11-118E18.2	-5.05	1.55E-02	MAGI1-IT1	-2.00	2.19E-02
OGN	-5.05	4.73E-02	C12orf36	-2.00	4.99E-02
AC003989.3	-5.04	4.53E-03	RP4-800G7.3	-2.00	2.29E-02
RP11-46O21.2	-5.03	1.32E-03	DCDC2B	-2.00	1.74E-02
RP11-174F8.1	-5.03	4.31E-03	RP11-353N4.6	-1.99	2.19E-02
RP11-26G10.1	-5.02	1.74E-03	SCN4A	-1.99	1.79E-05

RP11-58G13.1	-5.02	2.34E-02	SULT1A2	-1.99	2.92E-07
POU5F2	-5.01	6.36E-03	FAM87B	-1.99	3.17E-02
PEG13	-5.01	3.66E-03	AC013472.3	-1.99	3.39E-02
CTB-76P12.1	-5.01	6.79E-03	RP11-6N13.1	-1.98	7.75E-03
PLN	-5.01	1.75E-02	CH17-52D20.3	-1.98	5.88E-03
RP11-330C7.3	-5.00	3.29E-03	ARGFXP2	-1.98	3.61E-02
RN7SL370P	-5.00	6.10E-03	RP11-995C19.2	-1.98	1.56E-02
RP11-354P11.3	-5.00	9.80E-04	GPR68	-1.98	9.55E-04
RP11-461A8.5	-5.00	4.65E-02	TTC28	-1.98	4.69E-03
RP3-525L6.2	-5.00	4.49E-02	RP11-84A19.4	-1.98	4.07E-02
RP11-92K15.1	-5.00	1.13E-02	KRTAP2-3	-1.97	1.85E-10
MIR579	-5.00	3.76E-02	CLMP	-1.97	4.08E-06
RP1-177P22.1	-4.99	5.51E-04	RP11-1399P15.1	-1.97	4.06E-02
CTD-2538G10.1	-4.99	2.58E-02	CTD-3088G3.8	-1.97	1.25E-07
RP11-191J12.1	-4.99	2.64E-02	ESYT3	-1.97	3.61E-02
RF00019	-4.99	4.79E-02	AP000253.1	-1.97	4.60E-02
RP4-809F4.1	-4.98	2.08E-02	AC109333.10	-1.97	4.89E-02
RP11-58D2.1	-4.98	2.52E-02	RP11-798G7.8	-1.96	1.53E-03
RNU6-430P	-4.98	2.87E-02	ANXA10	-1.96	1.85E-05
NEGR1	-4.98	1.29E-02	RP11-286N22.8	-1.96	2.13E-02
RP11-395I14.3	-4.98	1.62E-02	TMEM232	-1.96	2.00E-02
RP11-4F22.2	-4.97	1.76E-03	AC012512.1	-1.96	2.29E-03
AL450226.2	-4.96	2.79E-02	TSHZ2	-1.96	1.66E-02
RP4-568C11.4	-4.96	9.01E-15	VGF	-1.96	1.92E-12
RP5-1154E9.6	-4.96	6.30E-03	RP11-44F14.2	-1.96	1.80E-02
CTB-139P11.2	-4.95	5.93E-03	SPOCK3	-1.95	5.01E-04
RP4-712E4.4	-4.95	1.72E-02	CTD-2547E10.6	-1.95	1.21E-02
AC080002.1	-4.94	4.06E-03	RP11-705C15.3	-1.95	7.25E-03
RP11-159M11.2	-4.94	2.11E-02	SPDYE1	-1.95	8.53E-03
AC007251.2	-4.94	4.89E-02	GRHL3	-1.95	2.05E-02
SLC38A4	-4.93	2.36E-03	AC012358.7	-1.94	4.07E-02
CTD-2566J3.1	-4.92	2.38E-04	SLC5A4	-1.94	3.72E-02
AC007790.4	-4.91	7.65E-03	HMGA1L5	-1.94	1.23E-02
RP11-295B17.6	-4.91	1.54E-03	APBA1	-1.94	1.28E-02
RP13-216E22.5	-4.91	1.35E-02	KRTAP2-4	-1.94	1.33E-07
RP5-1100E15.4	-4.91	4.63E-02	RAD51AP2	-1.93	3.25E-03
GPR52	-4.91	4.83E-04	RP4-814D15.2	-1.93	1.01E-02
RP11-296O14.2	-4.90	1.91E-02	AC005042.4	-1.92	3.60E-02
RP11-95J11.1	-4.90	2.38E-02	LINC-PINT	-1.92	1.34E-04
RP1-60N8.1	-4.90	4.17E-02	RP11-166O4.1	-1.92	2.25E-02
RP11-161H23.8	-4.90	1.45E-02	RP11-106D4.2	-1.92	1.04E-03
RP11-73M11.2	-4.89	4.08E-04	FAM186B	-1.92	1.49E-02
RP11-264L1.4	-4.88	1.45E-02	ADGRD2	-1.92	1.16E-05
RP11-474B12.1	-4.88	8.29E-03	RP11-31F15.1	-1.92	2.02E-03
RF00019	-4.87	4.63E-02	RP11-477J21.7	-1.92	3.01E-02
TAS2R30	-4.87	2.26E-02	IFITM1	-1.91	1.66E-04
RF00019	-4.87	4.70E-02	PRH1	-1.91	3.38E-02
RP11-572F4.1	-4.85	1.19E-02	EFCAB13	-1.91	7.65E-03
ZNF280A	-4.84	1.08E-07	RP11-191L9.4	-1.91	1.31E-02
RP11-15F12.3	-4.84	4.93E-02	SLC28A2	-1.91	1.19E-02
RP11-571F15.2	-4.84	1.75E-02	CTD-2538G9.5	-1.91	4.71E-02
CTA-797E19.3	-4.84	1.24E-02	CTA-217C2.2	-1.90	3.63E-02

RP11-750H9.7	-4.83	2.94E-02	ADAMTSL4-AS1	-1.90	2.54E-02
RNU6-681P	-4.83	3.39E-02	RP13-216E22.4	-1.90	2.38E-02
RP11-298J20.3	-4.83	4.08E-03	KCNMB2	-1.89	4.52E-02
RF00019	-4.82	1.57E-02	RP11-798G7.4	-1.89	4.69E-02
LRRN3	-4.81	1.09E-02	AC139100.3	-1.88	3.59E-02
RP11-122A21.2	-4.81	1.18E-02	ABI3BP	-1.88	3.44E-02
ST7-OT4	-4.81	1.10E-02	OR10H1	-1.88	2.80E-02
RP11-220M1.1	-4.81	4.16E-05	ERN2	-1.88	3.20E-02
RP11-153G4.2	-4.80	1.57E-02	B3GALT1	-1.88	1.16E-03
RP11-220I1.4	-4.80	1.05E-03	KLRD1	-1.88	8.19E-03
RP11-22B10.3	-4.79	9.91E-03	RP11-93B14.4	-1.87	1.78E-02
RP11-413N10.3	-4.79	4.94E-04	ABCA4	-1.87	1.55E-03
RP11-1110F20.1	-4.78	1.27E-02	ZBTB12B	-1.87	2.37E-02
RP11-417B4.2	-4.78	2.87E-03	RP11-304F15.3	-1.87	4.74E-03
AC007001.4	-4.78	3.63E-02	AC006995.8	-1.87	7.96E-03
RP13-204A15.3	-4.78	1.33E-03	RP11-927P21.2	-1.87	3.66E-02
RP11-282K24.3	-4.77	8.65E-03	RP11-626G11.6	-1.87	2.57E-02
RP11-399K21.11	-4.77	2.02E-03	AC093391.2	-1.86	1.24E-03
OR10A2	-4.77	6.97E-05	RP3-329A5.8	-1.86	1.26E-02
RP11-1396O13.1	-4.76	4.79E-03	C4orf47	-1.86	1.05E-03
RP11-686G8.1	-4.76	4.29E-05	TAC4	-1.86	1.88E-02
RP11-25J3.2	-4.76	3.79E-05	FHIT	-1.85	4.08E-07
RP11-201O14.1	-4.76	6.17E-03	RP3-522J7.7	-1.85	4.01E-02
RP11-330C7.1	-4.76	1.96E-02	FOXD4L4	-1.85	3.72E-02
LRRTM4	-4.75	1.93E-03	RP11-255B23.3	-1.85	3.81E-06
KIF6	-4.75	4.91E-02	CASP10	-1.85	9.01E-07
MIR181A1HG	-4.75	1.98E-04	LL22NC03-N64E9.1	-1.85	1.36E-06
RN7SL16P	-4.75	3.85E-02	UNC79	-1.84	2.10E-02
PSG5	-4.74	4.87E-02	TMEM125	-1.84	4.51E-12
RP11-274J7.2	-4.74	4.31E-03	MUC19	-1.84	8.82E-04
RN7SL285P	-4.74	7.27E-03	NECTIN4	-1.83	4.77E-03
RP11-801G16.2	-4.73	1.96E-02	PFN1P4	-1.83	3.74E-02
PRR26	-4.73	6.08E-03	RPL9P32	-1.82	9.91E-03
RP1-315G1.1	-4.73	1.92E-03	RP11-431K24.2	-1.82	2.28E-02
RP11-399K21.5	-4.72	3.70E-03	DUXAP10	-1.82	9.95E-19
CTD-2014D20.1	-4.72	1.07E-04	OR51B2	-1.82	2.98E-04
RP11-635L1.3	-4.72	1.98E-03	RP3-368A4.6	-1.81	8.42E-04
MIR1299	-4.72	4.89E-02	RP11-798G7.6	-1.81	1.64E-02
RP11-697H9.5	-4.71	3.86E-02	NCLP1	-1.81	3.91E-02
RF00100	-4.71	3.27E-02	KRTAP2-1	-1.81	1.39E-02
RN7SL756P	-4.71	4.32E-02	SHF	-1.81	1.03E-03
RP11-665J20.1	-4.71	2.81E-03	FOXQ1	-1.81	2.30E-02
RP11-360N9.3	-4.70	7.18E-03	RP11-548H18.2	-1.80	1.96E-02
RP1-261D10.1	-4.70	4.82E-03	RP11-927P21.1	-1.80	2.94E-02
LRRTM2	-4.70	5.04E-03	RP11-260O18.1	-1.80	2.78E-04
GPR18	-4.69	3.15E-03	RP11-36B6.2	-1.80	2.49E-03
RN7SL698P	-4.69	4.60E-02	C2orf78	-1.80	1.84E-02
RP11-1060J15.3	-4.69	6.11E-03	RP5-1171I10.4	-1.79	2.22E-02
RP4-633I8.3	-4.68	1.54E-02	TEX22	-1.79	4.37E-02
RP11-96C23.9	-4.68	2.13E-03	RP11-557N21.1	-1.79	2.36E-02
AC002044.1	-4.67	1.06E-02	AP001429.1	-1.79	4.06E-02
RP11-274A11.3	-4.67	5.31E-03	SPATA6L	-1.79	6.44E-03

RN7SKP158	-4.67	1.49E-02	RP11-172H24.3	-1.79	4.93E-02
RP11-226M10.3	-4.67	6.19E-05	KB-1507C5.2	-1.79	6.16E-03
P2RY13	-4.66	3.72E-02	RP11-366L20.3	-1.78	1.39E-03
RP1-292B18.3	-4.66	5.93E-03	TACR3	-1.78	3.96E-02
MIR4268	-4.66	1.10E-02	KLRK1	-1.78	3.72E-03
RP11-522L3.2	-4.66	8.06E-03	RP11-488P3.1	-1.78	2.59E-02
CTD-2540L5.9	-4.65	1.18E-03	RP11-448A19.1	-1.77	7.54E-03
MAGI1-AS1	-4.65	3.84E-04	AC073130.1	-1.77	4.60E-02
RP5-833A20.1	-4.64	3.10E-02	TMC2	-1.77	4.06E-02
AF127936.7	-4.63	1.45E-02	RP11-250B2.6	-1.76	1.70E-02
OR9A3P	-4.63	1.96E-02	APOL6	-1.76	1.85E-02
RP11-443F16.1	-4.63	2.26E-03	SDPR	-1.76	1.50E-02
RP11-1005I1.1	-4.63	4.66E-02	DUXAP9	-1.75	5.12E-16
RP11-829H16.5	-4.63	3.53E-03	MIAT	-1.75	4.28E-02
AC012513.3	-4.62	9.02E-03	RP11-11N5.1	-1.74	1.02E-02
SCN2A	-4.62	2.53E-08	CTB-13F3.1	-1.74	6.70E-03
RP13-204A15.4	-4.62	4.08E-04	LL0XNC01-36H8.1	-1.74	3.02E-02
RP11-661D19.1	-4.62	2.38E-03	RP11-509J21.1	-1.74	2.23E-02
RF00157	-4.61	2.96E-04	ZNF506	-1.73	2.60E-02
AC012066.1	-4.61	7.03E-03	HFM1	-1.73	6.33E-03
RP11-293A21.2	-4.61	1.49E-02	RP11-361H10.5	-1.73	4.21E-02
RP11-702L15.4	-4.60	6.90E-03	KCNK9	-1.73	4.04E-03
RP11-382D8.4	-4.60	1.74E-02	GGT5	-1.73	1.04E-02
RP11-390P2.2	-4.60	4.40E-03	NR3C2	-1.73	1.07E-03
RP11-223P11.3	-4.60	1.68E-03	HACD4	-1.73	2.33E-02
CTD-2006C1.2	-4.59	3.29E-03	RP11-848G14.5	-1.73	6.25E-04
AC008269.2	-4.59	2.25E-02	RPLP0P2	-1.73	2.09E-03
NANOGP6	-4.59	1.40E-02	CD74	-1.73	3.41E-02
RP11-697B24.1	-4.58	5.22E-06	CAPN12	-1.73	1.16E-05
ANGPT2	-4.58	3.35E-12	PDE1A	-1.72	1.57E-02
PBOV1	-4.58	1.62E-02	MYH11	-1.72	2.12E-02
AC008281.1	-4.58	1.46E-02	GREB1	-1.72	2.64E-09
RP5-1154E9.5	-4.58	4.50E-02	CTA-941F9.10	-1.72	2.00E-02
RN7SL220P	-4.58	3.02E-02	RP5-894A10.5	-1.72	1.82E-02
AC012370.3	-4.58	1.19E-02	ANKRD31	-1.72	3.69E-02
RP5-1049N15.2	-4.57	5.81E-03	RP11-27J8.3	-1.71	1.97E-03
RP11-332O19.2	-4.57	4.82E-03	RP11-40A8.3	-1.71	2.64E-02
CTB-73N10.1	-4.57	7.18E-03	RP11-326C3.2	-1.71	8.11E-04
RF00019	-4.56	2.96E-02	SUN3	-1.71	2.81E-03
AC068491.3	-4.55	3.61E-02	AC004951.6	-1.71	2.04E-02
RP11-397P14.3	-4.55	4.75E-02	RP11-356J5.12	-1.70	3.53E-05
RP11-473O4.3	-4.55	8.20E-03	NELL2	-1.70	2.74E-02
RP11-354E23.3	-4.55	8.47E-03	KLK8	-1.70	2.32E-07
RP1-290I10.4	-4.54	2.09E-02	CCDC7	-1.70	5.31E-03
CTA-339C12.1	-4.54	3.77E-04	RP11-583F2.1	-1.70	2.20E-02
RP11-211A18.2	-4.54	1.35E-02	PAH	-1.70	7.56E-03
AC092620.2	-4.54	5.39E-03	RP11-507K2.6	-1.70	4.69E-02
RP11-118E18.1	-4.54	9.98E-03	AC142293.3	-1.69	2.57E-02
CTC-551A13.1	-4.54	2.79E-02	RP11-151N17.1	-1.69	3.42E-02
CTD-3020H12.4	-4.54	3.91E-02	KIRREL2	-1.69	8.11E-03
RP11-324O2.3	-4.54	5.51E-18	AC008697.1	-1.69	2.33E-02
C3orf65	-4.53	1.14E-02	NEK5	-1.69	2.40E-07

MTND5P26	-4.53	8.52E-03	RINL	-1.69	1.77E-07
TACR1	-4.53	1.97E-02	ATP2C2	-1.68	4.13E-04
DNM3OS	-4.52	7.13E-03	GHRL	-1.68	3.34E-02
RP11-570L14.1	-4.52	2.90E-02	RP11-379B18.8	-1.68	2.59E-02
RP11-76I7.1	-4.52	1.40E-03	CLDN20	-1.67	2.74E-02
RP1-154J13.3	-4.51	4.10E-02	ELOVL2	-1.67	1.39E-02
OR51A10P	-4.51	7.07E-03	AC127904.2	-1.67	4.89E-02
RP5-951N9.1	-4.51	1.76E-03	RP11-164J13.1	-1.67	1.57E-02
AC013476.2	-4.50	3.53E-02	RP4-777D9.2	-1.67	8.04E-03
RP11-88B8.2	-4.50	1.10E-03	DNAH5	-1.67	9.13E-04
RP11-20L24.1	-4.49	9.59E-03	FGF9	-1.66	4.71E-02
RP11-426J5.3	-4.48	5.25E-03	DDX17	-1.66	5.72E-18
RP1-184J9.2	-4.48	1.94E-02	HLA-DOA	-1.66	1.71E-02
RP11-423E7.2	-4.48	5.76E-03	MKRN2OS	-1.66	4.05E-03
OXER1	-4.47	1.35E-03	DNALI1	-1.66	2.64E-02
RP11-357N13.2	-4.47	3.92E-03	RP11-379B18.4	-1.66	1.36E-02
RP11-388P9.2	-4.47	1.98E-02	AC083884.8	-1.65	4.43E-02
SLC28A3	-4.47	2.38E-02	SMIM5	-1.65	3.95E-02
RP11-138A9.1	-4.47	3.46E-03	RP11-21I4.3	-1.65	3.53E-02
RP11-556O9.3	-4.47	4.10E-02	ANKDD1B	-1.65	6.75E-03
RP4-728D4.3	-4.46	5.32E-03	PTPRB	-1.65	6.32E-04
NANOGP8	-4.46	2.94E-02	AC010148.1	-1.65	4.73E-02
RP11-298P3.1	-4.46	1.51E-03	BMS1P11	-1.65	8.06E-03
RP5-966M1.4	-4.46	3.09E-02	MUC2	-1.65	1.60E-02
RP3-403A15.5	-4.46	3.94E-02	TMEM200A	-1.64	3.03E-06
RP4-569M23.5	-4.45	2.24E-04	GRHL2	-1.64	2.17E-12
OMG	-4.45	9.49E-03	RP11-734K2.4	-1.64	4.48E-03
LXN	-4.45	1.73E-03	MATR3	-1.64	2.94E-03
LRRC9	-4.44	5.17E-04	RP11-399K21.6	-1.64	3.02E-07
RP11-430C7.2	-4.44	1.34E-03	RP11-278A23.2	-1.64	2.68E-02
EHF	-4.44	3.11E-62	AC067956.1	-1.63	1.67E-02
RP4-566L20.1	-4.44	4.32E-04	RP11-343C2.10	-1.63	4.65E-02
ERVFRD-1	-4.43	2.75E-02	RP11-219I21.2	-1.63	2.69E-03
RP11-522L3.11	-4.43	7.12E-03	ABO	-1.63	1.57E-02
SPTLC3	-4.43	2.09E-04	TJP2	-1.63	4.62E-02
TSLP	-4.43	9.13E-04	RP11-103B5.4	-1.62	3.29E-02
RP11-936I5.1	-4.43	2.82E-04	LA16c-60H5.7	-1.62	8.50E-04
RP13-339P19.1	-4.43	2.45E-02	ACSM4	-1.62	6.91E-03
RP11-6B19.1	-4.43	2.09E-04	KRTAP2-2	-1.62	2.97E-03
FAM196A	-4.42	1.75E-02	OR51B3P	-1.62	3.44E-02
RP11-463D19.1	-4.42	2.25E-03	SLC16A4	-1.61	1.88E-02
RP11-182B22.2	-4.42	4.60E-02	CTB-50L17.14	-1.61	1.30E-02
RP11-211A18.1	-4.42	2.34E-02	POU5F1B	-1.61	4.01E-02
PDHA1P1	-4.41	2.62E-03	LA16c-381G6.1	-1.61	1.04E-02
RP11-474P2.7	-4.41	1.11E-02	HOGA1	-1.61	6.59E-04
GCNT2	-4.41	2.04E-08	CTD-3203P2.2	-1.61	4.95E-02
OR10A4	-4.41	2.98E-02	RP1-80B9.2	-1.61	1.35E-02
RP11-330C7.2	-4.41	4.79E-03	PADI3	-1.61	2.01E-02
RP11-425D17.2	-4.40	1.82E-02	EPN3	-1.60	3.81E-03
RP11-363P13.1	-4.40	4.77E-03	RPL9P2	-1.60	4.74E-02
RP11-516C1.2	-4.39	3.12E-03	PLA2R1	-1.60	1.29E-04
RP3-391O22.2	-4.39	4.03E-02	KLK6	-1.59	7.73E-05

RP4-604K5.3	-4.39	9.90E-03	ARHGAP40	-1.59	3.04E-03
DDX18P5	-4.39	8.83E-03	MCAM	-1.59	1.08E-13
ART4	-4.38	9.72E-04	FAM166B	-1.59	4.23E-02
PKHD1	-4.38	1.70E-02	KLK13	-1.59	2.51E-02
AC064874.1	-4.38	2.34E-02	MEST	-1.59	3.87E-08
OR2D3	-4.37	3.96E-02	RP11-58H20.3	-1.58	3.86E-02
GRIN2B	-4.37	3.27E-28	RP11-798G7.5	-1.58	1.09E-02
RP11-1174L13.2	-4.36	4.32E-02	CCDC153	-1.58	3.94E-04
RP11-55J15.2	-4.36	1.74E-03	RAB40A	-1.58	4.13E-04
RP5-997K18.1	-4.36	2.68E-02	AKAP12	-1.58	2.37E-10
RP11-1396O13.2	-4.36	3.38E-03	MPIG6B	-1.58	6.16E-03
MROH9	-4.35	3.33E-03	FIRRE	-1.58	3.81E-06
RP11-380M21.3	-4.35	4.16E-02	AC004166.6	-1.58	1.45E-02
RP11-384L8.2	-4.35	2.63E-02	CITF22-45C1.3	-1.58	2.37E-02
ALK	-4.35	4.95E-04	PRSS51	-1.57	5.74E-04
AC106873.4	-4.35	4.01E-02	AC027119.1	-1.57	3.42E-02
RPL17P25	-4.34	2.85E-02	SPTSSB	-1.57	6.30E-03
RN7SL648P	-4.33	1.13E-04	FAXDC2	-1.57	2.75E-02
RP11-22L13.1	-4.33	3.05E-02	RP11-902B17.1	-1.57	1.40E-02
RNU6-879P	-4.32	4.29E-02	LCK	-1.56	4.58E-02
RP11-312P12.2	-4.32	3.77E-03	AC006042.6	-1.56	2.23E-02
MIR1255A	-4.32	4.41E-02	RP11-46C20.1	-1.56	3.63E-06
RF00017	-4.32	2.13E-02	TTYH1	-1.56	2.61E-02
A2M	-4.32	4.89E-07	HELLPAR	-1.56	8.34E-03
RP11-421E14.2	-4.32	1.36E-02	TAS2R5	-1.56	2.94E-02
OSR1	-4.32	6.18E-05	RP11-316C12.2	-1.56	3.66E-02
RP11-151A6.5	-4.32	1.29E-04	RP11-497H16.8	-1.56	1.40E-02
AC012501.3	-4.31	7.91E-03	ZMYND15	-1.55	1.57E-04
AC002075.3	-4.31	4.67E-02	BISPR	-1.54	2.57E-02
WDR64	-4.31	3.49E-07	RP3-394A18.1	-1.54	7.35E-03
CA9	-4.30	4.33E-04	KLK10	-1.54	1.14E-05
B3GALT2	-4.30	1.20E-02	NOTCH3	-1.53	1.33E-07
RP11-360N9.2	-4.30	6.10E-03	EPS8L1	-1.53	1.52E-08
RP11-30L3.2	-4.30	4.63E-02	AC007000.7	-1.53	3.91E-02
C8orf17	-4.30	2.71E-03	ANO7	-1.53	3.35E-02
RP11-95H11.1	-4.30	2.03E-02	MAST4	-1.53	6.63E-04
RP11-190D6.1	-4.30	1.20E-02	RP3-443E24.1	-1.53	2.36E-02
TMPRSS11D	-4.29	1.95E-03	N4BP2L2-IT2	-1.53	3.86E-03
ITPK1-AS1	-4.29	3.88E-03	RP11-382A18.1	-1.52	6.11E-05
RP11-319G9.3	-4.29	2.37E-04	AC004791.2	-1.52	3.10E-03
ELOA3	-4.29	2.53E-02	AC004041.2	-1.52	1.65E-02
RPL31P58	-4.29	2.56E-02	IZUMO1	-1.52	7.40E-03
AP004289.2	-4.29	1.18E-02	RP11-379B18.5	-1.52	5.17E-04
BEX4	-4.28	3.11E-06	RP11-786O7.1	-1.52	7.24E-03
XXbac-BPG55C20.3	-4.28	4.60E-02	AL035209.2	-1.52	3.11E-02
GLTSCR1-AS1	-4.28	3.09E-02	ZNF648	-1.52	2.09E-02
RP11-648O15.1	-4.27	3.79E-03	AMY2B	-1.52	4.41E-04
RP11-17E4.1	-4.27	4.85E-02	JPX	-1.52	4.70E-02
RN7SL449P	-4.26	3.14E-02	TRMT12	-1.51	1.56E-07
RP11-337A23.5	-4.26	1.57E-02	MEI1	-1.51	4.10E-02
LA16c-352F7.1	-4.26	4.10E-02	AC007038.7	-1.51	4.11E-02
RP11-350D23.4	-4.26	8.21E-03	RP11-37B2.1	-1.51	8.69E-03

RP11-460E7.9	-4.26	8.21E-03	TWIST1	-1.51	2.08E-02
RP11-66E20.2	-4.26	2.84E-04	SLC4A9	-1.51	3.61E-02
RP1-29C18.10	-4.25	3.75E-02	TMPRSS13	-1.51	1.61E-02
RP11-16C1.2	-4.25	5.01E-04	LINC00243	-1.50	2.97E-02
KLK5	-4.25	8.95E-04	GS1-124K5.14	-1.50	2.21E-04
COL6A6	-4.24	1.72E-02	HLA-DRB1	-1.50	3.25E-03
RP11-307I14.3	-4.24	2.40E-02	RP3-368A4.3	-1.50	1.03E-03
RP11-480I12.1	-4.24	1.07E-03	CDRT4	-1.50	2.67E-02
TMEM14EP	-4.24	2.55E-02	RP11-460E7.5	-1.50	1.91E-02
CTC-436P18.4	-4.22	2.81E-03	RP11-23J9.5	-1.49	9.90E-03
MIR4296	-4.21	3.01E-02	RP3-510O8.4	-1.49	4.65E-02
RP11-167O6.2	-4.21	8.52E-03	RP11-500G10.1	-1.49	3.20E-02
ADAM20	-4.21	1.05E-03	AC093375.1	-1.49	1.88E-03
MALAT1	-4.21	2.98E-04	NLRC4	-1.48	2.36E-02
RP11-175F9.1	-4.21	9.95E-03	MMP19	-1.48	2.59E-02
OR51K1P	-4.20	4.65E-03	SH2D2A	-1.48	7.86E-04
RP11-115C21.4	-4.20	4.20E-03	C6orf163	-1.48	4.82E-03
RP11-142L16.2	-4.20	1.09E-02	KIAA0825	-1.48	2.34E-02
ACSL5	-4.19	2.37E-29	SLCO6A1	-1.48	3.44E-02
RP11-820K3.3	-4.19	5.71E-04	RP11-350A18.1	-1.47	4.41E-02
CTC-458G6.3	-4.19	3.39E-05	RP11-83A24.2	-1.47	1.32E-02
RP11-533E19.3	-4.19	6.79E-03	MCF2L2	-1.47	1.75E-02
ASPN	-4.19	5.81E-03	RP11-1020A11.2	-1.47	3.05E-02
RP3-403L10.3	-4.19	2.20E-02	RP11-981G7.2	-1.47	2.61E-02
RP11-93O17.2	-4.18	6.63E-03	EYS	-1.46	3.94E-02
RP11-10E18.2	-4.18	1.90E-02	MIR193BHG	-1.46	4.52E-04
RP11-460N1.1	-4.18	1.91E-02	ST3GAL3	-1.46	5.00E-02
RBBP8NL	-4.17	7.19E-09	CTC-281F24.1	-1.46	2.38E-02
UBE2V1P1	-4.17	7.76E-03	RP11-166P13.4	-1.46	4.10E-02
CTD-2562G15.2	-4.17	2.18E-02	NHEJ1	-1.46	4.16E-02
ROBO1	-4.16	9.92E-04	RP11-503E24.2	-1.46	1.92E-02
CTD-2315M5.2	-4.16	1.36E-02	ESR2	-1.45	1.11E-02
RP11-55J15.1	-4.16	5.95E-06	YPEL4	-1.45	4.28E-02
ELOA3B	-4.16	1.74E-03	CCSER1	-1.45	1.25E-03
LL22NC03-79E2.1	-4.15	2.65E-04	FMN1	-1.45	2.95E-02
AP001271.2	-4.15	1.78E-03	BCL6B	-1.45	3.65E-02
RP11-199B17.1	-4.14	1.14E-02	RP11-806O11.1	-1.44	1.59E-02
RP11-793H13.12	-4.14	1.80E-02	AFAP1L2	-1.44	5.56E-03
THY1	-4.14	3.23E-03	AQP11	-1.44	2.56E-02
HSD17B2	-4.14	6.36E-03	FTX	-1.44	2.68E-04
RP11-409C19.2	-4.13	1.06E-02	RP11-188C12.2	-1.44	2.12E-02
RP11-162A12.3	-4.13	6.69E-03	PLB1	-1.44	9.83E-03
KCNJ13	-4.13	4.81E-04	RP11-398J13.1	-1.44	2.85E-02
RP3-471M13.2	-4.13	1.27E-02	AC156455.1	-1.44	7.12E-07
RP11-250H24.6	-4.13	1.19E-02	C1orf210	-1.44	2.02E-04
RP11-820K3.4	-4.12	2.43E-03	CAPN3	-1.44	2.68E-02
RP11-610P19.2	-4.12	6.59E-04	RP11-398K22.12	-1.43	4.31E-03
RP11-15J10.8	-4.12	4.48E-04	RP11-677M24.1	-1.43	9.13E-04
MIR181A2	-4.12	3.13E-02	MYO1F	-1.43	1.88E-02
RP4-654J19.1	-4.11	4.89E-02	KLRC4	-1.43	4.75E-02
CTA-305I2.1	-4.11	2.64E-02	PARP10	-1.43	9.83E-04
RP5-867C24.5	-4.10	1.56E-02	TPRG1	-1.43	1.07E-02

RP11-453N18.1	-4.09	2.25E-03	TMEM254-AS1	-1.43	4.63E-03
RP11-161I2.1	-4.09	6.10E-03	DYNC2H1	-1.43	5.66E-06
AC114765.2	-4.09	2.70E-06	FAM53A	-1.42	9.55E-04
RP11-351O1.2	-4.08	8.21E-03	RP4-778K6.2	-1.42	4.10E-02
RP11-329J18.4	-4.08	3.68E-02	AC137932.6	-1.42	4.41E-02
RP11-731D1.1	-4.08	1.84E-04	AC116366.4	-1.41	2.96E-02
RP11-405O10.2	-4.08	1.28E-02	AC092415.1	-1.41	4.03E-02
AL133245.2	-4.07	1.71E-02	KCP	-1.41	8.17E-05
RP11-481C4.1	-4.07	1.56E-02	RP4-563E14.1	-1.40	4.79E-02
RP11-357N13.6	-4.07	2.90E-04	MGAM	-1.40	1.57E-02
RF02119	-4.07	1.48E-02	PDZD2	-1.40	1.77E-02
RP11-270M14.1	-4.06	2.76E-02	ZNF410	-1.40	1.89E-02
RP11-328M4.3	-4.06	3.48E-02	MUC5B	-1.39	3.70E-02
RP4-695O20.1	-4.06	1.88E-02	CLDN3	-1.39	2.65E-03
RP11-58N10.1	-4.06	3.81E-03	FER1L4	-1.39	1.13E-03
RP11-44F21.4	-4.05	4.58E-02	LNX1	-1.39	3.34E-03
SFRP5	-4.05	5.54E-03	SEMA3D	-1.38	2.68E-02
RPL9P30	-4.05	3.87E-02	SSC4D	-1.38	8.78E-04
RP4-633I8.1	-4.04	1.28E-02	ITGB8	-1.38	3.11E-06
RP11-451F14.1	-4.04	1.85E-03	HRH2	-1.38	2.16E-02
RP3-368A4.2	-4.04	9.25E-03	CTF1	-1.38	1.73E-03
RP11-715N9.2	-4.04	9.91E-03	FBXL13	-1.37	2.12E-02
RP11-329J18.5	-4.04	4.68E-02	C9orf43	-1.37	1.55E-02
RP11-981G7.1	-4.03	6.11E-05	C3	-1.37	2.15E-02
RP11-974F13.3	-4.03	8.95E-04	AC005517.3	-1.37	3.64E-02
RP1-29C18.8	-4.02	6.88E-03	PLEKHA4	-1.37	1.56E-05
OR6A2	-4.02	4.88E-03	RP11-1023L17.1	-1.37	1.31E-02
RP11-504I13.2	-4.02	1.34E-03	ZFPM2	-1.37	2.46E-02
AC140134.2	-4.02	9.13E-04	ZNF350	-1.37	2.96E-02
RP11-52J3.3	-4.02	6.76E-03	TRPV4	-1.37	2.08E-02
RP11-756D7.2	-4.02	4.16E-03	NOV	-1.36	2.90E-02
RP11-221N13.2	-4.02	3.23E-04	DCDC1	-1.36	2.80E-02
PM20D1	-4.02	8.18E-04	CDK14	-1.36	1.75E-05
CA1	-4.02	5.23E-04	RP11-496N17.2	-1.36	1.01E-02
AC019080.1	-4.02	1.71E-02	SPDYA	-1.35	2.16E-02
C1QTNF7	-4.02	1.07E-02	RP11-458F8.2	-1.35	2.02E-02
RP11-509J21.2	-4.02	4.56E-02	PLXNC1	-1.35	2.05E-02
RP5-848E13.4	-4.01	4.42E-03	RP11-49K24.8	-1.34	3.77E-02
CEACAM8	-4.01	2.36E-02	C2orf88	-1.34	1.06E-02
CHST4	-4.01	7.95E-05	CTC-426B10.1	-1.34	1.67E-02
TAS2R13	-4.00	4.87E-03	PRR15L	-1.34	3.07E-03
RP11-230L22.4	-4.00	3.30E-02	RP11-631N16.2	-1.34	1.82E-04
MECOM	-4.00	7.58E-10	LGALS9	-1.34	4.74E-03
TCF24	-3.99	9.57E-03	RP11-15J10.4	-1.34	3.21E-02
RP11-342M21.2	-3.99	6.95E-03	AC004158.2	-1.34	1.15E-02
CH507-513H4.6	-3.98	7.75E-03	RP11-458F8.1	-1.33	2.40E-02
CH507-513H4.4	-3.98	7.75E-03	RSPO4	-1.33	6.16E-03
CH507-513H4.3	-3.98	7.75E-03	TIMP3	-1.33	2.06E-04
OR51I2	-3.98	7.07E-03	SUCNR1	-1.33	3.83E-02
RP11-464D20.6	-3.98	6.16E-03	ACVRL1	-1.33	3.43E-02
RP4-625H18.2	-3.98	2.07E-09	RASGRF1	-1.33	1.51E-03
RP11-522L3.7	-3.98	1.11E-02	HDHD2	-1.32	2.25E-02

Gene	Value	p-value	Gene	Value	p-value
RP11-746L20.1	-3.97	1.70E-02	CCDC30	-1.32	1.17E-02
CTA-243E7.2	-3.97	2.48E-03	OAS1	-1.32	2.99E-02
RP11-252K23.1	-3.97	1.48E-02	ANK3	-1.32	3.40E-05
POU5F1P5	-3.97	6.40E-03	RP11-70L8.4	-1.31	1.15E-03
RP11-527B17.2	-3.97	4.09E-02	CYP4F43P	-1.31	3.60E-02
TNPO1P1	-3.97	8.61E-03	ZNF84	-1.31	4.00E-05
RP11-748C4.1	-3.96	2.44E-02	NKPD1	-1.31	7.72E-03
RP11-181D10.2	-3.96	3.86E-03	RP11-573D15.2	-1.31	2.77E-02
AL589743.2	-3.95	2.54E-08	SLC1A3	-1.31	7.91E-03
CTA-797E19.1	-3.95	5.71E-03	KLK7	-1.30	3.10E-04
CTB-46B19.2	-3.95	1.14E-03	CTD-3051D23.1	-1.30	3.09E-02
MAGEA9	-3.95	2.36E-02	MUM1L1	-1.30	1.06E-02
CH17-80A12.1	-3.95	6.60E-05	PKDREJ	-1.30	8.40E-03
RF00004	-3.94	4.41E-02	RP11-452H21.4	-1.30	3.84E-02
AC104297.2	-3.94	8.93E-03	RP3-388N13.5	-1.30	1.87E-02
RP11-5N19.3	-3.94	3.85E-03	RP11-236F9.4	-1.30	2.70E-02
SULT1C2P1	-3.94	2.89E-02	HLA-DRA	-1.29	1.31E-02
CH507-513H4.5	-3.93	8.22E-03	DLEU1	-1.29	1.66E-02
MAGEA9B	-3.92	2.74E-02	SOCS1	-1.29	4.78E-02
AC074367.1	-3.92	4.64E-02	SEMA3A	-1.29	1.10E-06
GRIA3	-3.92	7.88E-03	RP11-1280N14.4	-1.29	1.78E-02
CTA-722E9.1	-3.92	7.15E-05	RP11-486B10.4	-1.29	2.91E-02
KCNS2	-3.92	1.30E-02	AC093642.1	-1.28	2.70E-03
RP11-204K16.1	-3.92	1.31E-02	RP11-793J2.1	-1.28	3.88E-02
RP5-1115A15.1	-3.92	4.90E-03	RP11-622O11.2	-1.28	1.74E-03
RPS20P31	-3.91	9.93E-03	AP000347.2	-1.27	1.94E-02
PZP	-3.91	5.30E-03	NTRK1	-1.27	1.93E-02
HMGN1L2	-3.91	7.98E-03	CACNA1D	-1.27	4.71E-03
AC010240.1	-3.91	3.23E-02	MT-RNR1	-1.27	1.09E-02
RP4-802A10.1	-3.91	4.12E-02	CTD-2516F10.2	-1.26	1.81E-02
RP5-979D14.1	-3.91	1.86E-02	ZNF780B	-1.26	2.96E-03
AC011747.6	-3.91	4.40E-03	RP11-645C24.2	-1.26	3.62E-02
MIR181A2HG	-3.90	6.70E-04	DFNB59	-1.26	1.35E-03
RP11-171G2.1	-3.90	9.62E-03	EPHA4	-1.26	2.09E-03
RP11-420B22.1	-3.89	3.04E-02	NAALADL2	-1.26	1.62E-02
RP11-356M20.3	-3.89	8.77E-03	SAMD12	-1.26	1.91E-06
CXCL17	-3.89	1.27E-03	PDZK1P1	-1.26	3.72E-02
RP11-820K3.2	-3.89	1.36E-02	ZNF704	-1.26	8.18E-04
RP11-264C15.2	-3.88	1.62E-02	AC011330.8	-1.25	4.06E-03
FGL2	-3.88	4.67E-04	RP11-290F20.2	-1.25	3.13E-02
RP11-829H16.4	-3.88	4.46E-02	RP11-446N19.1	-1.25	2.63E-02
RP4-569M23.4	-3.88	3.42E-03	TBC1D19	-1.25	1.82E-02
COL10A1	-3.88	8.42E-05	MAMDC2	-1.25	4.67E-02
RP11-553D4.2	-3.88	9.24E-03	SAT1	-1.24	1.72E-03
RP11-330L19.2	-3.87	4.28E-02	WDR66	-1.24	1.99E-03
ICAM1	-3.87	2.28E-23	CCDC64B	-1.24	9.44E-07
RP1-37M3.8	-3.87	2.10E-02	ACP7	-1.24	3.27E-02
RP11-264L1.3	-3.87	3.81E-02	BATF2	-1.24	2.25E-02
AC012363.9	-3.87	3.59E-03	NOTCH2NL	-1.24	4.12E-02
RP11-391L3.4	-3.87	9.67E-04	CTC-425O23.5	-1.24	6.34E-03
RP3-344J20.1	-3.87	2.59E-02	CACNA1A	-1.23	6.54E-05
AC079776.7	-3.86	1.20E-04	AKR1C1	-1.23	2.97E-02

AC004049.2	-3.86	6.65E-04	PARD3B	-1.23	4.04E-02
CTA-714B7.6	-3.85	9.44E-07	RP11-427L15.2	-1.23	1.67E-02
CTD-2024I7.13	-3.84	1.39E-04	SNORD3A	-1.23	2.30E-02
ANGPTL7	-3.84	1.49E-02	ZNF548	-1.23	8.25E-04
RP1-22N22.1	-3.84	5.62E-03	TMEM51-AS1	-1.23	1.03E-02
ELOA3D	-3.83	4.77E-03	AP001053.11	-1.23	4.60E-02
C9orf73	-3.83	1.96E-02	SQLE	-1.22	1.13E-06
RP11-160H22.1	-3.83	1.06E-02	RP11-390F4.3	-1.22	3.88E-03
AC004455.1	-3.83	8.68E-03	FOXP1	-1.22	6.65E-04
RP11-101O6.2	-3.83	8.11E-03	CEACAM19	-1.22	7.51E-03
MRPL37P1	-3.83	2.82E-03	KIAA1257	-1.22	1.94E-02
RP1-136O14.1	-3.82	1.57E-02	AC012358.4	-1.22	1.57E-02
GFY	-3.81	3.44E-31	MUC16	-1.22	1.26E-02
RP1-191J18.2	-3.81	1.38E-02	RP11-221N13.3	-1.22	4.92E-03
RARRES1	-3.81	3.70E-03	RP11-13A1.1	-1.21	1.99E-07
RP11-240G22.5	-3.81	3.81E-03	RP11-981G7.6	-1.21	1.19E-02
AC012513.4	-3.81	1.09E-03	POLR2J2	-1.21	2.25E-02
RP11-826F13.1	-3.80	1.88E-02	CACNB2	-1.21	7.07E-03
AC011239.2	-3.80	1.84E-02	ZBED3-AS1	-1.21	3.62E-02
RP1-267L14.3	-3.79	1.18E-02	CUBN	-1.20	8.54E-03
RP11-102C24.1	-3.79	1.68E-04	TVP23C	-1.20	3.83E-02
RP4-633I8.4	-3.78	2.51E-02	SPRN	-1.20	6.36E-03
RP11-230G5.2	-3.78	9.00E-25	RP11-536C12.1	-1.19	4.61E-02
RP11-19G24.2	-3.78	8.68E-03	ADGRE2	-1.19	1.69E-06
AC010240.2	-3.78	4.17E-04	MSH4	-1.19	1.24E-02
RP11-4K16.2	-3.78	1.99E-10	ANKK1	-1.19	3.15E-02
EIF4EBP3	-3.78	1.48E-02	BTC	-1.19	2.79E-03
CTD-2553L13.5	-3.78	3.20E-02	DDIT4	-1.19	1.62E-02
RP11-532F6.2	-3.77	4.32E-02	ICA1	-1.19	8.27E-05
RP11-315D13.1	-3.77	1.19E-02	RP11-1198D22.1	-1.19	1.91E-02
RP11-326L2.1	-3.77	6.83E-03	CCDC171	-1.18	9.40E-03
CTD-2179L22.1	-3.77	1.90E-02	RORC	-1.18	2.59E-02
RF00004	-3.77	4.82E-03	RASD2	-1.18	1.94E-02
RP11-484D18.2	-3.77	4.16E-02	SH3YL1	-1.18	8.86E-08
BHMT	-3.77	5.04E-03	PDE5A	-1.18	1.29E-02
ADAM28	-3.77	7.80E-05	SLC4A5	-1.18	3.96E-02
ANGPTL2	-3.76	2.68E-02	AREG	-1.18	1.31E-02
AL079295.1	-3.76	4.70E-03	SDCCAG8	-1.17	9.39E-04
ADCY1	-3.76	4.93E-02	CD24	-1.17	5.42E-04
AC007000.10	-3.76	1.65E-02	NLRC3	-1.17	2.99E-02
AP001439.2	-3.76	3.25E-02	ADAMTS6	-1.17	1.38E-02
RP11-399E6.1	-3.75	4.95E-02	TMEM9B-AS1	-1.16	4.33E-03
SMCR5	-3.75	7.07E-03	PLXNB3	-1.16	1.06E-03
RP11-104F15.7	-3.75	4.31E-03	ALOX12B	-1.16	4.23E-02
AC104389.31	-3.74	3.63E-02	RP5-1139B12.4	-1.16	3.62E-02
AC011242.5	-3.73	2.32E-02	BACH2	-1.16	8.50E-04
AC078883.3	-3.73	9.28E-03	RP4-740C4.5	-1.16	4.82E-03
RP11-197N18.8	-3.73	2.62E-03	OGDHL	-1.16	6.07E-04
RP11-2J18.1	-3.73	4.78E-02	ATP6V1C2	-1.15	4.48E-04
AC107620.1	-3.73	3.21E-02	SYNE1	-1.15	2.20E-02
TMEM148	-3.73	4.68E-02	PIGZ	-1.15	4.30E-03
FER1L5	-3.73	1.82E-26	STRC	-1.15	4.92E-03

RF00019	-3.72	3.44E-02	TTN	-1.15	3.62E-02
CTB-94B10.2	-3.72	7.88E-03	RP11-473M20.5	-1.15	4.30E-04
RP11-386I23.1	-3.72	5.49E-03	RP11-823P9.1	-1.15	2.38E-02
KBTBD12	-3.71	4.61E-03	DOC2A	-1.14	4.77E-05
RP11-354P11.8	-3.70	1.97E-02	LIPG	-1.14	5.78E-03
RP4-665N4.8	-3.70	2.23E-02	FCGBP	-1.14	2.32E-04
RP13-467E5.1	-3.70	9.47E-03	STAP2	-1.14	3.24E-02
LRRC19	-3.70	5.56E-03	AP000525.9	-1.13	1.67E-07
RP11-307P5.1	-3.69	2.15E-02	PABPC1L	-1.13	3.87E-02
SPATC1L	-3.69	8.68E-05	C21orf125	-1.13	3.93E-02
RP11-319E16.2	-3.69	3.05E-04	GUSBP3	-1.12	2.61E-02
RP11-362L22.1	-3.69	4.09E-02	RAD51B	-1.12	6.10E-03
RP3-405J10.5	-3.69	3.62E-02	MIRLET7BHG	-1.12	1.57E-02
RP1-224A6.8	-3.68	1.69E-03	RP5-875O13.7	-1.12	2.40E-03
AC004158.3	-3.68	1.19E-03	GPR135	-1.12	3.73E-02
ASAP1-IT2	-3.68	4.81E-03	RP11-429J17.7	-1.12	1.57E-02
OMD	-3.68	1.35E-02	CTHRC1	-1.12	1.19E-03
RP11-382E9.1	-3.68	1.09E-03	TMC4	-1.12	1.56E-04
RP11-88N11.1	-3.67	1.10E-02	BDH2	-1.12	1.01E-02
RP11-288K12.1	-3.66	1.02E-03	RP11-392P7.3	-1.12	2.65E-03
RP11-2H8.4	-3.66	2.44E-02	CR2	-1.12	2.05E-05
RP11-823P9.4	-3.66	1.47E-02	SLC43A1	-1.11	9.87E-03
RP11-356K23.1	-3.66	2.14E-02	RP11-1415C14.4	-1.11	2.44E-02
RP11-397P13.6	-3.65	3.36E-03	DIAPH2	-1.11	4.61E-04
ASPG	-3.65	1.43E-02	SLC7A8	-1.11	4.71E-02
COL3A1	-3.65	6.84E-07	RP5-1166H10.2	-1.11	3.12E-02
RP11-467J12.2	-3.64	1.75E-02	GUSBP2	-1.11	2.88E-02
CNTN2	-3.64	2.17E-04	PLIN5	-1.10	1.74E-03
RP5-1049G16.4	-3.64	1.41E-02	NLGN3	-1.10	6.35E-03
RP4-773A18.2	-3.64	3.99E-03	ICA1L	-1.10	2.80E-02
FUT9	-3.63	1.21E-03	ABCA12	-1.10	4.31E-02
RN7SL255P	-3.63	1.49E-02	CYP3A5	-1.10	1.82E-02
AC079781.9	-3.63	2.61E-02	DNAH6	-1.09	1.62E-02
AC005067.4	-3.62	7.31E-03	RASIP1	-1.09	1.60E-02
CTA-714B7.4	-3.62	2.31E-02	GOLGA8K	-1.09	1.29E-02
RP11-435O5.7	-3.61	2.14E-02	AC005336.4	-1.09	4.55E-03
OR13K1P	-3.61	1.32E-02	MAP2	-1.09	4.13E-04
RP11-201O14.2	-3.60	4.19E-02	RP11-392A22.2	-1.08	3.94E-02
RP11-319E16.1	-3.60	1.08E-02	RGS6	-1.08	4.99E-03
FAM205A	-3.60	8.57E-03	RP5-1090P18.1	-1.08	3.29E-02
RP11-635N19.2	-3.60	3.23E-02	RP11-126L15.4	-1.08	4.70E-02
C1orf195	-3.60	1.85E-02	CFAP74	-1.08	6.09E-03
TAS2R46	-3.60	5.23E-03	ALOX12	-1.08	1.18E-02
CTA-243E7.1	-3.59	3.97E-02	ANKHD1-EIF4EBP3	-1.08	3.04E-02
RP11-308D13.1	-3.59	3.33E-02	PSORS1C1	-1.07	3.52E-02
RP11-95I19.2	-3.59	4.41E-02	RP11-764E9.1	-1.07	2.70E-03
AC068491.4	-3.59	3.86E-02	RP11-10N23.2	-1.07	3.21E-02
SNORD65C	-3.58	4.10E-02	CTD-2047H16.4	-1.07	2.03E-02
POU5F1P4	-3.56	3.88E-02	CD72	-1.07	2.90E-02
RN7SKP163	-3.55	2.50E-02	ESPNP	-1.06	6.03E-03
EVI2B	-3.55	1.61E-03	DIABLO	-1.06	3.54E-02
RP11-1B20.1	-3.55	2.64E-02	RP11-465B22.8	-1.06	4.91E-02

RP11-600F24.2	-3.55	1.38E-02	ANKRD24	-1.05	7.12E-03
RP11-152N13.8	-3.54	4.70E-03	RP11-222A11.1	-1.05	3.95E-02
RP11-63K6.1	-3.54	4.37E-03	SIPA1L3	-1.05	5.27E-04
TMEM74	-3.53	1.61E-03	RP11-390P24.1	-1.05	1.60E-02
RP11-366L20.2	-3.53	1.18E-03	DNAH14	-1.05	1.31E-02
RP11-297P16.1	-3.53	1.77E-02	PHF14	-1.05	1.54E-02
AL355093.2	-3.53	3.15E-02	WDSUB1	-1.05	5.56E-03
RP11-449H3.1	-3.52	7.05E-03	RP11-514P8.12	-1.04	1.27E-02
RP4-591N18.2	-3.52	3.30E-03	C17orf100	-1.04	4.25E-02
MIR5702	-3.51	2.69E-02	RP11-848P1.2	-1.03	4.14E-02
RP11-18E13.1	-3.51	4.23E-03	PATJ	-1.03	3.81E-03
RP11-549L6.2	-3.51	3.35E-02	RNF43	-1.03	5.27E-03
RF00004	-3.51	1.31E-02	COL4A3	-1.03	1.36E-04
TM4SF18	-3.50	1.98E-04	ADAMTS17	-1.03	2.30E-02
RP11-74J13.6	-3.50	3.20E-02	GOLGA8T	-1.03	1.29E-02
OR52D1	-3.50	2.03E-02	RP11-21I4.1	-1.03	5.59E-03
RYKP1	-3.49	6.09E-03	MLYCD	-1.03	5.58E-03
RP1-78B3.1	-3.49	2.70E-02	GPR143	-1.03	3.45E-02
ENPP2	-3.49	6.61E-03	PARD6B	-1.03	1.44E-02
CTA-747E2.8	-3.48	3.56E-02	RP11-497H16.5	-1.02	3.51E-02
ECM2	-3.48	2.14E-03	RP11-1415C14.3	-1.02	2.76E-02
OR51B6	-3.47	2.30E-02	FOXP2	-1.02	1.85E-02
RP11-156F12.1	-3.47	1.43E-02	AC018865.8	-1.02	1.89E-02
ASB18	-3.47	2.62E-03	SPTBN5	-1.02	1.61E-02
RP11-714G12.1	-3.47	4.64E-03	TRIM15	-1.02	7.54E-03
DMRTA1	-3.46	6.75E-03	CD70	-1.02	4.03E-02
RNU6-780P	-3.46	4.52E-02	FAM86HP	-1.02	3.72E-02
RP11-216N14.7	-3.46	6.16E-03	RP11-250B2.3	-1.01	1.59E-02
RP4-635E8.1	-3.46	2.10E-02	ZFHX2	-1.01	2.26E-02
Z69666.2	-3.46	2.13E-03	RP11-429J17.8	-1.01	3.77E-06
RP1-168P16.1	-3.46	8.98E-03	RP11-556O5.4	-1.01	3.35E-02
CTA-280A3.2	-3.46	1.95E-02	SERPINF2	-1.01	2.90E-02
CTD-3083F21.5	-3.46	2.76E-03	AC009404.2	-1.01	8.09E-03
RP11-274A11.4	-3.46	9.83E-03	RP11-403I13.8	-1.01	4.60E-02
SNORD70	-3.46	4.66E-02	IGSF9	-1.00	4.13E-02
BTBD18	-3.45	5.68E-04	C4B	-1.00	5.79E-03
RP11-93G5.1	-3.45	1.32E-02	RP6-99M1.2	-1.00	6.00E-03
RP11-146E13.4	-3.45	1.71E-12	SGK1	1.00	3.71E-02
PLET1	-3.45	2.10E-02	DENND5B	1.00	1.18E-03
BNIP3P4	-3.44	2.46E-02	NUF2	1.00	8.20E-03
RP11-123N4.4	-3.44	4.89E-02	RP2	1.00	1.15E-02
RP1-78O14.1	-3.44	5.02E-03	DEGS1	1.00	4.82E-03
SCRG1	-3.43	2.06E-02	SLC16A14	1.01	2.87E-03
RNU4-25P	-3.43	2.81E-02	ORC1	1.01	2.01E-02
SNHG14	-3.42	3.94E-04	FOXC1	1.01	4.32E-03
RP3-412A9.17	-3.42	1.04E-03	PSMB6	1.01	2.26E-02
AL133245.1	-3.42	1.33E-02	RP11-568G11.3	1.01	9.46E-04
RP11-1023L17.2	-3.42	1.57E-02	ARHGAP11A	1.01	5.80E-03
RP11-561O23.9	-3.42	1.37E-03	KIFC1	1.01	1.62E-02
ABRA	-3.41	1.71E-02	HMMR	1.01	6.49E-03
CTD-2034L19.1	-3.41	1.17E-02	EML1	1.01	1.70E-02
OR13H1	-3.41	1.07E-02	LMNB1	1.01	1.46E-02

Gene	Value	p-value	Gene	Value	p-value
RP11-673C5.2	-3.40	2.26E-02	HCFC1R1	1.01	2.70E-03
RN7SL4P	-3.40	2.61E-02	PUSL1	1.01	3.87E-03
KB-1254G8.1	-3.40	1.42E-02	ASF1B	1.01	1.44E-02
RP4-569M23.2	-3.40	4.20E-03	EIF5A2	1.01	2.93E-03
CSMD3	-3.39	5.47E-03	FAM20C	1.01	1.56E-02
RP11-214J9.1	-3.39	2.41E-02	RP11-887P2.3	1.01	4.39E-02
ITGBL1	-3.39	1.75E-06	TAF5	1.01	1.90E-02
RP11-489M13.1	-3.39	3.22E-02	SH3TC2	1.02	1.70E-02
GPR82	-3.39	2.71E-03	LFNG	1.02	2.75E-02
RP11-665C16.1	-3.39	2.63E-02	MORF4L1	1.02	3.10E-04
RN7SKP71	-3.39	2.88E-03	LMNB2	1.02	6.90E-03
RN7SKP9	-3.39	3.66E-02	GNAZ	1.02	4.31E-03
RP11-138H8.8	-3.39	1.86E-02	GINS1	1.02	2.13E-03
AC073551.1	-3.38	5.99E-03	AURKB	1.03	1.21E-02
RP11-109N23.5	-3.38	2.83E-02	PCNA	1.03	1.35E-02
PSG8	-3.38	2.60E-02	ASRGL1	1.03	3.79E-03
C9orf131	-3.37	1.44E-02	RP11-673C5.1	1.03	9.45E-03
IL1B	-3.37	1.99E-02	CYP4F12	1.03	3.55E-02
RP11-697N18.4	-3.37	3.82E-03	NGRN	1.03	5.54E-07
RNA5SP123	-3.37	3.82E-02	ACTB	1.03	9.79E-03
MIR1207	-3.37	4.42E-02	HMGB2	1.03	6.20E-03
RP11-182N22.9	-3.36	5.81E-03	CHSY1	1.03	4.48E-05
RP11-22C11.1	-3.36	1.26E-02	AIP	1.03	5.96E-04
RP4-534N18.2	-3.35	2.20E-03	CALR	1.03	4.31E-03
RP3-442M11.1	-3.34	3.42E-02	HYAL3	1.03	8.66E-03
RP11-115D19.3	-3.34	1.45E-02	TPST1	1.03	6.55E-05
RP11-533K9.3	-3.33	1.99E-02	GPAT3	1.03	1.19E-02
KRT23	-3.33	3.88E-20	AP1M1	1.03	2.70E-03
BHMG1	-3.33	2.74E-08	PRPS1	1.04	9.80E-04
MIR374B	-3.33	3.51E-02	CSRP1	1.04	5.29E-06
CTD-3236F5.1	-3.33	7.60E-03	MCM4	1.04	1.97E-02
C17orf78	-3.33	7.51E-03	P2RY2	1.04	1.80E-02
AC018442.1	-3.33	2.37E-02	NCAPD2	1.04	4.10E-02
UTS2	-3.33	9.13E-04	IMP3	1.04	2.68E-02
RP11-356J5.11	-3.32	2.77E-02	EHD1	1.04	1.32E-04
RN7SL3	-3.32	1.10E-04	RP11-490H24.5	1.04	2.70E-02
RP11-401P9.7	-3.32	1.81E-02	CLSPN	1.05	4.30E-04
AP001442.2	-3.30	2.96E-03	FEN1	1.05	1.16E-02
ACTL10	-3.30	2.71E-02	NCAPG2	1.05	3.67E-04
AC026191.2	-3.30	4.25E-02	CSK	1.05	5.66E-03
RP11-330M2.6	-3.30	4.49E-03	OIP5	1.05	4.73E-02
TIGIT	-3.29	2.45E-03	STMN3	1.05	1.91E-02
RN7SL2	-3.29	2.56E-02	HJURP	1.05	7.60E-04
RP11-507C10.4	-3.29	6.10E-03	LINGO1	1.06	5.91E-03
RP11-613C6.4	-3.29	1.84E-02	NCAPG	1.06	2.24E-04
RP11-195E11.2	-3.29	3.86E-04	PRR11	1.06	1.24E-02
RP11-139F4.1	-3.29	2.64E-02	NEK2	1.06	3.84E-02
RP11-95G17.2	-3.28	2.12E-02	KIF4A	1.06	8.42E-03
RP11-126O1.4	-3.28	1.39E-04	FKBP4	1.06	5.51E-03
COL18A1-AS1	-3.28	4.32E-03	DGKG	1.06	6.86E-03
RP11-314B1.2	-3.28	3.74E-04	LARGE	1.07	2.25E-04
RP11-138H8.2	-3.28	4.32E-02	CIB2	1.07	5.81E-03

RP11-533K9.4	-3.28	9.90E-03	FURIN	1.07	3.81E-03
RP11-378G13.2	-3.27	2.20E-02	RAP2A	1.07	3.94E-04
RP11-492I21.1	-3.27	4.46E-03	GALNT9	1.07	8.35E-03
AC009502.2	-3.27	1.19E-03	CENPN	1.07	9.80E-04
CYP4Z1	-3.27	2.52E-02	INCENP	1.07	2.36E-02
ZNF29P	-3.27	1.50E-02	DUSP4	1.07	6.47E-05
RP1-21O18.3	-3.26	4.57E-02	MCM2	1.07	2.41E-02
MAPT-IT1	-3.26	3.49E-02	PGP	1.07	5.53E-03
PXDN	-3.26	6.10E-40	SPAG5	1.07	1.09E-02
RP11-286E11.1	-3.26	1.06E-02	MPP1	1.07	1.11E-02
RP11-733C7.2	-3.25	1.47E-02	FAM102B	1.07	1.99E-02
RP11-236F9.2	-3.25	1.01E-04	FLNA	1.08	1.68E-04
RP11-667K14.8	-3.25	1.80E-02	FAM96A	1.08	1.25E-03
HEPH	-3.25	4.15E-08	ECT2	1.08	5.02E-04
RP1-232P20.1	-3.25	4.83E-02	ANLN	1.08	3.88E-03
RP11-140H17.2	-3.25	4.13E-04	CDCA5	1.08	4.32E-03
RN7SKP203	-3.24	6.19E-03	ABCG1	1.08	2.83E-02
RP11-386J22.3	-3.24	2.25E-02	ESCO2	1.08	4.82E-04
SERPIND1	-3.24	3.80E-02	FAM64A	1.08	3.60E-02
RP11-83A24.1	-3.24	7.22E-03	EIF2S1	1.08	1.61E-04
RP11-157K17.5	-3.24	1.96E-02	CENPA	1.08	4.06E-03
AC097500.1	-3.24	8.16E-03	SMPD1	1.08	7.40E-03
RP11-104D3.2	-3.24	5.47E-03	CCDC167	1.08	2.75E-02
RP11-274J7.3	-3.23	1.38E-02	RPS6KA4	1.08	2.81E-03
RP11-49O14.2	-3.23	1.68E-02	RP11-54H7.4	1.08	3.66E-03
RP11-305O6.3	-3.22	3.52E-02	TOM1L2	1.08	2.51E-07
RP11-757O6.2	-3.22	2.75E-02	CFL2	1.08	2.89E-03
RP11-5L12.1	-3.22	3.81E-02	ALYREF	1.09	7.75E-03
RP11-55K22.2	-3.21	3.88E-02	TOP2A	1.09	5.03E-03
RP11-1078H9.5	-3.21	4.24E-02	NUSAP1	1.09	8.22E-04
MIR421	-3.21	1.23E-03	RNF182	1.09	3.26E-03
RP11-288C17.3	-3.21	4.57E-02	ANP32A	1.09	1.31E-03
RP11-343K8.3	-3.21	1.38E-02	NEURL1B	1.09	1.80E-02
AC012363.11	-3.20	1.69E-03	NCEH1	1.09	3.78E-05
CTB-102L5.7	-3.20	2.23E-02	LZTS1	1.10	4.80E-02
RP11-709A23.2	-3.20	2.91E-03	CMPK2	1.10	6.40E-03
GDAP1L1	-3.20	1.07E-02	DLGAP5	1.10	3.44E-02
RP11-1223D19.6	-3.19	7.19E-05	TPX2	1.10	6.63E-03
AL133243.4	-3.19	4.87E-02	IDH3A	1.10	4.27E-04
AC007036.6	-3.19	4.57E-02	SNX22	1.10	6.64E-04
RN7SKP271	-3.18	1.06E-02	E2F2	1.10	1.84E-03
RP11-176F3.9	-3.18	2.10E-02	NEBL	1.11	4.39E-05
RP4-633I8.2	-3.18	2.99E-02	KIF18B	1.11	4.06E-03
ID4	-3.18	4.81E-07	RP11-303E16.2	1.11	7.58E-03
GAPDHP42	-3.17	3.11E-02	GAS2L1	1.11	9.91E-03
RP11-119H12.4	-3.17	4.34E-03	MICB	1.11	6.20E-04
RPRM	-3.17	2.25E-02	HIRIP3	1.11	1.51E-03
RP1-29C18.9	-3.17	3.76E-02	AC068831.18	1.12	2.57E-04
CD33	-3.17	1.85E-12	FERMT2	1.12	1.47E-04
FHAD1	-3.17	2.30E-18	PBX1	1.12	1.86E-02
RP11-356K23.3	-3.17	2.30E-02	GNE	1.12	9.67E-08
TMC1	-3.17	4.46E-07	TYMS	1.12	3.77E-03

SPNS3	-3.17	2.52E-06	DNER	1.12	4.32E-03
RF00017	-3.16	4.27E-02	BUB1B	1.12	4.00E-03
AC129778.3	-3.16	3.21E-03	RGS2	1.12	4.40E-02
RP11-1197K16.2	-3.16	2.68E-02	RPS17	1.12	7.51E-05
AC092168.2	-3.16	6.08E-03	ITGB4	1.12	5.51E-03
RP11-6N17.2	-3.15	9.91E-03	COL24A1	1.12	2.29E-02
KLK11	-3.15	1.16E-03	TRIM6	1.13	4.19E-03
RP11-208G20.1	-3.15	2.54E-02	E2F1	1.13	4.00E-03
AC008062.1	-3.15	2.19E-02	SUV39H1	1.13	1.50E-02
RP1-224A6.9	-3.14	1.35E-02	FANCI	1.13	5.30E-07
PRSS37	-3.14	4.32E-03	RP11-187C18.3	1.13	1.18E-02
RP11-689D3.4	-3.14	3.10E-03	NEIL3	1.14	9.85E-06
RP4-549L20.2	-3.14	1.06E-02	RAET1L	1.14	4.23E-02
RP11-797J4.1	-3.13	1.77E-03	GTSE1	1.14	7.85E-03
RP11-296K13.4	-3.13	3.19E-02	STARD8	1.14	4.42E-03
RNA5SP195	-3.13	8.51E-03	GINS2	1.14	6.96E-03
RP11-529H22.1	-3.13	2.52E-02	TICRR	1.14	1.51E-04
AC064852.5	-3.13	9.94E-03	COMMD4	1.14	1.61E-02
RP11-61L19.1	-3.12	9.92E-03	NCAPH	1.15	3.34E-03
KIAA0226L	-3.12	2.43E-03	BUB1	1.15	1.33E-02
LYVE1	-3.12	2.47E-03	CHN1	1.16	7.45E-03
RPS3AP34	-3.12	3.68E-05	MAD2L1	1.16	3.20E-03
RP11-923I11.4	-3.11	1.40E-02	PIF1	1.16	2.12E-02
RP11-540O11.8	-3.11	4.10E-02	CDCA8	1.16	1.92E-03
CTD-2542L18.1	-3.11	1.94E-02	CRIP2	1.16	6.91E-03
RP11-131L23.1	-3.11	5.02E-03	MYBL2	1.17	1.09E-03
RP11-292B8.2	-3.11	3.00E-02	LGALS1	1.17	1.98E-04
ABC11-48400900C8.1	-3.10	1.74E-02	SCD	1.18	3.47E-04
AK5	-3.10	3.11E-02	AC000095.6	1.18	4.48E-04
RP11-333J10.3	-3.09	1.36E-02	RPP25	1.18	1.32E-02
RP1-102H19.7	-3.09	2.73E-02	AC093509.1	1.18	3.11E-02
CTA-414D7.1	-3.09	3.24E-03	LGI3	1.18	1.61E-02
ACP5	-3.09	1.56E-03	TUBA1C	1.18	2.91E-04
RP1-117O3.2	-3.09	1.50E-02	REEP1	1.19	3.33E-05
RP11-75C10.6	-3.08	4.40E-03	ADAMTS2	1.19	6.60E-04
RP11-620E11.1	-3.07	3.08E-02	KPNA2	1.19	4.85E-03
GPR15	-3.07	2.51E-06	TUBBP1	1.19	1.57E-02
RP11-289A15.1	-3.07	3.74E-03	MCM10	1.19	6.09E-04
BHMT2	-3.07	3.25E-02	TCF19	1.20	3.98E-05
RP11-460N11.2	-3.07	6.04E-04	CKAP2L	1.20	1.01E-04
RP11-615I2.3	-3.06	2.95E-02	CD276	1.20	9.92E-04
AC073326.3	-3.06	1.88E-02	MDGA1	1.20	2.03E-03
RP11-24B13.1	-3.06	1.33E-02	PCLAF	1.20	6.04E-04
RP11-506B4.3	-3.05	3.54E-02	TUBB	1.21	7.58E-04
RP11-150L8.4	-3.05	4.36E-02	PSMA4	1.21	1.06E-03
TTLL2	-3.04	2.60E-03	CDKN2D	1.21	1.55E-03
RN7SKP268	-3.04	2.25E-02	ATP1B1	1.21	7.74E-05
RP11-274J7.1	-3.04	2.85E-02	CDCA2	1.21	8.80E-03
NIPAL4	-3.03	2.25E-02	AURKA	1.21	2.94E-02
RP11-561N12.4	-3.03	4.64E-02	FASN	1.21	1.82E-03
RP3-425C14.5	-3.03	5.81E-03	ATP6V1D	1.21	7.13E-06
AC079466.1	-3.02	1.97E-02	SPC25	1.21	8.50E-04

RP11-506H20.2	-3.02	2.18E-02	HSPA8	1.21	2.97E-02
RP11-181K12.2	-3.02	4.30E-02	PAQR5	1.21	5.75E-08
AC129778.2	-3.02	3.66E-02	HCN4	1.22	1.06E-03
CTC-458G6.2	-3.02	5.56E-03	SH3RF2	1.22	2.01E-03
RP11-234K24.3	-3.02	2.07E-02	BIRC5	1.22	1.48E-02
CTB-75G16.3	-3.01	2.17E-02	PCSK9	1.22	3.66E-04
RP1-69D17.4	-3.01	6.04E-04	ZNF367	1.22	6.04E-04
LIPM	-3.01	4.58E-02	P3H2	1.22	3.92E-02
CTD-2653M23.1	-3.00	1.75E-02	HCN2	1.23	3.25E-03
RP11-616K22.2	-3.00	3.30E-02	PLK1	1.23	1.97E-02
RN7SL5P	-3.00	2.98E-02	PRICKLE1	1.24	1.28E-02
RP11-71H17.4	-3.00	3.54E-02	KLF2	1.25	7.15E-05
CTD-3010D24.3	-3.00	3.84E-03	MYBL1	1.25	4.66E-04
RP11-101E13.1	-3.00	3.68E-02	PSMD2	1.25	3.34E-03
RP11-56B16.1	-3.00	3.20E-02	SPC24	1.25	2.84E-03
RP11-123C21.2	-3.00	7.83E-03	RP11-121L10.3	1.25	4.83E-05
RP11-381O7.3	-2.99	2.53E-02	TGFBR3	1.25	7.97E-03
RP11-479G22.5	-2.99	5.18E-03	CEP55	1.25	3.24E-03
RPL9P16	-2.99	5.44E-03	H2AFX	1.26	8.50E-04
SMIM6	-2.99	2.05E-04	PTRF	1.26	9.02E-03
AP000240.6	-2.98	3.25E-02	WDR62	1.26	1.13E-04
AC079111.1	-2.97	3.30E-02	CCNF	1.26	3.65E-03
RP11-1223D19.5	-2.97	3.23E-04	ZCCHC24	1.27	1.52E-04
RNA5SP33	-2.97	3.66E-02	CCDC50	1.27	6.82E-09
RP11-453E17.4	-2.97	2.65E-02	GSG2	1.27	1.84E-03
RP11-187A9.2	-2.97	1.89E-02	TUBB4B	1.27	3.08E-03
RP11-115D19.1	-2.96	9.06E-12	MT1E	1.28	1.98E-03
CTA-407F11.6	-2.96	5.57E-03	NR2F2	1.28	6.93E-04
PROM2	-2.96	2.63E-11	EMP3	1.28	2.44E-08
VAV3	-2.96	3.79E-03	NRG4	1.29	2.06E-02
CHRNG	-2.96	3.88E-03	DPP4	1.29	1.29E-02
CHRND	-2.95	1.93E-02	MT2A	1.29	4.16E-05
RP11-545A16.1	-2.95	2.68E-02	SCN1B	1.29	1.18E-04
CTD-2047H16.2	-2.95	2.89E-04	GABRQ	1.29	9.59E-03
POF1B	-2.95	4.36E-05	EPHA8	1.30	2.11E-02
AC097500.2	-2.95	1.44E-03	RP11-620J15.3	1.31	9.75E-04
AP005232.1	-2.95	1.40E-02	FAM83D	1.31	1.52E-02
PSG3	-2.94	2.30E-02	PBK	1.31	2.65E-03
AP000925.2	-2.94	1.85E-02	HEG1	1.31	4.57E-06
RP11-666A8.1	-2.94	1.96E-02	PRKCDBP	1.32	4.88E-03
RP11-544A12.4	-2.94	2.92E-03	ABCB1	1.32	1.38E-03
RP11-100G15.12	-2.93	4.31E-02	CDC20	1.32	4.83E-03
RP11-119D9.1	-2.93	2.37E-02	FOXM1	1.32	2.09E-04
RP5-1142A6.8	-2.93	5.23E-03	DPYSL5	1.34	7.99E-04
AC012363.12	-2.93	3.01E-03	PLPP3	1.34	7.74E-05
RP11-351I21.10	-2.92	2.36E-02	C1QL1	1.34	2.18E-02
RP11-399D6.2	-2.92	9.51E-03	IFNE	1.35	3.56E-02
RP11-423G4.10	-2.92	8.84E-03	KIAA0319	1.35	1.38E-02
TUBG1P	-2.92	1.50E-02	CSPG4	1.36	3.33E-06
BIRC6-AS2	-2.92	5.22E-03	SHCBP1	1.36	1.50E-04
FGF1	-2.92	1.29E-04	CCNA2	1.36	6.59E-04
RP5-1041C10.3	-2.92	3.66E-02	ZNF488	1.37	2.86E-02

LINC00299	-2.91	1.74E-02	RP11-466P24.3	1.38	3.51E-02
RP11-1A15.2	-2.91	3.16E-03	TK1	1.38	1.38E-03
AC003958.2	-2.91	4.56E-02	NCMAP	1.38	1.77E-03
RP4-814D15.1	-2.91	7.07E-03	SH2D7	1.38	2.74E-02
SF3A3P1	-2.91	2.14E-02	TUBA1B	1.38	3.94E-05
HKDC1	-2.91	3.36E-08	EFR3B	1.39	5.46E-03
CTD-2373H9.3	-2.91	1.66E-02	PRSS23	1.39	5.69E-07
MAL2	-2.91	6.92E-28	RP11-752G15.6	1.39	6.07E-03
MIR1206	-2.90	2.41E-02	S100A4	1.40	2.06E-03
RP5-881P19.7	-2.89	4.16E-02	B4GALNT1	1.40	6.84E-04
OR51I1	-2.89	3.87E-03	RRM2	1.41	1.14E-06
AC005062.2	-2.89	6.58E-03	ARHGAP42	1.42	4.62E-10
CTC-210G5.1	-2.88	2.26E-02	CDK6	1.43	6.28E-05
AC005522.8	-2.88	1.62E-02	RP11-58O9.2	1.44	1.16E-03
RP11-450K4.1	-2.88	2.31E-02	MT1X	1.45	2.82E-03
KCTD12	-2.88	1.93E-08	ECM1	1.47	1.17E-04
RP11-61F12.1	-2.88	6.14E-03	RP11-573I11.2	1.48	1.74E-03
LA16c-390H2.4	-2.88	2.70E-02	SYNM	1.48	4.12E-07
CTD-2553L13.7	-2.88	3.38E-02	SMAD6	1.48	1.44E-03
ENTPD3	-2.87	4.57E-02	SIGLEC1	1.50	3.92E-02
RP11-1221G12.2	-2.87	4.07E-03	KIF23	1.51	4.94E-07
RP11-855A2.3	-2.87	2.31E-02	ATF5	1.51	8.89E-04
RP11-767N6.2	-2.86	8.42E-03	CLIC3	1.52	6.44E-03
RP11-428O18.4	-2.86	7.91E-03	PAPSS2	1.53	7.06E-06
EVI2A	-2.85	1.57E-03	CYP1A1	1.54	3.00E-03
CTB-131B5.2	-2.85	1.25E-02	MT-TM	1.54	6.26E-03
RP5-1065J22.4	-2.85	1.01E-02	RF00019	1.57	4.58E-02
SLC3A1	-2.85	2.43E-02	DRAXIN	1.58	4.94E-07
RP11-391L3.5	-2.85	3.39E-02	ETV1	1.58	2.94E-04
MROH3P	-2.85	4.38E-02	CTRC	1.59	3.73E-02
CEACAM1	-2.85	2.10E-05	TBXA2R	1.60	8.36E-03
MACC1	-2.85	3.39E-13	SPARCL1	1.60	8.83E-04
RP11-444I9.2	-2.85	5.48E-03	KATNAL1	1.61	4.12E-10
COL6A3	-2.85	4.30E-03	CDKN3	1.62	7.59E-07
GPR34	-2.84	3.64E-02	CPA4	1.62	9.39E-06
NCF4	-2.84	2.20E-02	PKM	1.62	7.57E-05
AC114765.1	-2.83	1.63E-05	LONRF2	1.64	3.35E-05
CTD-2349P21.6	-2.83	1.97E-03	S100A5	1.64	1.12E-03
AC114737.7	-2.83	1.98E-02	SEMA3C	1.65	1.52E-06
SNTB1	-2.83	1.80E-13	AC000095.10	1.65	1.42E-02
AC012363.7	-2.83	8.11E-03	CLU	1.65	5.22E-06
FAM47E	-2.82	2.13E-07	CREB3L3	1.67	1.81E-02
AL133243.2	-2.81	2.10E-05	PRC1	1.68	1.58E-06
POM121L6P	-2.80	3.83E-02	S100A10	1.69	1.23E-12
LPAR6	-2.80	1.39E-02	ZEB1	1.71	8.55E-06
RP11-1007J8.1	-2.80	4.95E-02	TNS4	1.71	3.10E-06
CTC-470E21.2	-2.80	4.83E-02	MB21D2	1.72	5.60E-06
RP11-631M6.1	-2.80	1.67E-03	PDGFC	1.73	6.53E-18
RP11-115J23.1	-2.80	4.77E-02	RP4-662A9.2	1.76	3.86E-02
RP11-181K12.1	-2.80	6.72E-03	AC012146.7	1.80	5.05E-04
AC013448.2	-2.79	2.97E-04	MYL2	1.84	5.85E-03
AC012363.8	-2.79	1.30E-02	COL12A1	1.85	6.10E-07

RP11-292B8.1	-2.79	3.63E-02	AC108463.2	1.85	1.75E-02
RP11-767N6.3	-2.79	2.03E-02	SYT11	1.86	2.07E-02
RP11-255N4.3	-2.79	3.55E-02	AC108463.1	1.91	3.88E-02
CTD-2349P21.3	-2.78	2.05E-04	CDKN2C	1.92	1.14E-03
OR2AG2	-2.78	1.19E-02	IQGAP2	1.95	1.81E-05
LCN2	-2.77	2.95E-02	IFITM10	1.96	9.63E-03
RP1-67A8.3	-2.77	3.64E-02	ITGAM	1.96	1.34E-04
ZNF154	-2.77	1.04E-03	HBA1	1.96	4.32E-03
FSIP2	-2.77	6.06E-05	MSX2	1.98	2.20E-11
RP11-474I11.8	-2.77	3.53E-02	HBA2	2.04	4.88E-04
HAAO	-2.76	1.58E-02	GJA1	2.06	3.35E-03
AL133243.1	-2.76	1.03E-03	TARID	2.17	2.00E-08
TAS2R18	-2.76	1.23E-02	RP11-69H7.2	2.18	3.09E-02
ZNF750	-2.75	6.20E-03	AL162759.1	2.23	4.11E-15
RP11-210N13.1	-2.75	2.64E-02	B3GALT5-AS1	2.25	8.72E-03
RP11-574E24.3	-2.75	2.52E-03	XRCC4	2.27	1.22E-19
FAM81B	-2.75	4.62E-02	RGS5	2.30	3.14E-12
C1orf106	-2.73	1.74E-16	MT-TI	2.31	4.87E-03
CH17-195P21.1	-2.73	1.33E-02	RP11-281P23.1	2.32	9.67E-03
RP11-668G10.2	-2.73	1.17E-02	RP11-23P11.2	2.44	1.84E-02
LBH	-2.73	1.95E-03	NPY1R	2.45	5.02E-03
TCL6	-2.73	9.80E-04	ERMN	2.50	3.17E-19
AP001627.1	-2.73	4.89E-02	LGR4	2.72	5.95E-15
RP11-1379J22.3	-2.72	1.15E-02	VIM	2.83	8.60E-13
RP11-700A24.1	-2.72	2.87E-02	BMP4	3.04	1.94E-21
TTC22	-2.72	1.68E-03	AC006262.5	3.08	3.55E-02
RP11-764D10.2	-2.72	2.69E-02	LGALS9B	3.15	1.48E-02
RP11-426D19.1	-2.72	7.42E-04	HTR3A	3.17	2.30E-05
RP3-471M13.1	-2.71	3.81E-03	RP11-267A15.1	3.19	1.06E-02
GPR183	-2.70	5.49E-03	RP1-14N1.2	3.20	1.16E-02
KRT35	-2.70	1.86E-02	MYBPH	3.26	3.74E-02
CHRNB2	-2.70	1.75E-02	RP11-80B9.1	3.28	2.13E-02
RP11-358M11.1	-2.69	3.00E-02	NTRK3	3.37	1.72E-03
HTR2B	-2.69	7.47E-03	UTS2B	3.39	8.95E-32
RP11-70L8.5	-2.68	1.96E-04	CCL26	3.45	5.53E-04
TAS2R31	-2.68	1.88E-02	PRSS33	3.46	3.79E-05
RP4-552O12.2	-2.68	1.06E-02	RP11-398E10.1	3.47	1.92E-02
RP11-437B10.1	-2.68	2.96E-03	NHLRC4	3.51	1.78E-03
RP11-618G20.2	-2.68	1.24E-02	FLG	3.52	5.30E-05
IGHG4	-2.67	1.92E-03	TGFB2	3.52	4.25E-26
CD302	-2.67	4.65E-02	C11orf86	3.58	2.75E-02
MIR3687-1	-2.67	3.29E-03	VCAN	3.67	2.54E-55
NCAM1	-2.66	4.11E-11	IGHA2	3.78	4.03E-02
RP11-294J22.7	-2.66	1.31E-03	IL16	4.02	3.82E-04
RP11-275F13.3	-2.66	1.65E-02	GNG11	4.62	3.80E-06
C1orf194	-2.66	1.91E-02	RGS7	4.65	2.16E-03
RP11-403I13.9	-2.66	1.86E-02	RGS4	4.70	3.03E-43
PLA2G4D	-2.65	4.92E-03	ACAN	5.02	3.67E-02
RP11-438E5.1	-2.65	9.26E-03	SLC30A10	5.49	8.25E-04